

AD-A134 827

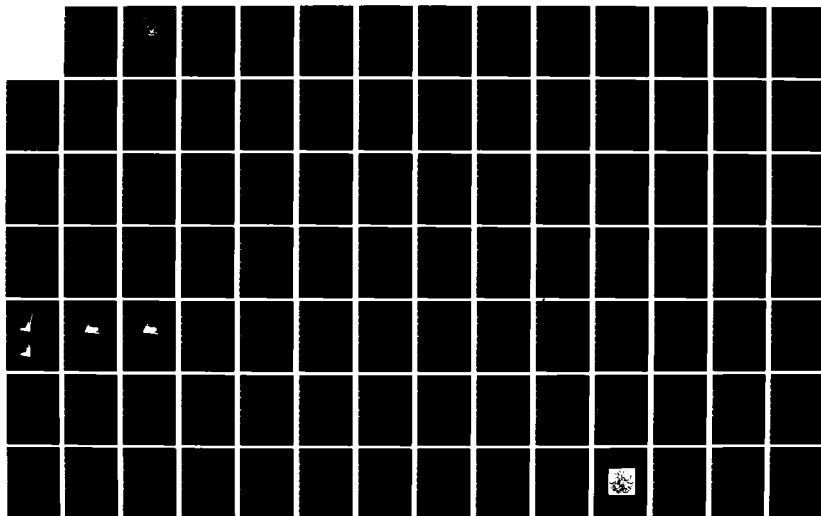
EFFECTS OF ATMOSPHERIC REFRACTION ON US GROUND WARFARE
(U) NAVAL POSTGRADUATE SCHOOL MONTEREY CA
T P MOURAS ET AL. SEP 83

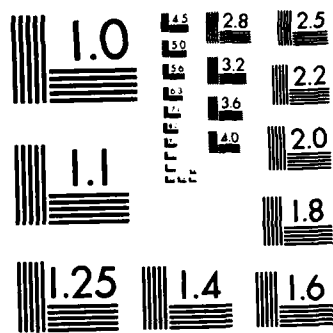
1/4

UNCLASSIFIED

F/G 28/14

NL





MICROCOPY RESOLUTION TEST CHART
NATIONAL BUREAU OF STANDARDS-1963-A

2

NAVAL POSTGRADUATE SCHOOL Monterey, California

AD-A134827



THESIS

EFFECTS OF ATMOSPHERIC REFRACTION
ON U.S. GROUND WARFARE

by

Theodore Paul Mouras

and

Charles Thomas Houser

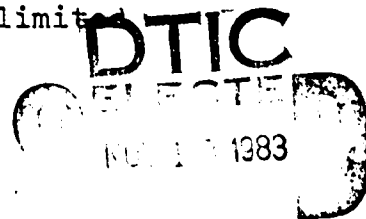
September 1983

Thesis Advisor:

G. E. Schacher

Approved for public release, distribution unlimited

DTIC FILE COPY



83 11 18 011

REPORT DOCUMENTATION PAGE		READ INSTRUCTIONS BEFORE COMPLETING FORM
1. REPORT NUMBER	2. GOVT ACCESSION NO.	3. RECIPIENT'S CATALOG NUMBER
	A134 827	
4. TITLE (and Subtitle) Effects of Atmospheric Refraction on U.S. Ground Warfare		5. TYPE OF REPORT & PERIOD COVERED Master's Thesis; September 1983
		6. PERFORMING ORG. REPORT NUMBER
7. AUTHOR(s) Theodore Paul Mouras and Charles Thomas Houser		8. CONTRACT OR GRANT NUMBER(s)
9. PERFORMING ORGANIZATION NAME AND ADDRESS Naval Postgraduate School Monterey, California 93943		10. PROGRAM ELEMENT, PROJECT, TASK AREA & WORK UNIT NUMBERS
11. CONTROLLING OFFICE NAME AND ADDRESS Naval Postgraduate School Monterey, California 93943		12. REPORT DATE September 1983
		13. NUMBER OF PAGES 316
14. MONITORING AGENCY NAME & ADDRESS (if different from Controlling Office)		15. SECURITY CLASS. (of this report) UNCLASSIFIED
		15a. DECLASSIFICATION/DOWNGRADING SCHEDULE
16. DISTRIBUTION STATEMENT (of this Report) Approved for public release, distribution unlimited		
17. DISTRIBUTION STATEMENT (of the abstract entered in Block 20, if different from Report)		
18. SUPPLEMENTARY NOTES		
19. KEY WORDS (Continue on reverse side if necessary and identify by block number) Atmospheric Refraction; Anomalous Propagation; Mirage; Optical Turbulence; Atmospheric Turbulence; Electromagnetic Propagation; Refractive Prediction; Ducting		
20. ABSTRACT (Continue on reverse side if necessary and identify by block number) This thesis investigates the effects of atmospheric refraction on military ground-force tactical systems which utilize EM energy propagating through the troposphere. Anomalous propaga- tion, mirages, and atmospheric turbulence are the three major atmospheric refractive conditions discussed. EM energy, from visible light to VHF radio is considered. The refractive characteristics of the atmosphere and the conditions that lead to significant refractive effects are		

reviewed. The means of predicting atmospheric refraction and the usefulness of such predictions, along with the probability of occurrence of atmospheric refraction is also discussed.

Specific examples of atmospheric refractive effects are provided in two forms: computer simulations and qualitative studies. A scenario is simulated showing the wide range of atmospheric refractive effects a typical ground force might anticipate in a desert environment. Finally, the thesis provides conclusions and recommendations for further studies.

Accession For	
NTIS GRA&I	<input checked="" type="checkbox"/>
DTIC TAB	<input type="checkbox"/>
Unannounced	<input type="checkbox"/>
Justification	
By _____	
Distribution/ _____	
Availability Codes	

Dist _____	
A-1	



Approved for public release, distribution unlimited
Effects of Atmospheric Refraction on U.S. Ground Warfare

by

Theodore Paul Mouras
Captain, United States Army
B.S., Virginia Military Institute, 1976

and

Charles Thomas Houser
Lieutenant Colonel, United States Army
B.S., University of Tampa, 1975

Submitted in partial fulfillment of the
requirements for the degree of

MASTER OF SCIENCE IN SYSTEMS TECHNOLOGY (ELECTRONIC WARFARE)

from the

NAVAL POSTGRADUATE SCHOOL
September 1983

Authors:

T. P. Mouras

Charles Houser

Approved by:

G. S. Schacher

Thesis Advisor

David E. Snider

Second Reader

John M. Boned
Chairman, Electronic Warfare Academic Group

G. J. Murphy
Academic Dean

ABSTRACT

This thesis investigates the effects of atmospheric refraction on military ground-force tactical systems which utilize EM energy propagating through the troposphere. Anomalous propagation, mirages, and atmospheric turbulence are the three major atmospheric refractive conditions discussed. EM energy from visible light to VHF radio is considered.

The refractive characteristics of the atmosphere and the conditions that lead to significant refractive effects are reviewed. The means of predicting atmospheric refraction and the usefulness of such predictions, along with the probability of occurrence of atmospheric refraction is also discussed.

Specific examples of atmospheric refractive effects are provided in two forms: computer simulations and qualitative studies. A scenario is simulated showing the wide range of atmospheric refractive effects a typical ground force might anticipate in a desert environment. Finally, the thesis provides conclusions and recommendations for further studies.

TABLE OF CONTENTS

I.	INTRODUCTION-----	9
II.	ATMOSPHERIC REFRACTIVE EFFECTS-----	11
	A. EM WAVE PROPAGATION IN THE ATMOSPHERE-----	11
	1. Wavelength Dependence of EM Propagation Effects-----	11
	2. Index of Refraction (n)-----	13
	3. Snell's Law-----	14
	B. REFRACTIVITY-----	20
	1. Refractivity (N)-----	20
	2. Anomalous Propagation, Mirage, & Optical Turbulence-----	25
	C. ANOMALOUS PROPAGATION-----	27
	1. Superrefraction, Subrefraction, and Ducting Defined-----	28
	2. Means of Describing Refraction-----	31
	3. Duct Characteristics-----	32
	4. Causes of Superrefraction, Ducting, and Subrefraction-----	40
	5. Consequences of Anomalous Propagation----	47
	6. Methods of Predicting Refractive Effects-	66
	D. MIRAGE-----	69
	1. General Description of the Mirage Phenomena-----	69
	2. Effects of Mirages on Optical Devices-----	77
	E. TURBULENCE-----	79
	1. General Description of Turbulence-----	79
	2. Principal Effects of Turbulence on Optical Propagation-----	90

a.	Scintillation-----	91
b.	Wave Front Tilt and Beam Spread-----	93
c.	Resolution-----	95
3.	Manifestation of Turbulence in Optical Systems-----	100
4.	Turbulence and MMW Propagation in the Atmosphere-----	106
F.	PREDICTION AND PROBABILITY OF OCCURRENCE OF ANOMALOUS PROPAGATION, MIRAGE FORMATIONS, AND TURBULENCE-----	107
1.	Anomalous Propagation-----	109
2.	Mirages and Turbulence-----	125
3.	Comparison of Mid-East and Central Europe-----	128
4.	Conclusions-----	134
III.	ATMOSPHERIC REFRACTION AND GROUND WARFARE-----	136
A.	INTRODUCTION-----	136
B.	EFFECTS OF ATMOSPHERIC REFRACTION ON TANK OPTICAL FIRE CONTROL SYSTEMS-----	137
1.	Atmospheric Conditions Creating the Gunnery Errors-----	140
2.	Expected Effects on Tank Gunnery-----	141
3.	Experimental Results-----	142
4.	Conclusions-----	149
C.	COMPUTER SIMULATION 1 - THE EFFECT OF REFRACTIVE CONDITIONS ON U. S. TACTICAL SYSTEMS, USING THE TROPOPLOT COMPUTER PROGRAM-----	154
1.	Tropoplot Program Description-----	155
2.	AN/FPS-16 Radar-----	156
3.	AN/VRC-12 Radio-----	160

4. Conclusions-----	161
D. COMPUTER SIMULATION 2 - THE EFFECT OF HORIZONTAL REFRACTIVE GRADIENTS ON AIRBORNE DIRECTION FINDING ACCURACY-----	161
1. General Description of Direction Finding and the Tactical Scenario-----	163
2. Algorithm Description-----	168
3. Results and Conclusions-----	173
E. SCENARIO-----	187
1. Scenario Background-----	187
2. Atmospheric Refractive Effects-----	190
a. Optical Effects-----	190
b. Effects on Communications and Electronic Warfare Systems-----	191
c. Effects on Noncommunications Emitters-----	193
3. Conclusions-----	194
IV. CONCLUSIONS AND RECOMMENDATIONS-----	196
A. CONCLUSIONS-----	196
B. RECOMMENDATIONS-----	198
APPENDIX A - IREPS-----	200
APPENDIX B - COMPUTER SIMULATION 1 LISTING AND OUTPUT--	212
APPENDIX C - COMPUTER SIMULATION 2 LISTING AND OUTPUT--	271
LIST OF REFERENCES-----	311
BIBLIOGRAPHY-----	314
INITIAL DISTRIBUTION LIST-----	316

ACKNOWLEDGEMENT

We would both like to express our gratitude and sincere appreciation for the guidance and patience extended to us by our thesis advisor, Professor Gordon Schacher. Without Professor Schacher's assistance, the problems involved in this thesis would have been insurmountable.

We would also like to extend our appreciation to Dr. Don Snider, of ASL, for his assistance as our second reader, and for the technical input he provided. Likewise, we would like to thank Professor Ken Davidson for his contributions to this thesis.

Several other individuals also provided technical input; thus, thanks is extended to Distinguished Professor E. C. Crittenden, Professor R. L. Kelly, Professor Jeff Knorr, Professor B. A. Milne, Professor Will Shaw, and LCDR Jim Corbin of the Geophysical Technical Readiness Center.

Finally, a special thanks to Melanie Mouras, for ruthlessly editing many of the sections in this thesis. Despite all the red ink involved, both of us are appreciative of her assistance.

I. INTRODUCTION

In order to enhance and extend surveillance and communications capabilities, modern ground warfare has become increasingly dependent on the entire electromagnetic (EM) spectrum. Uses of electromagnetic energy include airborne and ground target detection, weapons system tracking and guidance, command and control, and electronic warfare. Utilization of this energy requires an understanding of the phenomena that affect the propagation of EM waves as they travel through the atmosphere. After nearly 50 years of study, it is now widely accepted that dispersion, extinction, refraction, reflection, and diffraction all affect EM propagation significantly. Dispersion, extinction, and refraction are properties of the atmosphere, while reflection and diffraction are properties both of the atmosphere and of the terrain of the earth's surface. For radio/radar frequency (RF) and electro-optical (EO) systems, the physical factors listed impact on system performance above and beyond the more obvious effects of precipitation, wind, and temperature extremes.

The primary region of Army interest is the troposphere—the lower 10 to 20 kilometers of the atmosphere.¹ Within the troposphere, the main factor affecting RF propagation is refraction. E0 propagation, while greatly affected by aerosols and absorption in the troposphere, is also affected by atmospheric refraction. Thus, in order to best employ his assets, it is important that the ground forces commander be able to forecast and predict refractive conditions that degrade or enhance RF and E0 system performance.

It is the purpose of this thesis to examine the effects of atmospheric refraction on ground forces' tactical systems. Specifically, it will address the environmental conditions leading to the three major forms of atmospheric refraction (anomalous propagation, mirage formation, and atmospheric turbulence), and discuss their effects on EM waves propagating through the atmosphere. It will also address prediction and probability of occurrence of these three forms of refraction and it will end with a discussion of their effects on existing ground systems, (either through simulation or by presenting empirical test results). Recommendations and direction for future research directions will be found in the conclusion of the thesis.

¹ The specific height of the troposphere is a function of location and atmospheric conditions, on the average it is the thickest at the equator and narrowest at the poles.

II. ATMOSPHERIC REFRACTIVE EFFECTS

In this section the basic theory of EM propagation will be introduced. Since the purpose of this thesis is to describe the effects of atmospheric refraction on ground forces, this discussion will be limited to the troposphere.

A. EM WAVE PROPAGATION IN THE ATMOSPHERE

1. Wavelength Dependence of EM Propagation Effects

The electromagnetic wavelengths of interest to U. S. ground forces extend from those only micrometers (10^{-6} meters) in length to those several tens of meters long. This encompasses the full spectrum, from HF to visible - an EM region which is described in Figure 1.

Electromagnetic waves travel in a straight line in free space (vacuum), but in the atmosphere they are bent by several forces. The specific atmospheric effect and layer of the atmosphere that dominate in causing this bending depend on the propagating frequency. At wavelengths longer than very high frequency (VHF), approximately 30 MHz, the ionosphere is the primary influence. Since this thesis is concerned with the lower atmosphere, HF frequencies will, therefore, not be specifically addressed. Above 30 MHz, refraction in the troposphere is the controlling influence, and it will be these frequencies, from VHF to visible, that this thesis will address.

BAND	RADIO WAVES	MICROWAVES	INFRARED	VISIBLE LIGHT	ULTRAVIOLET
	HF	VHF	UHF	SHF	EHF
DEFINITION	30 MHz	300 MHz	30 GHz	3 THz	10 ¹⁴ Hz
	30 MHz	300 MHz	30 GHz	3 THz	10 ¹⁶ Hz
MILITARY USE	← 3 MHz TO 300 GHz →				
	LONG RANGE COMM	NAVIGATION AIDS	LASERS		
	FM RADIO	RADAR	THERMAL SIGHTS		OPTICAL SIGHTS
	TV				

Figure 1. Electromagnetic Spectrum

There is also a relationship between regions of the EM spectrum and the forms of refraction dominant in each region. The dominant effects at microwave frequencies are long range changes in refraction. At optical frequencies, absorption and small-scale refractive changes, in the form of mirage formations and atmospheric turbulence, are the dominant effects. In the millimeter wave (MMW) region the atmosphere is largely opaque due to molecular absorption by carbon dioxide and water molecules, except for a few regions (or "windows") of higher transmittance. Although little used until recently, much current research is focused on expanding the use of this region and in understanding the effects of atmospheric refraction on MMW propagation.

2. Index of Refraction (n)

Electromagnetic waves travel through matter via absorption and re-emission of electromagnetic energy by the atomic and molecular constituents of the medium. Thus, the speed at which these waves travel is affected by the density of the medium - the denser the medium, the slower the speed of EM propagation through it.

The "index of refraction (n)" is the ratio of the speed of electromagnetic waves in free space to their speed in the medium. Thus,

$$n = c/v, \tag{2.1}$$

where c is the speed in vacuum (speed of light) and v is the speed in the medium. We note that v is dependent on the constituents of the medium - in this case, the atmosphere. Note also that $n = 1$ in vacuum, and, therefore, n is greater than or equal to 1 for all media. For air,

$$n_{\text{AIR}} = 1.0003$$

In the troposphere, n_{AIR} is a function of temperature (T), water vapor content (e), and pressure (P), all of which are related to the density of the atmosphere and all of which vary systematically with climate and elevation. In general, the index increases with increasing density.

3. Snell's Law

The deflection of an electromagnetic wave across a discontinuity or boundary separating regions of differing values of refractive index is shown in Figure 2, and is described by Snell's law:

$$\sin \theta_1 / \sin \theta_2 = n_2 / n_1$$

Note in Figure 2 that the ray is bending (retarded) towards the higher n value, so that refractive bending is toward media of higher density.

Since the density of air generally decreases with altitude, the value of n will similarly decrease. Thus, in a "standard atmosphere" (a term used to describe average meteorological conditions), EM waves do not travel in a

straight line but bend slightly downward towards the earth's surface, the region of higher n . A list of the factors which, according to the National Oceanic and Atmospheric Administration (NOAA) [Ref. 1: p. 20], constitute "standard" conditions is provided in Table 1, while Figure 3 is a graphic illustration of the effect of index of refraction variation, with altitude, on EM propagation. When discussing changes of the index of refraction in the atmosphere, it is important to realize that there are no abrupt boundaries, as is implied in Figure 3. Changes in n generally occur over relatively large distances, when compared to the wavelengths affected. It is these gradual changes that create the smooth bending effect shown in Figure 4, as opposed to the sharp angles shown in Figures 2 and 3. Figure 4 also shows another of the effects of refraction in the troposphere, i.e., extension of the horizon. In essence, an EM ray directed above the geometric horizon is refracted and bent slightly around the surface of the earth, striking the surface at a distance greater than the geometric horizon. For example, J. Lake [Ref. 2: p. 22] states that, for microwave rays propagating in a standard atmosphere, the horizon is extended beyond the geometric horizon by approximately 30%.

Should the decrease in n , with altitude, be sufficiently great, a non-standard atmosphere will exist, where EM rays will bend downward more strongly than in a

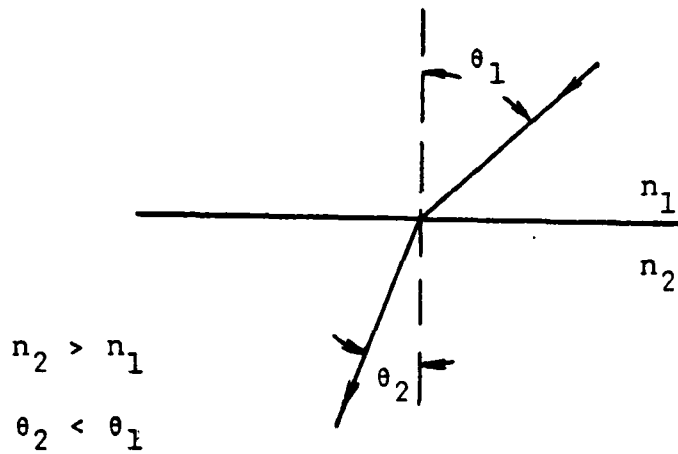


Figure 2. Snell's Law.

TABLE 1
 METEOROLOGICAL CONDITIONS FOR THE STANDARD ATMOSPHERE

At altitude $z = 0$ (sea level)

Pressure (P) = 1013.25 mb

Temperature (T) = 15°C (288.15K)

Acceleration (g) = 9.8 m/s²

Density (ρ) = 1.225 Kg/m³

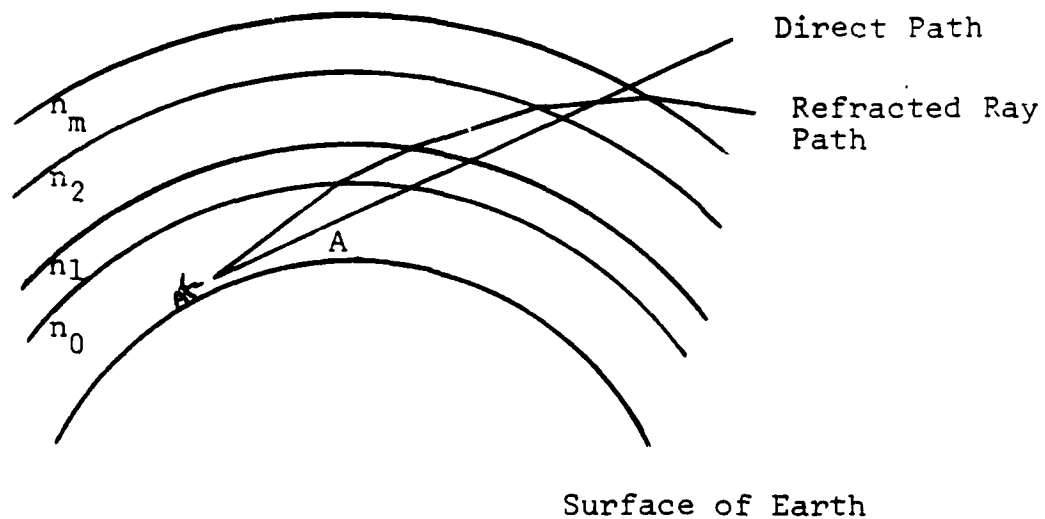


Figure 3. Path of microwave through the troposphere. The radar transmitter is located on the earth's surface and transmitting along path A. The atmosphere is assumed to consist of concentric shells each with a constant refractive index.

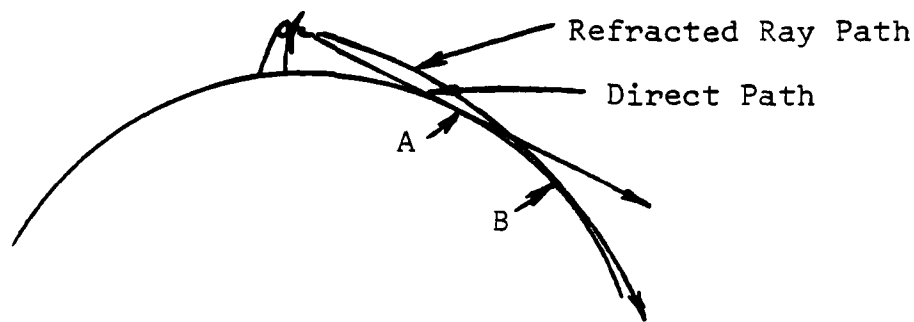


Figure 4. Extension of the radar horizon in the presence of refraction. A is the radar horizon in the absence of refraction (the geometric horizon) and B is the radar horizon in the presence of refraction.

standard atmosphere. This can lead to the most dramatic form of atmospheric refraction, called "trapping", where a horizontally launched ray is bent sufficiently so that it remains parallel to the earth's surface, extending the horizon to great distances. If we consider the atmosphere to consist of layers of varying refractive index, n , there is a critical angle of incidence needed to refract an EM wave completely back from a layer of lower n value to a layer of higher n value. At all angles of incidence smaller than the critical angle, EM rays are "trapped" by the layer of higher n . For all angles larger than the critical angle, the rays will be bent, but not so sufficiently as to be trapped. Thus, a region just above the trapped rays is formed, where fewer EM rays exist than if standard atmospheric conditions prevailed. This region is referred to as the radio or radar hole, the basic concept of which is shown in Figure 5. According to John Beach [Ref. 3: p. 82], the use of the word "hole" is not entirely accurate, since, under normal circumstances, there is no distinct critical angle, and leakage of EM energy into this region can occur by means other than direct propagation of the signal. There is, however, significantly less energy present in these radar/radio holes than would be present if no variation in n existed.

The critical angle for trapping, θ_c , as derived from Snell's law, is that angle, θ , which causes $\theta_2=90$. Thus,

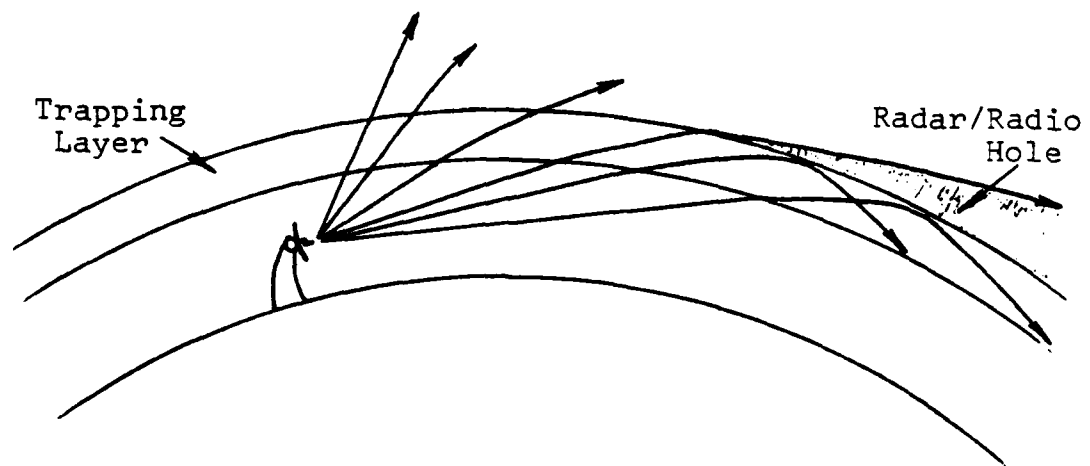


Figure 5. Radar/Radio Hole.

$$\sin \theta_c = n_2/n_1 \quad (2.3)$$

Since n only varies from about 1.00025 to 1.004 in the troposphere, $n_2/n_1 = .9998$ and $\theta_c \approx 89^\circ$. Hence, as shown in Figure 6, EM rays must be almost parallel to the layer in order to be trapped.

The index of refraction of the atmosphere does not always decrease with altitude. Should n increase with altitude, EM rays will be bent upward instead of downward. More will be said about this latter case, in discussions on subrefraction.

B. REFRACTIVITY

1. Refractivity (N)

The tropospheric index of refraction, n , is a characteristic of lower atmospheric properties. Specifically, at radio and microwave frequencies, n is a function of temperature, humidity, and pressure, and is related to these parameters by:

$$(n-1) \times 10^6 = (77.6 P/T - 5.6 e/T + 3.75 \times 10^5 e/T^2) = N, \quad (2.4)$$

where P is the barometric pressure in millibars, e is the partial pressure of water vapor in millibars, T is the

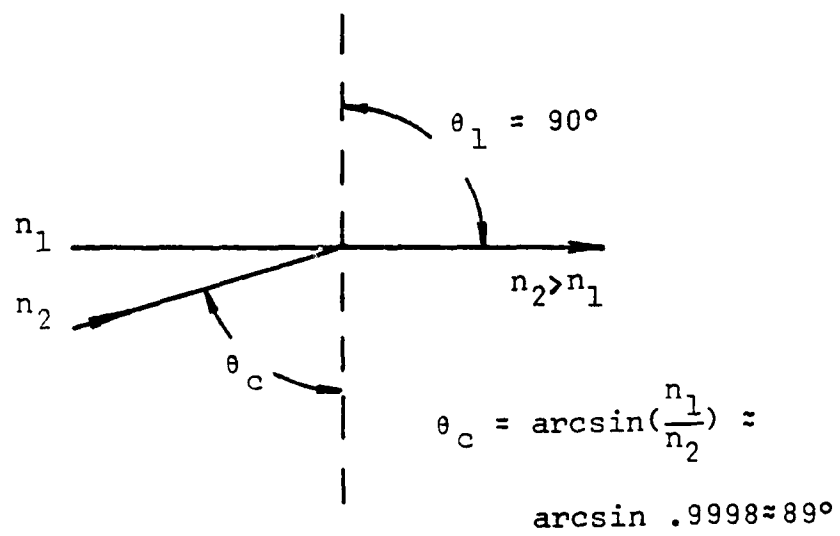


Figure 6. Critical Angle θ_c .

absolute temperature in Kelvin, and N is the refractivity, a parameter defined for the sake of convenience.

The second term in Equation 2.4 is often neglected, since its contribution to the calculation is very small compared with that of the other two terms, and the coefficient on the third term is usually modified so that the actual equation is generally:

$$N = (77.6 P/T + 3.73 \times 10^5 e/T^2) \quad (2.4A)$$

Beach [Ref. 3: p. 75] states that since the value of n at the earth's surface is usually between 1.00025 and 1.0004, the value of N generally lies between 250 and 400.

At optical frequencies the calculation of refractivity is modified to reflect the fact that water vapor has a negligible effect. Thus, for optical frequencies:

$$N = 77.6P/T \quad (2.5)$$

The significance of refractivity is not in the individual value of N for a given altitude, but, rather, in the gradient of N , (dN/dZ) , where Z is height. This is due to the fact that the electromagnetic wave path curvature depends, inversely, on the gradient of N . For microwave frequencies and a standard atmosphere, N decreases at a fairly steady rate of approximately 4×10^2 N per meter of

altitude. It is this characteristic that makes it convenient, in computations involving a standard atmosphere, to replace the actual earth's radius with a 4/3 earth radius. Using this geometry EM waves can be shown to propagate in straight lines rather than in curved or refracted lines, as shown in Figure 7. The value of using the 4/3 earth radius lies in its simplification of distance computations above the earth's surface, and in ray tracing. This geometry has been widely used in the modeling of radio communication and radar propagation. However, it must be remembered that the 4/3 earth representation is only an approximation of conditions that vary with meteorological conditions. The actual value may vary from 6/5 to 4/3 earth radius.

A vertical refractivity gradient causes EM rays to be bent with a radius of curvature given by:

$$r = -10^6 / (dN/dZ), \quad (2.6)$$

where the curvature is in a vertical plane.

Horizontal N gradients are normally not significant in EM propagation and are, therefore, usually assumed to be zero. In some circumstances, however, bodies of water either partially or completely surrounded by land may create horizontal N gradients which will have some effect on EM transmissions through the atmosphere above the land-water boundary region.

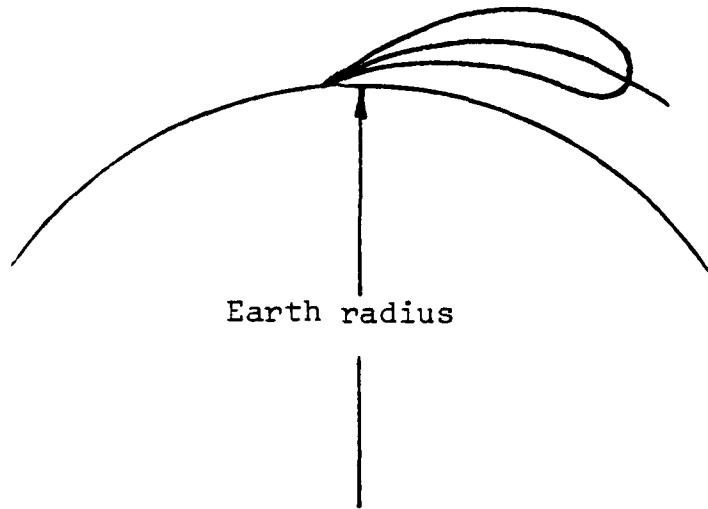


Figure 7a. Bending of antenna beam due to refraction by the troposphere.

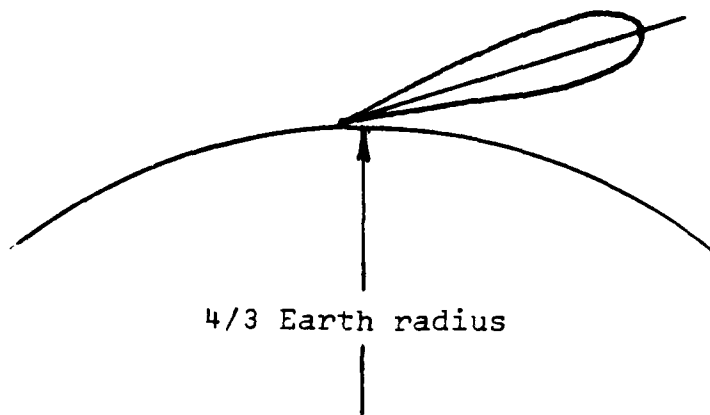
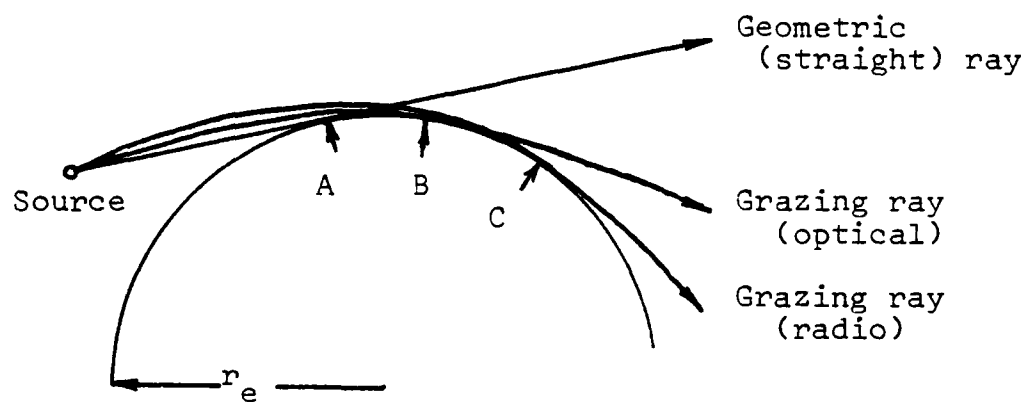


Figure 7b. Shape of antenna beam in $4/3$ earth representation.

2. Anomalous Propagation, Mirage, & Optical Turbulence

Refractivity effects are not the same across the EM spectrum. As previously shown, the calculation of N for the radio and radar portion of the spectrum is different than that for the optical portion (where the effect of humidity is ignored). Since the amount of bending is a function of the gradient of N , it is to be expected that the amount of bending is different for optical and microwave rays. This can be seen in Figure 8. Note the difference in the bending of the optical grazing ray and the radio grazing ray vis-a-vis each other and the geometric horizon.

Regions of strong refractivity gradients that are much larger in size than EM wavelengths cause anomalous propagation. Smaller scale regions with large N gradients also exist, in the form of mirages and atmospheric turbulence. Certain forms of atmospheric refraction, when located within the first several meters of the surface of the earth, and resulting from rapid changes in the temperature, can lead to mirage conditions which have a significant effect on optical transmission. Mirage formation is a form of anomalous propagation, but, for the sake of simplicity, the two will be discussed separately. They are best differentiated by relative size. Turbulence in the atmosphere creates fluctuations in the air index of refraction, resulting from inhomogeneities that vary in size from those of almost microscopic dimensions to those



- A Geometric horizon
- B Optical horizon
- C Radio horizon

Figure 8. Comparison of effect of refraction on optical ray and radio ray.

hundreds of meters in diameter. The wavelengths in the IR and visible range are most affected by turbulence, due to the small size of the refractive inhomogeneities relative to the wavelengths of radio and radar signals. Each of these three conditions will be individually addressed in the following sections, beginning with a discussion on anomalous propagation.

C. ANOMALOUS PROPAGATION

Anomalous propagation is a misnomer, referring to any propagation other than that in a standard atmosphere. Anomalous propagation is generally considered to be divided into three forms: superrefractive, subrefractive, and ducting. Although the name implies rare or infrequent, the refractive conditions listed above are far from infrequent. C. G. Purves [Ref. 4: pp. 13-14] states that in parts of the world, and during certain seasons ducting or trapping occurs more than 75% of the time. Although the frequency of occurrence of various propagating conditions will be addressed in more detail, let it suffice to say that anomalous propagation is far from uncommon.

Another point to address is the fact that superrefraction, subrefraction, and ducting occur on a macroscopic scale. They are characteristic of relatively large seasonal and/or atmospheric conditions, some of which will be discussed at the end of this section. This characteristic roughly separates anomalous propagation from the conditions leading to mirages.

1. Superrefraction, Subrefraction, and Ducting Defined

Equation 2.4 shows that if water vapor pressure decreases rapidly with height or if the temperature increases with height, N will decrease with height at a more rapid rate than under standard atmospheric conditions. Thus, the value of dn/dz becomes more negative. For small gradients a superrefractive condition exists, while when EM rays are curved parallel to the earth's surface trapping occurs and the phenomenon of ducting exists. Should the index of refraction increase, instead of decrease with altitude, a subrefractive condition exists. The meteorological conditions leading to these forms of anomalous propagation will be discussed in detail in Section II.C.4. of the thesis.

Superrefraction implies a gradient greater than that for a standard atmosphere, but not strong enough to form a duct. EM waves propagating in this region will be bent downward more than in normal (standard atmosphere) conditions but not sufficiently for trapping to occur. Superrefractive conditions will result in propagation distances beyond those expected in a standard atmosphere.

Trapping, or ducting, occurs when dn/dz is less than or equal to -157 . Signals traveling in a duct propagate in a manner similar to propagation in a "leaky" waveguide. Ducting is categorized into three subgroups: evaporative ducts, surface ducts, and elevated ducts. Evaporative ducts, most commonly created by evaporation off of the surface of

water, are present only to a maximum height of about thirty meters and can be much thinner. These ducts are present over the surface of the oceans of the world to some degree most of the time.

J. Beach [Ref. 3: pp. 78-80] states that surface ducts, which are usually stronger and generally extend higher in altitude than evaporative ducts, vary in thickness but are almost always less than one kilometer and usually are 300 meters or less in thickness. Surface ducts are characterized by the lower boundary being the earth's surface. Surface ducts, along with elevated ducts, occur much more frequently over land than do evaporation ducts.

Beach [Ref. 3: p. 80] in his discussion of elevated ducts states that elevated ducts begin at altitudes of from close to zero meters, absolute altitude, to 6 kilometers but generally no higher than 3 kilometers. The thickness of these ducts is similar to the surface duct.

When the index of refraction increases with altitude, a subrefractive layer is created. This type of layer is normally created by heating of the surface and thus exists in only a thin layer close to the earth's surface as shown in Figure 9. EM waves entering such a layer from above will be bent upward, as will rays traveling within the subrefractive region. Subrefraction is responsible for some of the more common forms of optical mirage (see Section D).

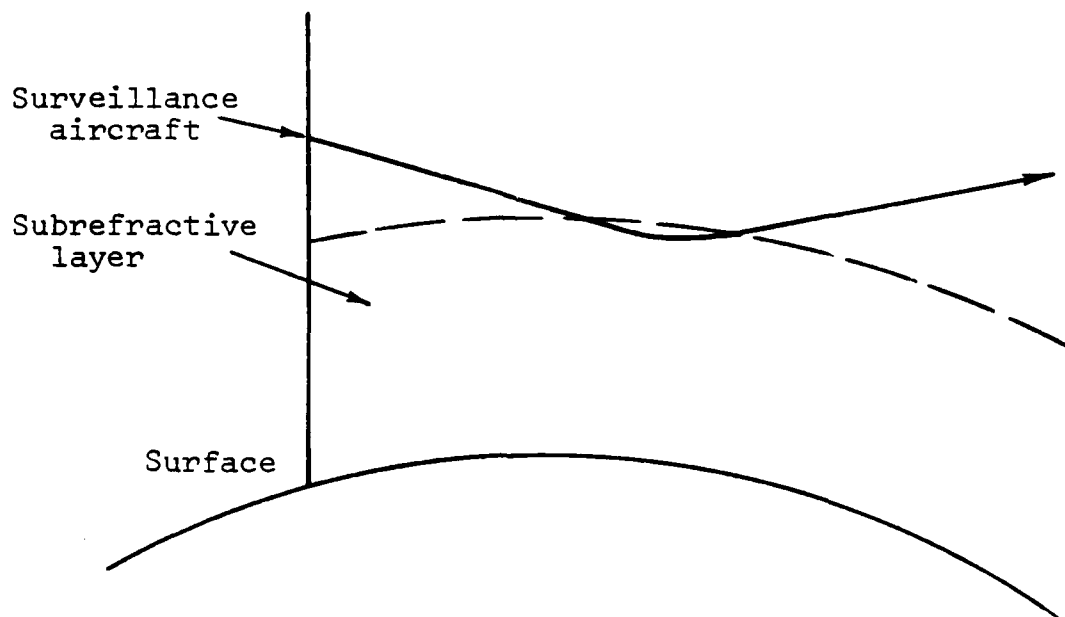


Figure 9. Description of Subrefraction. A subrefractive layer bends EM energy upward, away from the surface of the earth.

2. Means of Describing Refraction

As shown previously, the refractivity, N , is a parameter that normally decreases with height and is therefore not very useful in depicting refraction graphically. Two indices that are more commonly used for this purpose are B and M units.

B is defined by K. Davidson [Ref. 5: pp. 4-2 to 4-4] by adding 40 N units per kilometer to all N values

$$B = N_z + 40Z, \quad (2.7)$$

where N_z is the value of refractivity at height Z in kilometers. Thus, the B gradient is zero for standard atmospheric conditions.

Davidson goes on to describe the "modified refractivity" M , as being defined by adding 157 N units per kilometer to N , thus

$$M = N_z + 157Z \quad (2.8)$$

The M gradient is zero when EM ray curvature equals the earth's curvature. Since, in a standard atmosphere, M increases with height, layers in which trapping can occur will be readily apparent by the negative M gradient. Figure 10 shows the relationship between N , B , and M units.

Figure 11 shows the Navy Integrated Refractive Effects Prediction System (IREPS) classification of refractive conditions. See also Appendix A for more information on IREPS.

3. Duct Characteristics

Before describing the causes of ducting it is necessary to explain some of the characteristics of ducts. To begin, an important distinction must be made between the trapping layer and the duct. As shown in Figure 12, the trapping layer is the region where dM/dZ is less than zero. Consequently the EM rays are bent downward with a curvature greater than that of the surface of the earth, causing them to be trapped between the layer and the bottom of the duct. A duct is the region below the top of the trapping layer where the EM rays are confined or trapped and includes the trapping layer itself. The EM rays are trapped because they are partially confined between the top of the trapping layer (duct) and the bottom of the duct. The trapping layer is always at the top of the duct. The duct bottom can be located on the earth's surface (surface duct), or can be elevated above the ground (elevated duct).

The top of the duct is where the slope of dM/dZ changes from negative to positive. At this height M is no longer decreasing with height but begins to increase in value, as shown in Figure 13, for surface and elevated ducts. The bottom of the duct is located by dropping a line

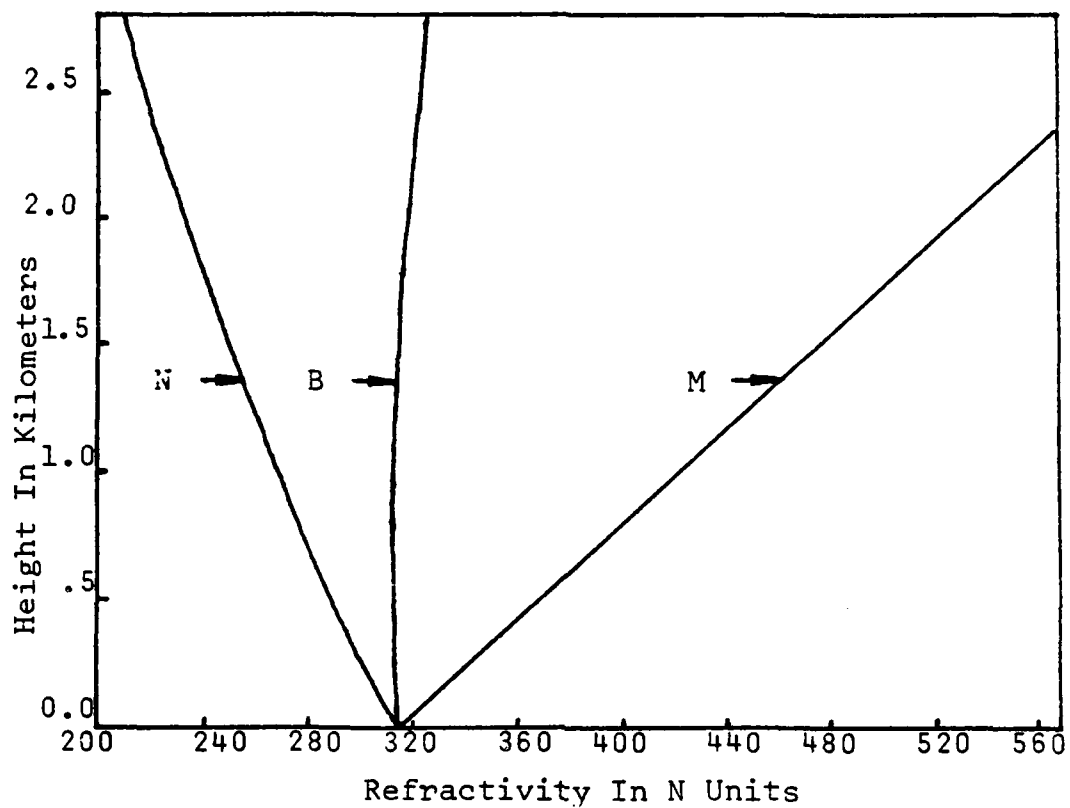


Figure 10. Profiles for N, B, and M units for a standard atmosphere.

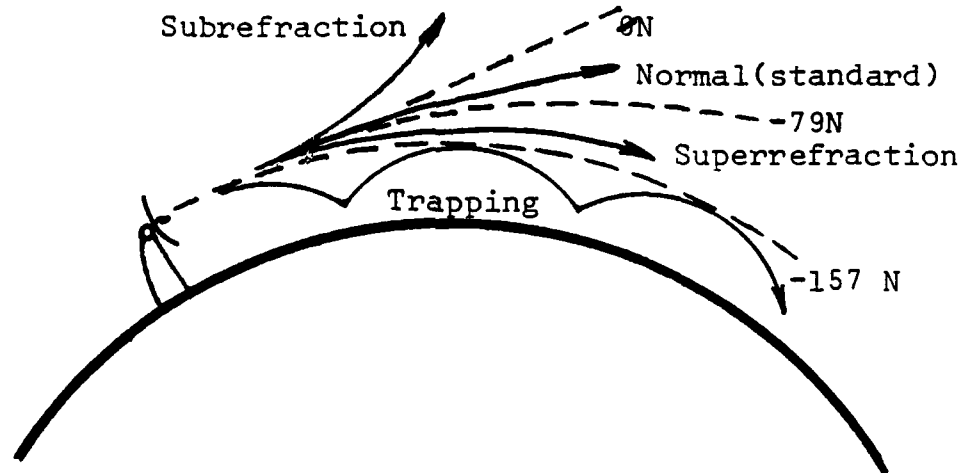


Figure 11. IREPS Classification.

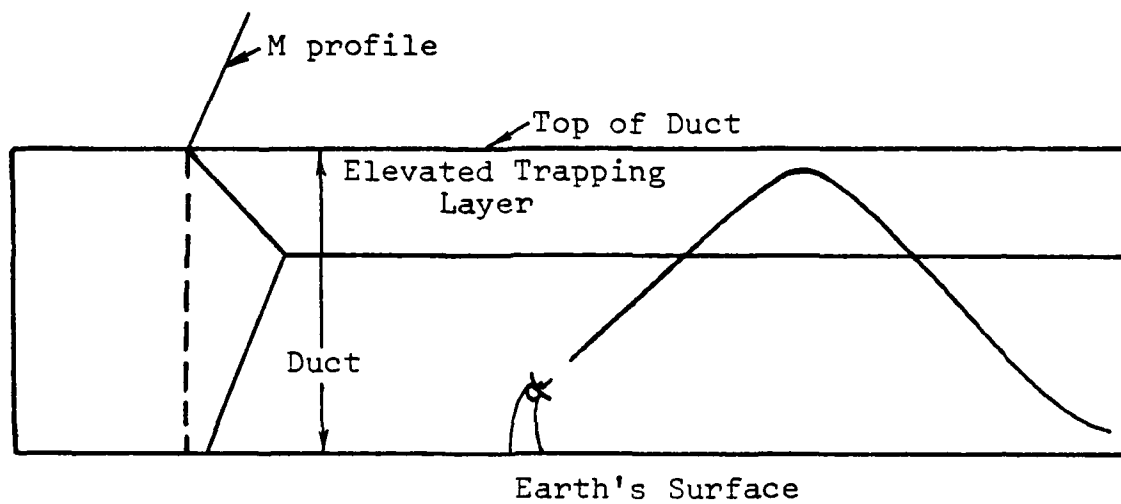


Figure 12. Duct Characteristics.

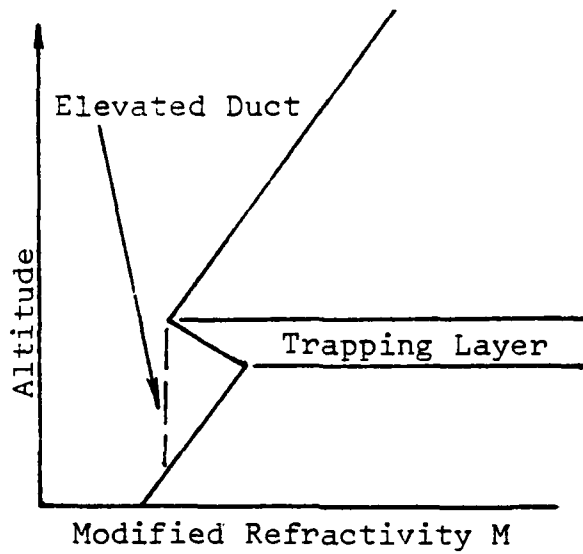


Figure 13a. Elevated Duct.

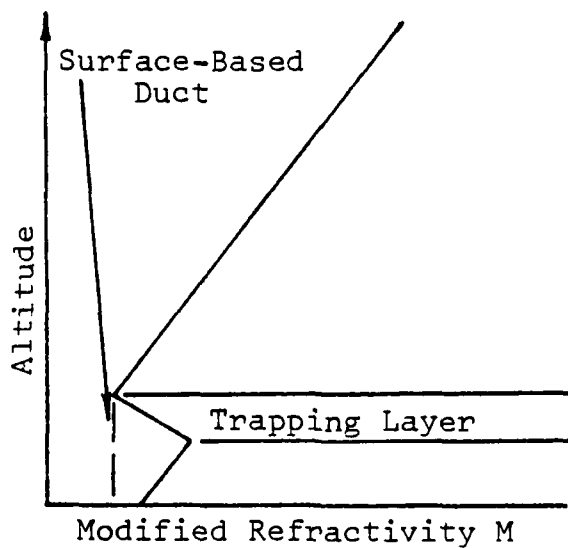


Figure 13b. Surface Based Duct With Elevated Trapping Layer.

vertically from the location of the top of the duct, in Figure 13, to the earth's surface (for a surface duct) or to the intersection with the M curve (for an elevated duct). The optimum coupling height into the duct is that point where dM/dZ goes negative. This is the point where a radar/radio transmitter will achieve the greatest extension of range due to the trapping effect of the duct. The strength of the duct is determined by the most negative value that dM/dZ attains and by the thickness of the negative layer. The more negative the value the stronger the duct. Note in Figure 12 that a surface duct can be caused by a surface trapping layer or an elevated trapping layer. The bottom of the duct is the location where the downward bent EM rays are turned back upward again. It is apparent from this discussion that ducts can vary considerably in thickness and, depending on the slope of the trapping layer, they can also vary considerably in intensity (strength of the duct).

As will be described later, not all EM frequencies are trapped within the duct and only those EM rays entering the duct or traveling through the duct at a very shallow angle will be trapped. Note that for the EM ray to be most effectively trapped the transmitter must be within the duct although EM signals can be coupled into the duct and trapped within it from an antenna located near but outside the duct. In addition, note that the trapped EM ray is either refracted back upward after reaching the bottom of an

elevated duct or reflected upward off the surface, as in the case of a surface or evaporation duct. In both of these cases at least part of the energy of the EM ray is lost due to surface absorption and diffuse scattering (surface and evaporation ducts) or lost through leakage through the bottom of the duct (elevated duct). Further, part of the EM ray is lost by leakage through the top of all ducts.

Diffuse scattering and absorption are greater over land than over water. M. L. Meeks [Ref. 6: pp. 13-26] states that these two surface characteristics result in the surface reflection coefficient, the value of which varies as a function of frequency, angle of incidence of the reflected ray to the surface, and the terrain surface itself. The lower the angle of incidence, the smoother the terrain, the more moist the surface, and the lower the frequency, the greater the amount of reflection of the EM ray. The reflection coefficient for water varies from approximately .85 to .99 and is largely a function of the sea state. The reflection coefficient over land is much more variable, ranging from as low as .15 to higher than .9. The reflective properties of various land surfaces and types of vegetation are still not completely understood.

The amount of EM energy lost as a signal travels through a duct is a complicated function of frequency, duct characteristics, and in the case of surface and evaporation ducts, the terrain's reflective characteristics. Due to

these losses and those resulting from atmospheric scattering and absorption it can be seen that there is a limit to just how far an EM signal can be propagated in the atmosphere. It is apparent from this discussion that ducting of signals is less effective in increasing EM signal range over land than over water.

As mentioned earlier, not all frequencies are trapped. It is the thickness of the duct itself that is the determining characteristic as to which frequencies are trapped. Duct thickness is therefore used to calculate the lower limit of those frequencies that are strongly trapped, as shown in the following formula from Davidson [Ref. 5: pp. 4-15]:

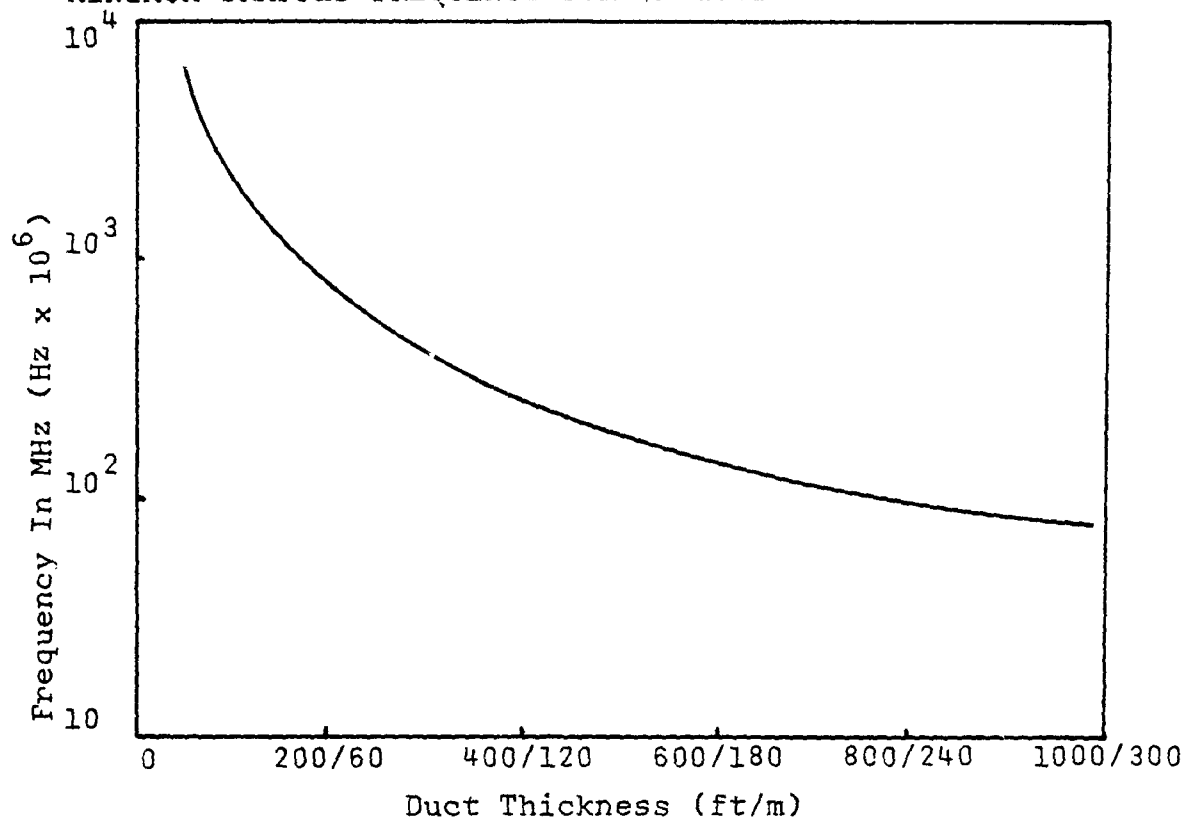
$$f_m = (3.6033 \times 10^{11})d^{-(3/2)} \text{ Hz} \quad (2.9)$$

Frequencies below f_m are still affected by the duct to a somewhat lesser extent. Table 2 shows values of f_m for various duct thicknesses.

It is important at this point to reiterate that not only does the thickness of the duct limit the frequencies trapped within a duct, but so too does the angle of incidence of the EM rays entering the trapping layer. As mentioned earlier, only EM rays incident at very shallow angles relative to the horizon will be refracted enough to be trapped. In actuality, angles above 1 degree from the earth's horizon are not trapped and, according to Skolnik

TABLE 2

MINIMUM TRAPPED FREQUENCY FOR VARIOUS DUCT THICKNESSES



Minimum Trapped Frequency (MHz)	Maximum Trapped Wavelength	Radar/Radio Band	Duct Thickness	
			Feet	Meters
150	2.0 m	A (VHF)	587	179
220	1.56 m	A (TAC UHF)	453	138
425	70.6 cm	B (TAC UHF)	294	89.6
1000	30 cm	D	166	50.6
3000	10 cm	F	80	24.3
5800	5.2 cm	G	51	15.6
9600	3.1 cm	I	37	11.2
10250	2.9 cm	J	35	10.7
30000	1	K	17	5.24

[Ref. 7: p. 450], refraction is troublesome only at angles of elevation of 5 degrees or less from the horizon in most microwave applications. Figure 5 provides a simplified example of the effect of angle of incidence on refraction, trapping, and creation of a radar/radio hole.

4. Causes of Superrefraction, Ducting, & Subrefraction

Superrefractive, subrefractive and ducting conditions are created by variations in water vapor and/or temperature in the atmosphere, brought on by a multitude of climatic and topographic conditions.

Evaporation ducts are created above the surface of large bodies of water by the rapid decrease in humidity above the water's surface. The humidity of the air immediately above the water is at the saturation point, but decreases quickly with height. Within the first thirty meters, an ambient level of humidity is reached, dependent on the climatic conditions prevailing. This rapid decrease in humidity causes M to decrease with altitude to a point where M will reach a minimum (the top of the duct) and then increase with altitude. Meeks [Ref. 6: p. 9] states that over land a similar situation is created after a rainfall, when the water evaporates from the ground. Snow, and particularly melting snow, can also lead to the creation of an evaporation duct over land. Overland evaporation ducts, however, are generally of short duration. Evaporation ducts will also occur over the continental land masses above

larger bodies of water. For the Navy, the occurrence and effects of evaporative ducts are very important and largely responsible for the development of the IREPS program which models the effects of superrefraction and ducting on EM communications and on surveillance systems.

Superrefractive conditions and surface and elevated ducts are created by the same climatic conditions. Which type of propagation condition occurs depends primarily on where the transition between two differing air masses forms and on the strength of the resulting refractivity gradient. Temperature inversions are the primary cause of superrefraction and ducting. As would be expected, superrefractive conditions are far more common than ducting.

A temperature inversion is a region of the atmosphere where there is an increase in temperature with height. As shown in Equation 2.4, a temperature inversion must be very strong to cause superrefraction by itself. If, however, a water vapor gradient is combined with the temperature inversion, superrefraction and ducting will more easily result. Thus, it is no surprise to find that superrefraction and ducting are more common over water (particularly oceans) than over land.

Ducting is characterized by the upper air being much warmer and drier than the underlying air. There are several meteorological conditions that can lead to this situation. Over land, the most common ducting is caused by radiation of

heat from the earth's surface on clear calm nights. This surface cooling creates a temperature inversion and a sharp decrease in moisture with height which will often lead to a surface fog in summer. Refractivity gradients are made even stronger if the ground is moist, a situation most common in summer and in winter over snow. Meeks [Ref. 6: p. 9] elaborates on the fact that in desert regions the temperature inversion created at night can be significant enough, in and of itself, to create superrefractive conditions and even ducting. Ducting is therefore most common over land at night, and will usually weaken or disappear, along with the weakening and disappearance of the temperature inversion, during the day.

Subsidence, the sinking of air from above, also is a common cause of ducting. As the air sinks it is warmed by compression capping the cooler air below and a strong inversion is formed. If the lower level air has a high moisture content, a strong humidity gradient will also be formed. Since subsidence is most often associated with high pressure areas, this type of ducting is generally a fair weather phenomena, characterized by light winds, and clear or low stratus skies. The presence of fair weather low stratus clouds that show a marked discontinuity at the top of the cloud mass will often indicate the presence of an inversion and a good possibility that superrefraction or ducting is present. Figure 14 shows temperature inversions created by radiation of heat and by subsidence.

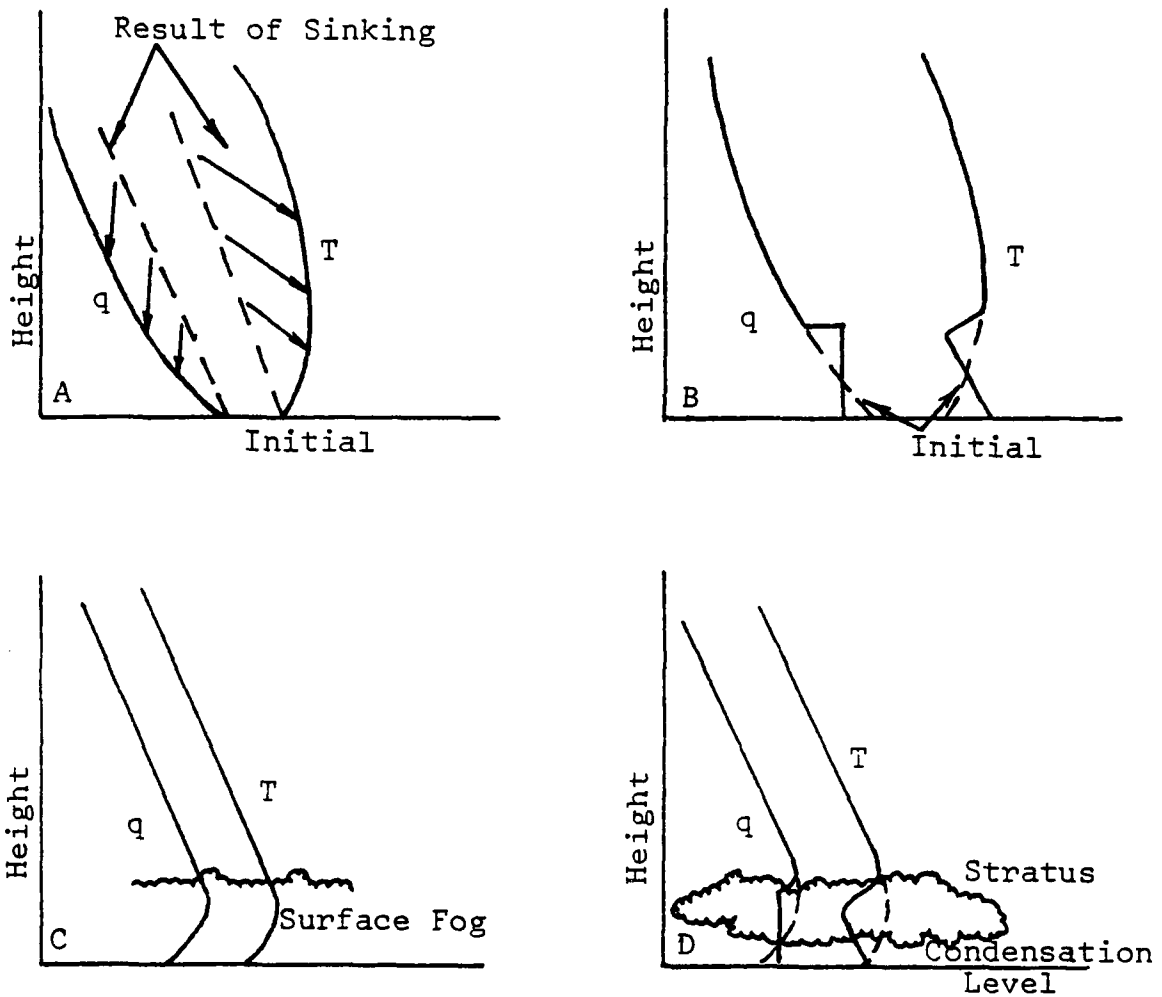


Figure 14. Types of Inversion: (A) Subsidence reaching the surface; (B) Subsidence above a mixed surface layer; (C) Ground Inversion caused by cooling of surface air; (D) Inversion caused by cooling and mixing of surface layer.

In temperate regions in the low and middle latitudes, ducting occurs most often in summer and does not usually occur during bad weather. Storms are characterized by the lower atmosphere being mixed by precipitation and winds, resulting in a more homogenous atmosphere. In arid regions humidity will have a lesser impact on the formation of anomalous propagation conditions but in temperate regions the air temperature may be high enough, particularly in summer, for the water vapor component of the atmosphere to be important. Seasonal variations in refractive conditions are strongest over large land masses and generally weakest over large bodies of water (oceans).

As described earlier, ducts over land generally are weakest or break up entirely during the warmest part of the day. This diurnal characteristic of the land² does not, however, occur significantly over large bodies of water. W. Thompson [Ref. 8: p. 3] additionally notes that in temperate regions, diurnal variations are more pronounced during summer months and less so in the winter. C. Samson [Ref. 9: p. 6] states that due to the rapidly changing thermal structure of the air near the earth's surface at

² The changes in the thermal structure are due to the effects on the atmosphere of the heating and cooling of the earth's surface.

sunset and sunrise, the most extreme changes in refractivity will occur at these times.

Skolnik [Ref. 7: p. 452] states that the main exception to the fair weather rule for ducting is the creation of ground ducts by thunderstorm downdrafts. These will usually last on the order of 1 hour or less and are small in spatial extent.

Coastal regions develop their own unique ducting conditions. As described in Davidson's notes [Ref. 5: pp. 7-30 to 7-31] the presence of ducting in coastal regions and straits is quite common and is due to the juxtaposition of marine and continental air masses at the surface. Offshore flow of warm dry air would lead to warm, dry, continental air overlying the cooler and more moist marine air. Offshore flow can be caused by: 1) local land to sea breezes induced by the differential heating of land and water areas and sea-breeze recirculation, and by 2) larger scale circulations in which an offshore flow occurs with a semi-stationary high pressure area located over land. Figure 15 shows both of these conditions.

In the latter situation, extremely strong ducts can be formed, some of which will extend well inland from the coast. The Santa Ana winds and monsoon circulations are characteristic of this type of offshore flow.

Subrefraction is the rarest of the anomalous propagation categories. The only regions where n increases

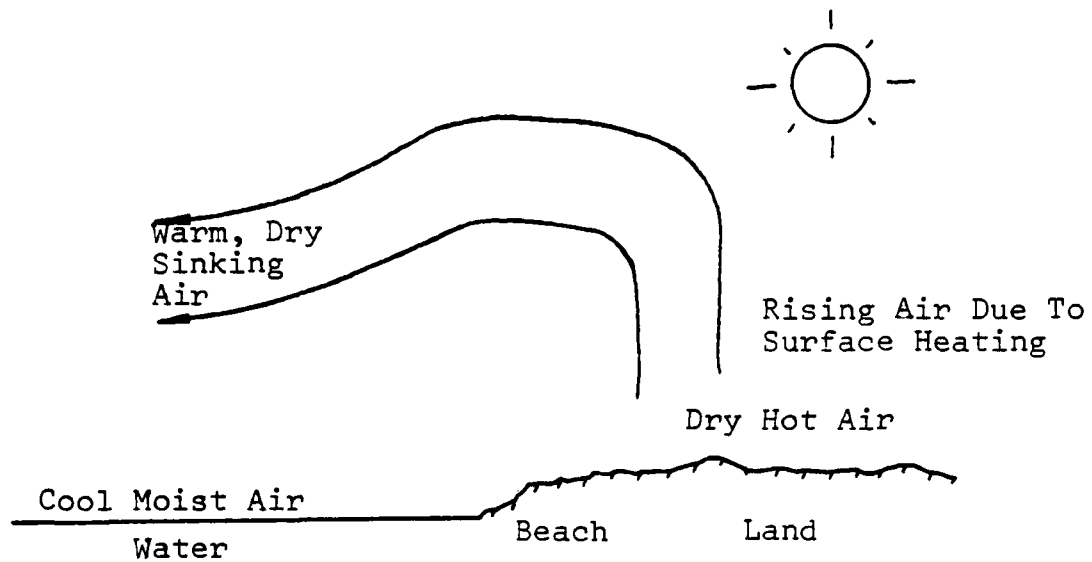


Figure 15a. Illustration of elevated layer occurrence due to local differential land-sea heating.

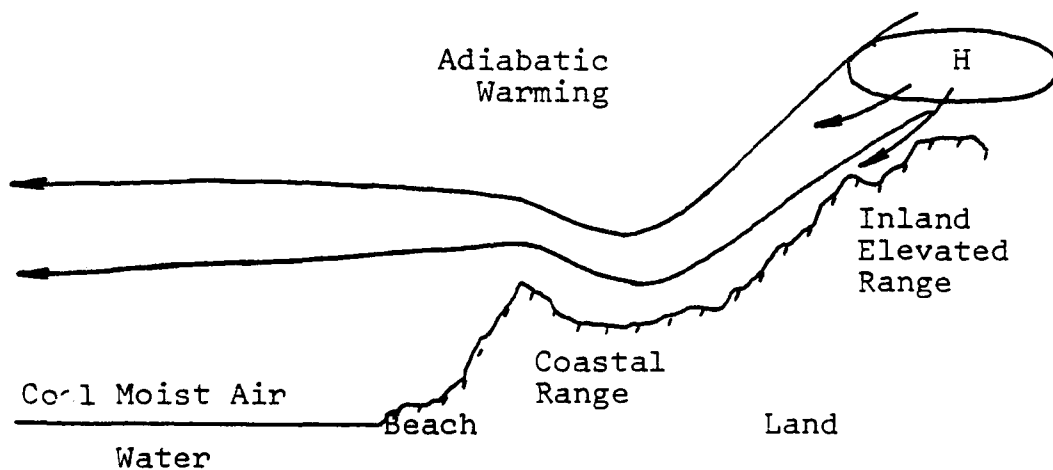


Figure 15b. Illustration of elevated layer due to synoptic scale driven offshore flow. Note adiabatic heating with downslope trajectory.

with height with any regularity are the deserts of the world and particularly those that are near large bodies of water. The sun heats the desert surface causing it to be very hot and dry, the temperature to decrease, and the water vapor to increase, with height. This subrefractive condition can be made even stronger by an onshore breeze which is characteristic of a high pressure area located at sea. The onshore breeze carries cool moist air that rises over the land.

Subrefractive conditions tend to follow a diurnal cycle and are strongest in the afternoon and usually disappear at night. In semi-arid and desert regions it is not uncommon to see strong subrefractive conditions forming in the afternoon, due to solar heating of the surface, and superrefractive conditions develop at night, due to radiation of heat from the surface.

5. Consequences of Anomalous Propagation

As described earlier, the effects of anomalous propagation vary with the wavelength and the gradient of the refractive index. Increases in the refractive gradient (due to superrefraction or ducting) result in an extension of the radar horizon, causing an increase in radar coverage beyond that expected for a standard atmosphere, as shown in Figure 4. Refraction can also lead to errors in the measurement of range and elevation angle by microwave systems. An elevation angle error is created by the bending

of the EM waves away from a straight path as they propagate to the target and back as shown in Figure 16. Range error is created by the increase in the effective path length due to refraction of the EM rays from the radar transmitter to the target and back to the radar receiver. Figure 17 shows range error as a function of the apparent elevation angle. An example of the type of range error that can be created by atmospheric refraction is that experienced by the FPS-16 air search and tracking radar at Mount Lemmon, Arizona. For this radar, range errors are generally between 30 and 40 yards over a 150,000 to 200,000 yard distance. In many instances this type of error is of little consequence, but, for accurate tracking of a target's location some compensation for the range error must be made.

Communications signals are affected by refraction in a manner similar to radar signals, leading to extended ranges in "line of sight" communications. However, the terrain over which the signals propagate will often have a greater effect on communications range than will refraction for ground based systems.

The effect of refraction on Direction Finding (DF) systems can, in certain circumstances, be significant. Harrington and Callaghan [Ref. 10: p. 3] state that changes in the refractive index, particularly if occurring horizontally, will lead to the same type of error in direction finding as the elevation angle error in a radar,

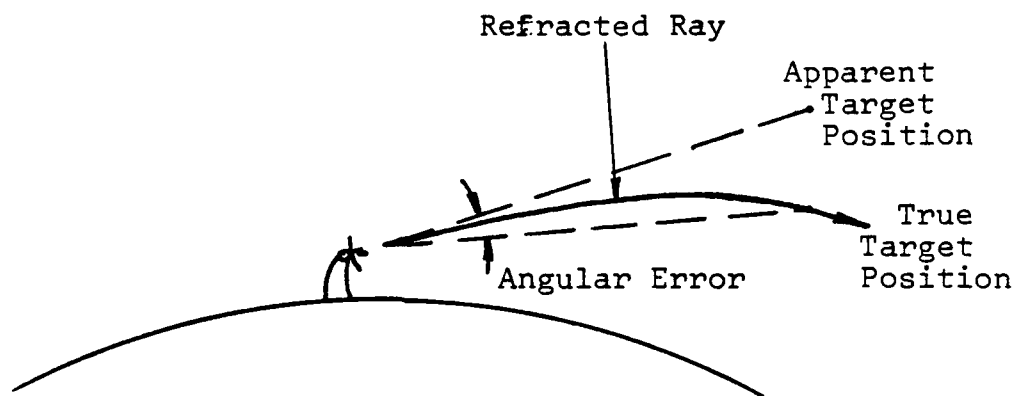


Figure 16. Angular Error Caused by Refraction.

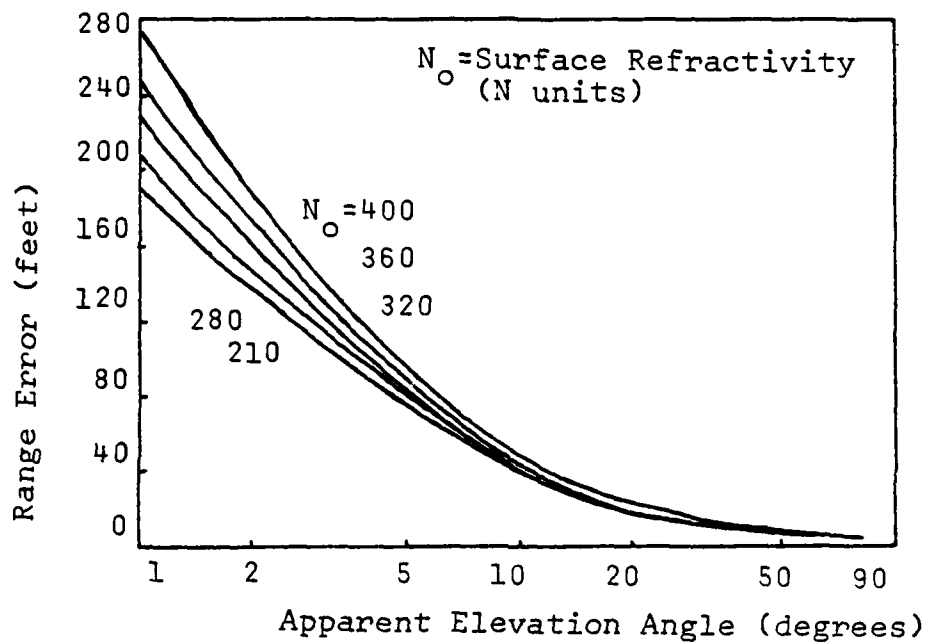


Figure 17. Range error as a function of apparent elevation angle, where apparent elevation angle is defined as the angle from the horizontal that the radar is aimed in order to locate the target (as opposed to the angle from the horizontal that the target is actually located). CRPL reference refractivity atmosphere (1958) is assumed. Note that the closer the apparent elevation angle is to the horizontal, the greater the range error.

as shown in Figure 18. An example of a situation that might result in a horizontal gradient is a signal transmitted across a body of water where the air is more humid than over land. Similarly, a signal traversing a wide valley, where the air is much drier than the surroundings, can result in an error in location of a transmitter.

Multiple modes on an EM signal propagating in a duct can result in variations in the strength of the EM signal at various points along the path due to interference. This spatial fading can be caused by multipath, or, as in the above example, by multimode interference, both of which can result in a condition where the vector sum of several components of a signal are not in phase. The variation in phase is a result of the difference in path length induced by refraction and/or path route. According to Skolnik [Ref. 7: p. 454] fading on the order of 20 dB can occur for radar systems experiencing multimode propagation. Fading can be greatly enhanced by the presence of ground and/or sky waves combining with the refracted signals (multipath). Beach [Ref. 3: p. 75] states that temporal fading will frequently occur near the radio horizon due to changes in the index of refraction leading to large changes in signal strength in the horizontal EM signal path.

In the presence of ducting, the effects previously described become more acute. The angle error in a ground based radar will become greater with a larger refractive

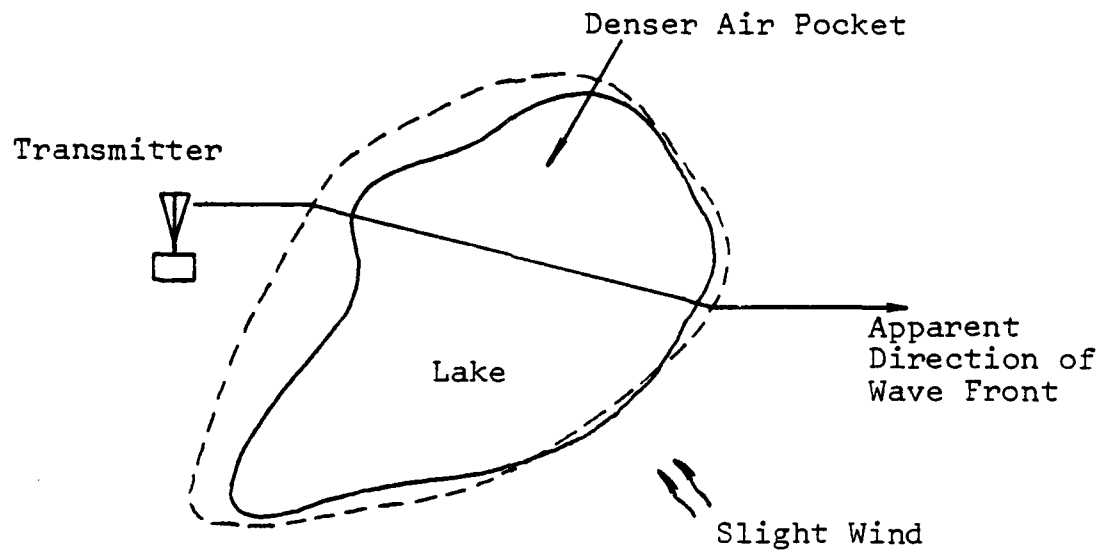


Figure 18. Signal Refraction because of change of humidity over a lake and its effect on D.F. accuracy.

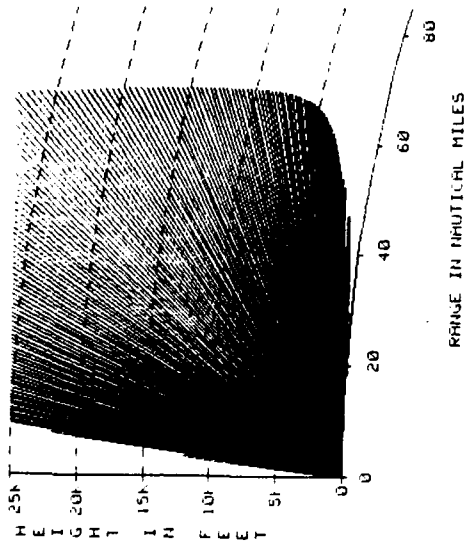
gradient and can often be more serious than the range errors induced. For those VHF, UHF, and microwave signals propagating nearly horizontal to the earth's surface, trapping can also occur, particularly if the transmitting antenna is located within the duct. When trapping occurs, the range of the EM signal within the duct is greatly extended beyond that expected in a standard atmosphere as shown in Figure 19. Thus, for surface based radar signals the coverage can be extended well beyond the expected radar horizon and, for communications signals, extraordinary ranges have been caused by the presence of surface based ducts. Examples of VHF signals propagating 2,000 miles without the use of satellites are well known. Likewise, electronic support measures (ESM) detection of these signals is greatly enhanced by the extension of the range of the propagating signal. For ground based DF systems, trapped signals can be a mixed blessing. Although the range at which a signal can be detected is extended, the accuracy of the direction finding can be degraded by the very nature of the ducted transmission.

The existence of radar/radio holes is indicated by regions in the atmosphere where EM signal strength is weaker in the presence of a duct than it would be in free space. The variables that dictate the existence and characteristics of a radar or radio hole are: the radar or radio transmitter height relative to the duct, the radar target or ESM receiver height relative to the duct, the operating

***** COVERAGE DISPLAY *****

SFSX

LOCATION: 09K
DATE TIME: 2-16-12



SURFACE SEARCH

SHADED AREA INDICATES AREA OF DETECTION OR COMMUNICATION

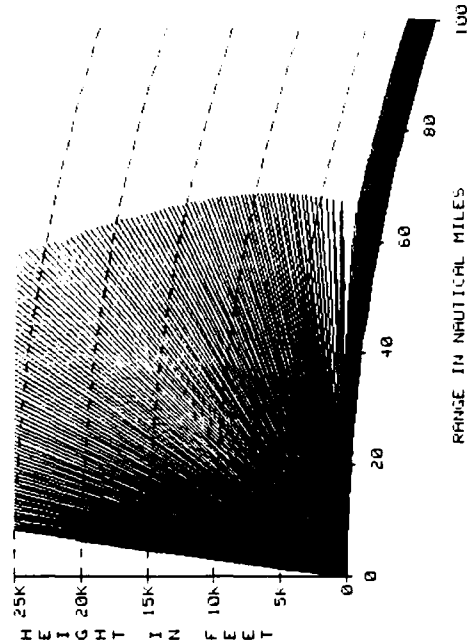
FREE SPACE RANGE: 50.0 NAUTICAL MILES
FREQUENCY: 5500 MHZ
TRANSMITTER OR RADAR ANTENNA HEIGHT: 170.0 FEET

A

***** COVERAGE DISPLAY *****

SFSX

LOCATION: 23 09H 061 11E CORRAL SEA
DATE/TIME: 2248Z 8 FEB 89 (C)



SURFACE SEARCH

SHADED AREA INDICATES AREA OF DETECTION OR COMMUNICATION

FREE SPACE RANGE: 50.0 NAUTICAL MILES
FREQUENCY: 5500 MHZ
TRANSMITTER OR RADAR ANTENNA HEIGHT: 170.0 FEET

B

Figure 19. Coverage diagram for a 5500 MHz surface based air search radar. A represents the radar coverage pattern in the absence of a duct or superrefraction while B represents the radar coverage pattern in the presence of a surface duct with a thickness of approx. 420 feet. In B note the extension of the radar's coverage along the earth's surface and the partial loss of coverage just above the duct. Note that these coverage displays were produced by the Navy IREPS.

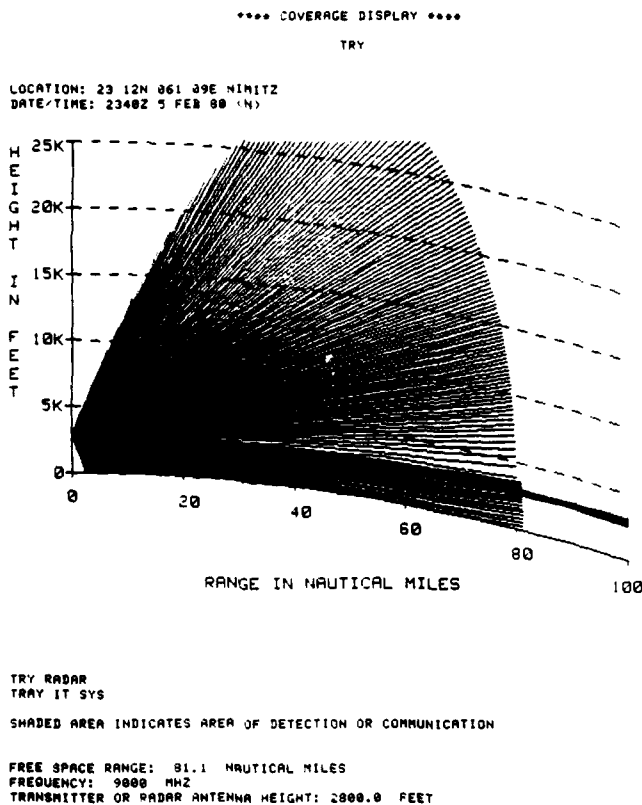
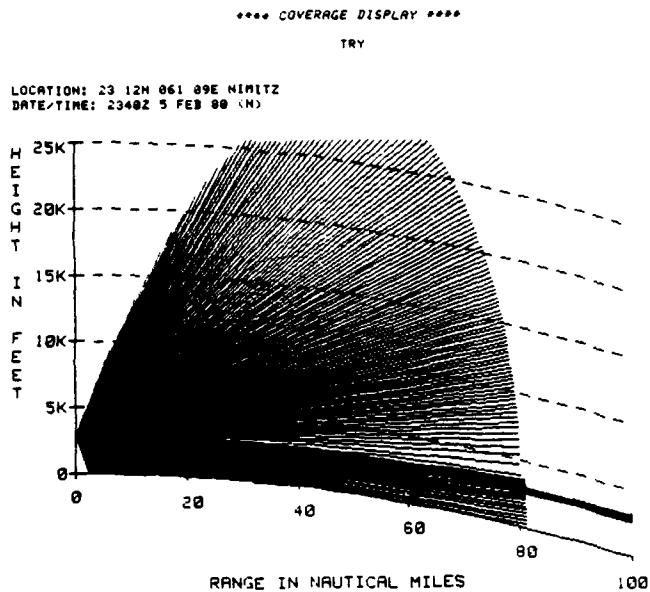


Figure 20. Coverage Diagram for a 9000 MHz airborne early warning radar transmitting within an elevated duct located between 2,590 feet and 3,220 feet above the surface. Note the extended coverage in the duct and the partial loss of coverage just above the duct. This coverage diagram like those in Figure 20 was produced by the Navy IREPS.



TRY RADAR
TRAY IT SYS
SHADED AREA INDICATES AREA OF DETECTION OR COMMUNICATION

FREE SPACE RANGE: 31.1 NAUTICAL MILES
FREQUENCY: 9000 MHZ
TRANSMITTER OR RADAR ANTENNA HEIGHT: 2800.0 FEET

Figure 20. Coverage Diagram for a 9000 MHz airborne early warning radar transmitting within an elevated duct located between 2,590 feet and 3,220 feet above the surface. Note the extended coverage in the duct and the partial loss of coverage just above the duct. This coverage diagram like those in Figure 20 was produced by the Navy IREPS.

farther away from the aircraft until a point is reached where the hole is no longer apparent.

Electronic countermeasures (ECM), ESM, and DF systems performance, as well as air to air communications and air to ground communications are also affected by elevated ducts, with the effect being most likely at higher frequencies. It has also been noted that the propagation of EM signals from transmitters located well below the elevated duct is greater in the duct than expected. One explanation mentioned by Skolnik [Ref. 7: p. 453) postulates that the EM signals are being scattered into and out of the elevated duct by variations in the index of refraction profile due to the "wavy" top of the duct, causing it to be similar to a nonuniform waveguide. Figure 21 shows examples of the effect that the position of the aircraft (whether radar or jamming) relative to the elevated duct has on the trapping of EM waves and on the effect of the radar/radio hole on EM waves.

For radar systems, the presence of surface or evaporation ducts can lead to an increased surface clutter return, both in magnitude and in coverage extent, masking targets over a much greater range. An example of this effect is shown in Figure 22. As described by Beach [Ref. 3: p. 85], if the clutter return is stronger than the target return at the same range, detection of the target may be seriously degraded or impossible. The strength of the

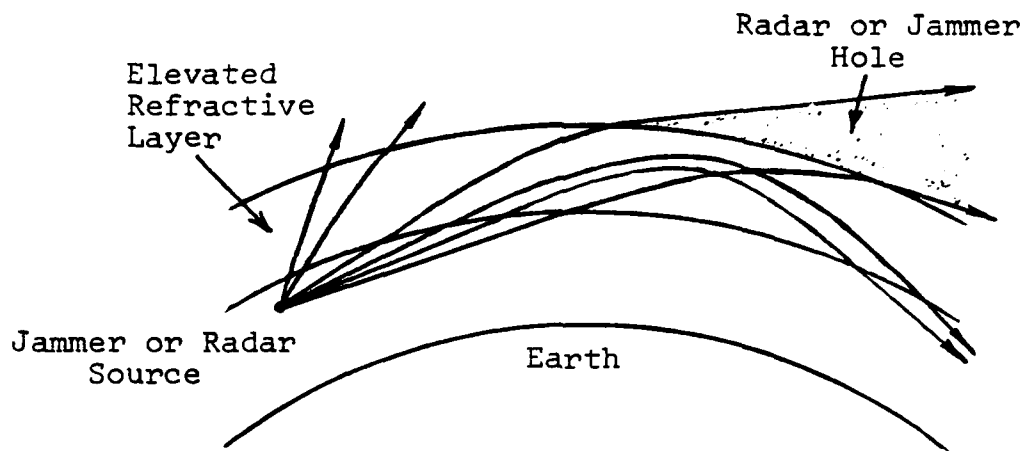


Figure 21a. Scenario of Jammer or Radar Source Below Elevated Refractive Layer.

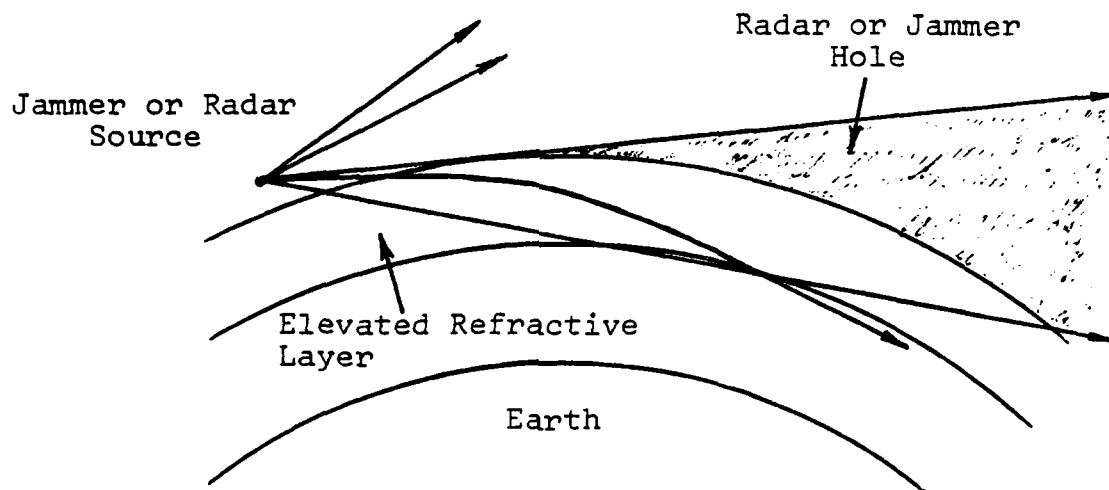


Figure 21b. Scenario of Jammer or Radar Source Above Elevated Refractive Layer.

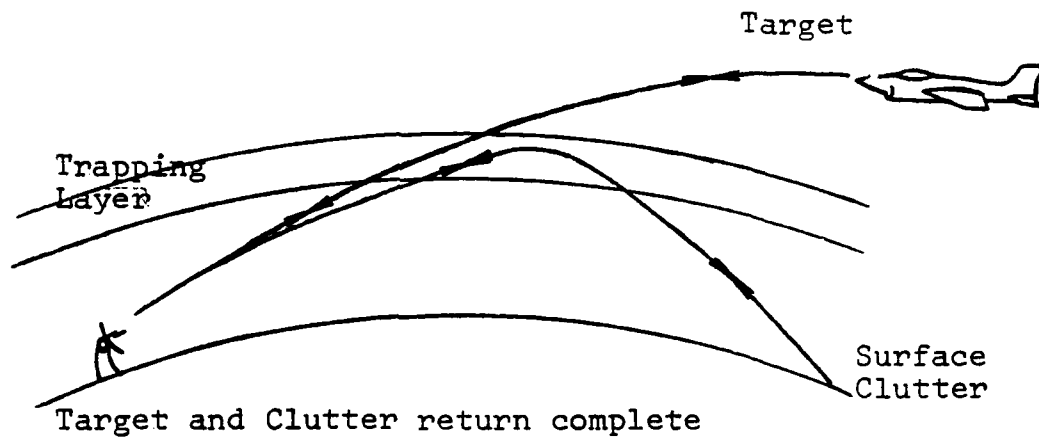


Figure 22. Air search radar geometry showing possible clutter return from rough surface at the same range as the air target for a surface duct.

clutter return is partially dependent on the strength of the duct. MTI radars can be seriously affected by the enhanced strength of the clutter return which may overcome the radar's ability to separate out a moving target from stationary clutter.

The fading phenomena described earlier can also become more severe in the presence of ducting and can lead to the "skip" effect in the presence of a surface duct. This phenomenon is characterized by periodic spatial gaps in radar coverage or communications signals. These spatial intervals give the appearance of rings on the radar display. Figure 23 shows the ray paths that characterize skip rings. Note that the appearance of skip rings is dependent on the surface reflectivity as well as the strength of the surface duct and the angle at which the EM ray is launched. Since water generally has a higher surface reflectivity than land this skip effect is more significant over the oceans of the world.

Subrefractive conditions can cause the creation of blind spots within the subrefractive zone for EM emitting aircraft (airborne early-warning and EW aircraft) located above the zone, as shown in Figure 9. Aircraft traveling close to the earth's surface, below the top of the subrefractive zone, can take advantage of this condition. In the case of airborne early-warning systems, penetrating aircraft will be able to move in much closer to the radar aircraft before being detected. As an example, Davidson

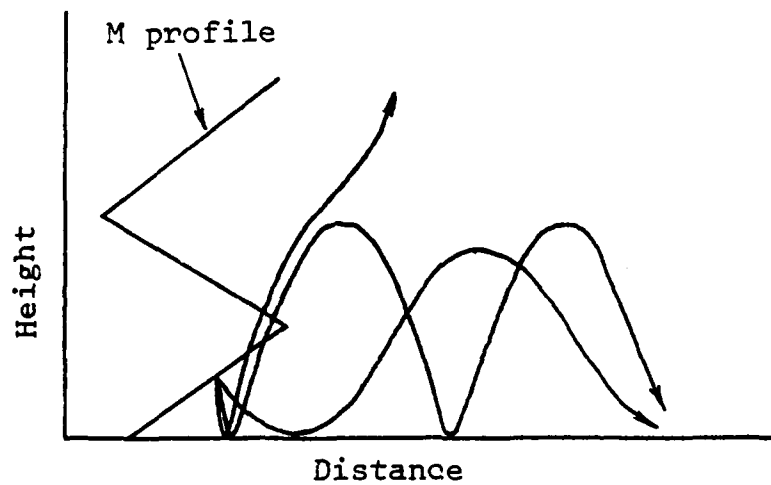


Figure 23. Skip Effects. EM rays from the transmitter will follow different paths depending on the angle they are transmitted at and the surface duct characteristics.

[Ref. 5: pp. 3-10] discusses the effects noted by an E-2C squadron. One of the phenomena noted was that for aircraft flying at approximately 25,000 feet ray angles of as much as 5 degrees below the horizontal were required to penetrate solar heated subrefractive conditions, seriously degrading the early warning ability of these systems. In a similar manner, air to ground communications can also be affected by subrefractive conditions.

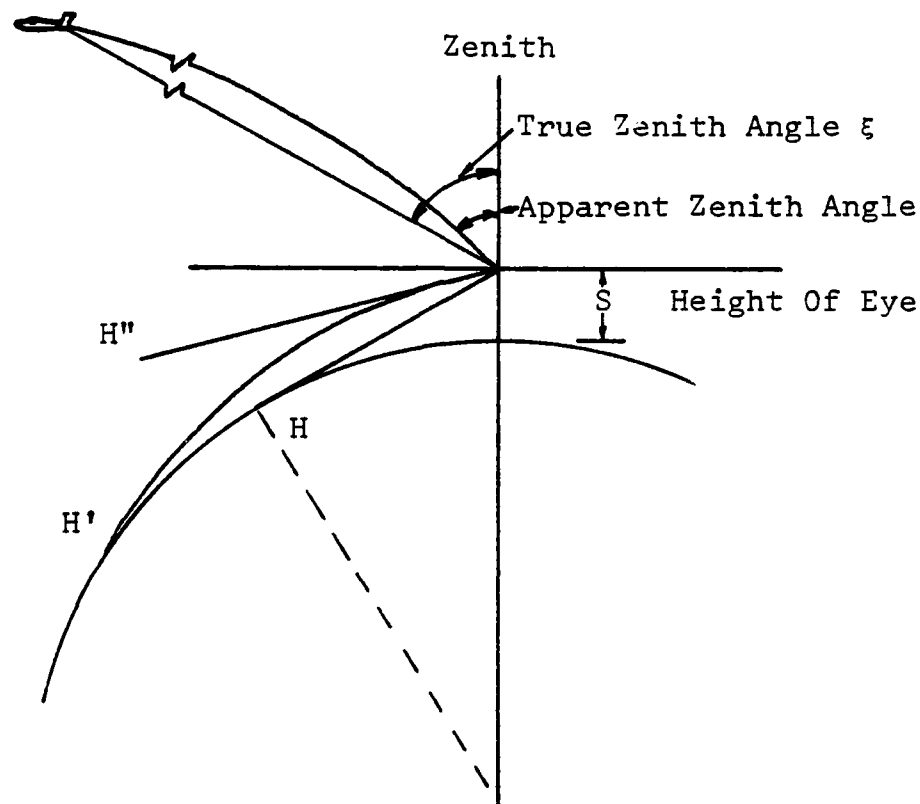
Optical wavelengths are affected by refraction in a manner similar to microwaves, but on a much reduced scale due to the relative ineffectiveness of water vapor gradients. Figure 8 shows that refraction does extend the optical horizon beyond the geometric horizon but not nearly to the extent that the radar/radio horizon is extended. Since there is usually little measurable difference in the refractive effects experienced by IR and visible wavelengths, which together form the optical region, they will generally be considered together in this thesis.

Refraction in a standard atmosphere causes the horizon seen by the observer to appear higher and more distant than the geometric horizon. McCartney [Ref. 11: p. 100] describes a formula, given by Bowditch, for calculating the distance to the optical horizon in a standard atmosphere as

$$\text{Horizon distance} = 3.839s^{1/2} \text{ km}, \quad (2.10)$$

where s is the height of the eye in meters. This relationship is shown graphically in Figure 24. Superrefractive and ducting conditions will extend the optical horizon even more, causing objects beyond and below the horizon to become visible. Extremely strong inversions near the surface of the earth will form a mirage, known as looming, leading to greatly extended optical horizons. This subject will be taken up in more detail in the section dealing with mirages. Figure 24 shows that optical waves traveling in the atmosphere are also subject to downward bending due to refraction, leading to range and angle errors in surveillance and tracking systems. The degree of bending is dependent not only on the refractive conditions prevailing but also on the zenith angle ξ . As described by McCartney [Ref. 11: p. 112], when the zenith angle is 75 degrees or less the effect of refraction in a standard atmosphere is largely ignored. For larger values of the zenith angle the effects become apparent particularly if ξ is greater than 90 degrees or if superrefraction or ducting conditions exist. When the beam path lies at such an angle, and is also tangent to the horizon, the refractive effect in bending and lengthening the path can be significant.

The effects of refraction on millimeter wave propagation in both a standard and non-standard atmospheres is an area not clearly understood at this time. The millimeter wave region of the EM spectrum has only recently been actively considered for application to communications,



- H - Geometric Horizon
- H' - Visible Horizon
- H'' - Apparent or Optical Horizon

Figure 24. Refraction Effects on Optical Transmission. The optical horizon is the visible horizon which appears to be displaced upward. Note also the angular and range error induced in optically tracking the aircraft by refraction.

surveillances and weapons system's guidance. The majority of the information currently available is largely theoretical. In a standard atmosphere, there is some reduction of signal strength and, like microwave signals, there are errors induced in range and angle estimation of radar targets. These effects appear to be rather small in standard conditions. T. Patton et.al. [Ref. 12: p. 170] states that in non-standard atmospheric conditions (anomalous propagation) there is some evidence of trapping of millimeter waves by surface ducts, but there has been little investigation of the effects of elevated ducts. Also, the importance of a water vapor gradient in the atmosphere on millimeter waves has not been adequately addressed although it does appear to be more significant in MMW propagation than in microwave propagation and less so in optical propagation. D. Snider, in private communications³, states that due to the difference in the responses to humidity of optical and millimeter wave energy, if there exists, simultaneously, a temperature inversion, created by heat radiation, and a slight increase in humidity with altitude, optical rays would bend downward, due to the temperature inversion, while MMW rays would bend upward due to the humidity gradient.

³ The discussion with D. Snider was in regards to the difference in the effects of atmospheric refraction on optical and MMW systems.

6. Methods of Predicting Refractive Effects

Calculating the refractivity of the atmosphere, detecting the presence of anomalous propagation and determining the effect of refractivity on EM wave propagation is very complex and as yet inexact. Characterizing the variation of atmospheric refractivity with altitude is usually done by making measurements of temperature, pressure, and humidity as a function of altitude using a radiosonde balloon. Based on these measurements, and utilizing Equations 2.4 and 2.5, a determination of the refractivity and its gradient at various elevations can be made. This information is generally sufficient to determine the presence of anomalous propagation phenomena.

The use of a radiosonde for measurement has a major drawback; it is generally a slow response instrument and somewhat inaccurate. Consequently the data collected by the radiosonde greatly limits the ability to accurately calculate refractive index gradients. Ongoing efforts are underway to develop and deploy smaller and more accurate means of measuring refractivity, directly or indirectly. Kaelin [Ref. 13: p. 124] in his thesis states that examples of new systems are the mini-refractionsonde and airborne dropsonde being developed by the Naval Air Development Center, Warmister, Pennsylvania. A direct and accurate, but not commonly used method of measuring atmospheric refractivity, is the airborne microwave refractometer.

A thorough and accurate table of climatological records that describe local geographic conditions will also provide a valuable means of at least probabilistically calculating the expected refractive profiles for a region. Forecasts of anticipated weather conditions can also be used to develop a general idea of expected refractive conditions. These two methods, one for prediction and the other for forecasting of refractive conditions will both be discussed further in Section E of the thesis.

To determine the effect of the existing refractive conditions, the frequency of the EM wave of interest must be known. The Navy's IREPS will take the condition of the atmosphere and the wavelength of interest and, using a desk-top computer, graphically display the refractive index calculated and the effect this condition has on various radar and radio systems working in the VHF, UHF, and microwave region of the EM spectrum. Likewise, the Navy is developing a computer based model to assess atmospheric effects (including refractivity) on electro-optical system's performance. This system, described by F. Snyder [Ref. 14], is called PREOS (Prediction of Performance Range for Electro-Optical Systems). The Navy eventually intends to unite IREPS and PREOS into a single prediction system. Figure 25 provides an example of a PREOS output and Figures 19 and 20 are examples of IREPS outputs.

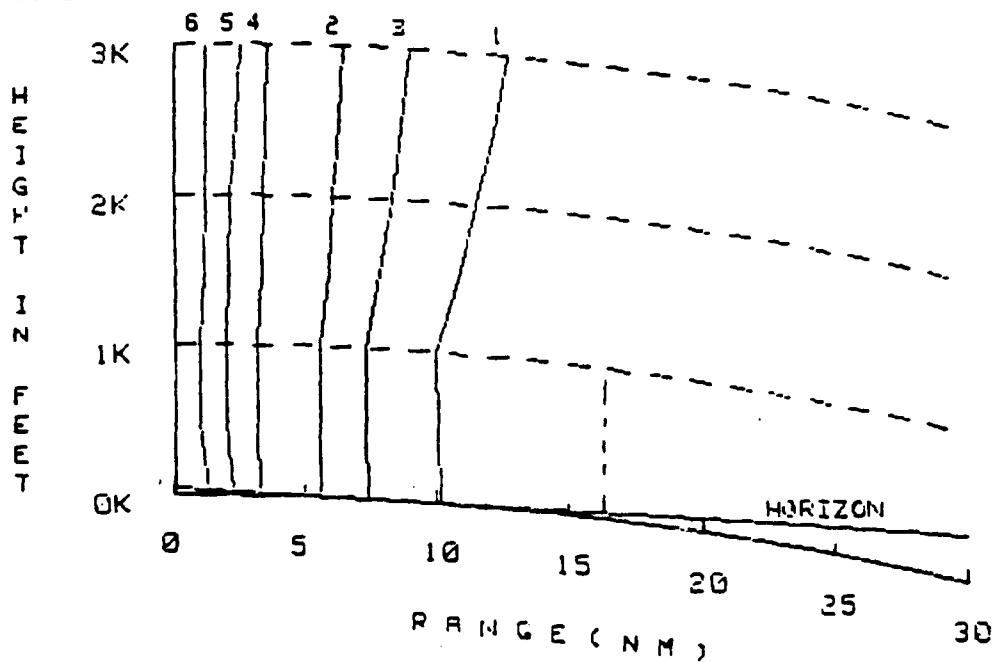
*** EO PERFORMANCE RANGES ***

A REAL FLIR

FLIR PERFORMANCE RANGES(NM):

#	TARGET TYPES	ALTITUDE LEVELS(FT)						
		GROUND	500	1000	1500	2000	2500	3000
1	CRUISER/DET	10.2	10.1	10.0	10.9	11.6	12.3	12.8
2	/IDENT	5.6	5.5	5.5	5.9	6.1	6.4	6.6
3	SUBMARINE/DET	7.5	7.4	7.4	7.9	8.4	8.8	9.1
4	/IDENT	3.3	3.2	3.2	3.3	3.4	3.6	3.6
5	SNORKEL/DET	2.2	2.0	2.0	2.1	2.2	2.4	2.6
6	PERISCOPE/DET	1.3	.9	1.0	1.1	1.2	1.2	1.3

LOCATION: NOSC
TIME: SEP 26 1979/1600



AIRBORNE FLIR
FAR IR BAND

PERFORMANCE RANGE CURVES INDICATE 50% PROBABILITY OF SUCCESS

Figure 25. Example of PROCAL-PREOS Output.

Before methods can be used to compensate for, correct, or take advantage of refractive effects on EM propagation, two things are necessary. First, accurate prediction and forecasting are needed. Some prediction means have been described here and in a later section prediction methods and forecasting methods will be described in detail. Secondly, an in-depth understanding of the effects of refraction on specific wavelengths and even specific systems that utilize propagating EM energy is needed. In the second half of the thesis several systems will be used to provide examples of refractive effects' wavelength dependence.

D. MIRAGE

One form of refraction of visible light that occurs in the lower atmosphere, with which almost everyone is familiar, is the mirage. Before discussing the effects of the several types of mirages on EM energy transmitted through the lower atmosphere, a general description of the conditions leading to mirage formation will be addressed. The majority of the information used in this discussion comes from an article by A. B. Fraser and W. H. Mach in a 1980 issue of Scientific American [Ref. 15: pp. 29-37].

1. General Description of the Mirage Phenomena

As with other forms of refraction, the atmosphere creates mirages by the bending of EM energy. As previously discussed, the index of refraction in the visible spectrum

is largely dependent on temperature, as seen in Equation 2.5. The greater the temperature gradient, the stronger the gradient of refraction and the greater the amount of bending of light. The portion of the atmosphere responsible for forming mirages is located in the first several meters above the surface. The exact form of the mirage is highly variable and is dependent on the solar absorption at the surface, the temperature gradient, the position of the object relative to the temperature gradient, and the position of the observer.

Light traveling through the shallow lower layer of the atmosphere will, due to the existing temperature gradient, travel in a parabola. The curvature of the ray can be upward or downward, depending on whether there is a decrease or increase of temperature as altitude increases. A general way to describe this phenomenon is to draw two light rays from an object, one moving directly to the observer's eye and the other following a parabolic path, as shown in the two-image inferior mirage in Figure 26. The first ray presents the light directly from the object. The second ray path is bent upward (due to a decrease in temperature at higher altitude) and thus appears to be light from an object which is located vertically below the actual object.

The simplest types of mirage to distinguish between are superior and inferior. In a superior mirage the temperature increases with height, as in superrefraction or

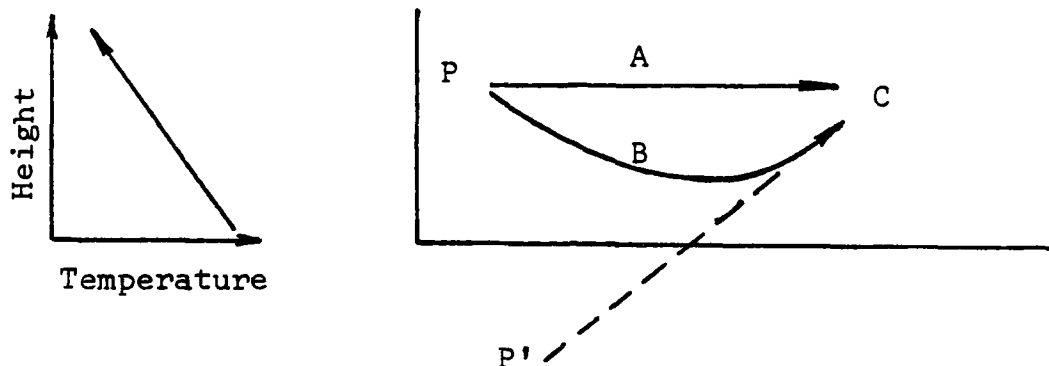


Figure 26. General Mirage Effect. Light ray A from object P is above the subrefractive condition and travels in a straight line to the observer C. Light ray B from object P travels through the subrefractive condition and thus creates a virtual image P' which is seen by the observer C.

ducting, and a horizontal surface will appear to be concave upward, presenting an impression to the observer, of being inside a shallow bowl. Figure 27A is a ray diagram of a superior mirage, showing that the image of the observed object is displaced upward. According to McCartney [Ref. 11: p. 100], although most mirages only involve relatively short distances (1 - 5 km), a superior mirage created by a very strong inversion can make objects located far beyond and below the optical horizon visible in a phenomenon known as looming.

An inferior mirage is created by a gradient in which temperature decreases with height (subrefraction). As described by Fraser and Mach [Ref. 15: p. 35], a horizontal surface altered by an inferior mirage will appear to be convex upward. The impression is also of a bowl, but this time the bowl is inverted and the observer is on top of it. There is thus an optical horizon created beyond which the surface being observed disappears. This phenomenon is referred to as sinking. The decrease of temperature, with altitude, which leads to this profile is common over enclosed bodies of water in the early morning and in desert regions in the late afternoon. Note that, with an inferior mirage, light rays from the bottom of the object may not reach the observer if this portion of the object is beyond the optical horizon, as shown in Figure 27b.

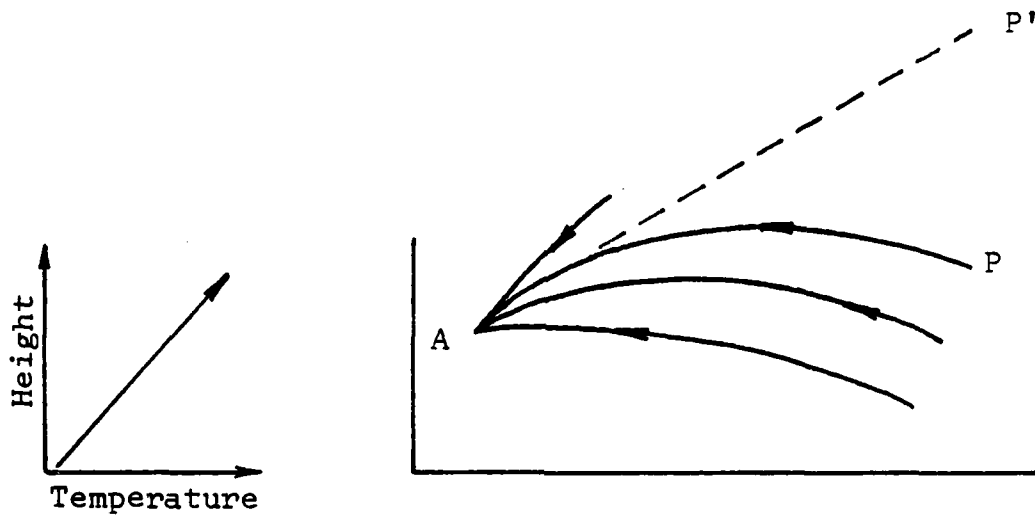


Figure 27a. Superior Mirage. The virtual image P'' is seen by the observer A as being above the actual object P.

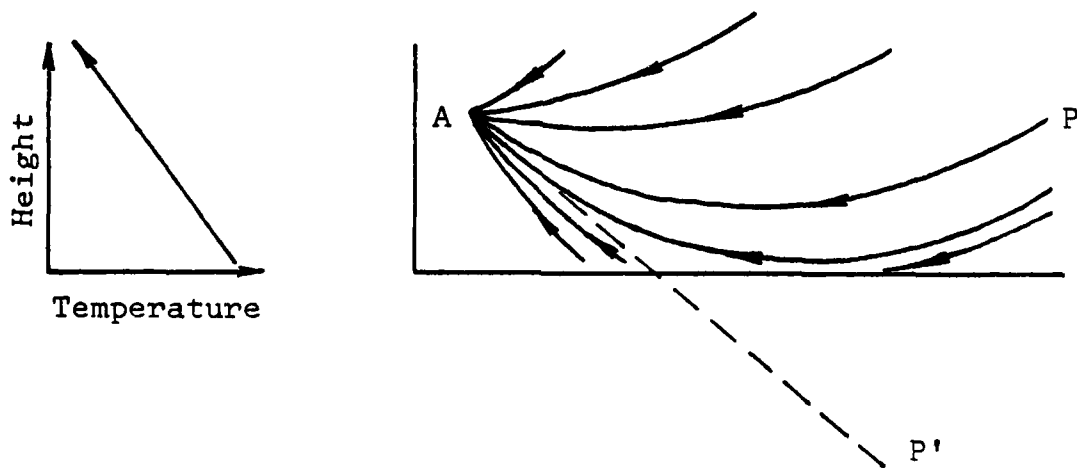


Figure 27b. This time the virtual image P' is seen by the observer A as being below the actual object P.

If the temperature gradient is constant with height, no distortion of the image will occur in a mirage, since displacement of all portions of image, upward or downward, will be the same. However, such a situation is not the general case, since some magnification or reduction of the image will usually occur. When an image is reduced in height, the condition is referred to as stooping. This occurs if the temperature gradient decreases as the temperature increases with altitude. Such a condition often occurs over lakes or inlets on a sunny afternoon, where warm air from the land is carried over the cooler water. A superior mirage is thus formed with the bottom of the image displaced upward more than the top of the image. The result to the observer is a squashed image of the object, and this image will appear to fluctuate in vertical dimension, as the day progresses.

A magnification of the image, or towering occurs, according to Fraser and Mach [Ref. 15: p. 35], in an inferior mirage when the image is displaced downward, but the bottom of the image is moved downward more than its top is. This happens when the temperature gradient increases as the temperature decreases with altitude and occurs over enclosed bodies of water in the early morning or over sun-heated ground later in the day.

The familiar mirage of the desert is the two-image inferior mirage. The "water" seen by the observer is actually an inverted image of the sky seen below the horizon. The same atmospheric phenomena that create the inferior mirage and towering create the two-image inferior mirage, i.e., the temperature and temperature gradient both decrease with height. The difference is that the temperature profile must be stronger, thus resulting in the ray being bent more significantly. Since the object rises so far above the surface that it is near the top of the temperature gradient, rays will travel both directly from the object and in a parabolic manner, similar to the simplified diagram in Figure 26. Because the ray of light passing through the region of strong temperature gradient is so strongly bent, it will not join the eye with the bottom of an object but will join the eye with the top of an object to provide a second, but inverted, image. As Fraser and Mach [Ref. 15: p. 35] state:

"The image is inverted because as the observer lifts his gaze slightly he is looking through a region of the atmosphere that has a weaker temperature gradient, so that the ray is less strongly curved. It will therefore join the eye to a point lower on the object rather than higher, as would usually be expected."

An object moving away from the observer will first appear as a single image, then as a double image, and then vanish from the bottom up. The presence of a double image will make the ground between the observer and the object appear

to be a water surface. The distance to the point where the "water" begins is the location of the optical horizon. As the temperature cools, the optical horizon is extended and the "water" recedes and, finally, vanishes.

According to Fraser and Mach [Ref. 15: p. 36], the most common form of the three-image mirage is caused by temperature increasing with height, for a distance, and then decreasing. This condition will occur over enclosed bodies of water on warm afternoons, and results in the surface of the water appearing as a "large, flattened letter S" - thus, the surface appears to fold over. If the inflection point is gentle, the surface will appear to rise up rather than fold over. An object at the distance where this occurs will be magnified, creating an example of the "Fata Morgana".

Fraser and Mach [Ref. 15: p. 36] feel that the occurrence of gravity waves in the atmosphere, along with the conditions leading to a three-image mirage, can result in the creation of the classic "Fata Morgana", which will sometimes appear as a high wall rising up above the surface or as a mountain range in the distance. This combination of stratified atmosphere and gravity waves causes a periodic oscillation of the refractive index. Energy imparted from surface winds and a countering force imparted by the earth's gravity are responsible for the waves. The oscillating bands of varying refractive indices will lead to the appearance of bright pilasters and dark windows in the

wall created by the "Fata Morgana", and are actually the image of the surface below the mirage.

Although there are other less common forms of mirage, those described above show some of the great variety of types and the atmospheric conditions leading to their creation. Such conditions can potentially disrupt the operation of optical systems.

2. Effects of Mirages on Optical Devices

As previously stated, there are a variety of forms of mirage, all dependent on the conditions of the atmosphere near the surface of the earth. The resulting refractive conditions are similar to those of anomalous propagation but are on a much smaller scale, though the line separating anomalous propagation from mirage is often unclear. The basic difference between these two forms of refraction are the local nature of the atmospheric conditions leading to mirage formation and the larger scale atmospheric conditions leading to anomalous propagation.

The effects of mirages are most apparent on optical systems. Generally, there is little difference in the effects of mirages on IR and visible wavelengths, even in the presence of strong refractive conditions. The effects on optical tracking systems can be quite significant, resulting in extension (superior mirage) or shortening (inferior mirage) of the optical horizon and distortion of the image (towering and sinking). Mirages such as the three

image mirage and the "Fata Morgana" can appear very solid and real, and, therefore, be quite misleading. Just as light from the object to the observer is strongly bent, so, too, will be any visible energy directed from the observer to a target in the mirage.

The effects of mirages can be significant for optical trackers, visible surveillance, and laser systems operating at low elevation angles within the mirage.

In a similar manner, optical systems using the IR spectrum will also be affected by refraction in mirage conditions. The PREOS model [Ref. 14] incorporates the ability to predict the amount of image distortion due to mirage effects.

The effect of mirages on radio wave and microwave systems will depend not only on the general type of mirage (inferior or superior), but also on the strength of the refractivity gradient and the mirage thickness. The effects will be the same as those predicted for surface based anomalous propagation, whether superrefractive, ducting, or subrefractive. The effect on microwave systems, such as radar, will only occur at very low elevation angles and at frequencies high enough to be above f_m , (Equation 2.9).

Prediction of mirage occurrence is difficult, since it is dependent on terrain, large scale atmospheric, and local atmospheric conditions. Mirages are generally associated with partially or fully enclosed large bodies

of water, such as lakes, sounds, or bays, and with hot desert regions. The probability of occurrence of mirage conditions and examples of the effects of mirages on specific systems will be addressed later.

E. TURBULENCE

Anomalous propagation and mirage conditions are created by relatively large scale, steady state variations in the refractive index of the atmosphere. Such refractive conditions affect EM signals at both the long and short end of the spectrum, from radio frequencies to visible light. The air is, however, never entirely motionless. Thus, much smaller scale variations in the index of refraction also exist. These random fluctuations of the index of refraction of the air are created by turbulent motion in the atmosphere coupled with temperature and humidity gradients. This turbulent motion includes inhomogeneities in the atmosphere varying in size from hundreds of meters in extent of those on the order of 1 mm in length. The effects of turbulence are largely confined to the shorter wavelengths (MMW, IR, and visible), due to the size of the refractive inhomogeneities relative to the size of the wavelengths.

1. General Description of Turbulence

The inhomogeneities in the atmosphere consist of varying sized regions (discrete cells) which fluctuate in temperature and water vapor content in time and in space.

According to Zuev [Ref. 16: p. 348], variation of 1 degree centigrade will result in a change in the refractive index of approximately 1×10^{-6} . Fluctuations of the temperature of the air at a given location may be as high as tenths of a degree and can vary over periods of milliseconds to seconds. Zuev further states that the variation of temperature over a horizontal path can be several degrees for points on the order of 10^2 to 10^3 m apart.

These inhomogeneities are themselves constantly changing in size and location. They are created and modified by wind shear and convection arising from vertical temperature gradients and from vertical water vapor gradients over lakes and oceans. As stated by F. Lutomirski et. al. [Ref. 17: p. 1]

"The most important factors affecting daily variations (in the index of refraction) are short wave solar radiation and long-wave terrestrial and atmospheric radiation, the mean wind speed, type of soil and ground cover, and ground surface roughness."

The overall effect of the inhomogeneities present in a turbulent atmosphere is to modify the characteristics of optical propagation through the atmosphere. The nature of the refractive effect is dependent on the operating wavelength, pathlength, and nature of the turbulence. Specifically, the size of the inhomogeneities is important to the overall effect of turbulence on optical and MMW transmissions. The size of the inhomogeneities created by wind shear and

convection will vary greatly from those hundreds of meters in size (outer turbulent scale) L_0 , to those, according to Zeuv [Ref. 16: p. 349], on the order of

$$l_0 = \sqrt[4]{\nu^3/e} \quad , \quad (2.11)$$

where l_0 is the inner turbulent scale, ν is the kinematic viscosity, and e is the rate of dissipation of turbulent kinetic energy. The inner scale l_0 , is the smallest size inhomogeneity that can exist due to viscosity while L_0 is the largest such region that can exist in which temperature can be expected to remain nearly constant. According to A. Cooper [Ref. 18: p. A-40], between these two scales there often exists a region of well established turbulence which can be described by the Kolomogorov spectrum as

$$\theta_n(K) \approx K^{-11/3} \quad , \quad (2.12)$$

where $K = 2\pi/l$ is the "turbulence wave number" representing the size of the eddy or inhomogeneity and $\theta_n(K)$ is the "inertial subrange" of well established turbulence.

The structure function of the refractive index between two points (r and r_1) of a medium with random inhomogeneities is

$$D_n(r) = [n(r_1 + r) - n(r_1)]^2 \quad (2.13)$$

where r is the distance between the two points. In a similar manner Zuev [Ref. 16: p. 349] defines the temperature structure function

$$D_T(r) = [T(r_1 + r) - T(r_1)]^2 \quad (2.14)$$

Atmospheric turbulence is generally described by the Kolomogorov model for fluid velocity turbulence. For the Kolomogorov turbulence model the two Equations 2.13 and 2.14 can be written equivalently for small scale turbulence, as

$$D_T(r) = C_T^2 r^{2/3} \quad , \quad (2.15)$$

$$D_n(r) = C_n^2 r^{2/3} \quad , \quad (2.16)$$

where C_n^2 is the refractive index structure value and C_T^2 is the temperature structure value. These relationships in Equations 2.15 and 2.16 only hold for limited separation values, when

$$l_0 \ll r \ll L_0 \quad (2.17)$$

The two structure constants are related by

$$C_n^2 = (79P/T^2 \times 10^{-6})^2 C_T^2 \quad , \quad (2.18)$$

and are the usual means of describing the turbulence level. According to F. Hall [Ref. 19: p. TuCl-1] C_n^2 can also be described as the difference in refractive index between two points, squared, averaged and divided by the $2/3$ power of the distance between them, or

$$C_n^2 = (n_1 - n_2)^2 / r^{2/3} \quad , \quad (2.19)$$

where r is the distance between the two points. Note that C_n^2 has the dimensions of length to the $-2/3$. Generally C_n^2 is the only parameter needed to describe small scale turbulence and, for this reason, is the parameter most often used in studying optical turbulence effects. Actual measurements of C_n^2 can be made by determining the difference in temperature between two sensitive, fast response thermometers located some distance apart or from the temperature power spectrum from one thermometer.

Values of C_n^2 in the lower atmosphere generally lie between 10^{-16} cm and 10^{-12} cm and vary widely with time and location. C_n^2 values, and therefore turbulence conditions, are considered to be light around 10^{-15} and severe around 10^{-13} . Variation in the value of C_n^2 occurs not only along a horizontal path, but also along a vertical path from the earth's surface to the top of an inversion. Turbulence will generally be strongest at the surface and at the top of an inversion. For such a vertical path C_n^2 normally decreases in value as

altitude increases until the inversion region is reached where C_n^2 values increase dramatically. Above the inversion there can also be significant turbulence depending on the wind and large scale weather conditions.

The usual result of the many factors affecting turbulence formation is the turbulence maximum in the early or midafternoon when heating of the surface is greatest and winds are light, and minima at sunrise and sunset when little heating occurs. Turbulence will occur at night, particularly if an inversion develops, but only if a light wind is present and will generally be weaker than during the day. Thus, turbulence shows a characteristic diurnal variation as shown in Figure 28, although the diurnal variations will be weaker when the sky is overcast. Table 3 provides a rule-of-thumb for predicting the occurrence of turbulence given existing meteorological and surface conditions. Figure 29 through 31 are actual plots of C_n^2 values for three different climatic conditions. Figure 29 is a desert region in summer, Figure 30 is a treeless area over snow, and Figure 31 is a wet grassland typical of many regions in Central Europe. Note the distinct diurnal cycle in each plot and that the strongest turbulence occurs over the desert region. Significant turbulence is recorded in the other two regions as well, particularly over the wet grassland.

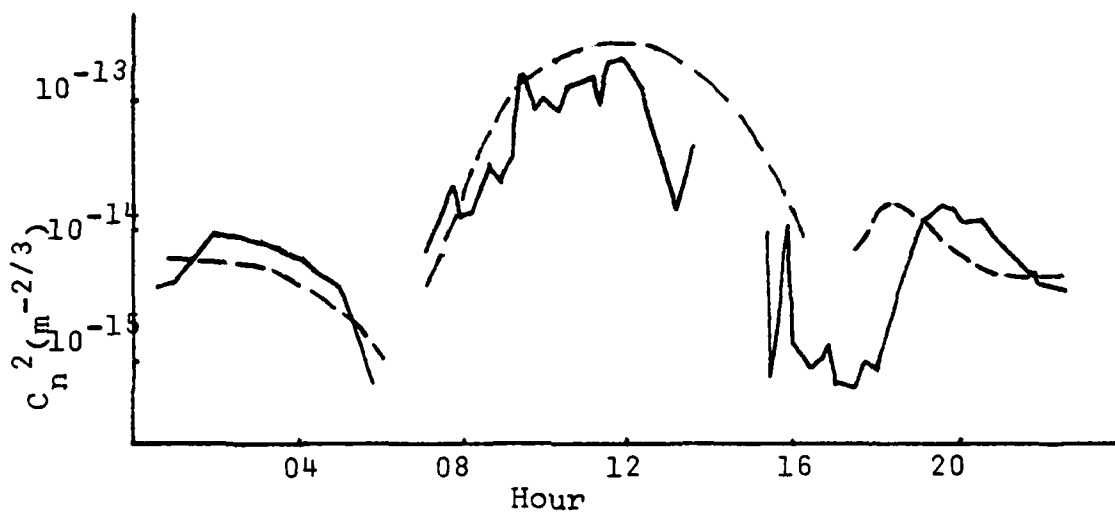


Figure 28. Diurnal Variation of Turbulence. The graph shows the measured values (solid lines) of optical turbulence at 1.5 meters above a grassy surface in a semi-arid region and those from bulk meteorological measurements (dashed lines).

TABLE 3
INTERIM RULES-OF-THUMB

Minimum thermal turbulence in the boundary layer is observed with the following atmospheric and earth-surface conditions:

- o Under a heavy overcast, day or night.
- o Over water or wet ground, day or night.
- o With winds exceeding $\approx 8 \text{ m sec}^{-1}$ ($\approx 15 \text{ kn}$), nearly regardless of surface heating or cooling, day or night.
- o During clear weather, for periods of 10 to 30 minutes shortly after sunrise and before sunset.
- o During generally unstable days, for brief periods in the shadows of transient clouds (the same effect may be obtained during nights that are generally stable).
- o In descending volumes of air, specifically between convective plumes in daytime, free-convection conditions.
- o On clear nights, with absolutely still air (any air motion can drastically change this situation).

Maximum thermal turbulence is generally found with the conditions:

- o Over relatively dry ground, with strong solar heating and light winds.
- o On clear nights with light but nonzero winds (the most unpredictable, sporadic turbulence is found under these conditions,
- o In the upper atmosphere, in stable strata associated with vertical wind shears.

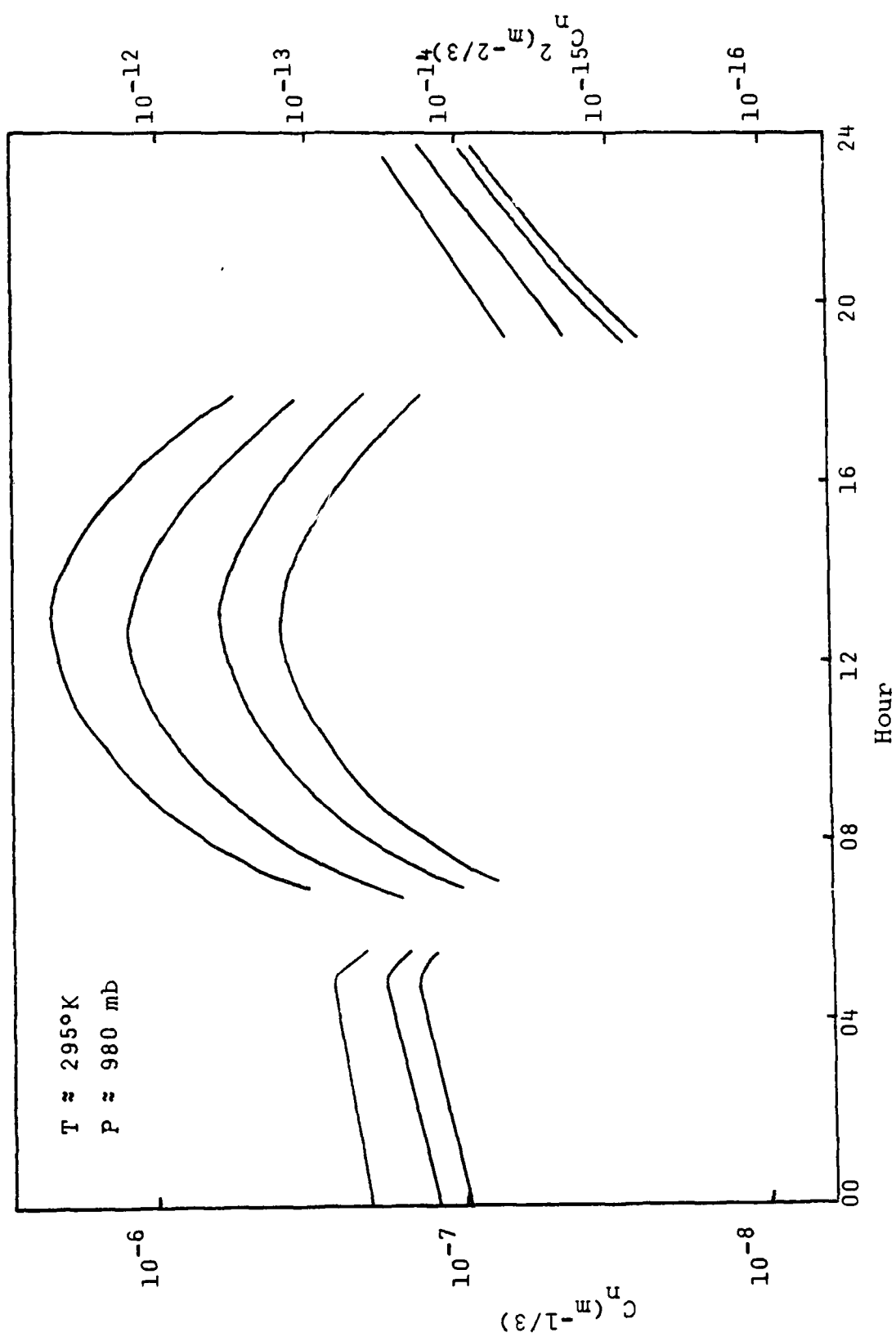


Figure 29. C_n vs mean solar time at 16, 8, and 2 meters (top to bottom) for a dry desert in summer.

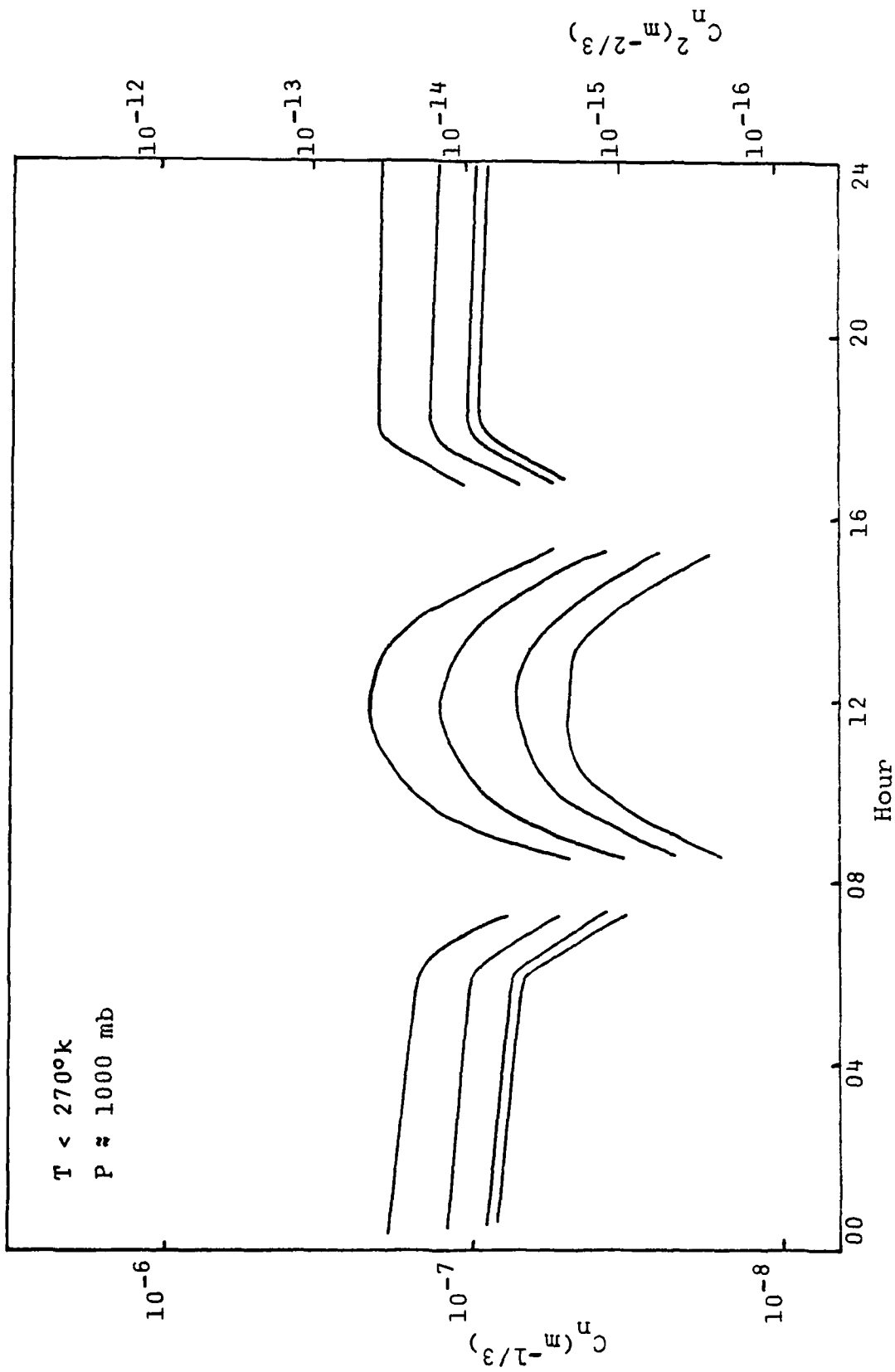


Figure 30. C_n vs mean solar time at .5, 2, 8, and 16 meters (top to bottom) for a snow covered treeless area.

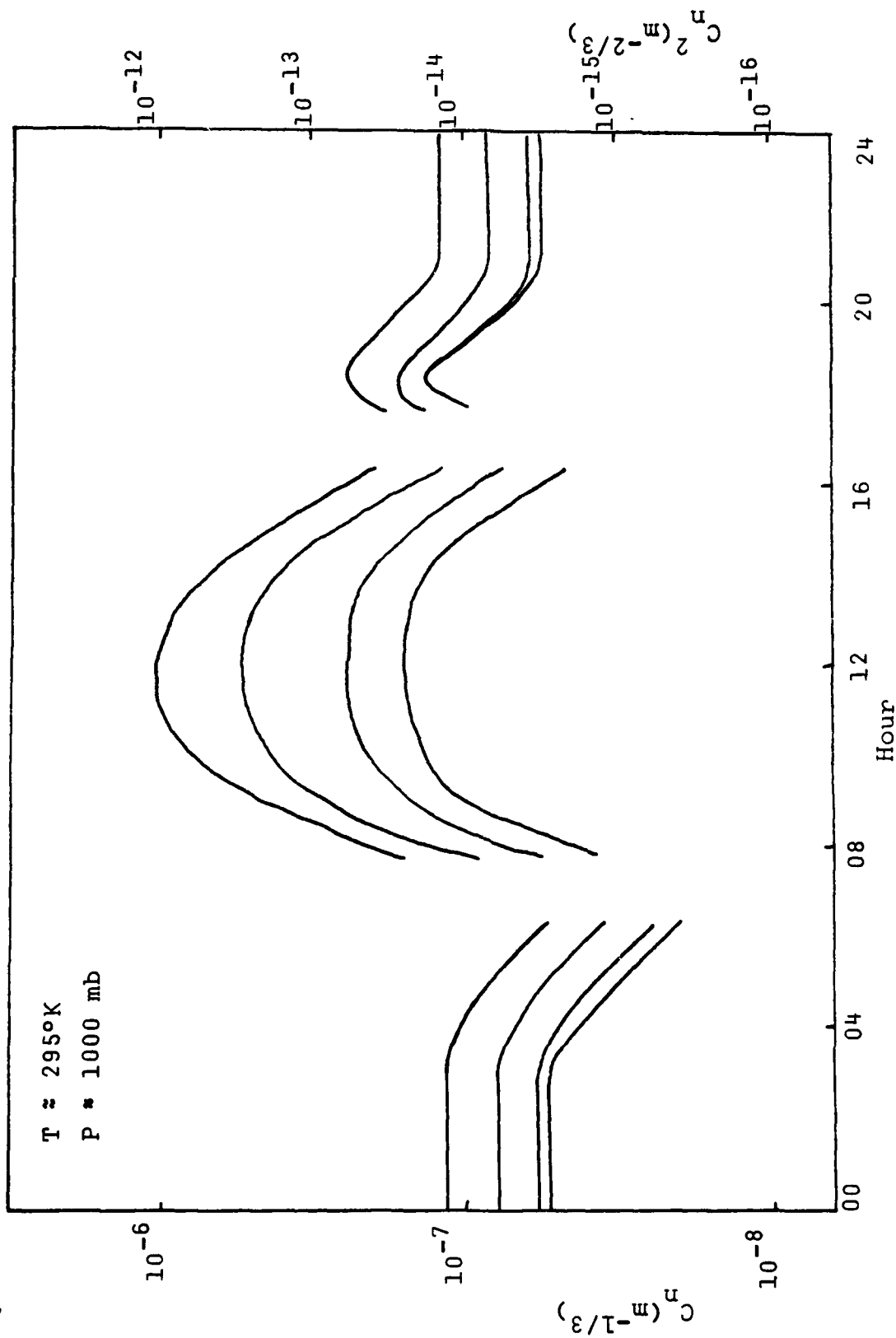


Figure 31. C_H vs mean solar time at .5, 2, 8, and 16 meters (top to bottom) for a wet green short-grass grassland.

2. Principal Effects of Turbulence on Optical Propagation

Turbulence in the atmosphere, along the optical path, affects the optical properties of focused beams and imaging systems. Point measurements of C_n^2 along an optical path often show wide variations in values due to temperature and water vapor variations. Due to this spatial variation in C_n^2 , a path integrated value is usually determined for the overall path. Often in calculations of the effects of turbulence on optical systems the value of C_n^2 used will be weighted for the calculation. These weighting functions will emphasize the effects of certain parts of the path (the center or ends) and may totally ignore other regions. The value of weighting will vary with the type of turbulence effect being considered, thus, care must be exercised in using "weighted" values of C_n^2 in calculations.

Instantaneous deviations in n due to turbulence can lead to a number of effects on optical systems to include: scintillation, wave front tilt or fluctuations in angle of arrival, beam spread, beam steering or beam wander, and degradation of the Modulation Transfer Function (MTF) or loss of resolution. Each of these effects will be considered separately, although it will be seen that many are closely related. E. Crittenden [Ref. 20: p. 2] states that H.T. Yura in his analysis of turbulence effects shows that the effects on an active focused beam system will be applicable to those

imaging systems as well, although the manifestation of the effect may be somewhat different.

a. Scintillation

Scintillation or beam breakup is due to the fluctuation of the intensity of a focused beam or image which has propagated through a turbulent medium. This characteristic sometimes referred to as "image boil" is caused by random bending of optical rays resulting in destructive and constructive interference patterns. These patterns vary with position and time. Figure 32 shows an example of scintillation of a laser beam. The twinkling of stars viewed from the earth is another example of scintillation.

The variance of the log amplitude intensity of a laser beam, as seen through a pinhole at the receiver, can be related to C_n^2 , the propagating wavelength, and the pathlength, according to E.C. Crittenden et. al. [Ref. 20: p. 16] by

$$\sigma_{\text{LnA}}^2 = 0.124 k^{7/6} C_n^2 z_o^{11/6}, \quad (2.20)$$

where $k = 2\pi/\lambda$ and z_o is the propagation pathlength. As expected, the greater the level of turbulence or the longer the pathlength, the greater the scintillation observed. It should also be noted that the shorter the optical wavelength the greater the scintillation effect. Equation 2.20 is only



Figure 32. An "open camera" photograph of a scintillating beam profile.

accurate for small amplitude fluctuations, for $2\sigma_{\text{LnA}}^2 \leq .8$. For higher turbulent levels, Equation 2.20 is used only to infer the approximate relationships between C_n^2 , pathlength, wavelength, and log amplitude variance.

Turbulence levels generally vary along the propagation path, rather than being homogeneous as implied by Equation 2.20. This fact must be considered in calculating the actual log amplitude variance, and Equation 2.20 can be rewritten (for spherical waves) as

$$\sigma_{\text{LnA}}^2 = .56 k^{7/6} \int_0^{z_0} C_n^2 w dz , \quad (2.21)$$

where w is a weighing function that emphasizes the C_n^2 values in the middle of the optical path and ignores those values at the path ends.

C_n^2 values can also be calculated from measurements of scintillation. According to Crittenden [Ref. 20: p. 16], however, in cases of nonuniform turbulence levels along the path of propagation such calculations may not be of any use in calculating other turbulent effects because of the different weighting functions involved.

b. Wave Front Tilt and Beam Spread

Wave front tilt or fluctuations in the angle of arrival of a beam or image are caused by bending of the entire wave front of an image or beam as it passes from one inhomogeneity to another. As would be expected, the inner

scale turbulent inhomogeneities have little effect on creating wave front tilt, but rather, it is the larger, outer scale, turbulence regions that lead to this phenomenon. The result of this effect is to cause "image dance", a movement of the apparent position of an object's location in an imaging system. This is the phenomenon that leads to the false apparent location of stars viewed from the earth's surface.

One characteristic of beam spread is the increasing of the width of an initially narrow beam as it propagates through the atmosphere. This expansion of the beam width and resultant decrease in intensity is due to the random refraction of the beam as it passes through a turbulent atmosphere. In essence, relatively small scale wave front tilt is occurring at many different locations across the beam profile. Long term beam spreading can be separated into two components: beam expansion as described above and beam wander. Beam wander is the movement of a beam from a straight path due to turbulent inhomogeneities that are much greater in length than the beam width, thus, refracting the entire beam. As expected, beam wander is a function of the beam diameter and the turbulence scale. Lutomirski [Ref. 17: p. 115] states that beam wander is closely related to wave front tilt and in cases where the only significant effect on a beam propagating through the atmosphere is wave front tilt, the instantaneous beam wander angle and wave front tilting angle will be equal.

c. Resolution

A cumulative effect of the various turbulence effects is an overall degradation of the image resolution of an object seen through the atmosphere. Characteristics of an object are said to be resolved if their images are discernible as being separate. This loss of resolution is characterized by a degradation of the Modulation Transfer Function (MTF) of the atmosphere by turbulence. The MTF describes the detail of an image, transmitted from one point to another, in terms of the spatial frequency. The MTF for a total optical system can be calculated by determining the MTF for the components (lens, mirrors, and atmosphere) and forming the product of these component values. Knowledge of the MTF of the atmosphere is important in predicting the effects of turbulence on low, medium and high power laser beams leading to beam wander and modification of the beam profile. However, in high power lasers the heating of the air must also be considered. To be entirely accurate, when discussing the MTF as it relates to optical systems, it is the Optical Transfer Function (OTF) that is discussed. The OTF describes both the phase and amplitude changes in the atmosphere. When only the amplitude changes are considered, the OTF is called the MTF.

Knowledge of the MTF can also aid in predicting the turbulence contributions to resolving ability, image

AD-A134 827

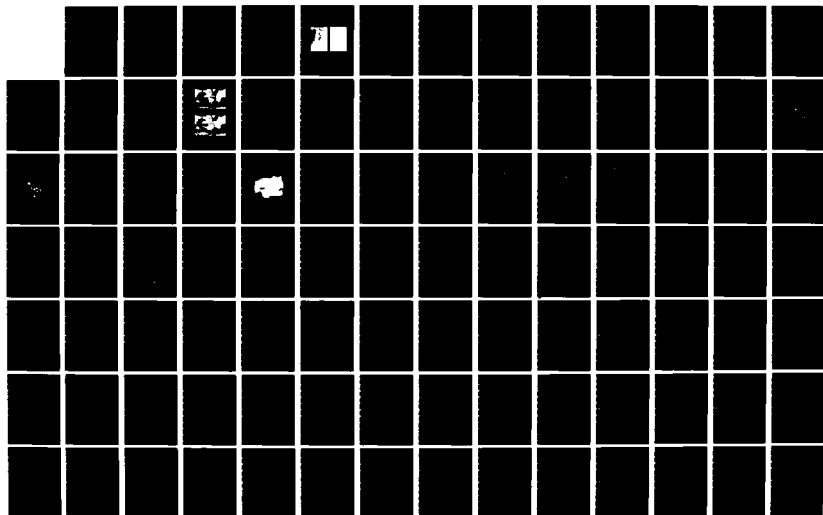
EFFECTS OF ATMOSPHERIC REFRACTION ON US GROUND WARFARE
(U) NAVAL POSTGRADUATE SCHOOL MONTEREY CA
T P MOURAS ET AL. SEP 83

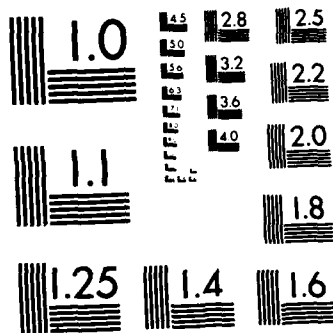
2/4

UNCLASSIFIED

F/G 20/14

NL





MICROCOPY RESOLUTION TEST CHART
NATIONAL BUREAU OF STANDARDS-1963-A

broadening, and image wander of imaging systems. Using weighting functions that emphasize the ends of the path, MTF curves can be developed from measured values of C_n^2 and λ .

For imaging systems, the Mutual Coherence Function (MCF) is the equivalent of the OTF and, in fact, the atmospheric MCF is the same function as the OTF but expressed in terms of different variables. The MCF is of considerable concern in coherent detection systems. It reflects the loss of transverse coherence of an initially coherent wave as it passes through the turbulent atmosphere. Knowledge of the MCF can also be used to provide information on atmospheric effects on laser propagation.

The OTF for a propagation system, along a path where the turbulence varies is described by Crittenden [Ref. 10: p. 14] by

$$M(f) = \exp\{-57.64 \lambda^{-1/3} f^{5/3} \int_0^{z_0} C_n^2 (z/z_0)^{5/3} dz\}, \quad (2.22)$$

where z_0 is range, f is the angular spatial frequency, defined as $f = 1/L$, where L is the spatial period of the distribution of the modulation of the amplitude (intensity) of the optical beam, and λ is the wavelength. The same function $M(f)$ is used to calculate the MCF of an imaging system but using different variables.

The most common parameter used to describe FLIR propagation through the atmosphere is the Minimum Resolvable Temperature Difference (MRTD). The MRTD implies the use of a standard four-bar pattern with an individual bar length to bar width ratio of 1:7. The MRTD is the minimum temperature difference between the bars and the background for which the bar pattern can be resolved at the 50% probability of detection level for a given FLIR. Figure 33 shows a four-bar MRTD test pattern such as that discussed above. As with other means of measuring resolution, the MRTD for a FLIR system can be greatly degraded by turbulence.

Figure 34 provides a comparison of line spread functions measuring the atmospheric OTF for two different levels of turbulence. Note that several of the effects of turbulence are occurring simultaneously. The cumulative effect of scintillation, image broadening, and image wander (wave front tilt) is to reduce the resolution of an image or degrade the shape and move the end point location of a beam.

As mentioned earlier, C_n^2 can be calculated from measurements of scintillation. Likewise, Crittenden et. al. [Ref. 21: pp. 13-1 to 13-2] states that measurements of the OTF and beam wander can also be used to calculate C_n^2 and with more ease than using scintillation.

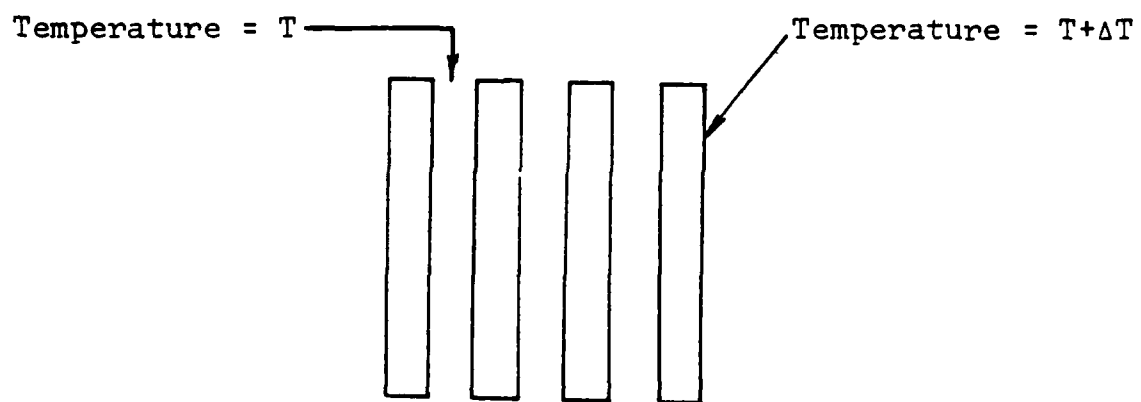
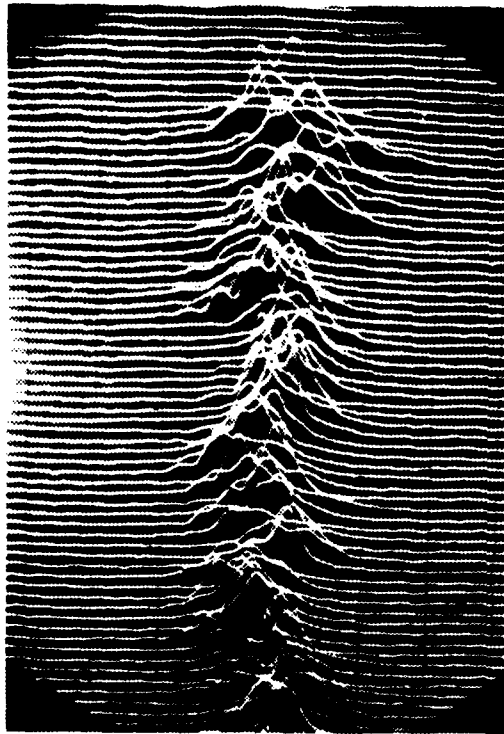
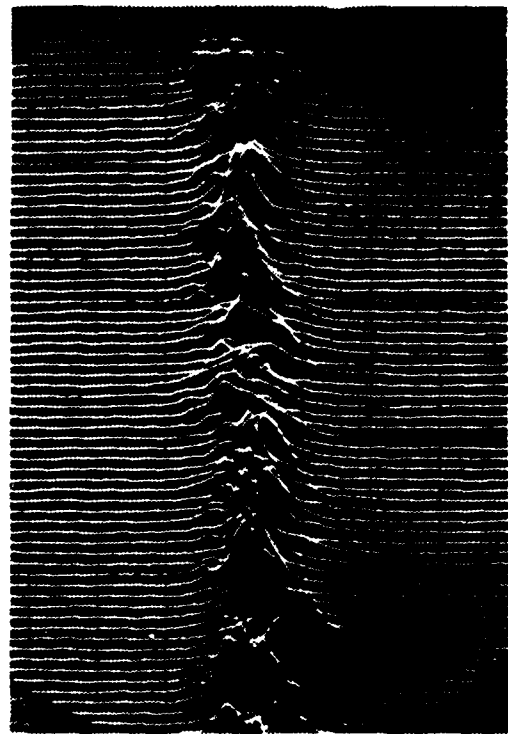


Figure 33. Standard Four-bar MRTD test pattern where the bars represent a blackbody source of temperature $T + \Delta T$ and the spaces represent the background temperature T , and ΔT is the difference between the background temperature and the targets temperature.



$$C_n^2 = 9.6 \times 10^{-16} \text{ m}^{-2/3}$$



$$C_n^2 = 19.36 \times 10^{-16} \text{ m}^{-2/3}$$

Figure 34. Line spread spectrum for two levels of turbulence. These photos show that associated with an increase of C_n^2 is a broadening of the image related to the OTF, increased detailed structure (scintillation) and an increase in the wander of the center (image wander).

3. Manifestation of Turbulence in Optical Systems

In beam forming optical systems, such as laser systems, scintillation may result in a few dB to upwards of 40 dB fluctuation above and below the average irradiance value. For a laser communications system this effect can be significant in degrading the bit error rate. Scintillation is less important at IR and longer wavelengths than at visible wavelengths. According to Lutomirski [Ref. 17: p. 230], recent studies have shown that at the longer wavelengths (IR) a coherent detection laser communications system is preferable, while at visible wavelengths, an incoherent detection system is best when turbulent effects are concerned. Beam wander can cause significant enough movement of a laser beam to degrade detection in an optical communications system or to sweep the beam off the target in a laser designation or laser weapon system. Wave front tilt will also cause a degradation of detection in an optical receiver, although this may be the simplest turbulence effect to correct. Beam spread can result in a reduction of the irradiance of a laser weapon and a sensitivity reduction in laser communications systems. The MCF can be used to determine the limiting mean irradiance from an initially coherent beam and the turbulence limited S/N ratio of an optical heterodyne (coherent) receiver. Table 4 consists of two tables listing several types of army laser systems and the types of turbulence induced degradation each system can suffer from.

TABLE 4
(a)

POSSIBLE TURBULENCE-INDUCED DEGRADATIONS FOR VARIOUS SYSTEMS

Tactical System	Comments	Possible Degradation			
		Scintillation	Phase Fluctuations (Loss of Resolution)	Angle-of-Arrival Fluctuations	Beam Spreading/Expansion/Dancing
Range finders	Usually pulsed (some limited to < one pulse/sec). Scintillation can affect minimum averaging time. Spreading can cause target spillovers.	X			X
Trackers	Degradations can be reduced by fast-tracking the center of gravity of the image.	X	X	X	X
Line scan cameras	Resolution determined by minimum spot size. For very small illuminated dimensions, the raster scan received signal may scintillate.	X			X
Semiactive bomb and missile guidance	Possible turbulence effects in direct target spillovers and scintillation of returned signal.	X			X
Target designators	Center of gravity tracking may improve designation.	X		X	X
Active gun-sights and bombsights	Ranging information fed into gunsight/bombsight.	X			X
Battlefield IFF ^a		X		X	X

^a Identification, Friend or Foe.

TABLE 4
(b)

TYPICAL TACTICAL LASER APPLICATIONS

Service	Program	Functions Performed						
		Range Finder	Tracker	Camera	Semiactive Guidance	Illuminator, Designator	Gunsight	
Army	Multi weapon fire-control system, UH-1B, AH-1G	X	X					X
	ALTD5					X		
	Night Vision Aerial Surveillance System, ASQ-127	X			X			X
	Night Vision Aerial Periscope, YO-3					X		X
	LRTS	X	X					
	Stab. Night Sights	X				X		
	ALERTS			X				
	AN/GVQ-10	X				X		X
	VVS-1	X						
	3-D Surveillance			X				
Navy	Bulldog				X			
	PDR/AR	X			X			
	LAAPS			X				
	A-4M	X			X	X		X
	Paveway				X	X		
	Pave Arrow	X	X		X			
	Pave Sword					X		
Air Force	Pave Knife AVQ-10				X			X
	Pave Spot	X			X			X
	Pave Gat	X	X		X			X
	Blind Bat	X			X			X
	Pave Hawk				X			X
	Pave Light				X			X

	LARS/Pave Mack			X
Air Force	Tropic Moon 3	X		X
	AVB-1	X		
	Compass Count		X	
	AVD-3		X	
	Alirats	X	X	X
	Multispectral Recon		X	

Turbulence will create the same effects on imaging systems but will often be manifested in a different manner than the effects on beam producing optical systems. Scintillation will create variations in the intensity of the image of the object being viewed and will thereby degrade detection and identification. Image wander can cause a degradation of detection ability, dependent on the type of imaging system used, specifically the nature of the detection method used by the imaging system. Image broadening may degrade both detection and identification. Wave front tilt can present a false apparent location of the object. Turbulence induced degradation of the resolution of an image can be quite severe, affecting detection, discrimination and identification. The limiting resolution due to turbulence can be determined from the MCF.

It is apparent from this discussion that turbulence effects on optical systems are varied, but generally result in a degradation of the system's operation. Some means have been developed to compensate for turbulence effects, a few of which will be mentioned.

Lutomirski [Ref. 17: p. 65] states that perhaps the easiest form of turbulence effects to correct is wave front tilt to the entire beam or image, if it occurs largely by itself. Mechanical or electronic tracking of the image can be used in a system to correct the displacement in the image plane, producing a nondegraded image.

Other forms of turbulence effects are not so easy to correct, particularly when several occur at once. Because of the small scale of turbulence effects, turbulence correction requires a resolution element related to the size of the turbulence scale. These elements must be small and response times very short, due to the rapidly changing nature of turbulence effects. This is the basis of adaptive optics, the purpose of which is to minimize turbulent effects on optical systems, both imaging and beam forming. The adaptive optics system senses phase shifts induced in the optical beam by turbulence and introduces a compensating phase shift to correct for this. In particular, the Coherent Optics Adaptive Technique (COAT) is basically a self-phasing phased array system. Errors in the phase of the incoming signal are sensed across the wavefront and corrected by the COAT system. The COAT output aperture is divided into many small segments whose phase can be controlled independently using mirrors or splitters, providing the means to correct phase errors in the incoming beam. This technique has been shown to improve to some degree the degrading effects of scintillation, beam spread and beam or image wander but can not as yet fully improve the system's performance to that at low turbulence conditions.

4. Turbulence and MMW Propagation in the Atmosphere

Although turbulence has been largely studied because of its performance degradation of optical systems, it has been theorized for some time that it may also adversely affect millimeter waves. Recent tests have confirmed this fact and have also shown agreement with theory in that there is a stronger dependence on the atmosphere's humidity at MMW than at optical wavelengths. Thus, in calculations involving the effects of turbulence on MMW propagation, both C_n^2 , the temperature structure value and C_Q , the humidity structure value, must be considered. Additionally, the cross correlation of these two parameters, C_{TQ} , must be included in determining turbulence effects. Scintillation and fluctuations in the angle of arrival of the beam in radar applications have been shown to be the primary turbulence effects at millimeter wavelengths. McMillan and Bohlander et. al. [Ref. 22: pp. 32-39], in their 1982 article on MMW propagation, provide a detailed discussion of the formulas used in calculating intensity fluctuations (scintillation) and angle of arrival fluctuations.

As described by McMillan and Bohlander [Ref. 22: pp. 33-36], results of tests at White Sands Missile Range in New Mexico show that scintillation effects, though present, are generally not expected to be significant on MMW radar systems. However, fluctuations of the angle of arrival of MMW beams are on the same order of expected angular accuracy

and, thus, can be significant in degrading angle tracking ability as shown in Figure 35. The results of the testing seem to indicate that turbulence effects on angle tracking may be smaller than those due to overall anomalous propagation effects. Although more data on this subject is necessary before the full nature of turbulence effects on MMW is known, the results to date appear to indicate that turbulence should be considered when discussing MMW applications.

F. PREDICTION AND PROBABILITY OF OCCURRENCE OF ANOMALOUS PROPAGATION, MIRAGE FORMATIONS, AND TURBULENCE

The effects of atmospheric refraction on EM wave propagation, regardless of severity, are of little real consequence unless these conditions occur with some frequency. Furthermore, to respond to these effects, it is necessary to be able to forecast their occurrence and/or determine their existence. Some discussion on meteorological conditions and characteristics of terrain that lead to the three major forms of atmospheric refraction has already been dealt with and will not be reiterated here, except, as needed, for clarity. Rather, this section will attempt to look at the larger scale causes and characteristics of atmospheric refraction and focus on the probability of occurrence of anomalous propagation, mirage conditions, and turbulence in various regions of the world. Finally, two specific regions, Central Europe and the Mid-East will be

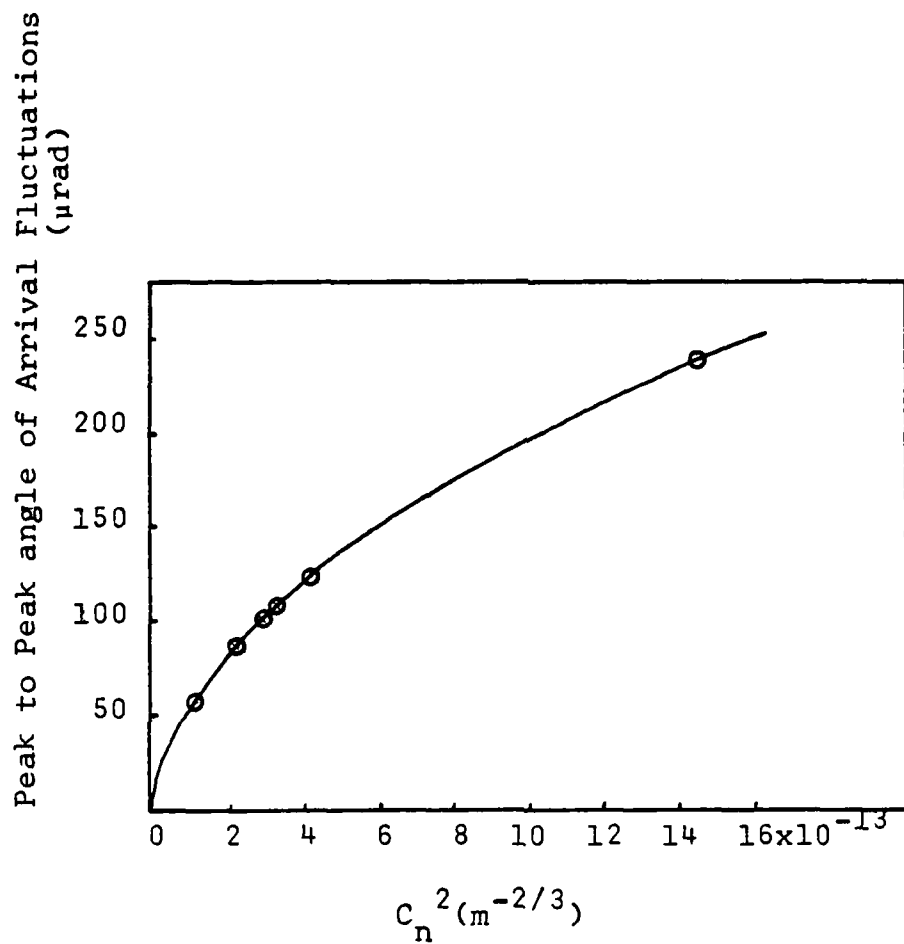


Figure 35. Calculated peak-to-peak angle-of-arrival fluctuations for millimeter wave signal.

looked at in some detail, not only because of the obvious military interest, but also to compare these two distinctly different areas.

Anomalous propagation will be examined first, for two reasons: first, because a larger body of information exists on this subject; second, because much of what is discussed concerning anomalous propagation can be directly related to turbulence and mirage forecasting and prediction.

1. Anomalous Propagation

A great deal of study has been conducted towards understanding the causes of anomalous propagation in its many forms, and in determining analytical methods of predicting its existence. Most of these have already been discussed. Forecasting anomalous propagation conditions can also be performed, given an understanding of the location and terrain features of the region of interest, the time of year and time of day, and existing large-scale weather conditions (air masses, high and low pressure regions, etc.), many of which interact closely.

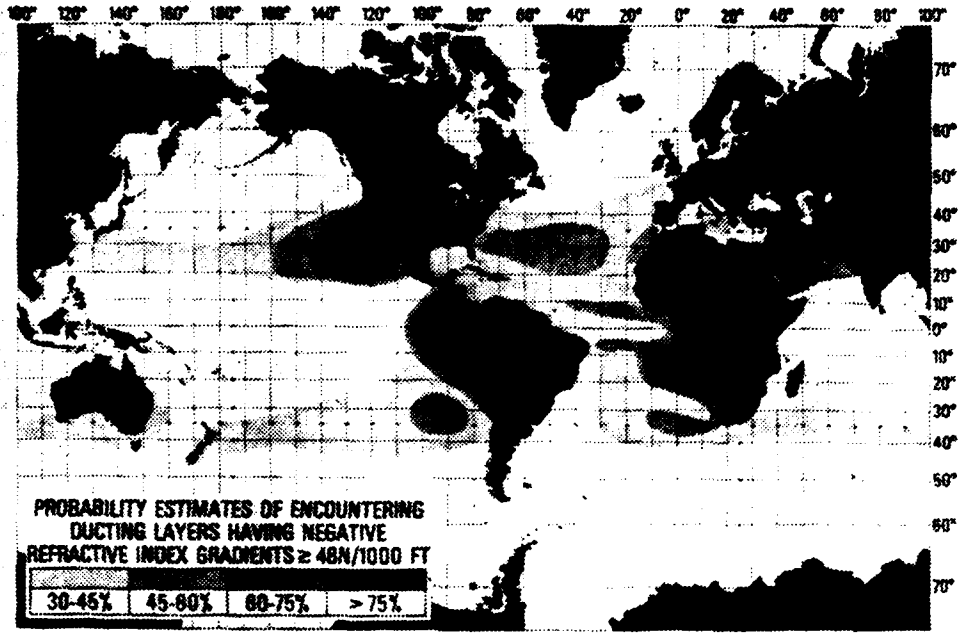
The general nature of the earth's surface, be it a large body of water or a large land mass, contributes to the expected refractive characteristics. This is due to the physical nature of the surface (mountains, desert, shallow tropical sea, etc.) and the effect of the surface on the air masses above. The persistence of superrefractive and ducting conditions over the oceans of the world is due largely to the

constant presence of moisture at low altitudes and the relatively slow changes of large air masses over these bodies of water. This persistence over water tends to decrease with distance (north or south) from the equator. Figure 36 shows this fact graphically.

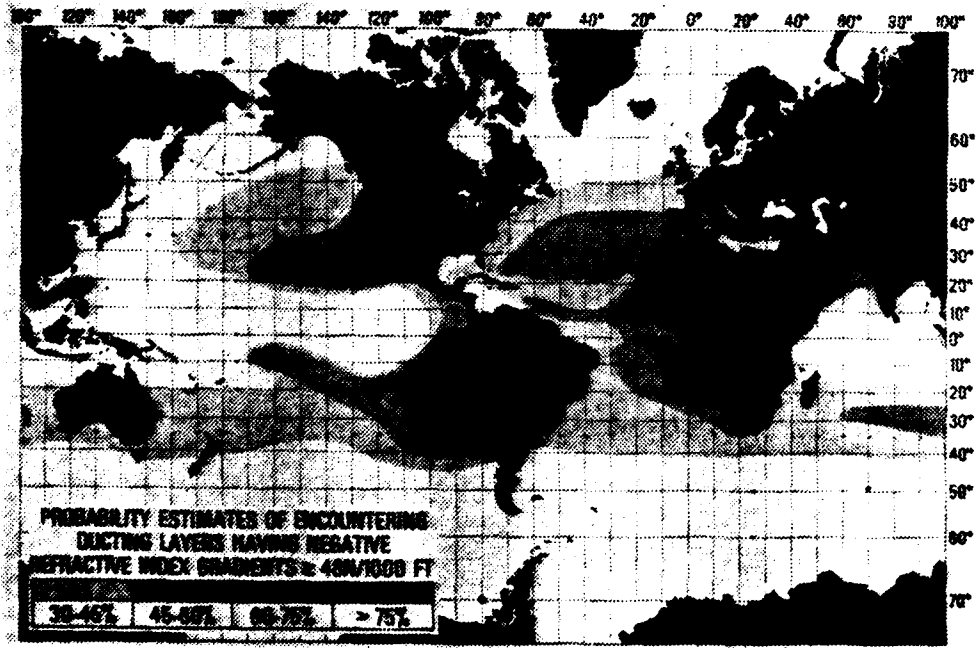
Over large land masses there generally is no such consistency in atmospheric conditions as exists over oceans. The humidity content and temperature of the air, as well as the large scale weather conditions (fronts and pressure regions) change much more rapidly over land than over sea. For this reason, persistent ducting is much rarer over land, and forecasting of anomalous propagation is generally more difficult.

The presence of certain terrain features also tends to have an effect on the occurrence and characteristics of refraction. High mountains will significantly affect the movement of air masses across the surface of the earth and impact on the creation of trade wind inversions and land-sea breeze recirculation. C. Samson [Ref. 9: p. 7] states that large river valleys may show patterns of refractivity differing markedly from surrounding regions due to stratification of the atmosphere by air drainage, above the valleys. Heating of large arid surfaces will often result in subrefractive conditions.

Large scale weather conditions are the most significant factor in forecasting overland anomalous propagation. Air



(a) February



(b) August

Figure 36. Regions of persistent oceanic atmospheric duct layers.

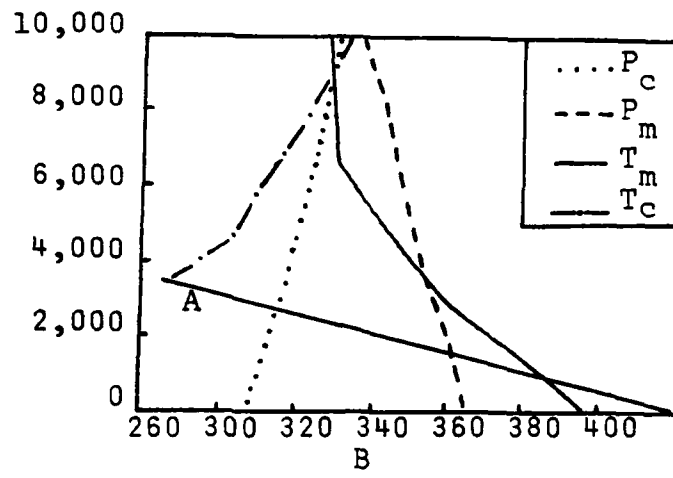
mass characteristics, the presence of high pressure regions, and the movement of fronts and cyclones are all important in the formation of anomalous propagation conditions.

Air masses are regions of air in which the properties of the atmosphere are relatively uniform. These air masses are formed in source regions which include large desert areas, tropical seas, and polar regions. The presence of a high pressure system over a source region enhances the development of the air mass. Source regions used in the classification of air masses are polar 'P', tropical 'T', continental 'C', and maritime 'M'. Table 5 describes the major air masses and their characteristics. Each of these air masses has a unique source region and movement pattern that varies seasonally. As would be expected, each also has a characteristic refractivity profile associated with it. Figure 37 shows the average profiles associated with these air masses.

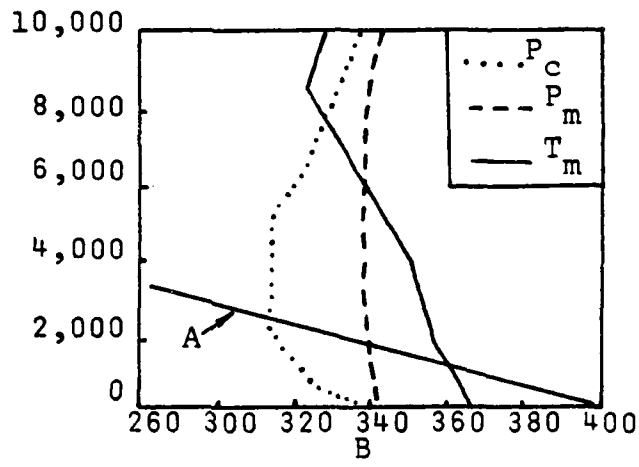
The profiles shown in Figure 37 can be modified by the presence of subsidence associated with high pressure regions. Large, permanent high pressure regions exist over the subtropical and mid-latitude oceans of the world, to some extent year-round. These high pressure regions shift toward the poles during each hemisphere's summer months and tend to drive the movement of frontal regions poleward. Frontal regions and cyclones, which are common in the mid-latitudes and polar regions, tend to destroy elevated layers, and, thus, no significant ducting or superrefraction

TABLE 5
AIR MASS CLASSIFICATIONS AND GENERAL DESCRIPTIONS

Air Mass	Source region(s)	Properties at Source
Polar maritime (Pm)	Oceans in latitudes greater than 50° (approx.)	Cool, rather moist; unstable
Polar continental (Pc)	Continents in vicinity of Arctic Circle; Antarctica	Cold, dry; stable
Arctic or Antarctic (A)	The Arctic Basin and (central) Antarctica in winter	Very cold and dry; very stable
Tropical maritime (Tm)	Sub-tropical oceans	Warm; moist, and rather unstable near surface, dry and stable above
Tropical continental (Tc)	Deserts in low latitudes: primarily the Sahara and Australian deserts, but also south-west U.S.A. and Mexico in summer	Hot and dry; unstable



(A) Summer



(B) Winter

Figure 37. Typical B-profiles in the source region for (A) Summer and (B) Winter. A is the ducting gradient.

is expected in the vicinity of fronts or of traveling low pressure regions (cyclones). Due to the persistence of these traveling weather patterns in extreme northern or southern (polar) regions, anomalous propagation is generally a rare and intermittent occurrence at and near the poles.

Coastal regions will reflect the variation in humidity and temperature related to the ebb and flow of maritime and continental air masses by exhibiting extreme horizontal and vertical refractive gradients.

Over land, and to a lesser extent over water, there tends to be a distinct seasonal variation in the occurrence of anomalous propagation. This can generally be tied to the prevailing large-scale weather conditions and to the intensity of solar irradiance.

Many of the smaller oceanic islands show little seasonal change in refractivity patterns, due to the fact that their climates are dominated by the maritime air masses. Islands large enough to affect these air masses will, on the other hand, often develop distinctly seasonal refractive gradient patterns.

Continental regions, particularly those in the mid-latitudes, tend to show significant seasonal variation in refractive characteristics, with the greatest occurrence of superrefractive and ducting conditions occurring in the summer months and early fall. This is, in part, due to the

shifting of the subtropical high pressure regions, higher mean temperatures, and the greater amount of moisture present in air masses in summer.

Seasonal shifts in the prevailing wind patterns, such as the monsoon circulations, lead to distinct seasonal variations in the refractive patterns of regions thus affected.

Many regions will also show strong diurnal variations in refractivity gradients due to surface changes in temperature, humidity, and, in some regions, shifts in wind direction. In general, according to Samson [Ref. 9: p. 9], continental and coastal regions tend to show anomalous propagation as occurring most often between 2000 and 0700 LST with the fewest occurrences between 1200 and 1500 LST. Oceanic islands show just the opposite trend in the occurrence of anomalous propagation. Subrefraction in desert regions also occurs most often in the late afternoon. As was mentioned earlier in this thesis, it is not uncommon in semi-arid and desert regions to see subrefractive conditions develop in the afternoon and superrefractive conditions form at night. Figure 38 shows this graphically, along with the resulting effects on IR rays. These diurnal characteristics, which tend to be strongest in the warmer summer and early fall months, are superimposed on the large scale changes in air masses.

Forecasting anomalous propagation conditions involves many variables. However, studies of meteorological data

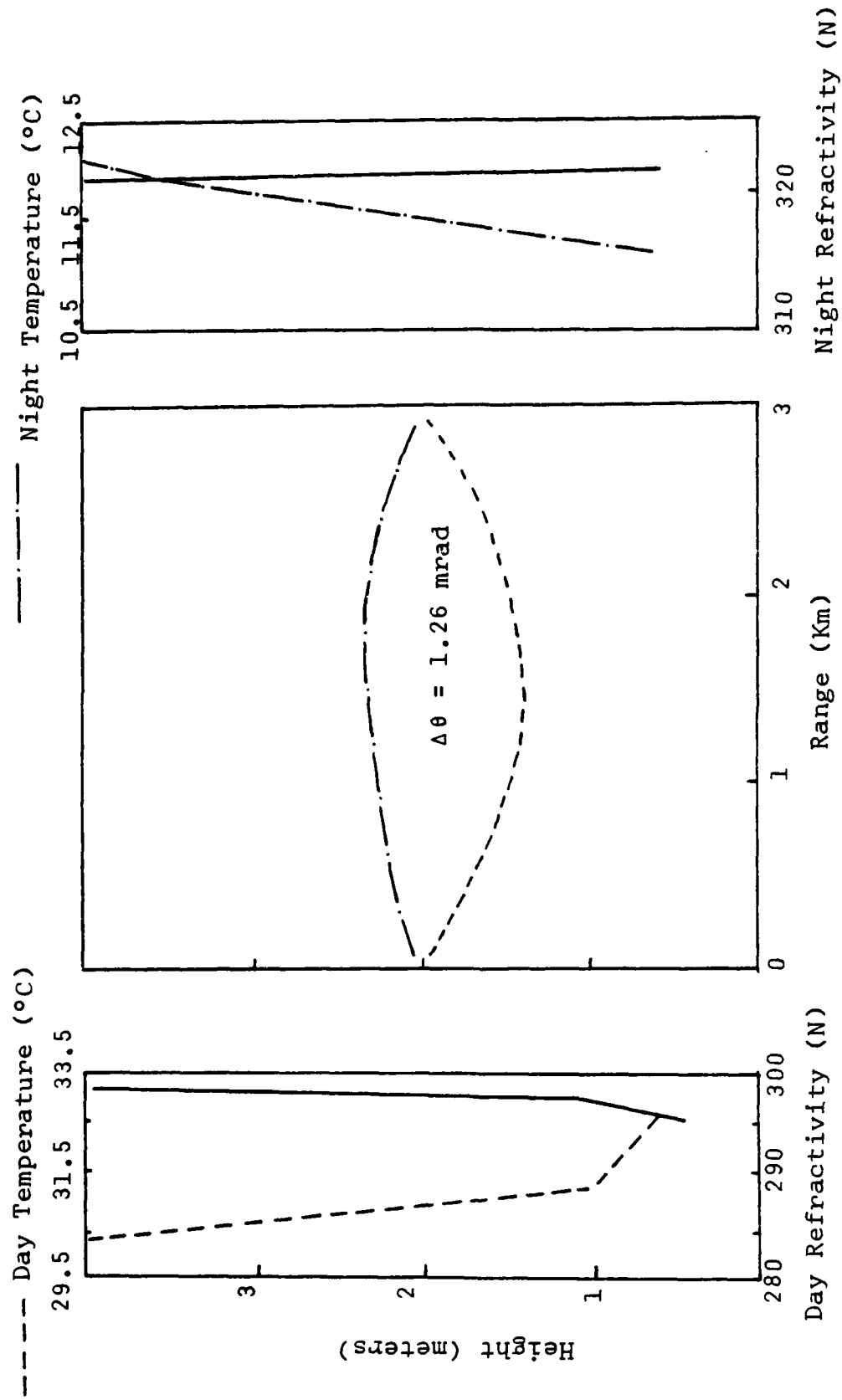


Figure 38. Desert Diurnal Refractive Characteristics and their effect on Infrared Propagation.

collected from weather stations located worldwide has led to the development of distinct climatic types, which are terrain types with similar climates found across the earth's surface. Table 6 is a list of climatic types and their associated meteorological and refractive characteristics.

Meteorological data collected at weather stations has been used to prepare climatic charts reflecting the percentage of time superrefractive conditions or ducting occurs, on the average, across the surface of the earth. These charts provide some idea as to the probability of occurrence of superrefraction, surface ducting, and elevated ducting in any region of interest where sufficient data has been collected, and also reflect the seasonal variation in anomalous propagation over most of the earth's surface. Figure 39 and 40 are representative of the types of graphic output climatic charts can present. These figures show the percent of occurrence of surface ducts, elevated ducts, and superrefractive layers. Note that Figure 39 is of Northern and Central Europe and Figure 40 is of the Mid-East. It is readily apparent that the percent of occurrence of surface layers and elevated layers varies a great deal between the two regions, and that coastal areas tend to show a greater occurrence of ducting than do inland regions. Charts like these, while helpful, do not show the percentage of time that subrefractive conditions occur, nor do they explain whether the anomalous propagation that they describe is

TABLE 6
CHARACTERISTICS OF CLIMATIC TYPES

TYPE	ANNUAL MEAN N, IN N UNITS	ANNUAL RANGE OF N, IN N UNITS	CHARACTERISTICS
I. Mid-Latitude Coastal	300-350	30-60	Stations near the sea or in lowlands and rivers. Located in latitude belts between 20° and 50°. Generally subtropical stations with marine or modified marine climate.
II. Subtropical-Savanna	350-400	30-60	Composed of lowland stations between 30° N and 25° S latitude. Rarely located far from the ocean. Tropical stations in this category exhibit definite rainy and dry seasons typical of Savanna climate.
III. Monsoon-Sudan	280-400	60-100	Monsoon climates generally found between 20° N and 40° N latitude. Climate produced by seasonal extremes of rainfall and temperature. Sudan climates located across central Africa from 10° N to 20° N latitude. Characterized by seasonal extremes of rainfall in a hot climate.
IV. Semiarid-Mountain	240-300	0-60	Found in desert and high steppe regions as well as mountain observatories at elevations greater than 1000 meters m.s.l. This group characterized by year round dry climate.

TYPE	ANNUAL MEAN N, IN N UNITS	ANNUAL RANGE OF N, IN N UNITS	CHARACTERISTICS
V. Continental-Polar	300-340	0-30	Widespread occurrence in middle latitudes and polar regions. Characterized by moderate or low temperatures. Mediterranean climates are included in this group due to low range resulting from characteristic dry summers.
VI. Isothermal-Equatorial	340-400	0-30	Tropical stations at low elevation between 20° N and 20° S latitude. Found almost exclusively along seacoasts or on islands. Characterized by monotonous, rainy climates.

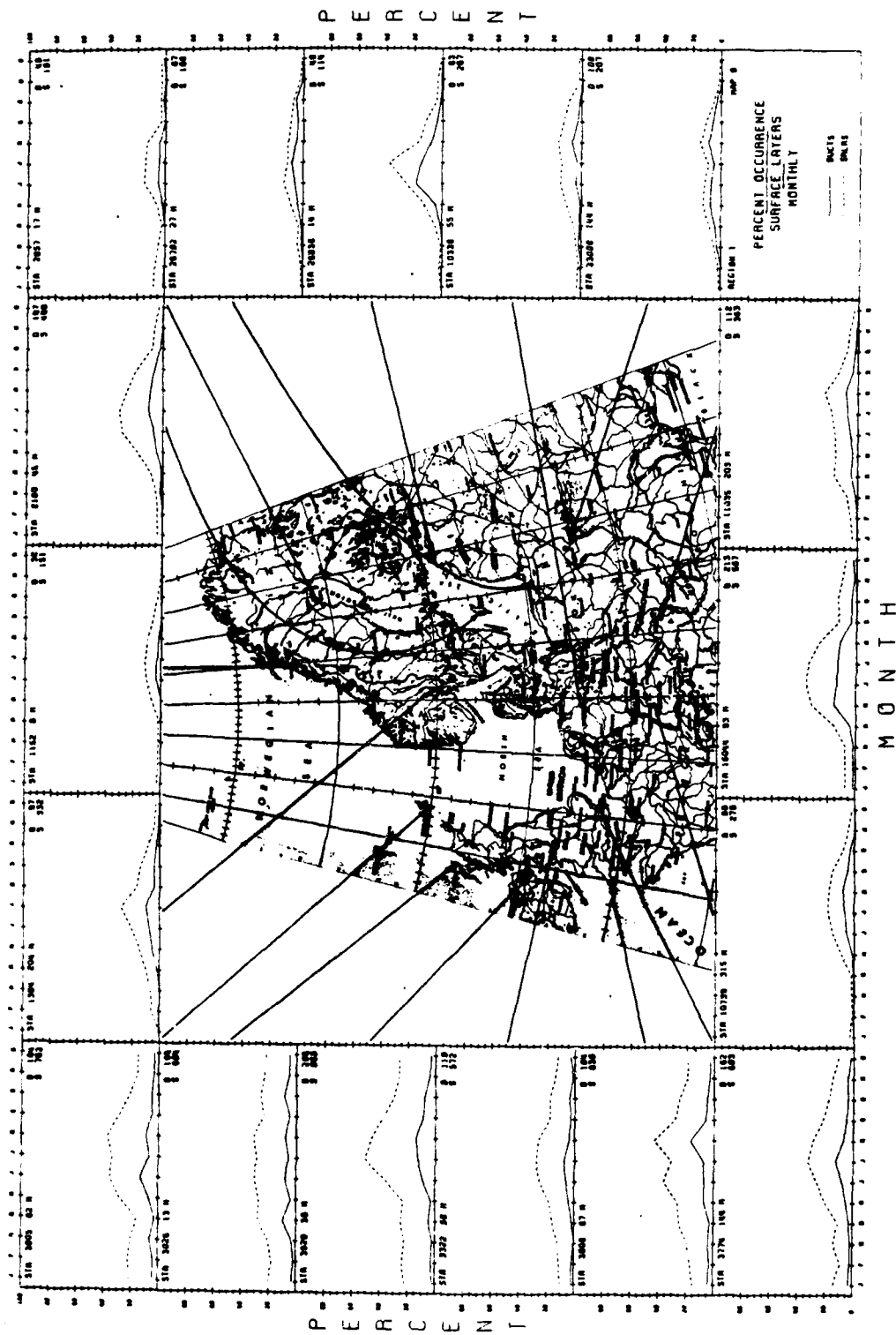


Figure 39A. Percent Occurrence of Surface layers for Northern and Central Europe.

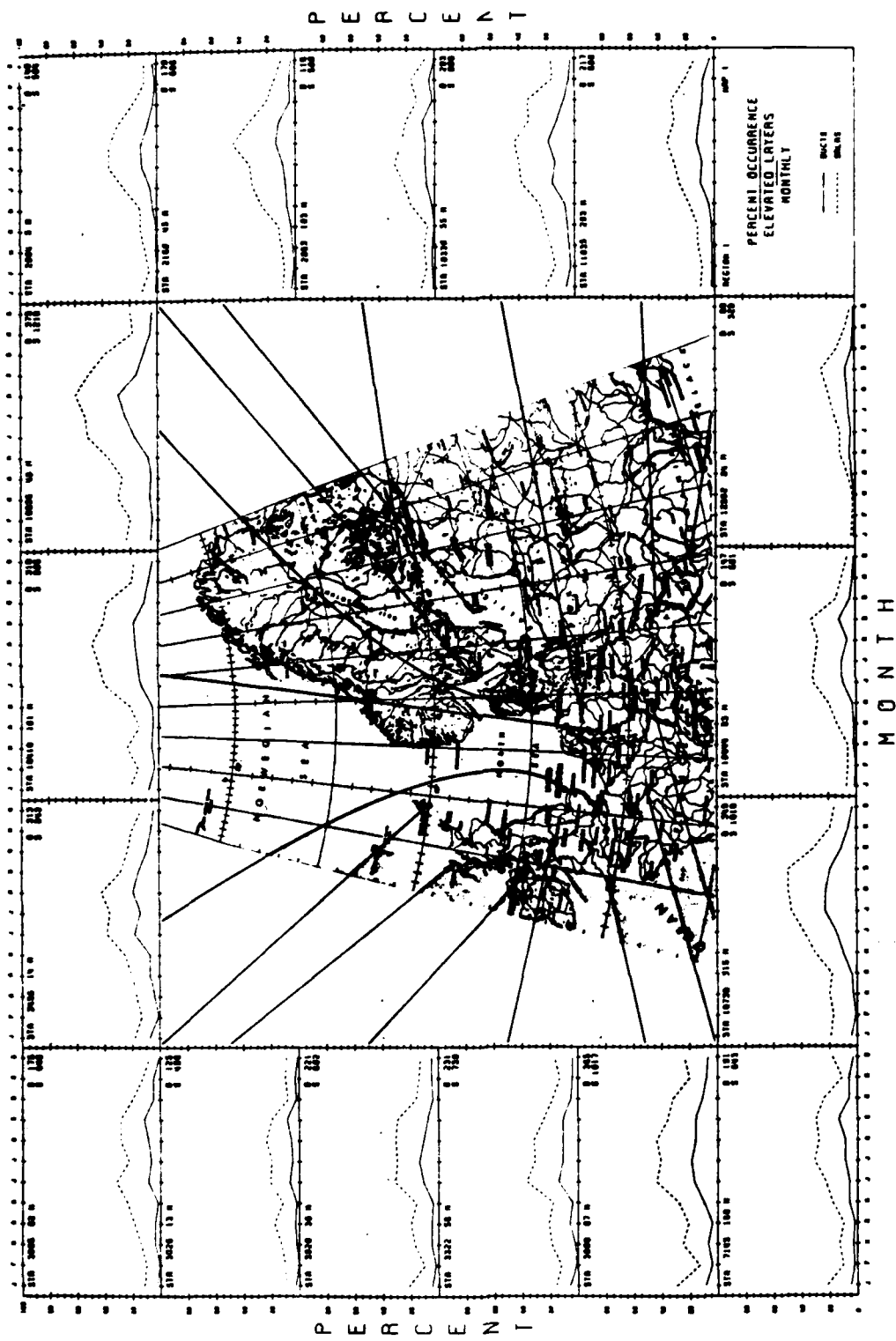


Figure 39B. Percent occurrence of elevated layers for Northern and Central Europe.

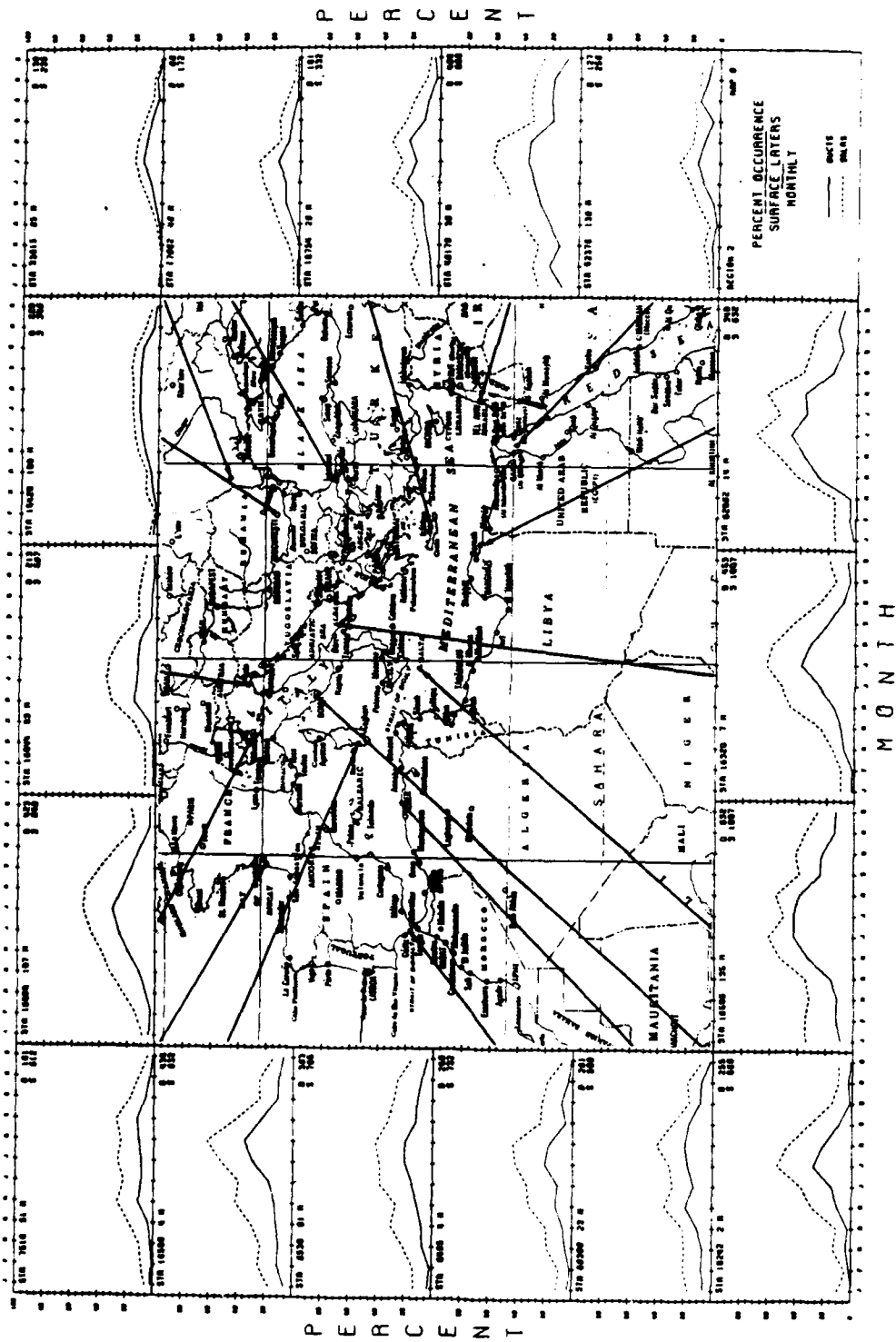


Figure 40A. Percent occurrence of surface layers for the Mediterranean region, to include the Mid-east.

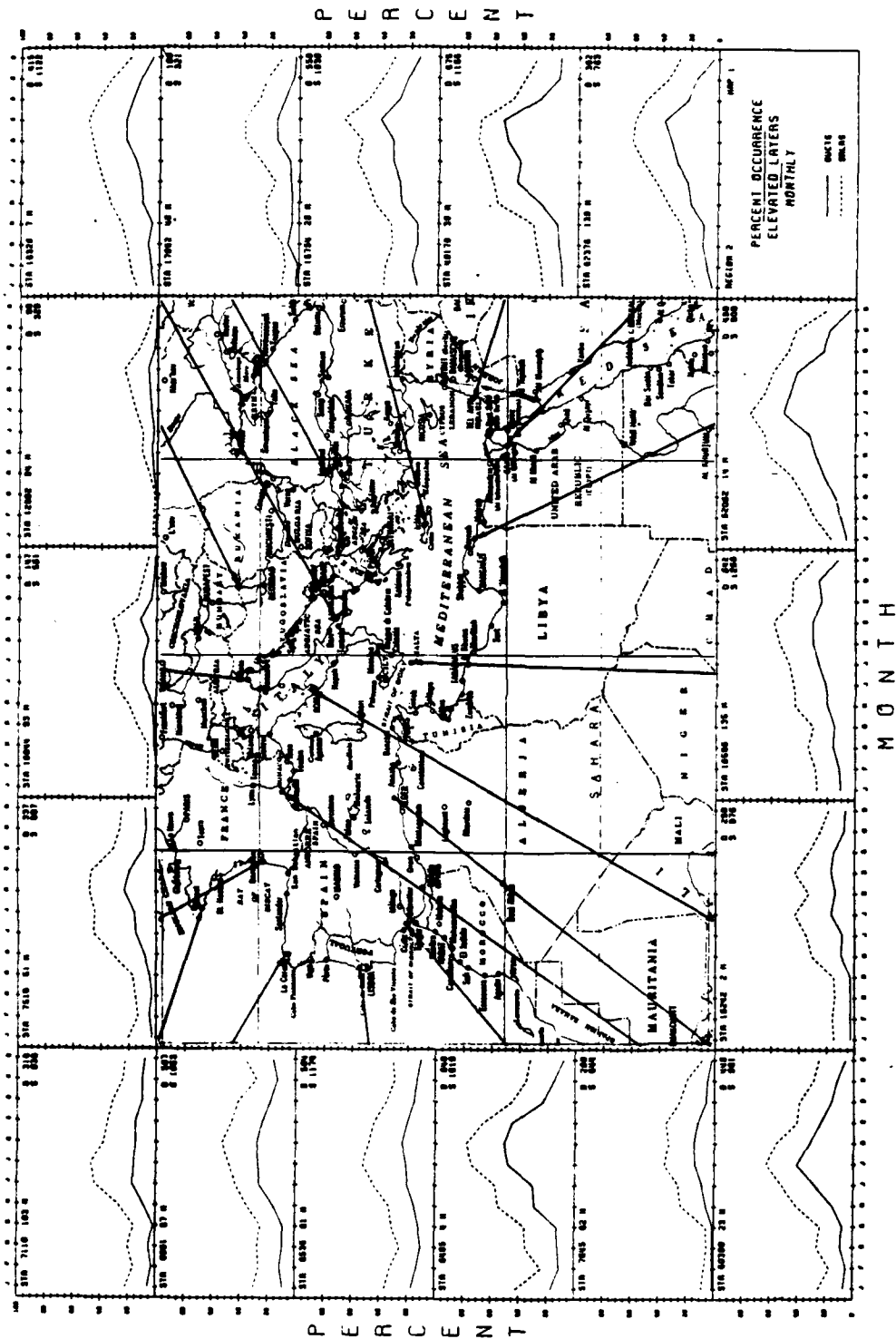


Figure 40B. Percent occurrence of elevated layers for the Mediterranean region, to include the Mid-east.

Forecasting turbulent conditions is, perhaps, more difficult than other forms of refraction, since the interplay of surface roughness, solar irradiance and wind strength is difficult to predict. Likewise, the direct measurement of C_n^2 is not always possible, however, Wesely and Alcaraz [Ref. 23: p. 9] state that an indirect method has been demonstrated. With this method, C_n^2 is calculated using sensible and latent heat flux components of the surface energy budgets, which are available in meteorological literature. This method is most accurate for heights of 4 meters or less, where comparison of values of C_n^2 determined by the indirect method and by direct measurements of C_n^2 appear to agree closely, and thus provide a reasonably accurate means of predicting turbulence over land. Just as with mirage conditions and subrefraction, turbulence conditions occur most often, and with the greatest strength, in desert regions in the late afternoon, but, as seen earlier, significant turbulence does occur elsewhere and at different times of day.

Although few actual climatic charts of turbulence conditions currently exist, over land solar heat flux charts and irradiance charts are available, and provide a fairly accurate idea of those regions where significant over-land turbulence can be expected. Figure 41 is an example of such a radiation chart. Note that, in general, the further away from the equator, the less solar radiation is received.

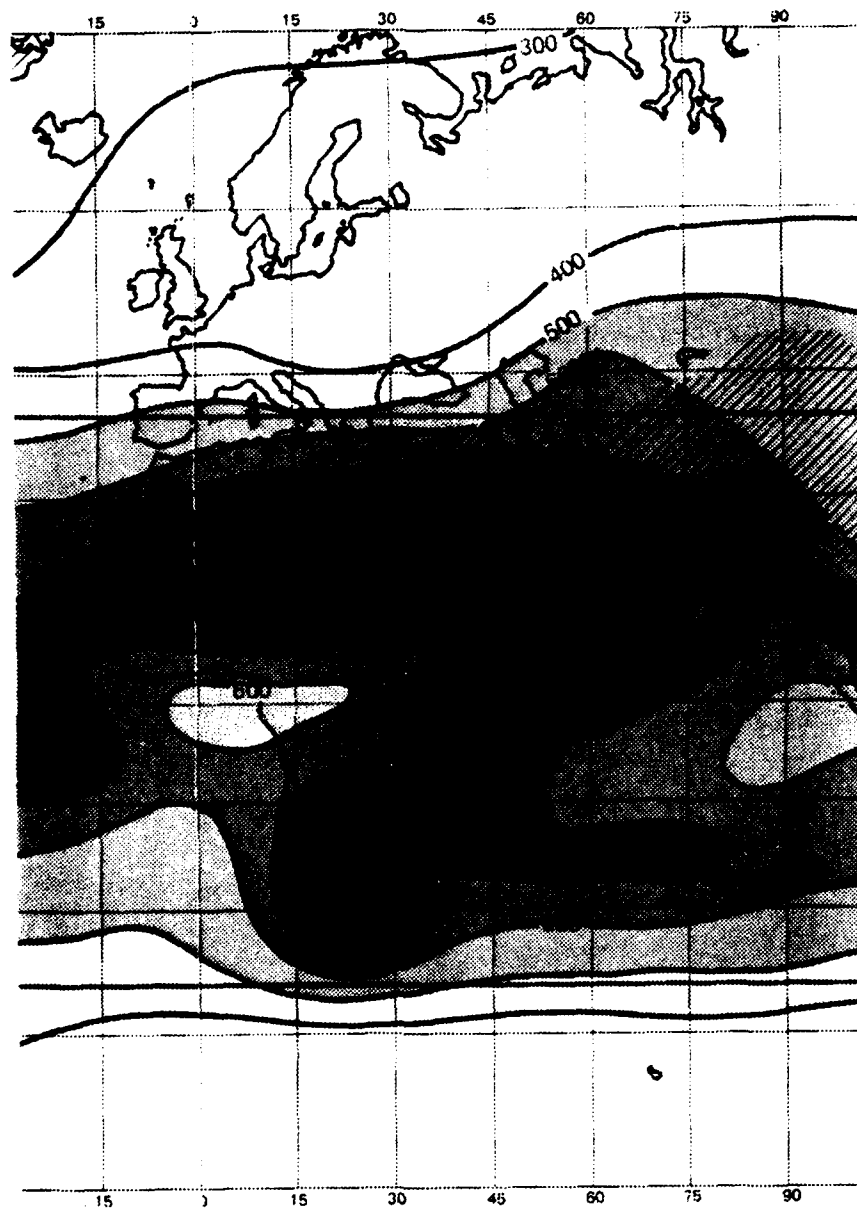


Figure 41. Solar radiation chart of eastern hemisphere measured in kJ/cm^2 .

3. Comparison of Mid-East and Central Europe

The Mid-East and Central Europe are two distinctly different regions in terms of both terrain and climate. The Mid-East generally is typified by a hot, dry climate with relatively little seasonal variation in temperature and humidity except for its southeastern areas, which are affected by monsoons. Much of the interior is rocky desert with coastal mountain ranges rising up along the Mediterranean Sea. Coastal regions on the Mediterranean Sea exhibit mild Mediterranean climates, while similar regions on the Arabian Sea are significantly affected both by continental air masses and by maritime air masses.

Central Europe has a continental climate, characterized largely by cold winters and cool-to-warm summers. There is a moderate amount of precipitation year-round and relatively high humidity in the summer months. Coastal regions tend to experience some modification of the continental climate by maritime air masses. The terrain varies from relatively flat, open land in the north to wooded, hilly, and mountainous terrain to the south.

It should come as no surprise, judging from the differences in climate and terrain, that the refractive characteristics of these two regions are distinctly different, as shown in Figure 39 and 40. The Mid-Eastern desert shows a significantly higher year-round incidence of both surface and elevated superrefractive conditions.

Before going any further, it must be noted that all measurements for the Mid-East are from coastal areas, and, thus, do not provide an accurate indication of the refractive conditions in the interior. Figure 42, however, shows that the incidence of superrefraction and elevated ducting decreases with distance from the coastlines - in the Mid-East, and in Europe as well. Figure 42 also highlights the seasonal nature of ducting and superrefraction by showing the wide variations between the average percent of annual occurrence of refractive conditions and the percent of occurrence for each month, given with the maximum occurrence of ducting and superrefraction.

Figures 39 thru 41 provide a good indication of general refractive conditions for these two regions. From these figures it is apparent that superrefraction and ducting occur far more commonly in the Mid-East than in Central Europe. Coastal areas in both regions show the greatest incidence of these forms of anomalous propagation, with the Mid-East coastline along the Arabian Sea showing an extremely high year-round incidence. Europe has a strong seasonal variation in the percent of occurrence of these two forms of anomalous propagation, whereas, in the Mid-East, this occurs only along the Mediterranean coast.

Subrefractive conditions, mirage formation, and optical turbulence are far more common in the Mid-East because of its hot, dry climate. Some incidence of mirage

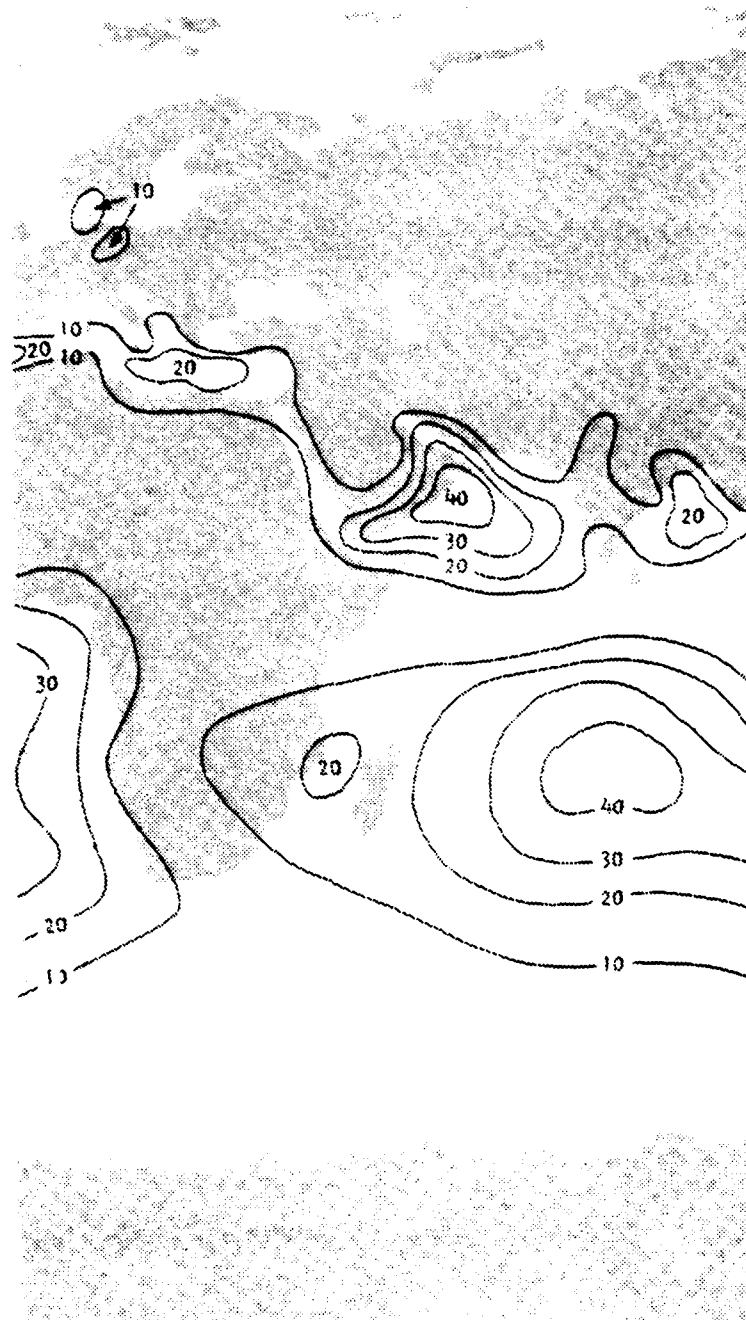


Figure 42A. Annual percent occurrence of elevated ducts.

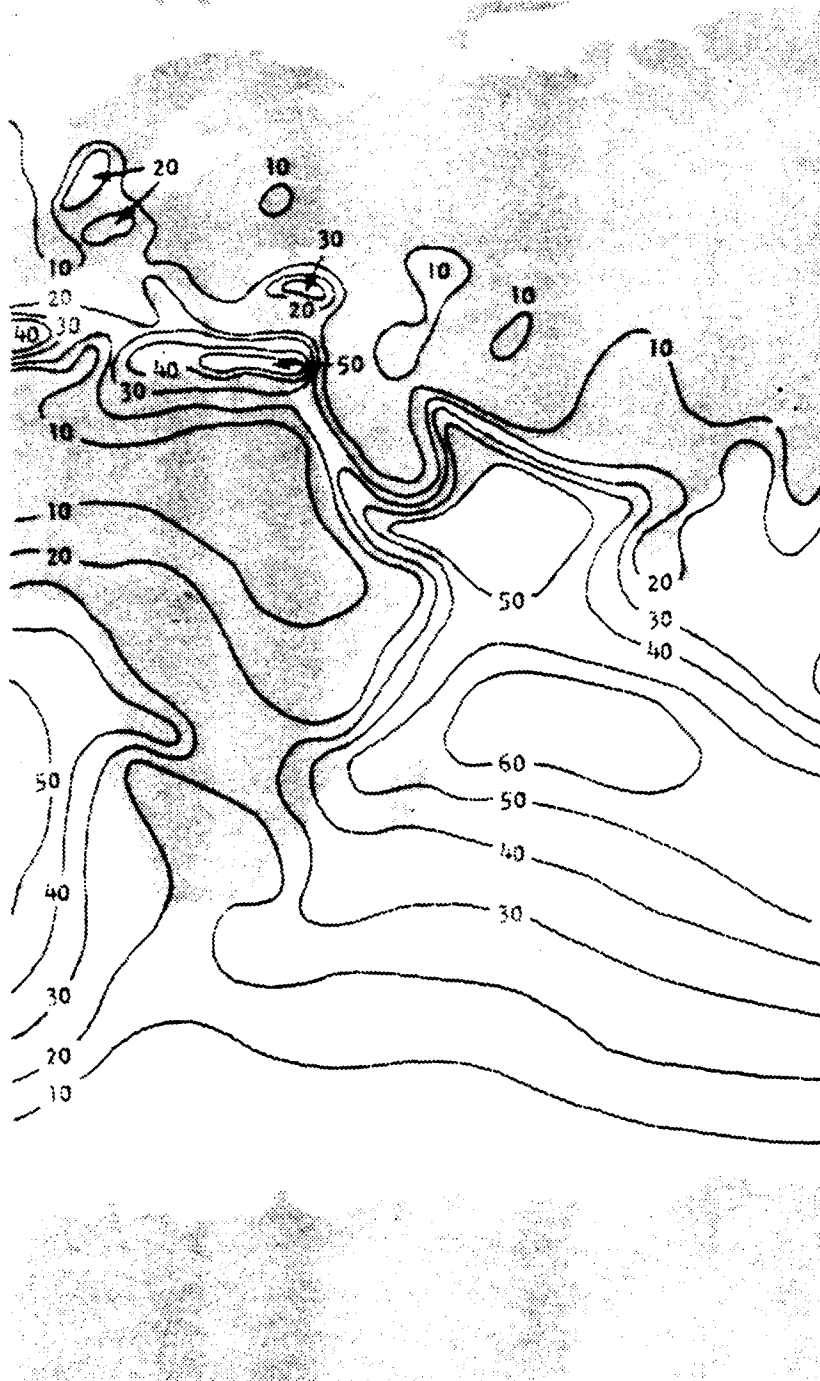


Figure 42B. Percent occurrence of elevated ducts during the month of maximum occurrence. This month of maximum occurrence varies from region to region.

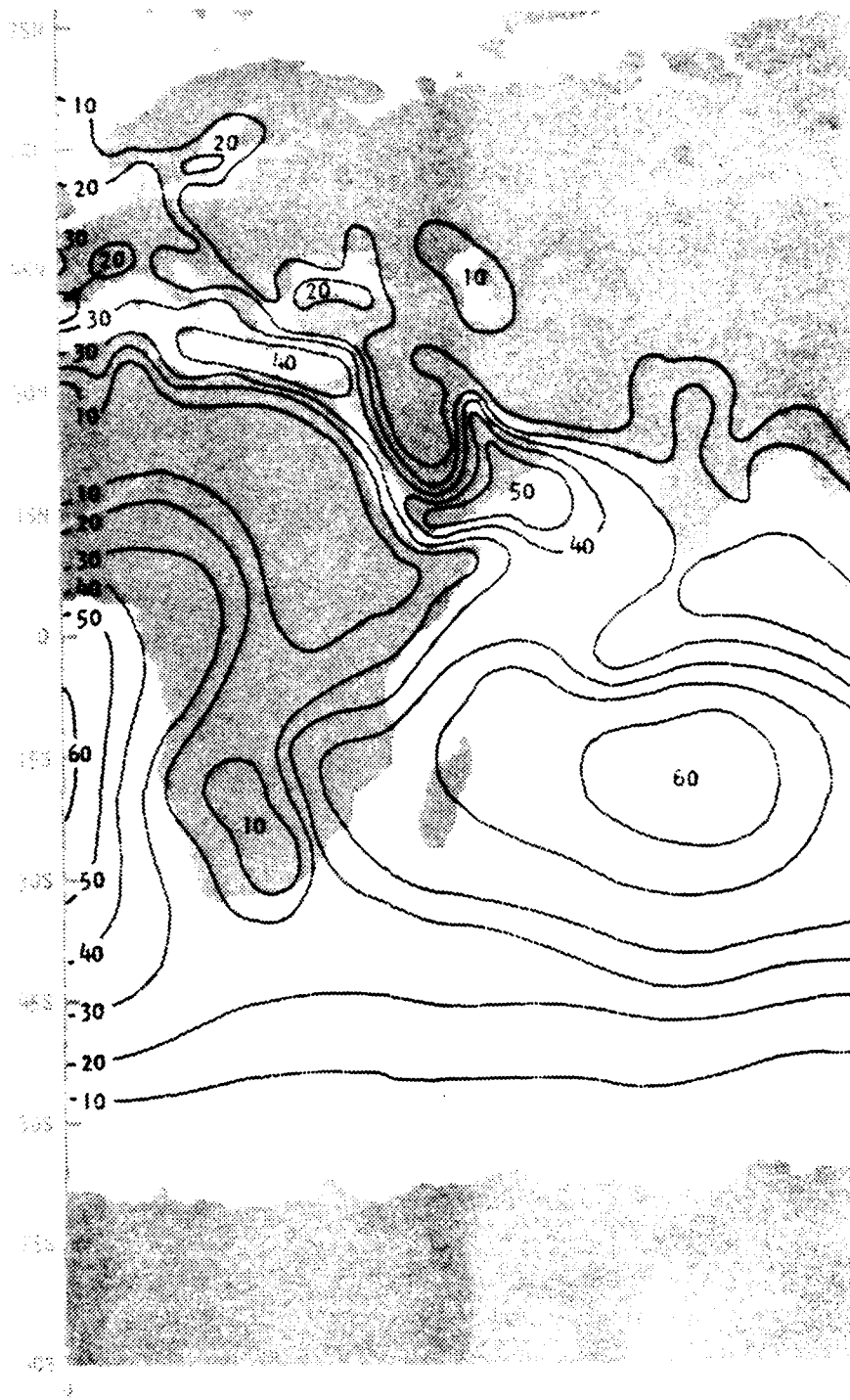


Figure 42C. Annual percent occurrence of superrefractive layers (SRLRS).

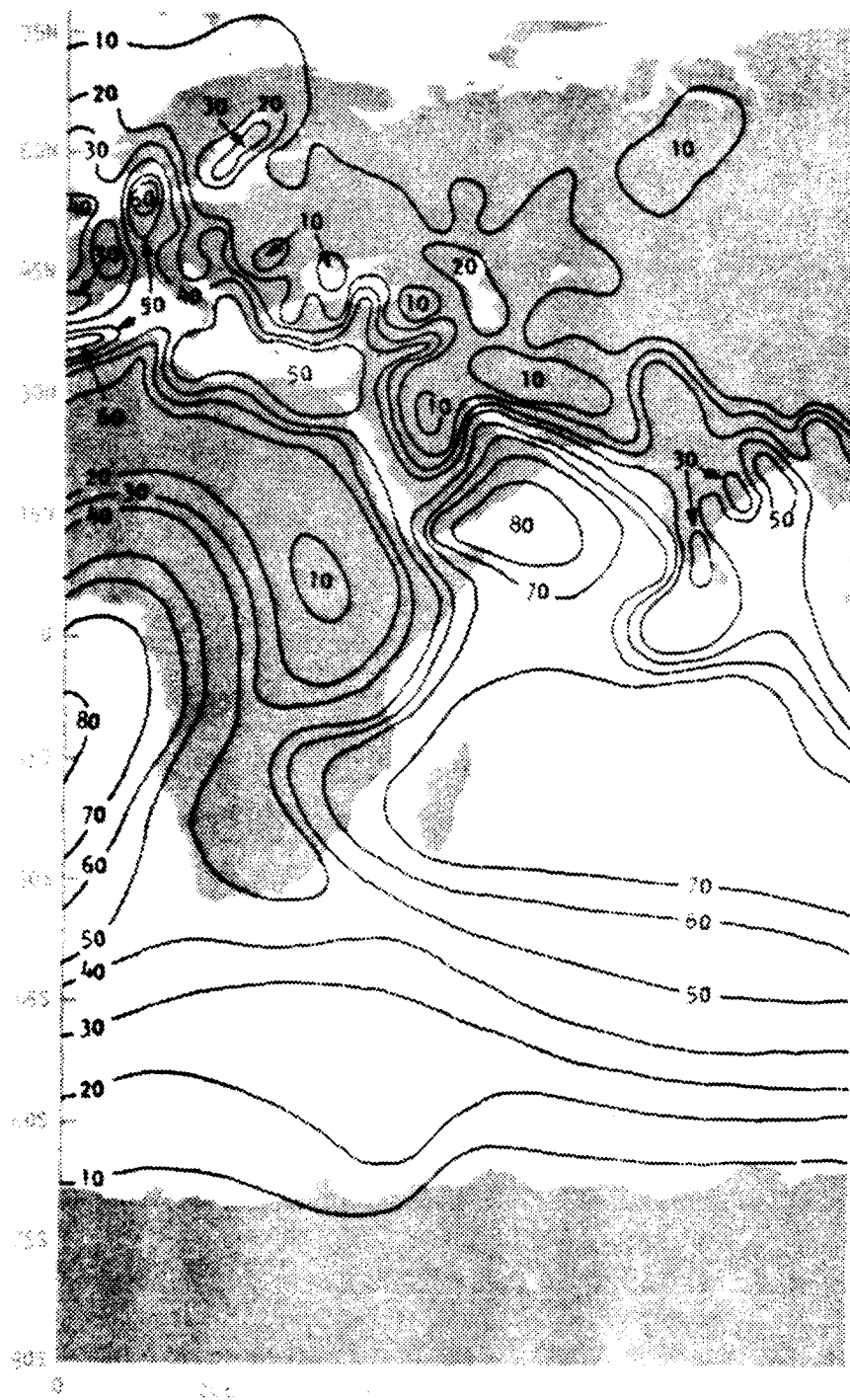


Figure 42D. Percent occurrence of superrefractive layers (SRLRs) during the month of maximum occurrence. This month of maximum occurrence varies from region to region.

formation is found in Europe, particularly over relatively large bodies of water and in the more arid south, but only during the warmer summer months. In the Mid-East, these conditions occur year-round and are fairly regular phenomena. By referring to Figure 41, it can be seen that the Mid-East receives a far higher level of solar irradiation annually than does Europe, and this provides the primary ingredient for the formation of subrefraction, mirages and optical turbulence.

4. Conclusions

Although it can be shown, with some accuracy, just what percentage of the time superrefraction and ducting can be expected to occur worldwide, and, to a lesser extent, subrefraction, mirage formation, and optical turbulence, it is difficult to determine just where the occurrence of these refractive characteristics becomes "significant". Such decisions must be based on each specific weapons system (or component of a weapons system) affected, and on the nature of the effects, as well as on the expected probability of occurrence of anomalous propagation. Much research is being conducted by the U.S. Army at the Atmospheric Sciences Laboratory at White Sands Missile Range and at the U.S. Army Electronic Proving Grounds (EPG) at Fort Huachuca, Arizona. The research concerns the refractive effects for specific regions of the EM spectrum, and on specific weapon systems.

What can be determined by the results of this discussion is that the various forms of atmospheric refraction are not rare, and may even be the norm in certain regions of the world at certain times of the year. Due to the wide regional variability in refractive forms and in probability of occurrence, it becomes apparent that each region of the earth poses a unique refractive problem. For this reason, when considering military operations in a specific region, the potential refractive conditions should not be approached in generalities, but, rather, should be addressed specifically to the region of interest.

III. ATMOSPHERIC REFRACTION AND GROUND WARFARE

A. INTRODUCTION

In Section II of this thesis, the three major forms of atmospheric refraction were discussed. The characteristics of each of these forms and their effects on EM waves propagating through the atmosphere were elaborated on at length in sub-Sections C through E. Those discussions showed the wide diversity of both the forms of refraction and their effects across the EM spectrum. Sub-Section F described the factors affecting the ability to predict and forecast atmospheric refractive conditions, contained a general discussion of the probability of occurrence of the various forms of atmospheric refraction across the earth's surface, and concluded with a description of the conditions characteristic of the Mid-East and Central Europe.

The purpose of this background was to show that atmospheric refractive conditions which have a measureable effect on EM signals should not simply be considered as so rare or unpredictable that they can be "written off" as inconsequential. Rather, it has been shown that, at times, these conditions are quite common, can have a significant impact on EM signal propagation, and are reasonably predictable. Of course the probability of occurrence and

ability to forecast the three major forms of refraction varies from region to region (and often season to season) across the earth.

With this general background as a foundation, the remainder of this thesis will now discuss specific examples of the effects of atmospheric refraction. This will be done in two ways - by use of computer simulations and by qualitative study. The examples will cover the full EM spectrum and are intended to enhance the reader's understanding of this subject as important for the employment of weapon systems utilizing the EM signals propagating through the atmosphere.

B. EFFECTS OF ATMOSPHERIC REFRACTION ON TANK OPTICAL FIRE CONTROL SYSTEMS

This example is based on private communications⁴ with Dr. Don Snider of the Atmospheric Sciences Laboratory (ASL) in White Sands, New Mexico. This section discusses the effects of superrefractive and subrefractive conditions on the accuracy of tank fire. The tank's optical fire control system (using both visible light and IR energy) and current

⁴ The communication with Dr. Snider concerned the effects of atmospheric refraction on tank optical fire control accuracy.

tank gunnery techniques (boresighting, synchronizing, zeroing of the main gun, and firing at center-of-mass) are addressed.

Current tank gunnery doctrine, as described in FM 17-12 [Ref. 24: pp. 4-9 - 4-10], requires boresighting and synchronizing both sights and main gun, followed by zeroing the tank weapon systems prior to firing the tank's main gun and machine gun(s). Boresighting establishes a convergent relationship between the axis of the tube of the main gun and its direct fire sight. Synchronization insures that main gun and sights remain aligned when they are elevated and when they are depressed. The tank crew is expected to fire from boresight using telescope and periscope during the day and, if so desired, the IR night vision sight at night. At the same time the crew must compensate for drift, cant, parallax, tube droop and winds on the battlefield. As would be expected, there are a great many potential sources of error involved in tank gunnery. The magnitude of the sources of error will vary depending on internal and external conditions (relative to the tank) and on the weapon and ammunition being fired.

Figure 43 shows a typical tank fire control error budget. It is currently thought that the most important cause of error in firing the kinetic energy (KE) round is round-to-round variation and loss of zero or improper zero. For the slower HEAT round, crosswinds and air temperature extremes

ERROR SOURCE (mr)	KE		HEAT	
	AZ	EL	AZ	EL
MUZZLE VELOCITY	-	.036	-	.106
RANGE ERROR	-	.015	-	.068
JUMP DISPERSION	.050	.050	.050	.050
CROSSWIND & GUST	.078	-	.564	-
RANGE WIND	-	.001	-	.035
AIR TEMPERATURE (MACH NO)	-	.008	-	.106
ATMOSPHERIC PRESSURE	-	.008	-	.131
AIR TEMPERATURE	-	.021	-	.342
OPTICAL PATH BENDING	-	.005	-	.005
EARTH RATE	.080	.080	.128	.128
SYNCHRO NETWORK	.109	.109	.109	.109
BORESIGHT	.030	.030	.030	.030
ROUND-TO-ROUND	.300	.300	.270	.240
ZEROING	.194	.214	.250	.203

Figure 43. Typical tank fire error budget. KE is the Kinetic Energy round and HEAT is the High Explosive Antitank round.

are thought to cause the greatest errors in azimuth and elevation. Note that, originally, the figure shows optical ray bending causing only minor errors in elevation.

It was the contention of the ASL report that the full effects of atmospheric refraction were not being considered in current tank gunnery doctrine, particularly those effects created in a hot/arid or semi-arid environment. The ASL proposed that refraction was affecting tank gunnery in two ways. First, atmospheric refraction could be inducing major elevation errors at ranges beyond 1500 meters. Second, those elevation errors currently blamed on other sources could actually be due to refraction.

1. Atmospheric Conditions Creating the Gunnery Errors

As was previously described in Section II, atmospheric refraction patterns tend to follow a distinct diurnal pattern over land. During the day, the surface is heated up by the sun, and, in hot/arid or semi-arid regions this heating can cause an atmospheric temperature structure, such that the temperature decreases rapidly with elevation. This condition can cause optical turbulence, subrefraction, mirage formation, or a combination of all three. At night, the earth's surface re-radiates the heat absorbed during the day into the atmosphere, often leading to the creation of a temperature inversion. This inversion is the exact opposite of the temperature structure that characteristically forms in the late afternoon. About one-half hour before sunset,

and some time just after dawn, a condition is formed when the heat radiating from and into the ground is roughly equal.

Local weather conditions, such as the presence of a high pressure region, can have a significant impact on atmospheric refraction. Depending on the weather conditions present, the diurnal characteristics described above can be affected in such a manner as to enhance or degrade either the subrefractive condition, the superrefractive condition, or both. Thus, atmospheric refractive conditions can vary significantly through the day, and from one day to the next.

The ASL report was primarily concerned with the effect of going from a subrefractive condition during the day to a superrefractive condition (characterized by the temperature inversion) at night, then back again to the subrefractive condition.

2. Expected Effects on Tank Gunnery

Since optical signals bend toward the denser medium, the direction of bending for the diurnal condition described above would be opposite for day (subrefraction) and night (superrefraction). This is graphically shown in Figure 38. If a target were located at a given range, its image would appear to shift upward at night and downward during the day. Figures 27A and 27B show such effects, created by a very strong temperature inversion (superior mirage) and an equally strong subrefractive condition (inferior mirage).

It should be noted that a mirage need not be present for the upward and downward shifting of an image to occur.

Bending of optical rays can cause a gunner to aim at an image point which is high at night or low during the day, as shown in Figure 44. Since most tank crews boresight and zero their tanks during the day, the effects of subrefraction due to surface heating are largely removed. But this can result in a much greater error at night, as shown in Figure 45. It should be reiterated here that there is little difference between the amount of refractive bending of visible light and of IR energy. Thus, the same errors occur going from an optical fire control system using visible light during the day to one that uses IR at night.

3. Experimental Results

An experiment was conducted by the ASL to determine whether the theorized refractive effects do, in fact, occur. An American tank, using currently-deployed optical fire control equipment and current gunnery doctrine, was used in the experiment, which took place at White Sands Missile Range. An eight foot by sixteen foot target was used. The tank was boresighted, synchronized, and zeroed during the day, and compensation was made for as many external and internal sources of error as possible. Special effort was made to maintain the correct boresight while firing. If the boresight was off by .1 mils or more the gun was re-boresighted.

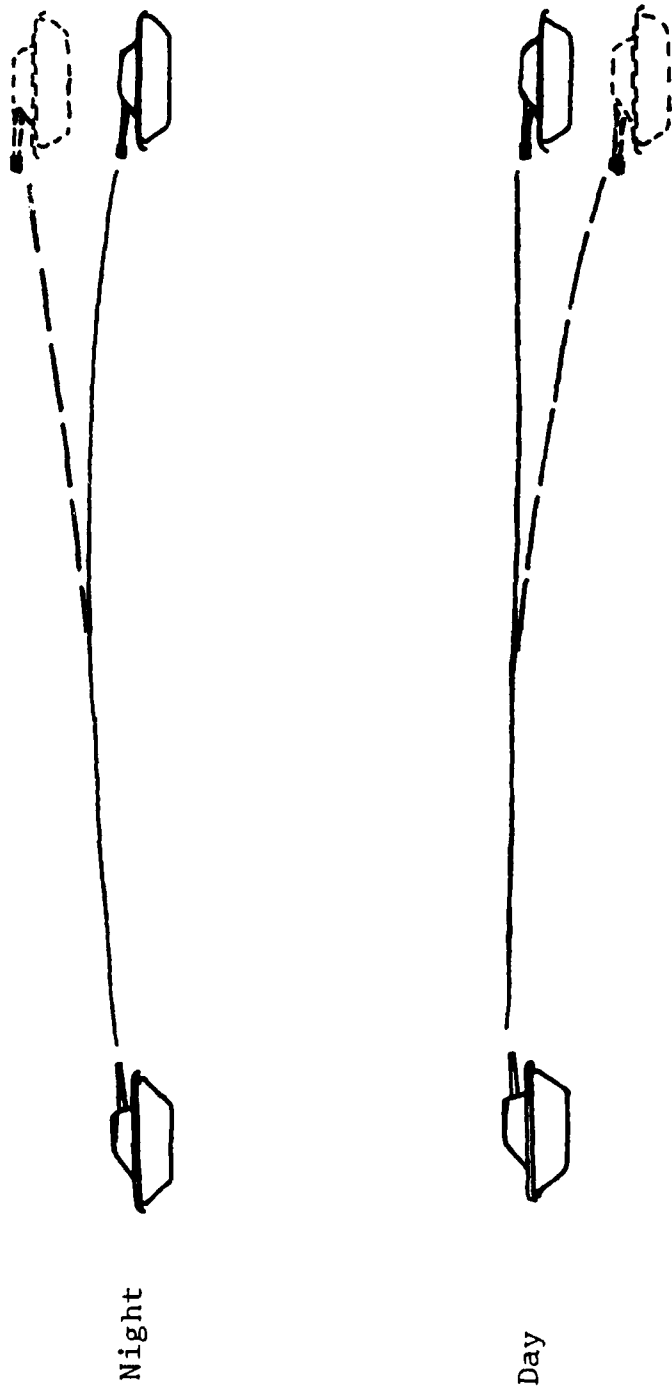


Figure 44. Firing from a neutral boresight and zero (dawn or dusk). The dashed tanks are the images actually seen and aimed at.

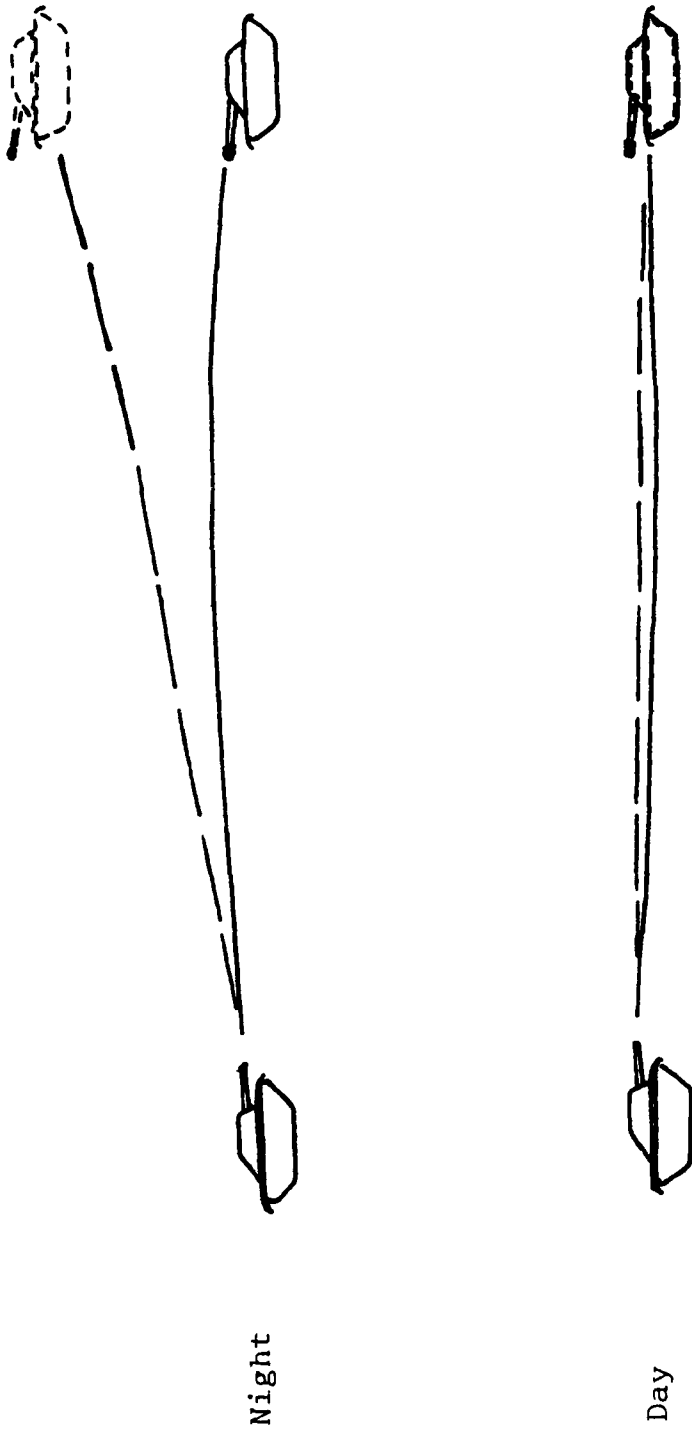


Figure 45. Firing from daytime boresight and zero. The dashed tanks are the images actually seen and aimed at.

Once the main gun had been satisfactorily zeroed, a series of 5-round shot groups was fired over a two-day and three-night period. The results of these firings are shown in Figure 46. This figure clearly shows that the centers-of-impact of the nightfired groups were higher on the target than those of the day groups. The group shifts are measured relative to the center of impact of the zero confirmation group.

The inversion and temperature lapse strengths can be deduced by the relative distance between the day and night 5-round groups. As can be seen, the greatest distance between shot groups occurred between the first night and the first day, and the differences between the groups progressively became less and less. On the first night the air was calm and clear, resulting in the creation of a strong superrefractive condition. The second night the sky was hazy, weakening the superrefractive condition. On the third night a front moved in, bringing winds and clouds which all but eliminated the superrefractive condition. The correlation between shot placement and weather conditions shows that refractive errors and tank fire accuracy are greatly affected by weather conditions.

A statistical analysis was performed by the ASL, proving that the day shots and night shots were from two statically different populations. The results of this

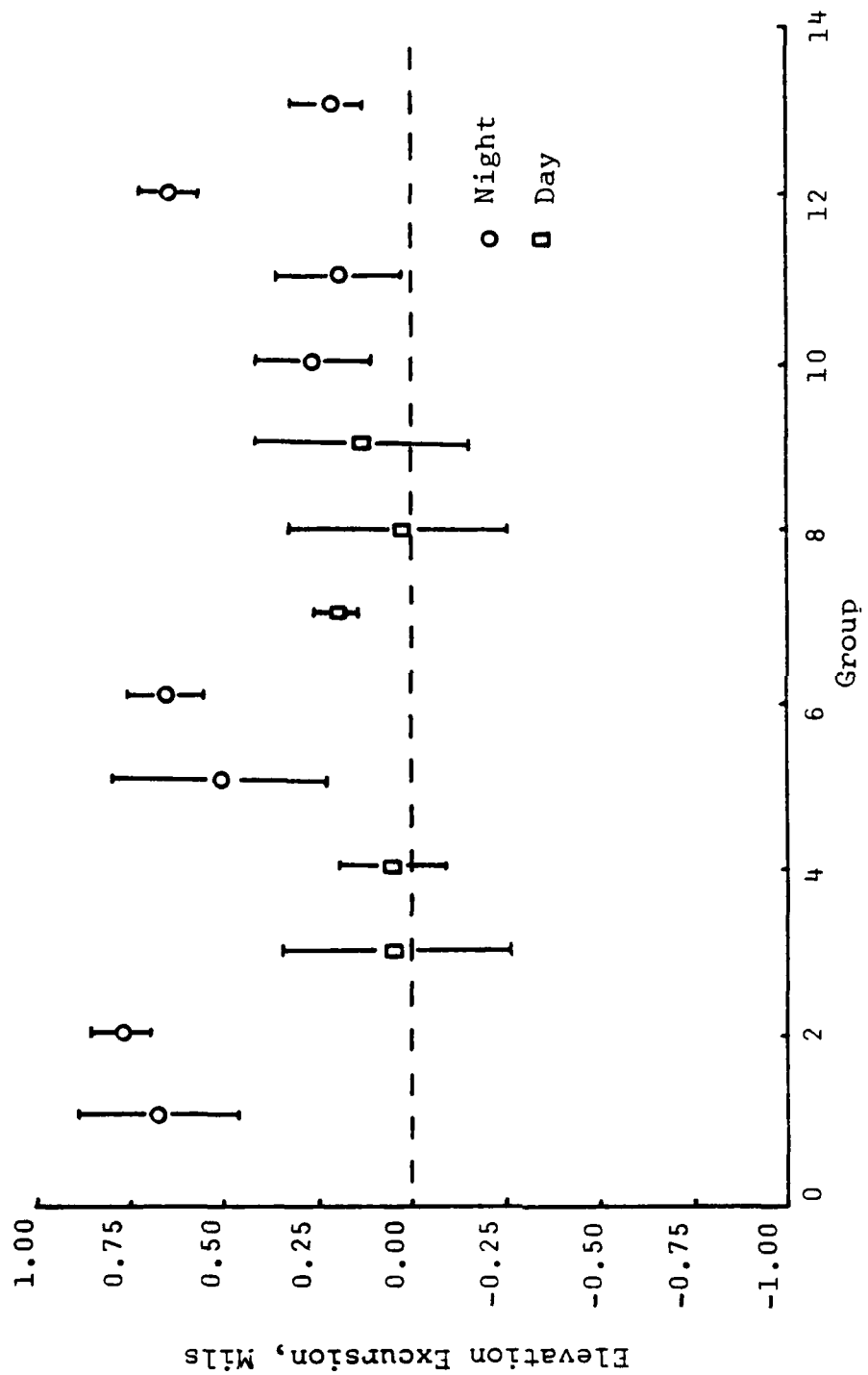
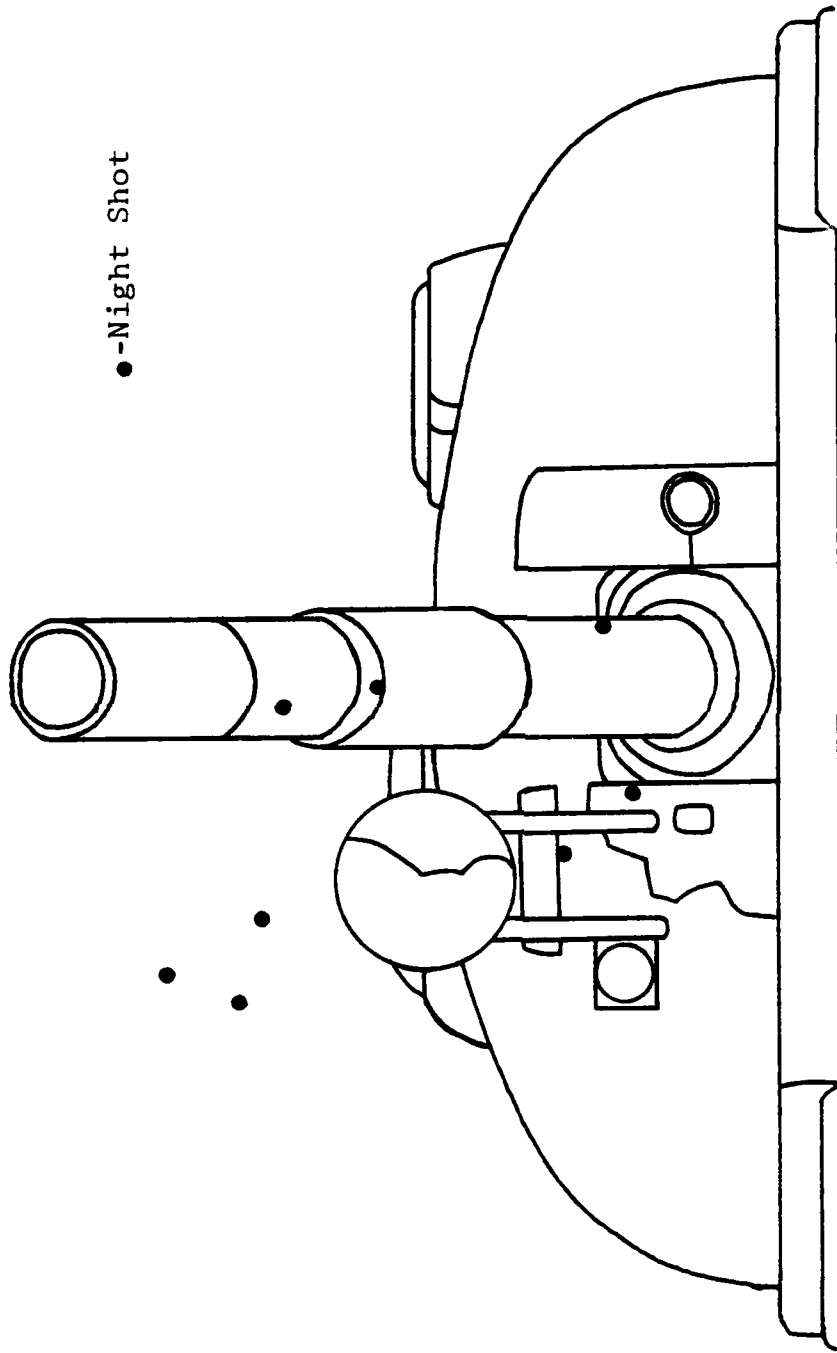


Figure 46. 5-round group centers of impact of tank main gun fire.

analysis showed, at a 95% confidence level, that the distance between the two shot centers was at least 46 cm.

To bring the effect of the difference between shot groups into perspective, Figure 47 shows how many of the night shots would have missed the target if the gunner had actually been shooting at a silhouette of a T-62 tank while aiming at the base of the turret. This figure is based on the results of a vertical T-test of the 5-round shot groups, which determined the one sigma standard deviation in elevation and azimuth for each group.

Although the above statistical analysis does show significant differences between day and night shot groups, it does not prove that the differences are due to refraction. To prove this relationship, temperature measurements at various altitudes above the ground were made concurrently with the firings. These measurements were made at .5 meter intervals from 0-to-4 meters above ground level (AGL). Apparent elevation angle measurements using a theodolite were also made just prior to each firing. These measurements were made so that the line-of-sight of the theodolite was roughly parallel to the tank's, and was at the same height AGL. A regression analysis was then conducted, which showed a definite correlation between the temperature gradient, the theodolites observed absolute elevation variations, and the shot pattern elevation shifts during



●-Night Shot

Figure 47. Silhouette of T-62 tank indicating that many night shots would have missed the target when using a daytime zero.

firing. These interactions showed a significant relationship between refraction and firing errors, as shown in Figures 48 and 49.

In order to assess the importance of these refractive effects, based on the probability of occurrence of the necessary refractive conditions, the ASL investigated the frequency of occurrence of those atmospheric conditions which led to the most significant firing errors. Figures 50 and 51 give a general idea of the frequency of occurrence of clear skies and light winds in southern Germany and in Iran, which would roughly indicate the occurrence of refractive conditions. Note that, for both cases, these conditions can be quite common at certain times of the year.

4. Conclusions

The results of the ASL experiment showed that a definite and systematic day/night shift in elevation angle can occur for certain meteorological and surface conditions. The values measured agreed closely with what was predicted by theory. The magnitude of the measured effect was as great as .8 mr. At longer ranges even larger effects would be expected. Because the occurrence of temperature gradients most conducive to the greatest refractive effects is characteristic of hot/arid and semi-arid regions, it is expected that gunnery errors of this type will occur most frequently in the desert regions of the world.

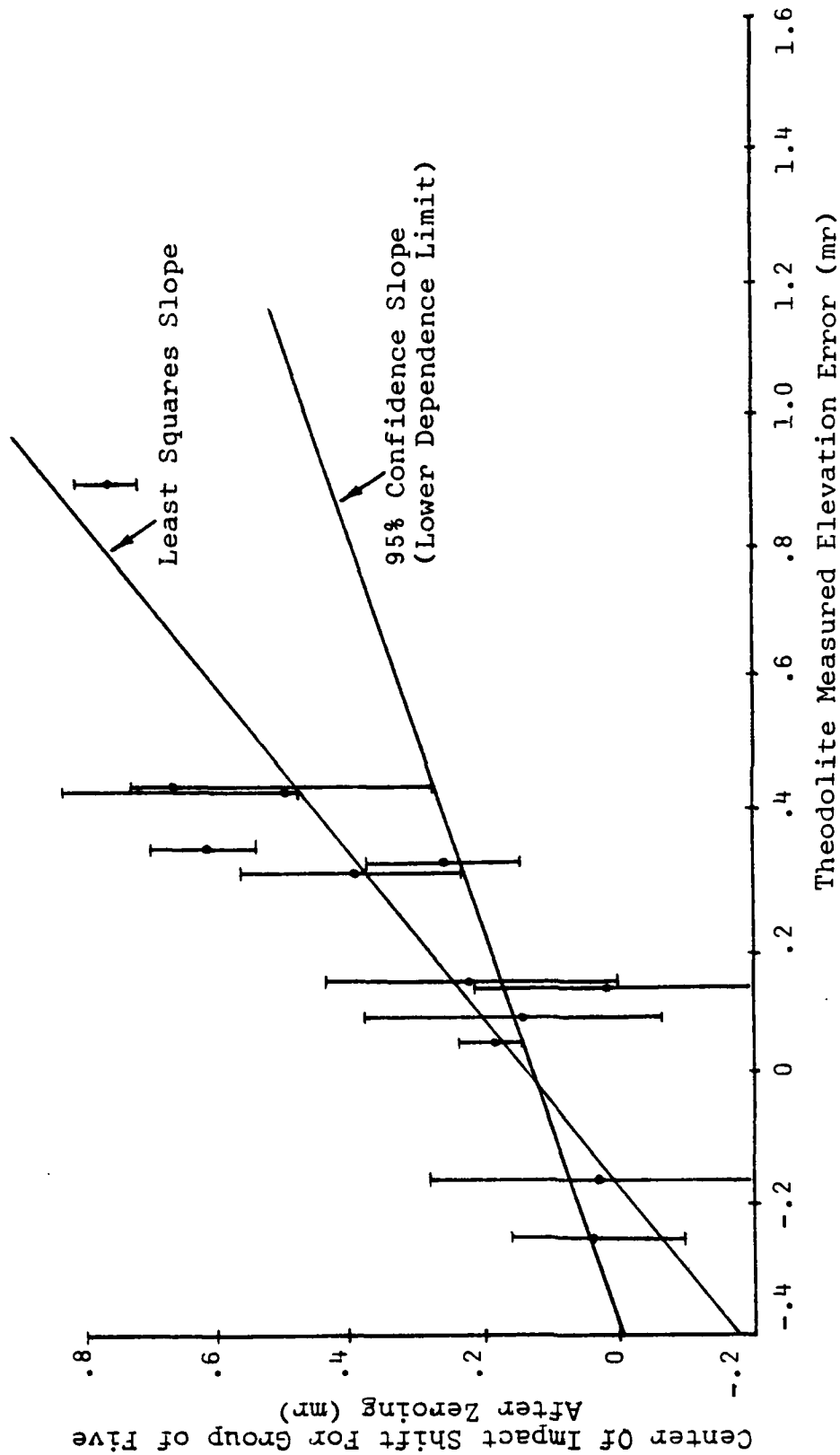


Figure 48. Test Results vs Predictions. If the 95% line slope were zero or negative, there would be no correlation between variables. This graph, however, shows that there is a definite correlation between the theodolite's observed absolute elevation variations and the shot patterns elevation shifts during firing.

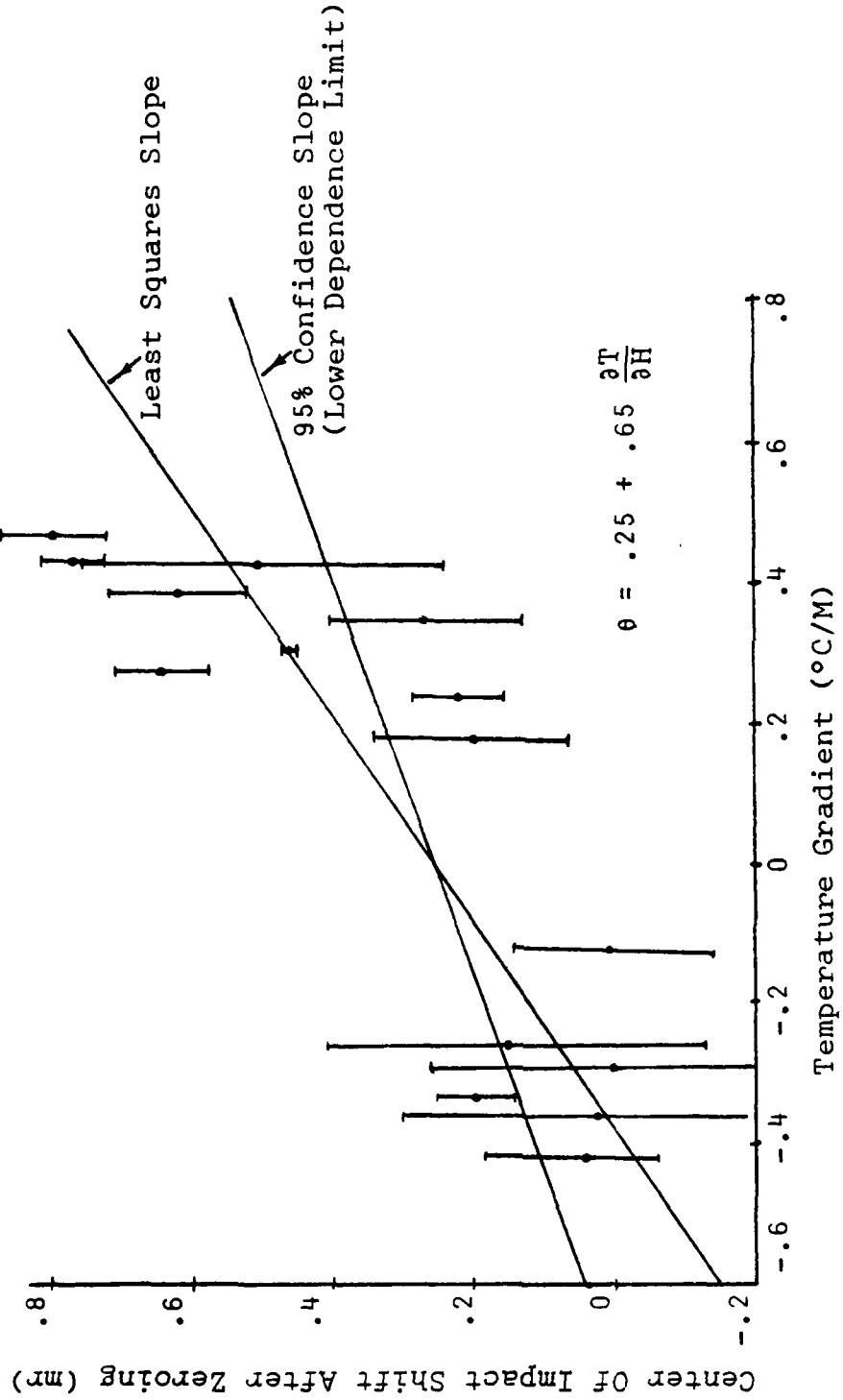


Figure 49. Firing Errors vs Temperature Gradients. The slope of this graph compares well with a theoretical slope of .75.

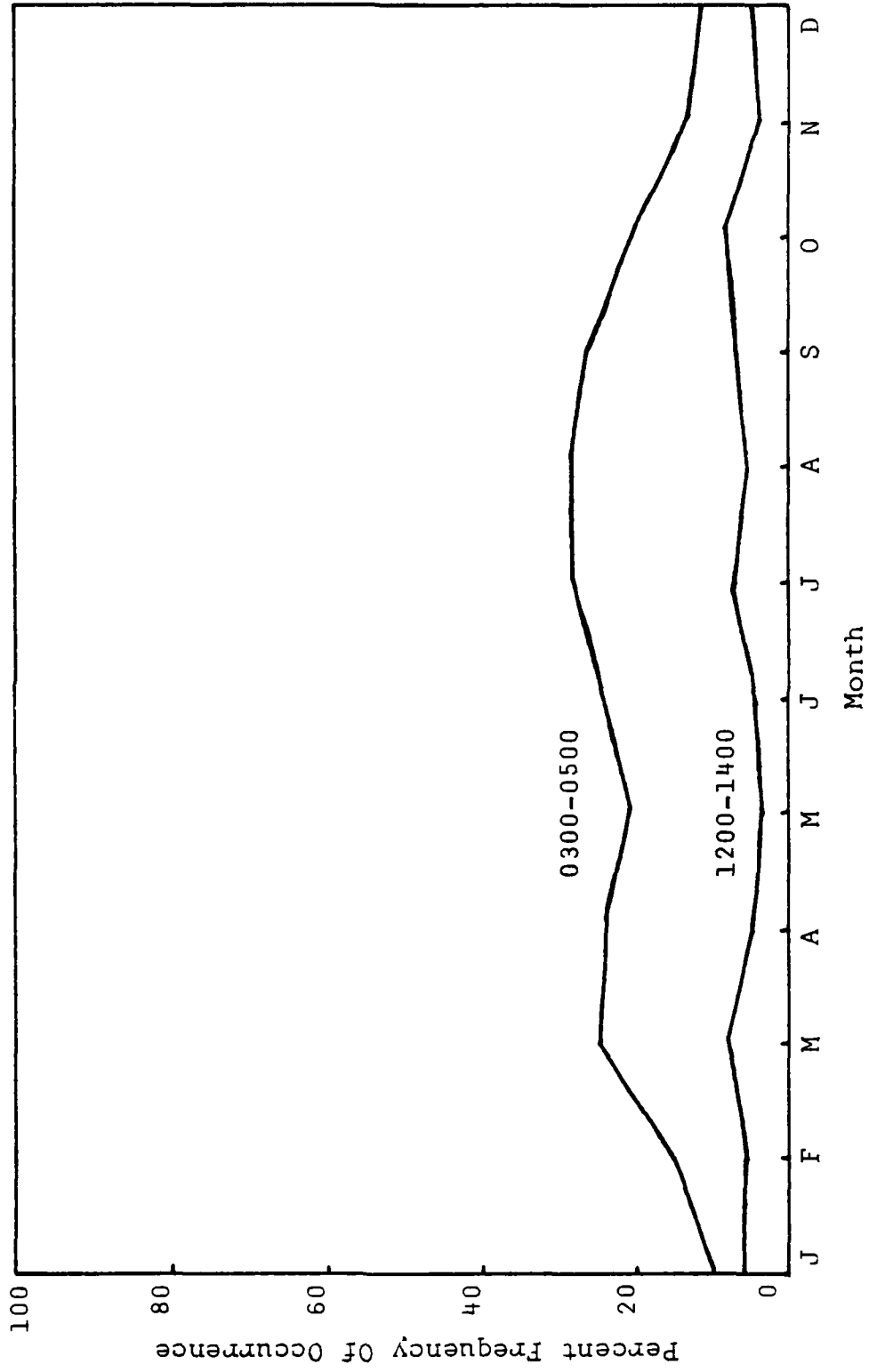


Figure 50. Percent frequency of occurrence of clear skies and windspeed from 0 to 5 knots for Grafenwohr, F.R.G.

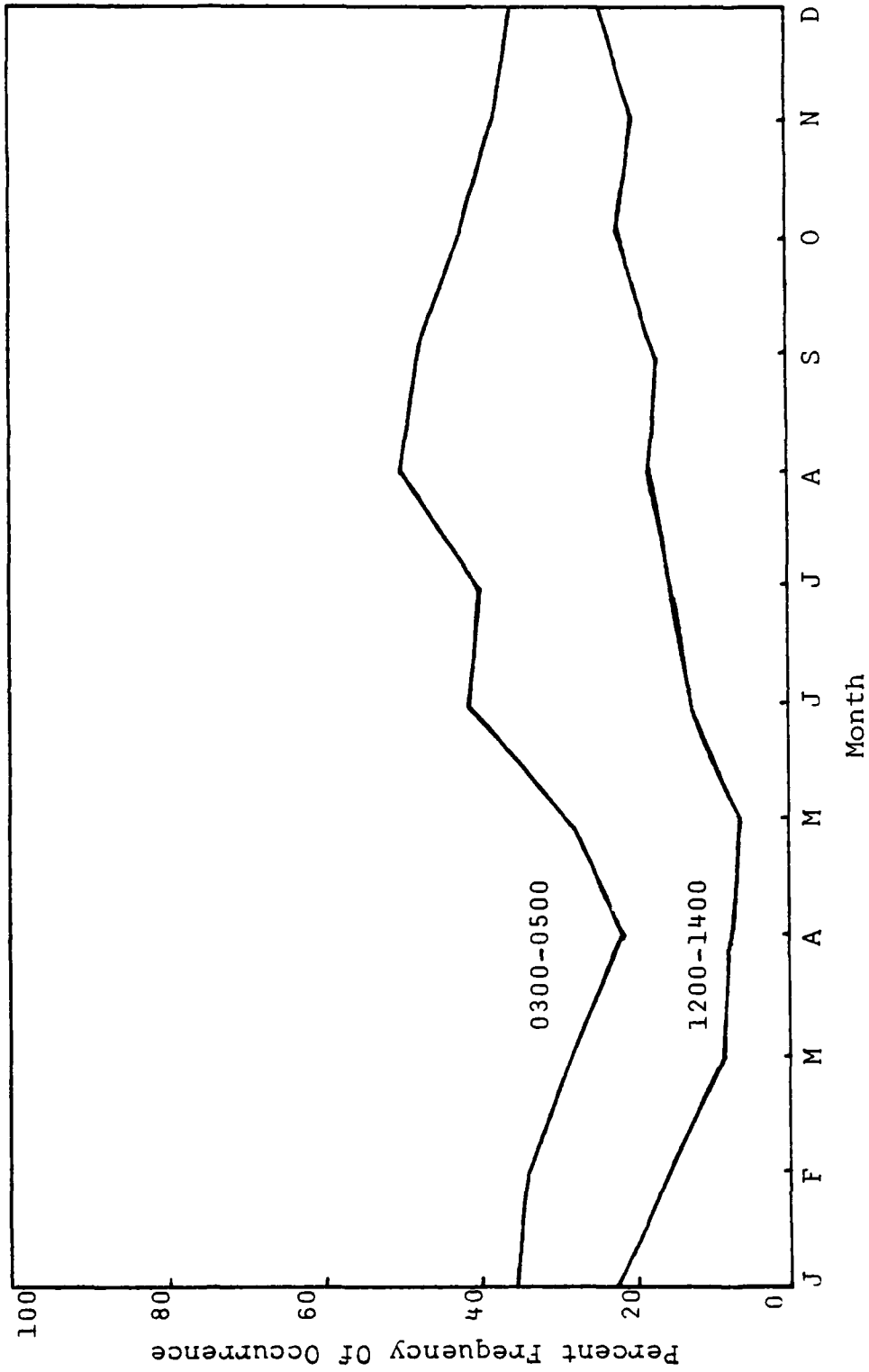


Figure 51. Percent frequency of occurrence of clear skies and windspeed from 0 to 5 knots for Tehran/Mehrabad Iran.

This type of effect is a characteristic of the atmosphere and not of any particular sight design. The ASL is developing two refractive prediction models for use with tanks. The first model would use a micro-computer, require extensive input, and provide an accurate prediction of existing refractive conditions. The second model would be small enough to be placed within the fire control computer of the tank, and would only use input readily available to a tank commander. The output of this model would provide the tank commander with the guidance needed to correct for predicted refractive effects. Another idea would be to develop simple rules-of-thumb which could be used by a tank commander to predict refractive conditions and to provide recommended compensatory actions.

Theory predicts a similar effect at MMW. If true, these effects must also be considered in any research currently under way into using this region of the EM spectrum.

C. COMPUTER SIMULATION 1 - THE EFFECT OF REFRACTIVE CONDITIONS ON U.S. TACTICAL SYSTEMS, USING THE TROPOPLOT COMPUTER PROGRAM

The purpose of this section is to explore atmospheric refractivity effects on actual army systems operating in the RF spectrum. A computer program called "Tropoplot" was used, which predicts long term median tropospheric transmission loss over irregular terrain. This computer

program was originally written in FORTRAN by the Environmental Science Services Administration (ESSA) research laboratories for Control Data Computers [Ref. 25]. The program was updated for use on IBM computers by LT James M. Callaghan [Ref. 26]. A copy of the program is included in Appendix B.

1. Tropoplot Program Description

The Tropoplot program uses a single surface refractivity value, and, although developed primarily to describe the effects of atmospheric refractivity on RF signals, calculates other effects, such as knife-edge diffraction. The surface refractivity value is related to a refractive gradient through a relationship described by Bean and Dutton [Ref. 27: p. 63]. However, the relationship does not provide gradient values which result in ducting and therefore the program is not used to evaluate systems operating in the presence of ducts. Other phenomena which affect communications systems, such as short and long term fading adjustments to median attenuations, are accounted for in the program by using factors taken from actual measurements made on various communications systems. All variables except the surface refractivity were held constant for the data runs in order to investigate only the effect of refractivity over the transmission path.

An interdecile range is used to characterize the terrain. The ESSA report and the Callaghan thesis describe the interdecile height correspondence of various types of terrain. This relationship is shown below.

TYPE OF TERRAIN	ASYMPTOTIC VALUE (meters) OF THE INTERDECILE HEIGHT
Very smooth plains or water	0 - 5
Smooth plains	5 - 20
Slightly rolling plains	20 - 40
Rolling plains	40 - 80
Hills	80 - 150
Mountains	150 - 300
Rugged mountains	300 - 700
Extremely rugged mountains	700 +

The program is usable for frequencies from 20 MHz to 40 GHz over distances of up to 2,000 kilometers. The surface refractivity can be varied from 250 to 400 N units. The ESSA research laboratories [Ref. 25: p. 1] have made empirical measurements for comparison with the program results and have found them to be satisfactory.

2. AN/FPS-16 Radar

The first system used in the program was the AN/FPS-16 air tracking radar. This high power system can be found at permanently fixed sites. The interdecile range for "smooth plains" was used. The transmission and reception line losses were not available, but were estimated to be 2 dB. Many of the system's parameters are provided in the signal strength data input section of Appendix B's data run output.

A "generic" radar warning receiver (RWR) with characteristics typical of fielded systems was assumed to be located on an aircraft at a radar range of approximately 125 km and an altitude of 610 meters. This example was used due to its similiarity to the "standoff" type mission profile that might be flown by current army surveillance and signals intercept airborne platforms.

During the data runs, the surface refractivity was varied from 250 N units to 400 N units in steps of 30 N units. The range at which the receiver could detect a signal varied from 117 km (at 250 N units) to 138 km (at 400 N units). This represented a fairly significant increase in the distance at which an RWR will detect the radar signal.

The next step involved use of the IREPS program to compare the same radar in the presence of a strong duct and in standard atmosphere. Although IREPS is not intended for use over land, the comparison is helpful in exploring the similarity of conclusions for Tropoplot and IREPS. The outputs to the Tropoplot program is provided in Appendix B.

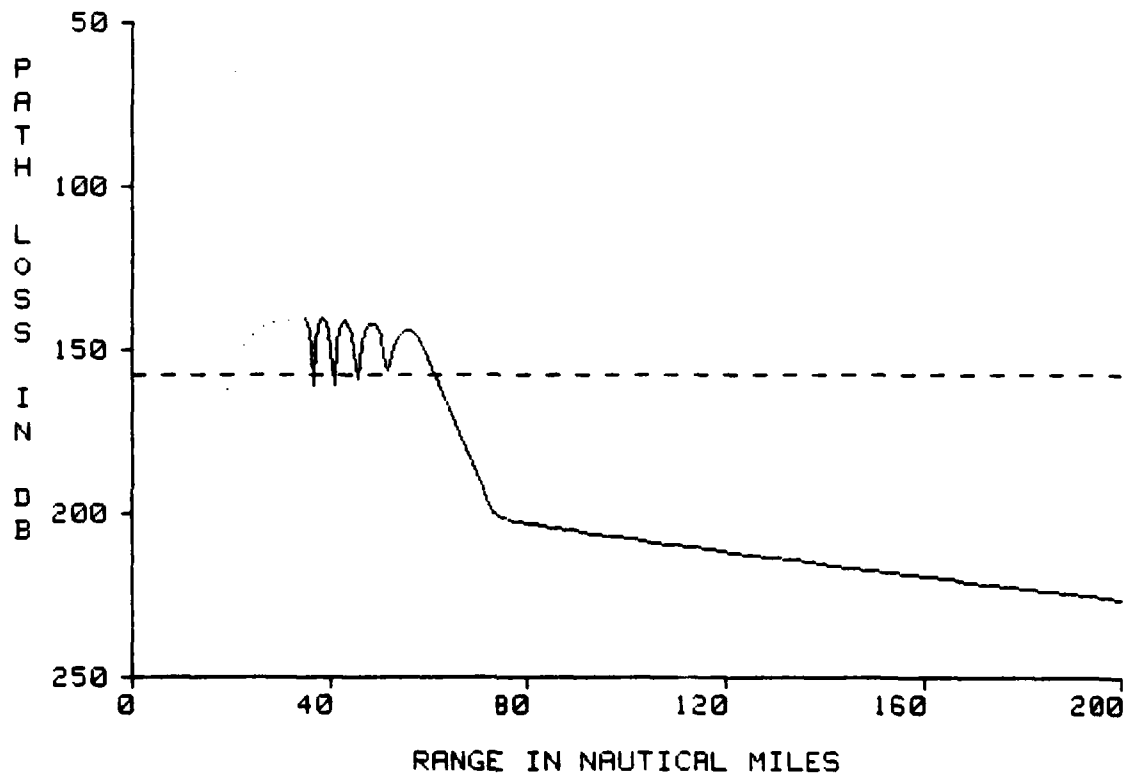
The IREPS results, shown in Figures 52 and 53, cannot be meaningfully compared with the Tropoplot results for several reasons, including the fact that reflective coefficients are different for land and sea water. However, the loss diagram for IREPS in a standard atmosphere versus that for a surface based duct is interesting. It shows a

**** LOSS DISPLAY ****

FPS-16 TRKING RDR (DET)

LOCATION: NOT SPECIFIED

DATE/TIME: STANDARD



FREE SPACE DETECTION RANGE BASED ON 50% POD OF A 1 SQ M AIR TARGET.

DASHED LINE INDICATES DETECTION, COMMUNICATION, OR INTERCEPT THRESHOLD

FREE SPACE RANGE: 163.8 NAUTICAL MILES

FREQUENCY: 5025 MHZ

TRANSMITTER/RADAR HEIGHT: 65.0 FEET

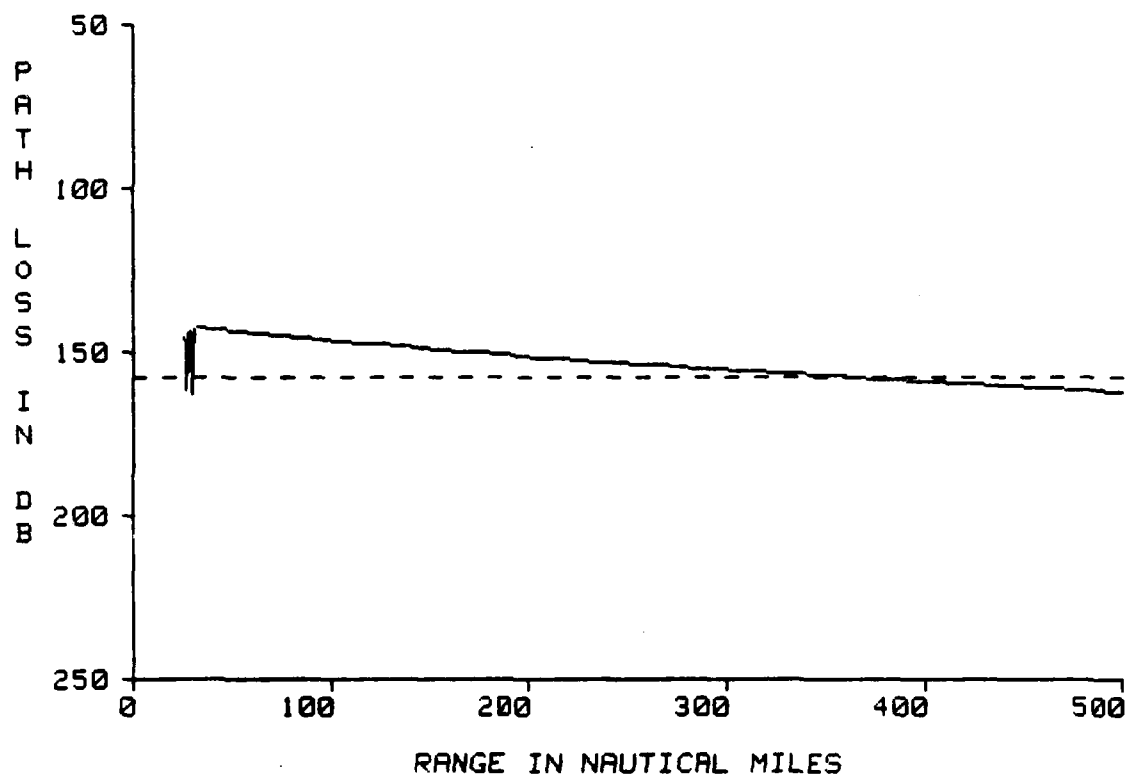
RECEIVER/TARGET HEIGHT: 2000.0 FEET

Figure 52. IREPS loss display for the FPS-16 tracking radar in a standard atmosphere.

**** LOSS DISPLAY ****

FPS-16 TRKING RDR (DET)

LOCATION: 38N 008E
DATE/TIME: SB DUCT 540 FT



FREE SPACE DETECTION RANGE BASED ON 50% POD OF A 1 SQ M AIR TARGET.

DASHED LINE INDICATES DETECTION, COMMUNICATION, OR INTERCEPT THRESHOLD

FREE SPACE RANGE: 163.8 NAUTICAL MILES
FREQUENCY: 5825 MHZ
TRANSMITTER/RADAR HEIGHT: 65.0 FEET
RECEIVER/TARGET HEIGHT: 2000.0 FEET

Figure 53. IREPS loss display for the FPS-16 tracking radar operating in a surface based duct.

loss which causes the radar's minimum detectable signal threshold to be reached at about 74 nm in a standard atmosphere. This is actually the horizon limited value for the given heights of the transmitter (65 ft.) and target (2000 ft.). In a strong surface based duct, the path loss is much less and the threshold is reached at about 350 nm. The loss diagrams are included in Appendix B.

3. AN/VRC-12 Radio

The second system examined was a tactical radio with parameters similar to the AN/VRC-12 series used extensively by the U.S. Army for tactical VHF communications. The parameters were obtained from the U.S. Army Intelligence School, at Ft. Devens, Massachusetts, and from FM 24-24 [Ref. 28: pp. 1-12] and FM 24-25 [Ref. 29: pp. 2-16]. Parameters that were not available were estimated, and are considered to be close to those which actually exist.

For this scenario, two radios are assumed to be operating over a fairly smooth surface with their antennas placed on terrain which allows for an antenna height of ten meters above the immediate land in order to enhance communications. The refractivity was again varied from 250 to 400 N units, although the increments were increased to 50 N units.

In this example, the results were less impressive than in the previous case. The maximum range for reception only varied from 24 km to 26.1 km. Although not shown, a

simulation of a ground surveillance radar was run, using actual parameters, which also resulted in little or no change in the maximum detection range of 3000 meters, regardless of surface refractivity.

The results of these latter computer runs suggest that refractivity may not be critically important for shorter range, lower power systems, a fact that is not totally unexpected.

4. Conclusions

Although it does appear that refractivity plays a critical role in the quantitative effects on RF signal propagation, further study, using a program for irregular terrain with strong vertical refractivity gradients, as opposed to a surface refractivity value, is necessary to define more precisely the critical ranges for refractivity. At present, there do not appear to be any programs which have this capability.

D. COMPUTER SIMULATION 2 - THE EFFECT OF HORIZONTAL REFRACTIVE GRADIENTS ON AIRBORNE DIRECTION FINDING ACCURACY

Airborne Direction Finding (DF) systems provide critically important support to U.S. Army tactical commanders. Systems which will provide enhanced accuracy are currently being planned or fielded. In general, accuracy is dependent on the system's ability to measure individual lines of bearing (LOB) to the target emitters and on the precision

with which the navigation system can determine the airborne platform's location. Five major causes of error, which are independent of a DF system but which affect its ability to measure LOB's are reflections, re-radiations, diffraction, refraction, and fading signals [Ref. 10: p. 2]. The purpose of this section is to investigate the impact of refraction on DF accuracy through the use of computer simulation.

It is important to recognize typical situations where refraction could cause problems. These include geographic areas where rapid changes in temperature and humidity (and sometimes pressure) occur in the horizontal plane. Such areas include broad river valleys, or large bodies of water surrounded, at least partially, by land, and coastal regions. In such areas the geometry involved in taking LOBs may vary greatly, depending on where the refractive gradient occurs in relationship to the emitters and the DF platform. This simulation used a fixed situation from which it is possible to extrapolate to other circumstances. This procedure is explained further in sub-Section 4.

This section is organized into several sub-sections. Section 2 provides a brief general description of DF and of the tactical scenario used in the simulation. Section 3 is a basic description of the program, including the assumptions and algorithm. A copy of the program is included in Appendix C. The final section describes the simulation runs, the results of the simulations, and the conclusions.

It was necessary to reduce the amount of output from the simulation since a large number of LOBs, fixes, and other data was generated on each "flight" across the tactical area. The thesis contains examples of the pertinent data and graphic representation of the output in this section and in Appendix C. In addition, it would be possible, but not practical, to do a number of sensitivity analyses by changing the variables in different combinations. For example, the depth of the refractive area, the horizontal gradient, or the depth of the emitters could be changed, either singly or in combinations. However, the purpose here was to make representative changes in the variables from which it would be possible to draw definitive conclusions.

1. General Description of Direction Finding and the Tactical Scenario

Airborne DF systems operate, basically, like ground based systems, except that they must also determine the aircraft's location at all times. This is normally done using an inertial navigation system (INS) with some type of external update. The aircraft flies a preplanned course, often a "racetrack" pattern, while taking LOBs on target emitters. These are entered into emitter LOB files and are eventually correlated into fixes, a term used to describe the target's calculated location. The emitter files may be sorted by frequency or by other parameters. Most systems use further correlation or refinement to "throw out" some of

the fixes which do not fit the main distribution of fixes. Reports on emitters usually include an elliptical error probable (EEP) to allow for the expression of a confidence factor in the fix accuracy. The simulation computes an "average" fix based on all of the correlated fixes.

A simple type of DF system uses a "two-bearing" cross (TBC) to produce fixes. In this system the point where two LOBs cross is a fix. The accuracy of the fix improves as the angle formed by the two LOB's approaches ninety degrees. In this simulation, a TBC routine is used to produce fixes.

The simulation used a corps level DF mission along a corps front of 200 kilometers. This is reasonable for a three division front. A single aircraft was used, although some systems use two or more in order to provide geometry that will allow almost instantaneous fix determination without having to fly long distances. The aircraft flew at a cruise speed of 200 knots and required a little over 30 minutes to fly the front. To simplify the simulation, the aircraft flew the same baseline on each sweep of the corps area.

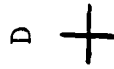
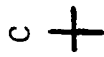
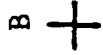
Four emitters were used in the scenario and their distance from the corps FLOT could be varied (see Figure 54). The deeper locations are particularly applicable to the tactical concerns of a corps. Since emitters located close to the corps boundary would be difficult to accurately fix, due to poor geometry, the emitters in the simulation

Emitter A



Y-Coordinate

X-Coordinate



Note: All X and Y Coordinates
Are Variable

200 Km Aircraft Baseline

Figure 54. Diagram of the Tactical Area

were placed well within the corps lateral boundaries. Of course, in an actual situation, some compensation could be made for this geometry problem, such as an interface with DF assets of any adjacent corps. Three of the emitters (A, B, and C) are set up to evaluate errors from refraction and Emitter D is used to compare other types of error, such as DF system error or platform location reporting error, with refractive error. Emitter D, therefore, is not affected by refractivity. All of the emitters can move about within the 200 kilometer area which corresponds to the aircraft baseline. The aircraft was assumed to be flying parallel to an area with a refractive gradient similar to that found along a coastline, taking fixes on land based emitters. The gradient area has a uniform horizontal refractive gradient (see Figure 55). The depth of this area can be varied in order to evaluate the effects on lines of bearing which are bent over long or short distances. Any refractive gradient value can be used, except zero.

With the exception of Emitter D, an LOB departs the emitter in a straight line, passes through an area where it is refracted, and departs that area in a straight line which, like the previous straight line, is tangent to the arc. The LOB arrives at the baseline, where the angle of arrival and the position are recorded (see Figure 55).

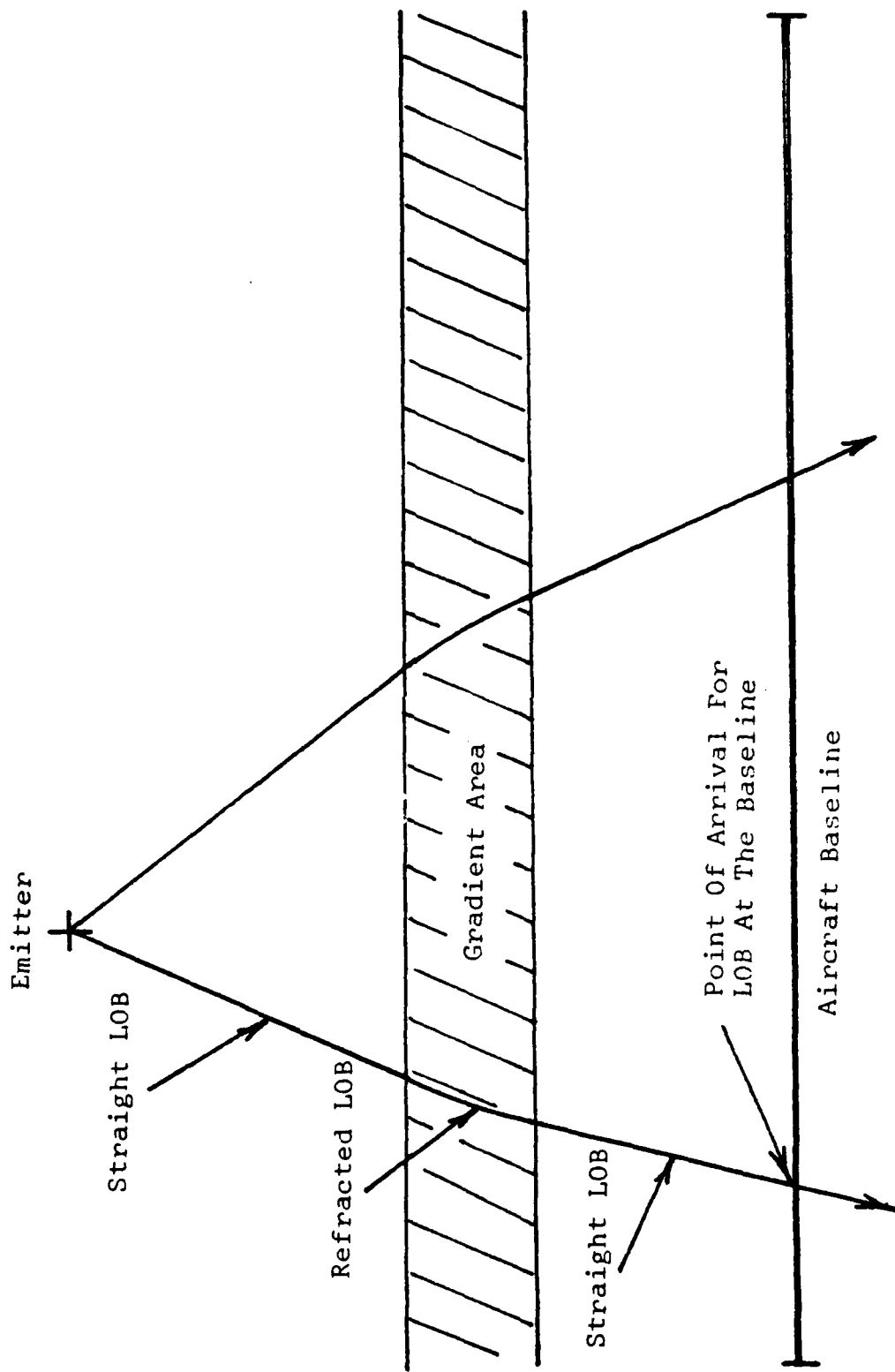


Figure 55. Geometry of lines of bearing from an emitter.

The program does not examine the effects of vertical changes in refractivity since the ray tracing problem becomes extremely involved when working with both horizontal and vertical ray tracing.

2. Algorithm Description

Throughout the program, a concerted effort was made to eliminate as many assumptions as possible, or, at the very least, to make assumptions which closely resembled real world circumstances. In addition, a graphic output was chosen over other output forms, such as statistical tables, as graphs are most effective in quickly evaluating where the fixes were computed.

The following assumptions are pertinent to the understanding of the simulation:

1. Flat earth geometry.
2. LOBs are taken every 15 seconds and emitters are selected using a uniform distribution.
3. LOB angles are taken with respect to the aircraft's longitudinal axis.
4. All emitters can be received at all times during the flight.
5. The aircraft track is along the $Y = 0$ axis. The emitter depths assume a standoff range in order to provide aircraft survivability in a high-threat air defense environment.
6. Emitter positions are fixed for each mission.

In reference to Emitter D, a set of preset flags controls the "on-off" condition of the variables. These are described in the first part of the program (see Appendix C). Basically, these flags control introduction of LOB error, navigation error (drift or random), and navigation system update. During the majority of the simulation runs, LOB system error was used only with Emitter D. This allowed comparisons with the other Emitters (A, B, and C) which had refracted LOBs, but which were not subject to system error. Navigation error was not used as a variable in any of the runs, since earlier simulations showed it to be less of a factor than LOB system error. One simulation run was made in which Emitters A, B, and C were affected by both refraction and system error, as noted in the data (see sub-Section 3).

During the simulation, the flags were turned on only when a comparison of system error versus refractivity error was desired.

The algorithm which follows can be described quite briefly, even though the program itself is fairly large. An aircraft is started on a track with constant updating of its actual and reported positions. It selects an emitter, calculates the LOB to the emitter, and stores both the LOB and the position where the LOB was received. In the case of Emitter D, the actual and reported aircraft positions are recorded. After each LOB is taken, position on the track is

checked. If the aircraft is at a boundary of the corps area, a subroutine is called in to correlate the LOBs into fixes, calculate an "average" fix, and plot the output or summarize the output statistically.

In order to validate the results, simulation runs were made using identical programs, except that variable values were reported after each step. A check was then made of selected data, both qualitative and quantitative. For example, the LOBs were checked qualitatively to ascertain whether their values approached that of a normal drawn from the baseline to the emitter, as the aircraft approached the normal. They were checked quantitatively by using a hand-held calculator to verify the angles. Many other checks were made, including a run with the dN/dX (refractive gradient) value close to zero in order to determine if any fix error was present. As a final check, large variations in gradient area and refractivity were introduced to insure they had the expected effects on the fix accuracy.

Figure 55 illustrates the basic geometry used in the simulation. The LOB on the left would be placed into one file and that on the right into a second file. Later, after the aircraft had reached the end of the baseline, the two files would be checked and the two LOBs would be correlated into a fix. The correlation routine checks every possible combination of LOBs which produce fixes.

The program can calculate a dN/dX value from inputs of temperature, pressure, and humidity for two different areas separated by a "gradient" area, as used in the simulation. In addition, a dN/dX value can be inserted into the program to facilitate sensitivity analysis. Different types of data can be produced by use of "write" statements located throughout the program. For example, the program will print out all of the LOB angles along with the locations where they were taken.

An outline of the basic algorithm follows:

Initialize variables.

Calculate a dN/dX value.

Use a random number routine to vary aircraft start on track.

Establish a loop to control round trips of the corps front.

Update actual aircraft position.

Check to see if aircraft has completed left to right sweep; otherwise continue.

Option for random nav. error, update reported position.

Option for drift nav. error, update reported position.

Option for LOB error.

Select emitter from uniform distribution.

Check aircraft position, if past point where a normal drawn from the emitter to the baseline would hit the baseline, set storage flag (Emitter D only).

For Emitters A, B, and C use a slightly different routine to calculate the angles - one which depends on the aircraft location on the baseline.

Calculate angle to selected emitter, in radians.

Convert angle to degrees.

Calculate location where LOB was taken (Emitters A, B, and C).

Check to see if the aircraft position is past the normal points (A, B, and C).

Call a subroutine to store the LOB, actual and reported aircraft position (Emitter D).

Call a subroutine to store the LOB and the position where the LOB was received (A, B, and C).

Check to see if a right to left sweep is complete.

 If complete, call a correlation subroutine.

 Otherwise, continue flying and taking LOBs.

Update aircraft position.

Go to emitter selection.

End of loop.

Subroutine to store LOBs (4).

 Select one of two LOB files based on flag.

 Store LOB, actual position, and reported position in proper file (D).

 Store LOB and position received in proper file (A, B, or C).

 Return to main program.

Subroutine to correlate LOBs.

 Establish 2 loops to check every possible combination on LOBs in the storage files for each emitter.

 Establish a counter.

 Add 2 LOBs together and make a check for acceptable geometry. This is optional: for further information, see text.

 Determine vertex angle and convert to radians.

Calculate distance between both LOBs at baseline.

Convert LOB angles to radians.

Calculate length of one side of two-bearing cross from vertex to baseline.

Calculate the Y coordinate.

Add in Y nav. error (D).

Calculate the X coordinate.

Add the X coordinate to reported aircraft X position.

Keep a running total of the X and Y coordinates for all fixes.

End of loops.

Call plot routine for fixes.

Calculate average X, Y, and average fix error.

Call plot routine for X, Y, and average error.

Return to Main Program.

3. Results and Conclusions

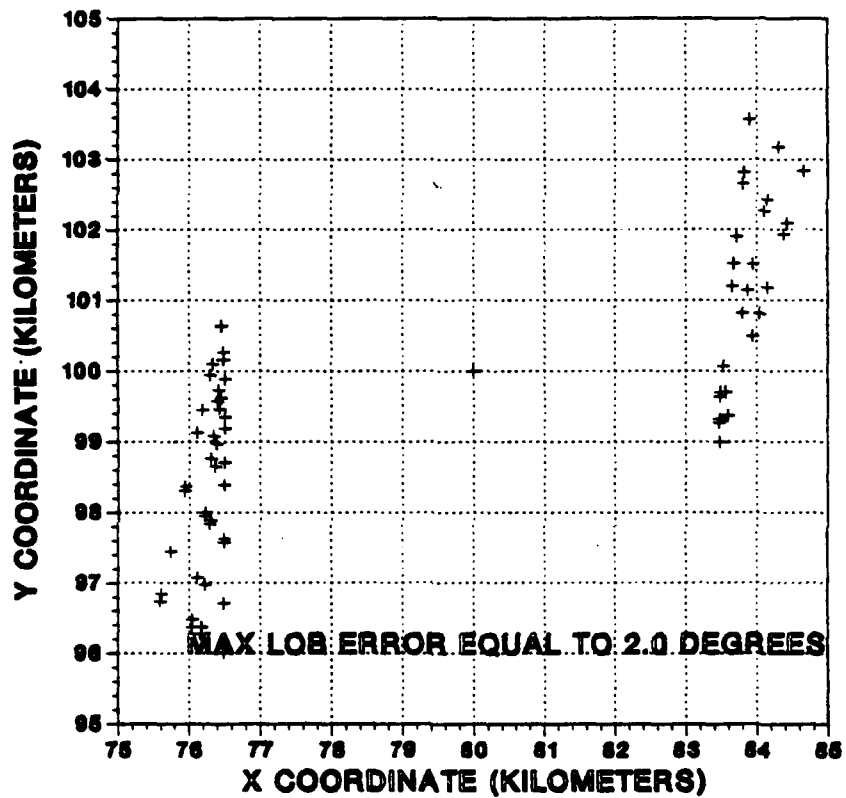
The graphs and tables in this section and in Appendix C, represent the data resulting from the multiple runs of this program. Since one graph for each emitter could be produced on each sweep of the corps area, it was necessary to limit the amount of output considerably. This was done through condition statements which allowed for sampling of data via collection from selected sweeps. Due to the uniform distributions used and the geometry, there were differences from sweep to sweep, as would be expected in the real world. Therefore, data used for comparison purposes were taken from the same sweep.

One of the first problems encountered concerned "angle gating". This problem is related to the geometry of the two-bearing cross used to determine fixes. Ideally, an angle of ninety degrees formed by two LOBs (known as the vertex angle) would give the best fix. However, because of various factors, including width of baseline, emitter depth, emitter proximity to corps boundaries, and the necessity to have several fixes for better averaging, it was necessary to specify an angle gate which would provide acceptable geometry and yet allow for several fixes on each sweep for each emitter. This was done by using a hand-held calculator to determine the maximum and minimum possible vertex angles for each emitter at all ranges. Throughout the data runs, the accuracy was highly sensitive to the angle gates. This results from the fact that narrowing the gates eliminates some of the outliers in the data.

The first simulation run checked the program by using a dN/dX value close to zero to indicate negligible fix error. The results showed that double precision was required in the program (due to division errors by numbers close to zero). The results are shown in data Table C-1 in Appendix C.

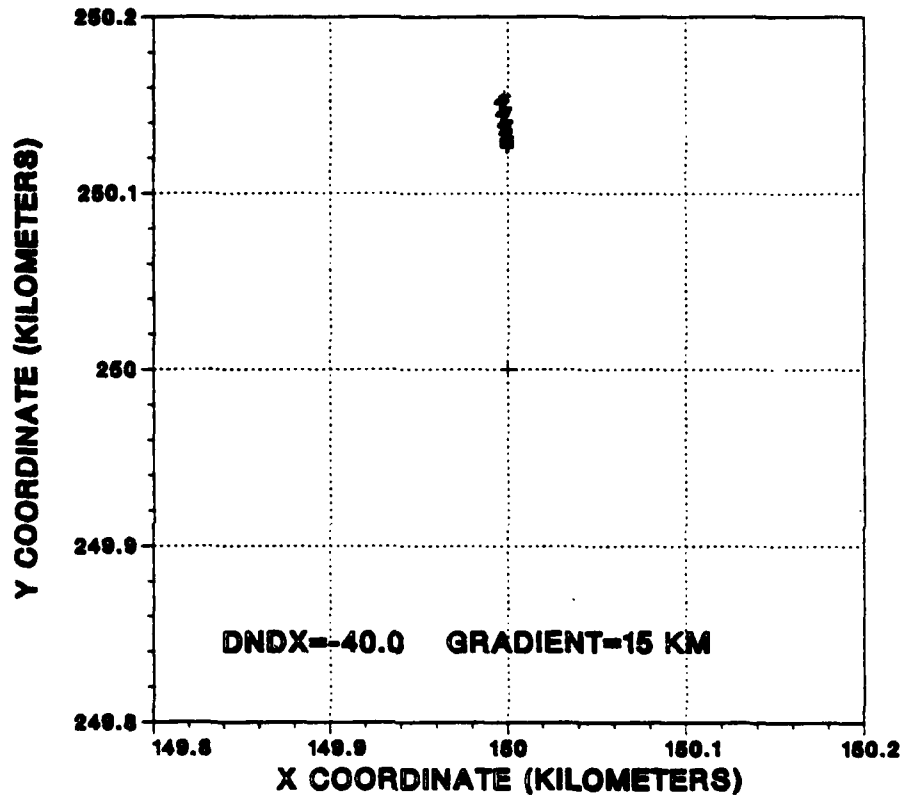
The initial simulation runs compared the effects of different amounts of refractivity on the fixes. The data is presented in Graphs 1, 2, and 3, on the following pages, and summarized in Tables C-2, C-3, C-4, and C-5, in Appendix C. The size of the gradient area was held at a constant 15 kilometers

COMPUTED FIXES FOR EMITTER D



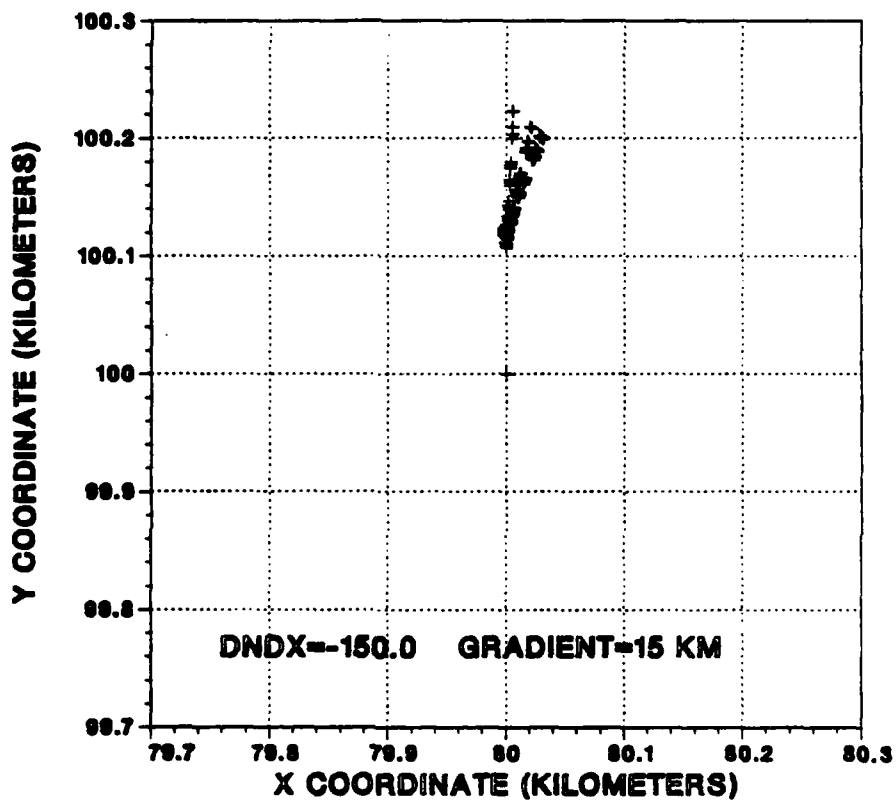
Graph 1.

COMPUTED FIXES FOR EMITTER C



Graph 2.

COMPUTED FIXES FOR EMITTER A



Graph 3.

during these runs. The output shows that the refractive index did have an effect on fix accuracy, but there were no cases where the error was as high as fixes produced with an LOB system error of 2.0 degrees (Emitter D). Even with $dN/dX = -150.0$, the errors for Emitters A, B, and C did not exceed 500 meters. Part of this is due to a "cancelling" phenomenon, which will be explained further.

A gradient of -150 N units could not occur over a 15 kilometer area since the range of N values would greatly exceed the norm. However, there is a case where the geometry could cause individual LOBs to travel for a fairly long distance through a strong gradient. This situation is illustrated in Figure 56. The individual LOB departs the emitter and travels in a direction which roughly parallels the refractive gradient. This results in the ray being bent over a longer distance, thus introducing greater error. Although extensive changes to the program would have been required to reproduce this particular geometry exactly, simulation runs were made with large gradients over areas of 15 to 30 kilometers in order to investigate the effect of strong gradients and longer distances on LOB accuracy. The results are shown in Graphs 4, 5, and 6, on the following pages, and are summarized in Tables C-6 and C-7 (Appendix C). As shown, this situation produced the greatest error from refractivity, particularly for the deepest Emitter (C), where the error exceeded 700 meters. The data appeared to

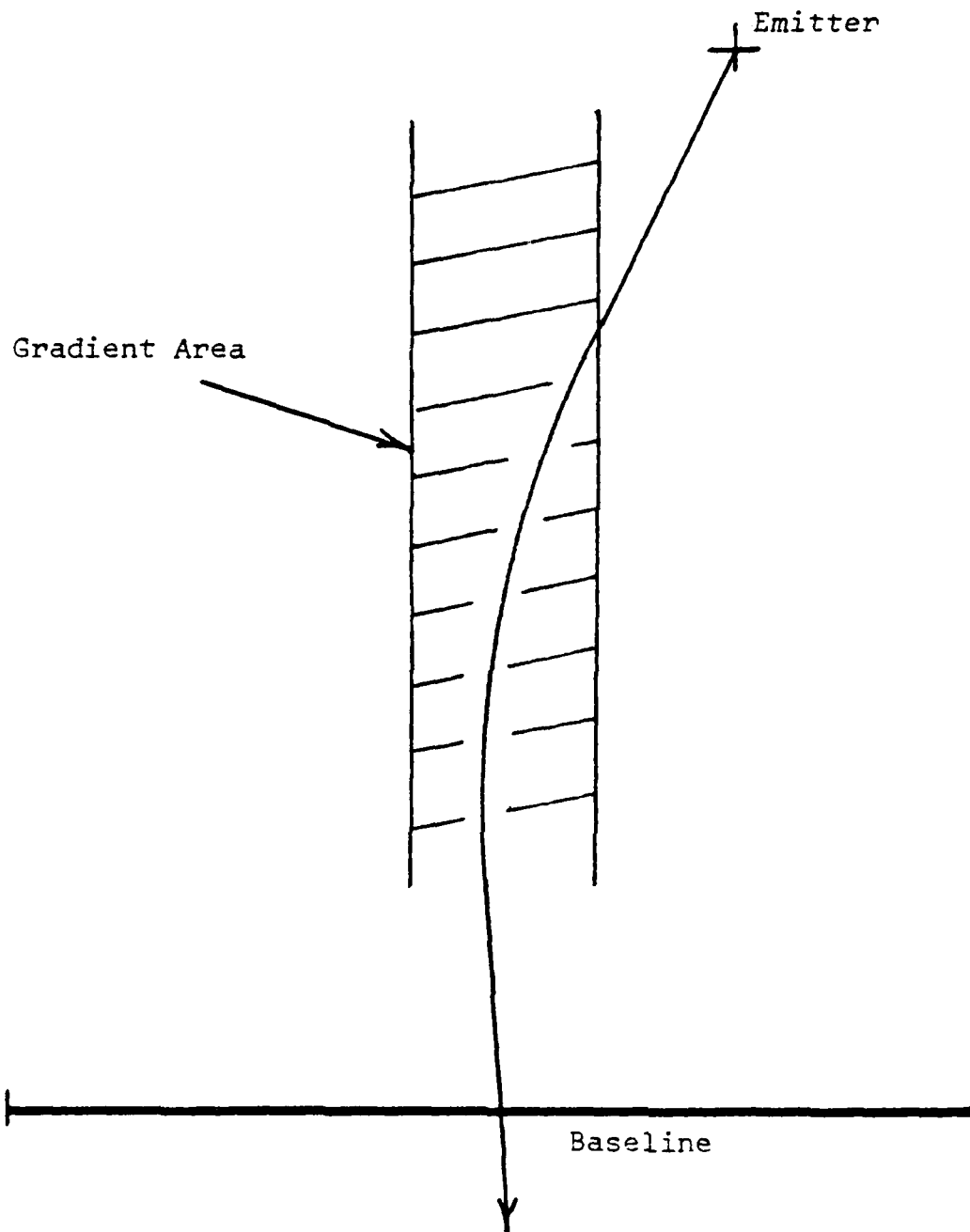
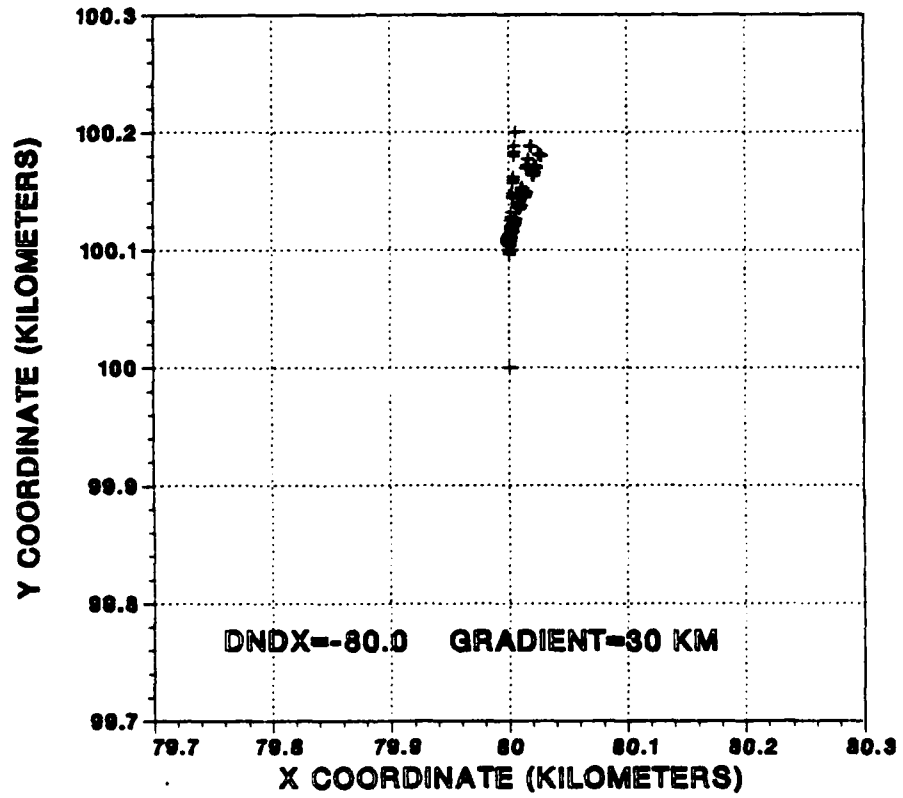


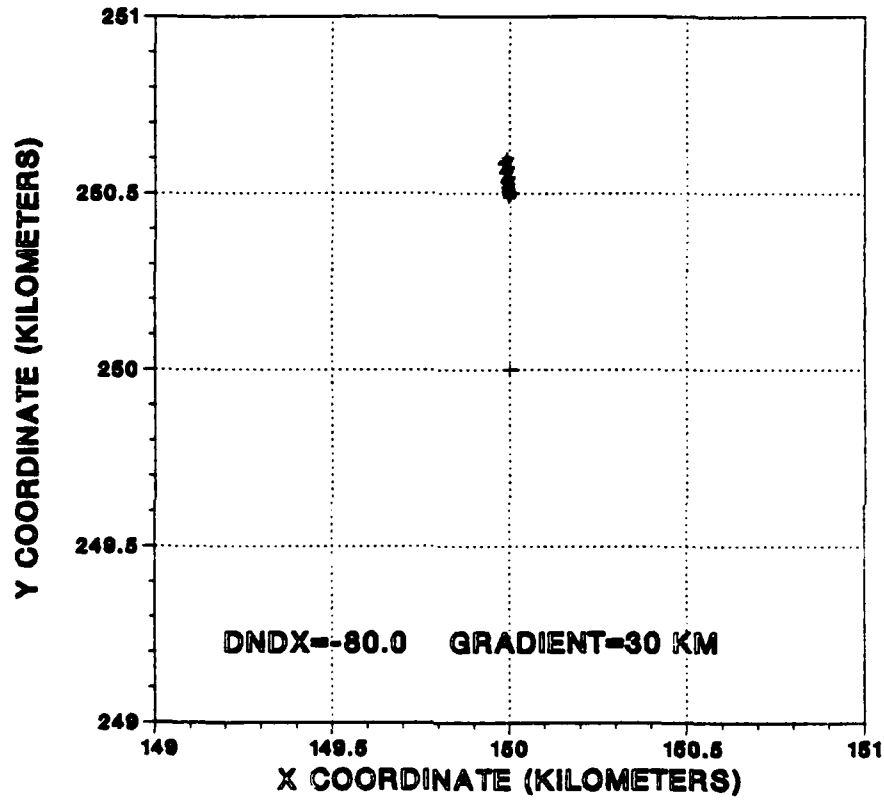
Figure 56. Diagram of a Retracted Line of Bearing Using Alternate Geometry.

COMPUTED FIXES FOR EMITTER A



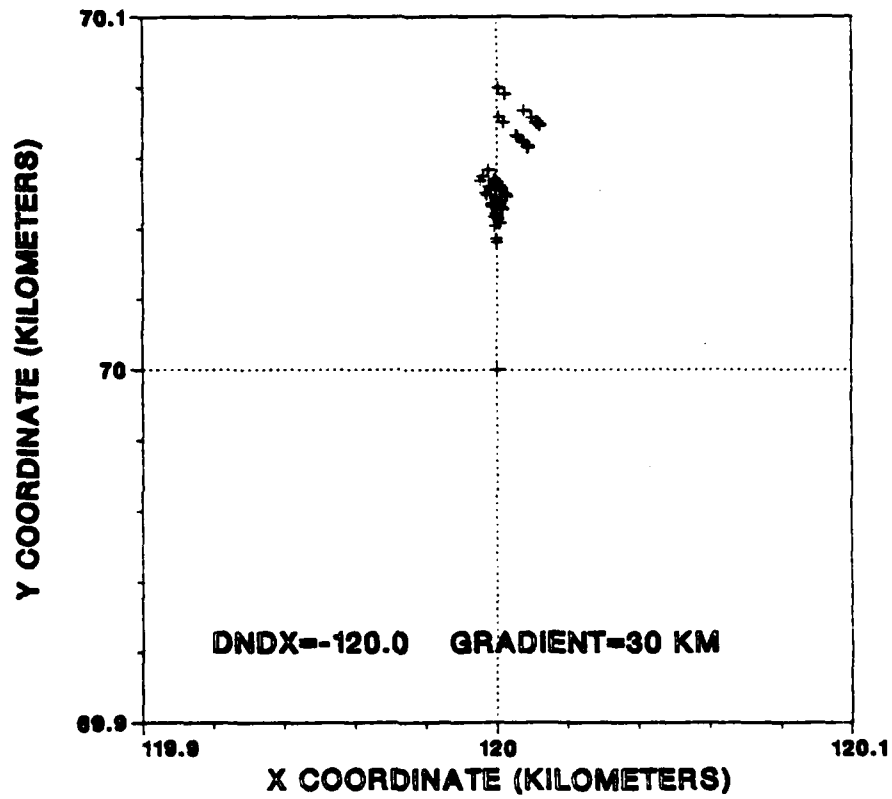
Graph 4 .

COMPUTED FIXES FOR EMITTER C



Graph 5.

COMPUTED FIXES FOR EMITTER B

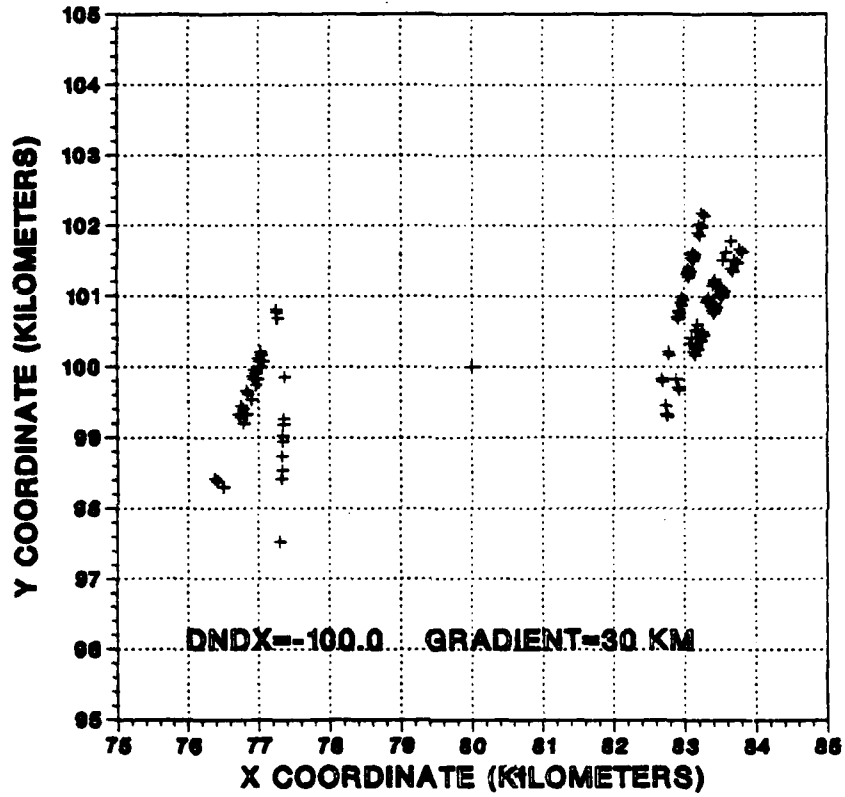


Graph 6 .

reflect some "cancelling" effect. This resulted when LOBs refracted in one direction were correlated with LOBs refracted in the opposite direction, causing some lateral error to be cancelled out. The error, therefore, occurred mainly in range (Y-coordinate) and is shown in the fix data by the reported fix being deeper in range than the actual location. In order to investigate this further, a run was made where refracted LOBs from Emitter A were correlated with straight LOBs in a situation like that depicted in Figure 54 (i.e., refraction occurs over a large area). An LOB system error of 1.5 degrees was also introduced. The results are shown in Graphs 7 and 8 on the following pages, and Table C-8 of Appendix C. Note that Emitter A's fix error greatly increased from previous runs, exceeding Emitter D's error in fifty percent of the cases.

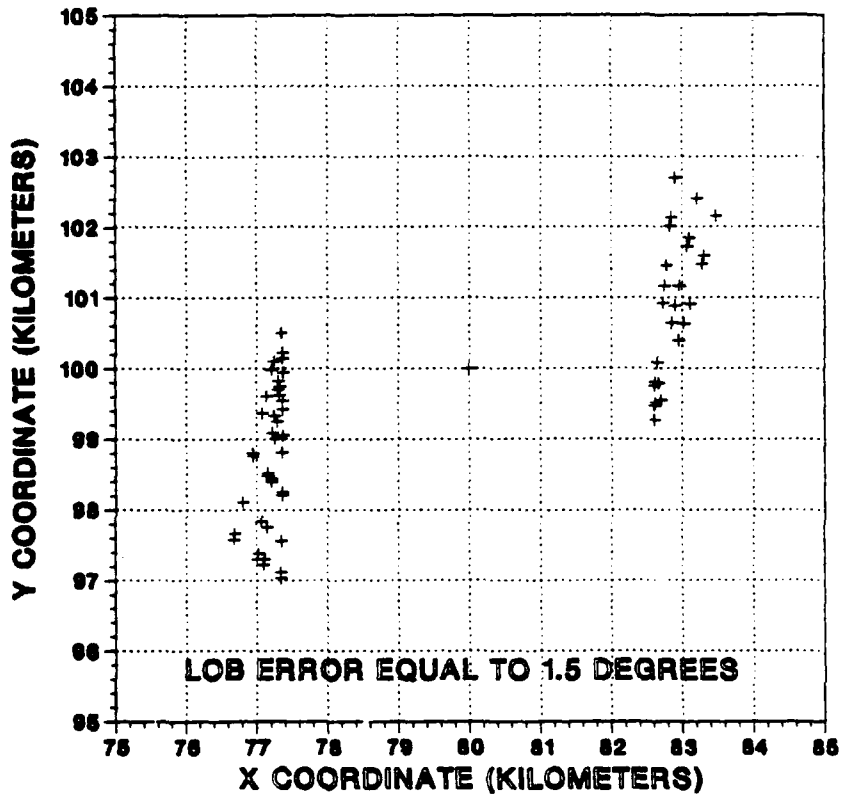
The primary conclusion to be drawn from the simulation is that horizontal refractive gradients can be a problem under certain conditions, but that, generally, system errors will induce greater LOB inaccuracy than will refractive effects. The worst case is the problem shown in Figure 56, where the LOB is refracted over a long distance and the refracted LOBs are correlated with straight LOBs. However, if the possibility of these conditions exists, measures can be taken to minimize their impact. For example, the correlation software routine could ignore fixes produced by LOBs which came through an area of suspected strong refractivity, or a

COMPUTED FIXES FOR EMITTER A



Graph 7 .

COMPUTED FIXES FOR EMITTER D



Graph 8 .

correction factor could be introduced for refracted LOBs. Since good refractivity data would be very difficult to obtain in the emitter area, the software routine could employ a predictor system for LOBs to check for any that consistently arrive at the baseline at a different angle than would be expected. This would require close operator interface and an assumption that the baseline of the aircraft is long enough to allow sufficient LOBs to be taken which do not pass through an area of strong refraction. Although correction tables are sometimes used to correct DF errors arising from known refractive conditions, they are not a practical solution for mobile DF systems [Ref. 10: pp. 4-7].

This simulation pointed out several areas which could be studied further. These include a computer simulation which exactly reproduces the geometry of Figure 56 or one which looks at a time-of-arrival system working in an area of strong refractive gradients. The latter could involve some extensive work, since vertical gradients could not be considered independently. Both vertical and horizontal bending would affect the time of arrival.

The magnitude of the effect of horizontal refractive gradients is dependent on many factors, including the emitter depth, the strength of the gradient, and the distance the LOB travels through the gradient. In many cases, the effects of inherent system errors will be greater than any refraction induced errors. Since refractivity errors are

often random and difficult to predict, attempts to correct or compensate for them may be hard to implement. Although improved software routines and other techniques may be effective in improving accuracy, the best procedure may be to recognize possible areas of strong refractivity and to use the fix results accordingly.

E. SCENARIO

The purpose of this Section is to show, by means of a general ground combat scenario, the large number and variety of U.S. Army systems that could be affected by atmospheric refractivity and the wide range of the resulting effects.

1. Scenario Background

To provide an extreme but not unusual atmospheric refractive situation, a Mid-Eastern coastal scenario will be used. A mechanized division, with the necessary corps supporting assets, has deployed to this region during a period of increased tension, but before any actual combat has occurred.

The mechanized division has three brigades on line, a tank battalion held in reserve, and a strong covering force forward of the front line of troops (FLOT). Since this description is not meant to be a lesson in ground combat operations, little further effort will be spent on describing the disposition of or organization for combat of the elements of the division.

The division has one flank anchored in a coastal mountain range, adjacent to another U.S. division, and the other flank is anchored in the sea. The division is currently located in a blocking position across a major high speed avenue of approach, as shown in Figure 57.

The division is deployed in an arid, desert region, characterized by large areas of sand and rock of generally good trafficability, interspersed with impassable semi-forested mountains, sand dunes, and ravines. Very little vegetation exists in the region except on the upper slopes of the coastal mountain range. The temperatures at this time of year range from the 70's at night to 110 degrees during the day. Days and nights are often clear, but, vision can quickly be obscured by violent sandstorms.

In this scenario, two days and one night will be considered. On the first day the extreme daytime temperature leads to the creation of a strong subrefractive condition over the coastal strip which is strengthened by an inferior mirage from the coastal range to the sea. The high temperatures and onshore breeze also lead to high turbulence, throughout the day, along the coastal strip.

That night, a high pressure area begins moving slowly into the region, enhancing the superrefractive condition created by the radiation of heat from the desert surface. Some turbulence exists but not nearly so severe as that which existed during the day.

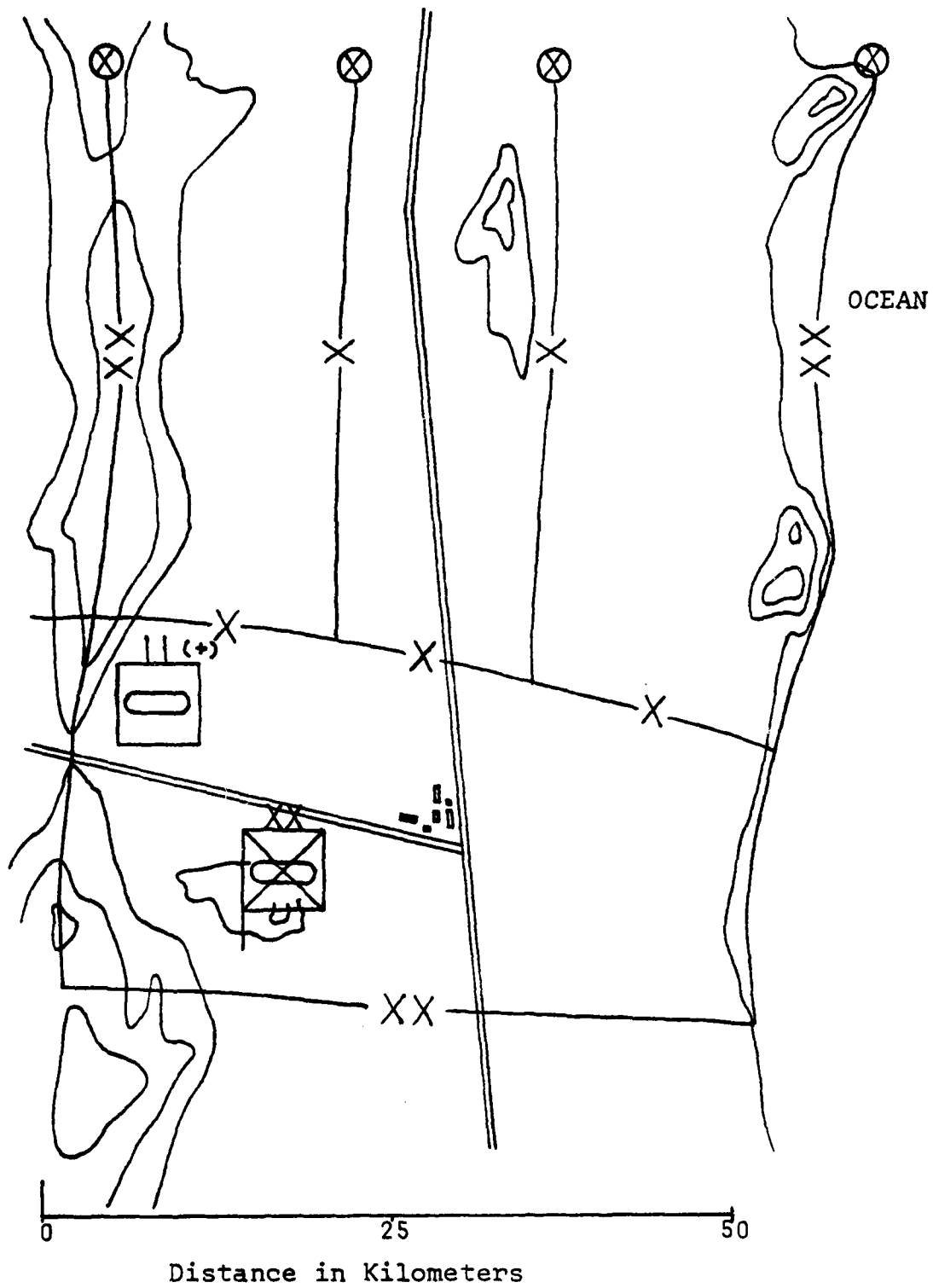


Figure 57. Example Scenario.

During the second day, the high pressure area leads to the creation of an offshore flow of dry, hot air and results in the creation of a strong elevated layer and surface duct that extends inland almost to the coastal range.

2. Atmospheric Refractive Effects

a. Optical Effects

The presence of the subrefractive condition, inferior mirage, and optical turbulence on the first day will significantly affect many of the division's optical surveillance, fire control, and tracking systems.

The distance at which the mirage begins will limit visual observation, by ground observers, of areas to the front of the division's covering force. Mirages can significantly affect optical systems as close as 1000 meters. In any combat, this near boundary of the mirage can reduce the detection and engagement ranges and accuracy of direct-fire weapons, particularly if optical turbulence is also severe. In a like manner, the presence of the mirage condition and optical turbulence could also reduce the effectiveness and range of laser rangefinders and laser designators.

Some relief from these adverse refractive effects can be gained by placing observers as high above the surface of the coastal strip as possible. Those observers located above the top of the mirage, either on the surrounding high ground or in aircraft, will be unaffected by the mirage.

Another adverse refractive effect would result if the division's tank main guns are boresighted and zeroed during the first day and fired the first night or second day. As explained in Section III.B., the result of such a situation could be significant reduction in tank main gun accuracy during night firing and during the second day.

Some bending of IR paths will occur at night due to the superrefractive condition, but the effect of this on FLIR systems would probably be insignificant.

The ducting on the second day would result in a weakening or total absence of the inferior mirage seen on the first day. Thus, visual observation and laser designation and rangefinding systems would be more effective on the second day, although optical turbulence might still be quite strong.

b. Effects on Communications and Electronic Warfare Systems

Desert regions, in general, have an adverse effect on RF communications. Some of the effects include difficulty in adequately grounding communications systems, existence of a weak HF ground wave, and a generally low surface reflectivity, all of which lead to a significant shortening of HF, VHF, and UHF communication ranges.

The presence of the subrefractive condition on the first day, although causing some bending of ground-to-ground communications signals and ECM jamming signals, will

not result in any additional significant loss of range. This is not necessarily the case for air-to-ground communications and jamming. The existence of the subrefractive layer over the surface of the coastal strip will set a limit on the minimum angle, from the aircraft to the ground station, at which communications will be dependable between the two stations. This latter effect will also place some limit on friendly airborne communications intercept and direction finding (DF) capabilities for platforms located behind the FLOT and attempting to acquire and DF hostile communications emitters. The height of the aircraft above ground, the distance to the ground communications system, the power output of the airborne system, and the strength, height, and extent of the subrefractive condition are all critical in determining the overall effect.

The accuracy of airborne and ground based DF systems can also suffer from a horizontal atmospheric refractive gradient created by the juxtaposition of land and sea air masses along the coastal zone. These errors can be quite significant, as shown in Section III.D.

The night time superrefractive condition and the ducting occurring during the second day, both of which are surface based, will tend to extend communication ranges of those signals operating within these conditions and above or near the minimum trapping frequency, f_m . This will serve to increase the distance between ground based units, for which

AD-A134 827

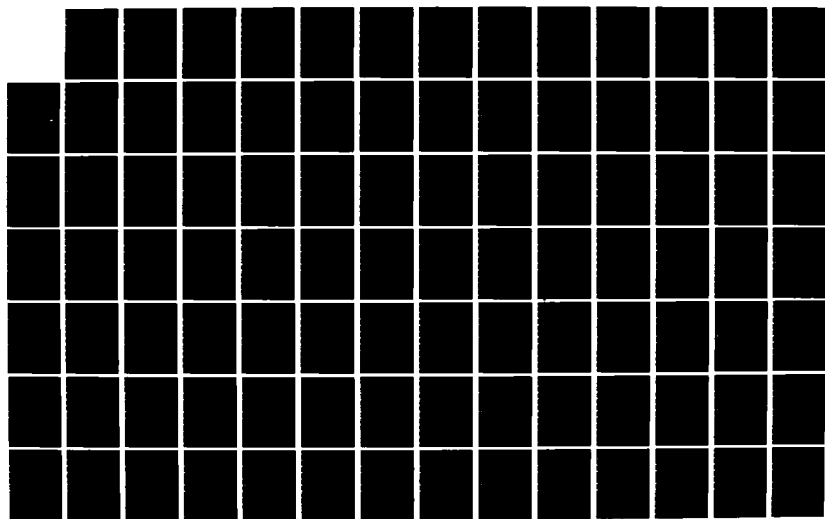
EFFECTS OF ATMOSPHERIC REFRACTION ON US GROUND WARFARE
(U) NAVAL POSTGRADUATE SCHOOL MONTEREY CA
T P HOURAS ET AL. SEP 83

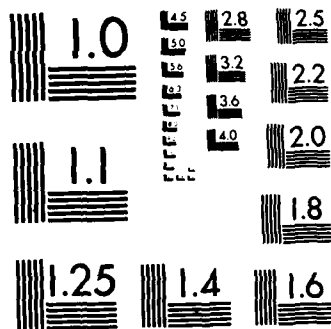
3/4

UNCLASSIFIED

F/G 20/14

NL





MICROCOPY RESOLUTION TEST CHART
NATIONAL BUREAU OF STANDARDS-1963-A

communications will be considered reliable, and also the distance from jammer-to-target at which jamming will be effective. Communication intercepts of distant hostile emitters will similiarly be enhanced. In a like manner, hostile Electronic Warfare (EW) units will be able to jam, intercept, and DF friendly communications from greater distances. Terrain features may, however, override the effect of the superrefractive condition, and, in any event the actual enhancement may be only a few kilometers for ground based systems, as shown in Section III.C.

c. Effects on Noncommunications Emitters

The division's noncommunications emitters, primarily radar, are spread throughout the division and serve a variety of purposes.

The accuracy of the division's counterbattery/ counter mortar radars may be degraded by the subrefractive, superrefractive, and ducting conditions. The extent and nature of such atmospheric refraction produced errors in the Firefinder radar is currently a subject of interest.

Ground surveillance radar systems will suffer very little from atmospheric refractive effects, since these systems are operated over relatively short ranges and are directed along the surface of the earth.

Ground based air defense radars, however, can be adversely affected by all forms of atmospheric refraction. The first day's subrefractive condition will result in errors in both angle and range, but will be unlikely to

affect early warning or tracking radars significantly. The first night's superrefractive condition will cause radar signals to bend in the opposite direction from those propagating during the day, and will thus cause angle and range errors in air defense radars; but, again, because of the nature of the radar's purpose, these errors will probably be insignificant. The strong ducting occurring on the second day will result not only in larger angle and range errors than those occurring at night, but will also, in all probability, result in the development of radar holes. These radar holes could cause reduced detection ranges for early warning radars.

Airborne radars, such as the side-looking airborne radar (SLAR), will suffer a reduction in range as a result of the subrefractive conditions occurring on the first day, if the aircraft is flying above the condition. The superrefractive and ducting conditions of the first night and second day may result in an extended range for the SLAR system, but this would depend on the height at which the aircraft is flying and the height of these refractive conditions.

3. Conclusions

It can be seen that a multitude of combat systems as well as surveillance and intelligence gathering systems are affected by atmospheric refractive conditions. An ability to predict the existence of such conditions can go a long

way towards explaining irregular or "unusual" effects on army ground systems. The ability to forecast atmospheric refractive conditions will also provide an opportunity to take advantage of those effects that can enhance certain capabilities and to compensate for those that will degrade other capabilities.

IV. CONCLUSIONS AND RECOMMENDATIONS

A. CONCLUSIONS

It has been the purpose of this thesis to highlight the effects of atmospheric refraction on ground force's systems that utilize EM waves propagating through the atmosphere. To this end, the various forms of atmospheric refractivity in the troposphere have been described, and their characteristic effects on EM waves have been examined. Additionally, specific examples and simulations were used to expand and to reinforce some of the points brought out earlier in the thesis.

From the discussions, examples, and simulations presented herein, a number of points should be apparent. First, atmospheric refraction in several related but different forms does affect the propagation of EM waves traveling through the atmosphere. Second, the specific effects of atmospheric refraction on the different regions of the EM spectrum will vary, not only with wavelength, but with the form of the refractive condition. Third, to some degree the forms of atmospheric refraction can be forecast, given certain meteorological parameters. In a like manner, knowledge of the earth region of interest can be used to predict what form or forms of atmospheric refraction to expect. Fourth, specific military systems using the EM

spectrum are affected by refractive conditions in the atmosphere, and these effects result in the associated weapons system's performance also being affected. Fifth, the significance of atmospheric refraction on any given system is dependent on the form of the refraction, the strength of the effect, the form and purpose of the affected system, and the tactical scenario. There is, therefore, no easy answer to the question of whether atmospheric refraction is significant to a system's performance or whether it occurs often enough to be considered a significant effect. This latter consideration is dependent on the system affected and on the region of interest. Sixth, tactics can be developed to compensate for or to utilize certain atmospheric refractive effects. Finally, it should be apparent that atmospheric refractive effects on ground warfare should be given consideration by the tactical commander.

The ability to forecast, predict, and understand the effects of atmospheric refraction allows the commander to avoid being surprised by many of the "unexpected" and "unexplained" problems that occur in systems using EM radiation. This ability also provides the commander with opportunities to use certain refractive effects to his own advantage.

The tank gunnery results and the simulations in this thesis indicate that the U.S. Army's primary problems with atmospheric refraction will occur in the electro-optics

spectrum. There are some cases in the RF spectrum where refractive effects are fairly significant, as when lines of bearing travel for long distances through a refractive gradient. However, the effect on electro-optics (and possibly millimeter waves) over relatively short distances is more significant. Due to the shorter operational ranges of most EO systems, as compared with RF systems, the possibility of detecting and correcting refractive problems in this region may also be greater.

In short, it is hoped this thesis has shown atmospheric refraction to be worth further consideration and study. In the next sub-section a list of recommendations for the direction of further studies, is provided.

B. RECOMMENDATIONS

Following are recommendations for further study of the effects of atmospheric refraction on ground warfare, and additional recommendations as to when and where this subject should be considered.

1. Further study of the wavelength dependence of refractive effects is needed.
2. Atmospheric refraction should be a consideration in system design, particularly in system testing.
3. Study is needed concerning atmospheric refractive effects on specific systems (e.g. AH64 FLIR, Firefinder Radar, JSTARS, etc.).

4. As a result of studying the effects of atmospheric refraction on specific systems, methods should be developed to compensate for and/or take advantage of these effects.

5. An effort should be made to relate the effects of dispersion, extinction, reflection (multipath), and diffraction into the overall picture of atmospheric propagation.

6. Further study is needed on determining the causes of atmospheric refraction in its many forms, and into those meteorological parameters needed to forecast atmospheric refractive conditions accurately.

7. A greater understanding of the reflection coefficients for various vegetation and terrain types and their impacts on EM propagation is needed before a prediction model can be developed.

8. Development of a systems prediction model along the lines of the Navy's IREPS model is a must.

9. Once a prediction model is under development, a study will be needed to determine who, within the Army's organization, will measure the meteorological parameters needed to predict atmospheric refractive effects.

Determinations must also be made as to whom the responsibility for operating the prediction model will be given, to whom the data will be disseminated, and to whom the data will be disseminated.

APPENDIX A

IREPS

The U.S. Navy has been aware of the effects of the atmosphere, particularly of atmospheric refractivity, on EM waves since at least World War II. However, until recently the exact nature of these atmospheric refractive effects, and therefore an ability to accurately predict them, has been non-existent.

With the introduction of an Integrated Refractive Effects Prediction System (IREPS) by the Naval Ocean Systems Center (NOSC) of San Diego, the Navy has now developed the capability to predict atmospheric refractive conditions at sea. IREPS uses a desk-top programmable computer (HP 9845) with a graphic display to provide evaluations of the effects of refraction on surveillance, communication, electronic warfare, and weapon systems. This system is currently being installed on all Navy aircraft carriers, to be used as an aid in developing tactics to assess, compensate for, and take advantage of refractive effects at sea. Eventually, other atmospheric effects will also be integrated into the IREPS program, along with the PROCAL-PREOS airborne FLIR performance model, in order to develop a more comprehensive prediction system for future use.

It is important to note that the effects of concern in IREPS are only significant at EM frequencies above 100 MHz, are considered only for the lower atmosphere (troposphere), and only over water.

1. Products of IREPS Model

There are eight basic products that can be generated by IREPS, according to the IREPS Revision 2.0 User's Manual [Ref. 30: p. 30]. Each product is dependent on a variety of data that must be entered into the program. For the first product, only the latitude and longitude are needed, but for the remaining seven products, a variety of on site environmental data are required. Each product is displayed on the minicomputer screen, and can be printed on an 8 1/2-by-11-inch page. The eight products are:

a. The Historical Propagation Conditions Summary

Figure 58 is an example of the Historical Propagation Conditions Summary. This product provides a description of the refractive average conditions for the geographic location specified by an input longitude and latitude. A refractive profile can also be generated for this region by season and by conditions of darkness.

b. The Environmental Data List

Figure 59 is an example of the Environmental Data List, used primarily for checking values of radiosonde data entered into the program, such as pressure, temperature, and relative humidity. Values that are produced and printed

HISTORICAL PROPAGATION CONDITIONS SUMMARY

Specified location: 32 00 N 117 00 W
 Radiosonde source : 72290 32 49 N 117 07 W
 Radiosonde station height: 487 Feet
 Surface obs source: MS120 35 00 N 120 00 W

PERCENT OCCURRENCE OF ENHANCED SURFACE-TO-SURFACE RADAR/ESM/COM RANGES:

FREQUENCY	YEARLY			WINTER			SPRING			SUMMER			AUTUMN		
	day	nit	d&n	day	nit	d&n	day	nit	d&n	day	nit	d&n	day	nit	d&n
100 MHz	3	3	3	2	3	3	3	2	2	5	3	4	3	4	3
1 GHz	35	20	28	34	23	29	31	17	24	37	18	27	36	24	30
3 GHz	41	26	33	39	29	34	38	21	29	44	22	33	42	31	37
6 GHz	53	35	44	52	40	46	50	30	40	53	28	40	55	42	48
10 GHz	75	61	68	74	65	69	75	60	68	75	54	65	75	65	70
20 GHz	88	93	85	87	85	86	88	83	86	89	80	84	88	83	86

SURFACE BASED DUCT SUMMARY:

PARAMETER	YEARLY			WINTER			SPRING			SUMMER			AUTUMN		
	day	nit	d&n	day	nit	d&n	day	nit	d&n	day	nit	d&n	day	nit	d&n
Percent occurrence	25	22	23	18	26	22	24	15	20	33	21	27	23	27	25
AVG thickness Kft		.44			.28			.40			.70			.38	
AVG trap freq GHz		.89			.86			1.4			.55			.78	
AVG lyr grd -N/Kft			91			88			90			94			93

ELEVATED DUCT SUMMARY:

PARAMETER	YEARLY			WINTER			SPRING			SUMMER			AUTUMN		
	day	nit	d&n	day	nit	d&n	day	nit	d&n	day	nit	d&n	day	nit	d&n
Percent occurrence	42	54	48	28	38	33	47	65	56	56	72	64	37	41	39
AVG top ht Kft		2.5			2.7			2.6			2.2			2.6	
AVG thickness Kft		.60			.42			.64			.78			.56	
AVG trap freq GHz		.20			.30			.18			.11			.21	
AVG lyr grd -N/Kft			70			72			71			68			71
AVG lyr base Kft		2.2			2.5			2.2			1.7			2.3	

EVAPORATION DUCT HISTOGRAM IN PERCENT OCCURRENCE:

PERCENT OCCURRENCE	YEARLY			WINTER			SPRING			SUMMER			AUTUMN		
	day	nit	d&n	day	nit	d&n	day	nit	d&n	day	nit	d&n	day	nit	d&n
0 to 10 Feet	7	6	6	6	6	6	7	4	5	8	6	7	6	7	6
10 to 20 Feet	9	16	13	10	15	12	8	15	11	9	19	14	9	16	12
20 to 30 Feet	17	27	22	16	25	20	17	26	21	19	33	26	16	24	20
30 to 40 Feet	17	21	19	15	20	17	18	24	21	20	23	21	14	19	16
40 to 50 Feet	11	10	11	10	11	11	12	11	11	11	9	10	11	10	11
50 to 60 Feet	6	5	6	6	6	6	6	5	6	6	3	5	7	5	6
60 to 70 Feet	4	2	3	5	4	4	4	2	3	3	1	2	5	4	4
70 to 80 Feet	2	1	2	3	1	2	2	1	2	2	1	1	3	2	2
80 to 90 Feet	2	1	1	2	1	1	2	1	2	1	1	1	2	1	2
90 to 100 Feet	1	1	1	1	1	1	1	1	1	1	0	1	1	1	1
above 100 Feet	24	9	17	27	11	19	23	11	17	20	5	12	27	11	19
Mean height Feet	71	45	58	77	48	62	70	48	59	63	35	49	76	48	62

GENERAL METEOROLOGY SUMMARY:

PARAMETER	YEARLY			WINTER			SPRING			SUMMER			AUTUMN		
	day	nit	d&n	day	nit	d&n	day	nit	d&n	day	nit	d&n	day	nit	d&n
% occur EL&SB dcts			4			3			5			6			3
% occur 2+ EL dcts			8			4			9			14			6
AVG station N			330			321			329			343			326
AVG station -N/Kft			19			16			20			24			18
AVG afc wind Kts	9.0	9.1	9.1	8.7	10	9.1	10	9.3	9.4	8.7	8.5	9.6	8.3	9.1	9.0

Figure 58. Historical Propagation Conditions Summary Product.

IREPS REV 2.0

**** ENVIRONMENTAL DATA LIST ****

LOCATION: 31 56N 118 36W
DATE/TIME: 17 JUN 0045Z

WIND SPEED 12.0 KNOTS

EVAPORATION DUCT PARAMETERS:
SEA TEMPERATURE 18.2 DEGREES C
AIR TEMPERATURE 15.1 DEGREES C
RELATIVE HUMIDITY 89 PERCENT
EVAPORATION DUCT HEIGHT 28.0 FEET

SURFACE PRESSURE = 1000.0 MB
RADIOSONDE LAUNCH HEIGHT = 60.0 FEET

LEVEL	PRESS (MB)	TEMP (C)	RH (%)	DEW PT DEP(C)	FEET	N UNITS	N-Kft	M UNITS	CONDITION
1	1,000.0	15.1	89.0	1.8	60.0	340.0	-20.2	342.9	SUPER
2	1,000.0	14.2	87.0	2.1	201.6	333.8	15.6	347.2	SUB
3	993.0	13.9	95.0	0.8	476.6	336.8	-10.9	359.6	NORMAL
4	982.0	13.3	97.0	0.5	785.3	333.4	-176.4	371.0	TRAP
5	972.0	20.4	25.0	20.8	1,071.8	282.9	27.2	334.2	SUB
6	962.0	21.5	34.0	16.6	1,364.9	290.9	-20.9	356.2	SUPER
7	949.0	21.5	27.0	19.9	1,751.3	279.7	-9.4	363.5	NORMAL
8	862.0	20.6	25.0	20.8	4,477.3	254.0	-9.5	468.2	NORMAL
9	850.0	19.7	25.0	20.7	4,873.5	250.2	-7.6	483.4	NORMAL
10	807.0	20.0	25.0	20.7	6,339.1	239.0	-6.0	542.3	NORMAL
11	726.0	14.5	34.0	15.8	9,299.4	221.2	-8.9	666.1	NORMAL
12	700.0	11.8	34.0	15.5	10,305.6	212.2	-----	705.3	-----

SURFACE REFRACTIVITY: 341 --SET SPS-40 TO 344

Figure 59. Environmental Data List Product.

out in the Environmental Data List are the dewpoint depression, altitude, N unit, N unit gradient, M unit and a description of the refractive condition.

c. The Propagation Conditions Summary

Figure 60 is an example of the Propagation Conditions Summary, showing the existence of refractive conditions for a specified region at a given date and time. The summary provides a plot versus altitude diagram of N units and M units. The extent of any duct present is shown by the use of shaded areas in the block on the right hand side of the summary. A brief statement on the performance of several types of EM systems operating in the specified region is provided at the bottom of this summary.

d. Surface-Search Radar Range Tables

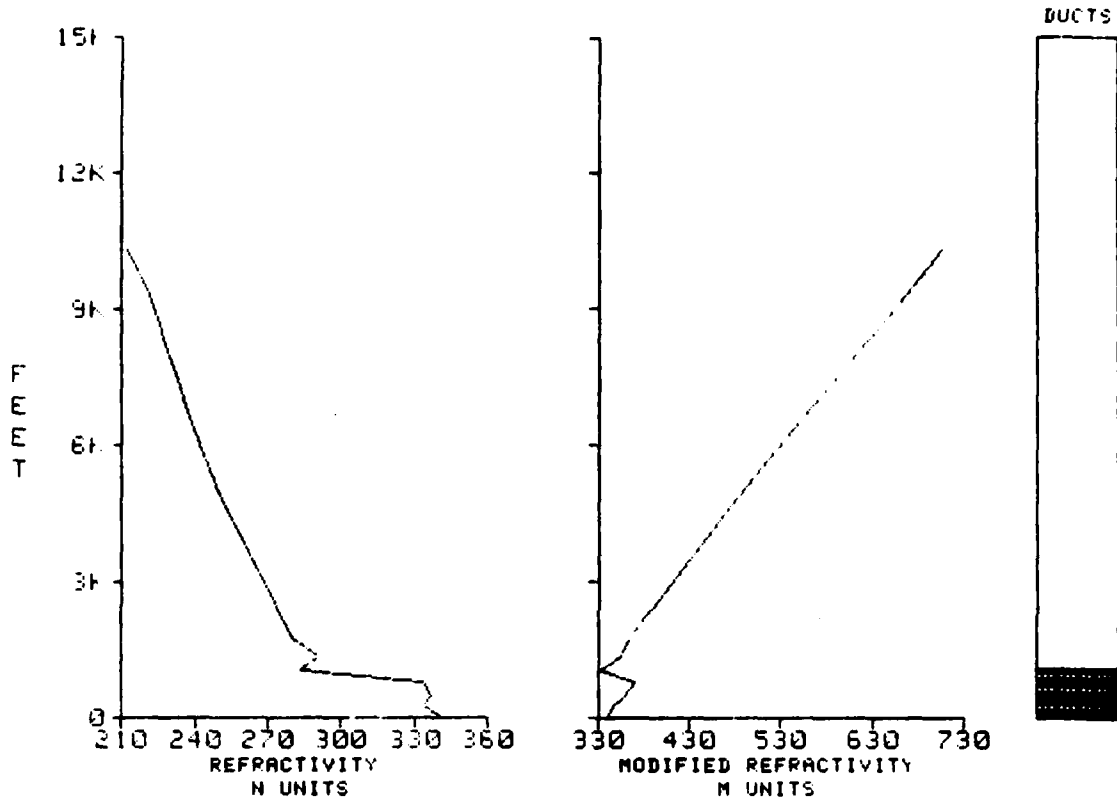
Figure 61 is the Surface-Search Radar Table format. This product provides detection range predictions for naval surface-search radars. An actual example of the output is not provided since the predicted range values are classified CONFIDENTIAL.

e. The Coverage Display

Figures 19 and 20 are examples of the Coverage Display product. This product shows the area of coverage of a specific type of radar or radio emitter on a curved earth range-versus-height plot. The shaded area is the area of detection or communication for the system represented. The impact of atmospheric refraction on a system can be seen

**** PROPAGATION CONDITIONS SUMMARY ****

LOCATION: 31 56N 118 36W
 DATE TIME: 17 JUN 0045Z



WIND SPEED= 12.0 KNOTS

EVAPORATION DUCT HEIGHT= 8.5 METRES
 = 28.0 FEET

SURFACE-TO-SURFACE
 EXTENDED RANGES AT ALL FREQUENCIES

SURFACE-TO-AIR
 EXTENDED RANGES FOR ALTITUDES UP TO 1,072 FEET
 POSSIBLE HOLES FOR ALTITUDES ABOVE 1,072 FEET

AIR-TO-AIR
 EXTENDED RANGES FOR ALTITUDES UP TO 1,072 FEET
 POSSIBLE HOLES FOR ALTITUDES ABOVE 1,072 FEET

SURFACE REFRACTIVITY: 341 --SET SPS-48 TO 344

Figure 60. Propagation Conditions Summary Product.

***** SURFACE SEARCH RADAR RANGE TABLE *****

LOCATION:
TIME:

SURFACE SEARCH RADAR:

RADAR ANTENNA HEIGHT: FEET

U S SHIP TYPE/CLASS	DETECTION RANGE IN NM		
	MIN	AVG	MAX
CV/CVN			
CG/CGN			
DD/DDG			
FF/FFG			
LCC			
LHA			
LPH			
LKA			
LPD			
LSD			
LST			
RE/RF			
AO/AOE/AOR			

SOVIET SHIP TYPE/CLASS	DETECTION RANGE IN NM		
	MIN	AVG	MAX
KIEV CLASS			
MOSKVA CLASS			
CLG			
CG/CC/CA			
DD/DDG			
FRIGATE			
CORVETTE			
OSA/STENKA CLASS			
PRIMORYE CLASS AGI			
LENTRA CLASS AGI			
OKEAN CLASS AGI			

EVAPORATION DUCT HEIGHT= METRES.
= FEET

Figure 61. Surface Search Radar Range Table Format.

graphically by comparing printouts of the radar coverage with and without refractive effects present. Note also that the presence of a radar hole can be seen in this product by the shape of the coverage pattern above the duct.

f. The Loss Display

Figure 62 is an example of a Loss Display showing one-way path loss in dB versus range. The dashed line on the printout is the threshold for detection, communications, or intercept. The solid line is the system's signal. Thus, a determination of where the signal would be strong enough to be detected can be estimated from this product.

g. The Radiosonde Observation Analysis

This product is provided largely to assist meteorological personnel, and consists of a radiosonde listing, a skew T, a log P thermodynamic diagram, and an encoded upper air observation message.

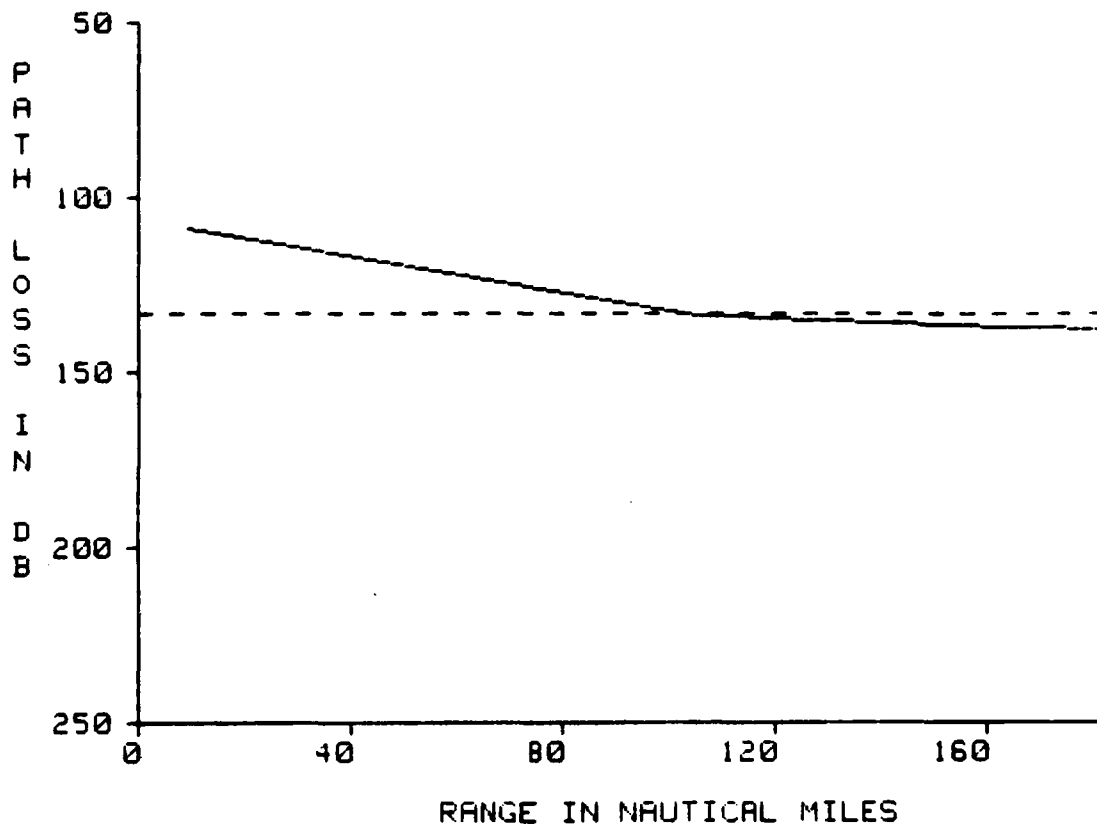
h. The ESM Intercept Range Table

Figure 63 is the format for the ESM Intercept Range Table. This table provides the maximum intercept range for several different Naval ESM systems versus a variety of hostile emitters. An actual example is not provided since much of the information on the hostile emitters and on the predicted values is classified.

**** LOSS DISPLAY ****

SURFACE UHF COM

LOCATION: 31 56N 118 36W
DATE/TIME: 17 JUN 0045Z



BASED ON A 200 NM FREE SPACE COMMUNICATIONS CAPABILITY
TO A SURFACE SHIP PLATFORM

DASHED LINE INDICATES DETECTION, COMMUNICATION, OR INTERCEPT THRESHOLD

FREE SPACE RANGE: 200.0 NAUTICAL MILES
FREQUENCY: 300 MHZ
TRANSMITTER/RADAR HEIGHT: 130.0 FEET
RECEIVER/TARGET HEIGHT: 100.0 FEET

Figure 62. Loss Display Product.

***** ESM INTERCEPT RANGE TABLE *****

LOCATION:
TIME:

ESM RECEIVER: MLR-1 CV

EMITTER CLASS: SOVIET

EMITTER	FREQ (MHz)	MAX INTERCEPT RANGE (nmi)
KNIFE REST A		
KNIFE REST B		
CROSS BIRD		
SQUARE HEAD		
HIGH POLE		
FAN SONG E MG		
TOP TROUGH		
BIG NET		
TOP SAIL		
HIGH LUNE		
SCOOP PAIR		
HEAD NET		
SLINNET		
LOW SIEVE		
BALL END		
HIGH SIEVE		
FRONT DOOR		
TRAP DOOR		
STRUT PAIR		
STRUT CURVE		
FAN SONG E MT		

EMITTER	FREQ (MHz)	MAX INTERCEPT RANGE (nmi)
HEADLIGHT		
MUFF COB		
POP GROUP		
BASS TILT		
DRUM TILT		
OWL SCREECH		
SQUARE TIE		
SNOOP TRAY		
PEEL GROUP		
HAWK SCREECH		
TOP BOW		
SNOOP PLATE		
DONETS		
DONETS-2		
POT HEAD		
LOW TROUGH		
SUN VISOR		
NEPTUNE		
DON KAY		
DON/DON-2		

EMITTER CLASS: U.S. NAVY

EMITTER	FREQ (MHz)	MAX INTERCEPT RANGE (nmi)
SPS-43A		
SPS-29		
SPS-37		
SPS-37A		
SPS-32		
SPS-40		
SPS-49		
IFF INT		
TACAN		
SPS-39		
SPS-42		
SPS-40		
SPS-52		
MK-26		
SPS-39A		
MK-35/MOD 8		
SPS-33		
SPS-30		
SPN-43		
SPN-6		
SPS-10		
SPG-49 ACU		
SPG-51		
MK-37		
SPS-5,9,11-15		
MK-13		
MK-34		

EMITTER	FREQ (MHz)	MAX INTERCEPT RANGE (nmi)
SPG-53A		
MK-60		
SPG-34		
SPG-50		
SPQ-9A		
MK-25/MOD 3		
MK-35/MOD 2		
MK-56		
MK-25/MOD 2		
MK-87		
SPN-35		
SPS-46		
SPS-53		
CPR 1500		
CPR 2900		
LN 66		
RAYTHEON 2502		
RAYTHEON 2040		
RAYTHEON 1900		
DECCA 202		
DECCA 914		
HEL-H 1079		
SPS-55		
SPN-12		
MK-115		
SPG-53B		
SPN-41		

EVAPORATION DUCT HEIGHT= METRES
= FEET

Figure 63. ESM Intercept Range Table Format.

2. Limitations of the IREPS Model

There are a number of limitations in the IREPS model, some of which are being corrected. These limitations include:

- a. Limited frequency range.
- b. Neglect of the effect of land and sea clutter.
- c. Assumption of horizontal homogeneity in the refractive structure.
- d. Limits on the maximum and minimum ground based antenna height.
- e. Exclusion of the effects of sea-reflection interference on airborne systems.
- f. Assumption that all EM systems are horizontally polarized.
- g. Absorption is not accounted for.
- h. Limits exists on the consideration of low level elevated ducts.
- i. The coverage diagram is not applicable to all radar applications.

3. Applicability of IREPS to Over-land Refractive Prediction

While IREPS is proving to be of considerable value to the Navy even with its wide range of limitation, its applicability over water does not imply that it will work equally well over land. IREPS in its present form, because it was designed for over-water use, does not account for

terrain features, vegetative effects, soil type, or variation in the surface reflective coefficient, all of which have great effect over land. In addition, the nature of atmospheric refractivity over land is much more transient and localized than over water, and this must also be taken into account in developing an over-land model. The basic design of IREPS, however, may prove to be viable in the development of an over-land model and, at the very least, is worthy of further study in this regard.

APPENDIX B

COMPUTER SIMULATION 1 LISTING AND OUTPUT

This Appendix contains the program and output for Simulation 1. Each computer run is summarized in four pages: Summary of the Parameters, a Transmission Loss Table, A Loss Diagram, and a Signal Strength Table. The latter contains the refractivity value. The type of system (either radar or communications) can be identified by the frequency at the top of the first output page for each run.

THIS PROGRAM IS USED IN A MASTER'S THESIS BY TOM HOUSER AND
 TED MOURAS TO EVALUATE THE EFFECTS OF REFRACTIVITY ON
 GROUND TACTICAL SYSTEMS OPERATING IN THE RF SPECTRUM.
 IT IS A MODIFICATION OF A PROGRAM WRITTEN BY THE ESSA
 RESEARCH LABORATORIES IN 1968 AND FURTHER UPDATED BY SCHOOL
 LT. JAMES H. CALLAGHAN AT THE NAVAL POSTGRADUATE SCHOOL
 IN JUNE 1973. ITS PURPOSE IS TO PREDICT LONG-TERM
 TROPOSPHERIC RADIO TRANSMISSION LOSS OVER IRREGULAR TERRAIN.

IMPLICIT REAL*8(A-H,O-Z)
 COMMON /MM/ F, D, NS, A, DH, DHS, S, E, POL, KM
 COMMON /MP/ H1E, H2E, H1G, H2G, DLS1, DLS2, DL1, DL2, DL, DLS, TE1, TE2, TE, KL
 COMMON /MDS/ AG, AD, AS, AC, AED, MD, AH50, AH5, D5, MS, AES, DX, H5
 COMMON /ML/ DO, DL, D01, D02, A0, A1, K1, K2, AL, ALS, A0G
 DIMENSION SO(100), SA(100), DB(100)
 REAL*8 NS, MC, MDO, MS, MSS, MDS, KI, K2, K3, K4, LBF

READ IN DATA FROM DATAFILE TROP01--SEE FILE FOR EXPLANATION
 OF DATA VARIABLES.

19 READ (5,20,END=9999) ITERR, IDB, DIST
 20 FORMAT (2I10, F10.5)

25 IF (10B.NE.1) GO TO 24
 23 READ (5,23) TXPO, TXAG, RXAG, TRLL, RXLL, RXIN
 23 FORMAT (6F10.2)
 DOB=10+DLOG10(TXPO)+TXAG+RXAG-TRLL-RXLL

24 IF (ITERR.LT.4) GO TO 26
 21 READ (5,21) NSS, SS, EE, DHH
 21 FORMAT (I10, 3F10.5)

26 READ (5,22) POL, F, H1G, H2G
 22 FORMAT (4F10.5)

COLORADO PLAINS TERRAIN DATA

CCCCCCCCCCCC

CCCCC

CC

CC

CC

CCCC

```

C
NS=290.
S=.005
E=15.
DHS=90.
ITERR.EQ.2) GO TO 3
IF (ITERR.EQ.3) GO TO 5
IF (ITERR.GT.3.AND.ITERR.LT.6) GO TO 7
      WRITE OUT COLORADO PLAINS TERRAIN HEADING
      CCCCC
2  WRITE (6,2) ('1',////////,54X,'---- COLORADO PLAINS ----',/)
   FORMAT 9
   GO TO 9
      COLORADO MOUNTAIN TERRAIN DATA
      CCCCC
3  DH=650.
   DHS=650.
      WRITE OUT COLORADO MOUNTAINS TERRAIN HEADING
      CCCCC
4  WRITE (6,4) ('1',////////,53X,'---- COLORADO MOUNTAINS ----',/)
   FORMAT 9
   GO TO 9
      OHIO TERRAIN DATA
      CCCCC
5  NS=312.
      WRITE OUT OHIO TERRAIN HEADING
      CCCCC
6  WRITE (6,6) ('1',////////,60X,'---- OHIO ----',/)
   FORMAT 9
   GO TO 9
      C

```

```

USER TERRAIN DATA
7 NS=NS S
  S=SS
  E=EE
  DH=DHH
  DHS=DHH
WRITE USER TERRAIN HEADING
8 WRITE (6,8)
  FORMAT ('1',////////,53X,'--- USER TERRAIN DATA ---',/)
WRITE OUT SIGNAL FREQUENCY
9 WRITE (6,27) F
27 *FORMAT (////,2X) SIGNAL -F- (MEG-HERTZ)',02X,F10.5,//////////)
  *FREQUENCY (F)

CALCULATION OF H1E AND H2E
H1E=H1G
IF (H1G.LE.2.0) GO TO 12
IF (H1G.GE.2.0.OR.H1G.LE.5.0) GO TO 10
Z1=5.0
GO TO 11
10 Z1=1.0+DSIN(3.1415927*H1G/10.0)
11 H1E=H1G+Z1*DEXP(-2.0*H1G/DH)
12 H2E=H2G
IF (H2G.LE.2.0) GO TO 15
IF (H2G.GE.2.0.OR.H2G.LE.5.0) GO TO 13
Z2=5.0
GO TO 14
13 Z2=1.0+DSIN(3.1415927*H2G/10.0)
14 H2E=H2G+Z2*DEXP(-2.0*H2G/DH)
15 CONTINUE
A=6370./((1.-0.4665*DEXP(.005577*NS))
DL S1=DSQRT(.002*A*H1E)
DL S2=DSQRT(.002*A*H2E)
DL S=DL S1+DL S2
DL I=DL S1*DEXP(-.07*DSQRT(DH/DMAX1(5.0D0,H1E)))

```

```
DL2=DL S2*DEXP(-.07*DSQRT(DH/DMAX1(5.0D0,H2E)))
DL=DL1+DL2
TE1=(.00065/DLS1)*((DLS1/DL1-1.)*DH-3.077*H1E)
TE2=(.00065/DLS2)*((DLS2/DL2-1.)*DH-3.077*H2E)
TE=DMAX1(TE1+TE2),(-DL/A)
```

```
START OF "DELTA-DISTANCE" LOOP
```

```
DMAX=0.0
DO 300 IDIS=1,100
D=DIST*IDIS/100.0
IF (IDIS.EQ.100) D=DIST
IF (D.GT.DL S) GO TO 40
```

```
CALL SUBROUTINE "LOS"
```

```
CALL LOS
```

```
STORE ATTENUATION (ACR) AND DISTANCE (D) DATA
```

```
SD(IDIS)=D
ACT=ACR+32.45+20*DLOG10(F)+20*DLOG10(D)
SA(IDIS)=ACT
GO TO 300
```

```
CALL SUBROUTINE "DIFF"
```

```
40 CALL DIFF
SD(IDIS)=D
ACT=ACR+32.45+20*DLOG10(F)+20*DLOG10(D)
SA(IDIS)=ACT
AE=AO G-K1*D0-K2*DLOG10(D0)
ADX=AE0+MD*DX
IF (-RXIN.LT.DDB-ACT+30.0) DMAX=D
```

```
END OF "100 POINT DISTANCE" LOOP
```

```
300 DB(IDIS)=DDB-ACT+30.0
```

```

CCCCC
WRITE "DISTANCE, TRANS-LOSS" HEADING AND DATA.
301 WRITE (6,301)
   FORMAT (1X,5(3X,'DISTANCE',2X,'TRANS-LOSS ',2X))
3011 WRITE (6,3011)
   FORMAT (5(6X,:(KM)',7X,:(DB)',5X),///)
DO 303 K=1,20
302 WRITE (6,302) (SD(K+20*(N-1)),SA(K+20*(N-1)),N=1,5)
303 FORMAT (2X,5(F8.4,-----,F6.2,6X),/)
CONTINUE

```

SCALE GRAPH FOR ATTENUATION.

```

70 SCAL=0.0
   SCAL=SCAL+1.0
   SCA=SCAL*6.0
   IF (SA(100).LE.SCA) GO TO 71
   GO TO 70
71 RA1=SD(100)
   RA2=0.0
   RA3=SCA
   DO 80 I=1,6
   SCAA=(SCA/6)*I
   IF (SCAA.GE.SA(1)) GO TO 81
80 CONTINUE
81 RA4=SCAA-SCA/6

```

PLOT TRANS-LOSS (DB) VS DISTANCE (KM).

```

CCCCC
WRITE (6,72)
72 FORMAT (1,1,48X,'PLOT OF TRANS.-LOSS VERSUS DISTANCE',///)
   IF (IDB.NE.1) GO TO 723
   DDC=DD8+30.0
   WRITE (6,722) DDC
722 FORMAT (1,1,1X,48X,'TO FIND SIGNAL STRENGTH FROM GRAPH, SUBTRACT 1
   *RANS.-LOSS FROM',F7.2,///)
723 CALL UTPLOT (SD,SA,100,RA1,RA2,RA3,RA4,2,0)
85 WRITE (6,85)
   FORMAT (1,1,1X,'TRANS-LOSS (DB)',30X,'DISTANCE (K-METERS)',)
   IF (IDB.NE.1) GO TO 308

```

```

CCCC
WRITE "DISTANCE AND SIGNAL STRENGTH" HEADING AND DATA
304 WRITE (6,304)
  FORMAT(11,3X,1,---, SIGNAL STRENGTH VERSUS DISTANCE FOR GIVEN SYST
  *EM PARAMETERS ---,1X,5(3X, DISTANCE,2X, SIG-STRENGTH
  *,1X))
3041 FORMAT(1X,5(5X,(KM),.8X,.4X),///)
  DO 306 K=1,20
305 WRITE(6,305) (SD(K+20*(N-1)),DB(K+20*(N-1)),N=1,5)
306 FORMAT(2X,5(F8.4,---,F8.2,6X),/)
  RXGG=RXIN
307 WRITE(6,307) RXGG,DMAX
  *FORMATT(///,9X,*** FOR A RECEIVER INPUT LEVEL OF ,F07.2,
  *, DBM ,DISTANCE BETWEEN ANTENNAS CAN BE AT LEAST',F07.2,
  *, KM ,***,)

```

WRITE OUTPUT PARAMETERS

```

CCCCC
308 IF (ITERR.EG.5) GO TO 69
WRITE(6,74)
74 FORMAT(11,52X,--- PROGRAM PARAMETERS ---,///)
  IF (POL.GT.0.0) GO TO 61
WRITE(6,60) //,15X,'POLARIZATION (POL), ---
  *FORMATT(--- HORIZONTAL,/)
  GO TO 63
61 WRITE(6,62) //,15X,'POLARIZATION (POL), ---
  *FORMATT(--- VERTICAL,/)
63 WRITE(6,64) F,SNS TE,DIST,AE,OH,DL,S,ALS
64 FORMAT(15X,
  *SURFACE CONDUCTIVITY (S) --- MEG-HERTZ ,//,
  *SURFACE REFRACTIVITY (NS) --- MHO/METER ,//,
  *SUM OF ELEVATION ANGLES (TE) --- N-UNITS ,//,
  *DISTANCE BETWEEN ANTENNAS (DIST) --- RADIANS ,//,
  *ATTENUATION BELOW FREE SPACE (AE) --- K-METERS ,//,
  *F7.2 , DB

```



```

*15X, ' INTERDECILE RANGE OF TERRAIN HEIGHT (DH) -----
*15X, ' SUM OF SMOOTH-EARTH HORIZON DISTANCES (DLS) -----
*15X, ' DIFFRACTION ATTENUATION AT DISTANCE DLS (ALS) -----
WRITE(6,65) E,AES,H2G,H1G,AED,K1,K2,MS
65 FORMAT(15X, ' PERMITTIVITY OR RELATIVE DIELECTRIC CONSTANT (E) --
*15X, ' ESTIMATED SCATTER ATTENUATION BELOW FREE SPACE (AE
*15X, ' STRUCTURAL RECEIVER ANTENNA HEIGHT ABOVE GROUND (H2
*15X, ' STRUCTURAL TRANSMITTER ANTENNA HEIGHT ABOVE GROUND
*15X, ' ESTIMATED DIFFRACTION ATTENUATION BELOW FREE SPACE
*15X, ' COEFFICIENT THAT DEFINES SLOPE OF A SMOOTH CURVE OF
*15X, ' COEFFICIENT THAT DEFINES SLOPE OF A SMOOTH CURVE OF
*15X, ' SLOPE OF THE CURVE OF SCATTER ATTENUATION AS VERSUS
*15X, ' DISTANCE (MS), ADX, MD
WRITE(6,66) DX,ADXM,DXM,ADXM,DXM,ADXM,DXM,ADXM,DXM,ADXM,DXM,ADXM
66 FORMAT(15X, ' ARE EQUAL (DX) ATTENUATION WHERE DIFFRACTION AND SCATTER ATTENUATI
*15X, ' ARE EQUAL (ADX) SLOPE OF THE CURVE OF DIFFRACTION ATTENUATION AS VE
*15X, ' ARE EQUAL (MD) SLOPE OF THE CURVE OF DIFFRACTION ATTENUATION AS VE
IF (IDB.NE.1) GO TO 69
67 WRITE(6,68) TXPO,TRLL, TXAG, RXGG, RXLL, RXAG
68 FORMAT(15X, ' SIGNAL STRENGTH DATA INPJIT ----',,/,/,/,/,/,/,/,/,
*15X, ' TRANSMITTER POWER OUTPUT -----
*15X, ' TRANSMITTER TRANSMISSION LINE LOSS -----
*15X, ' TRANSMITTER ANTENNA GAIN -----
*15X, ' RECEIVER SENSITIVITY -----
*15X, ' RECEIVER TRANSMISSION LINE LOSS -----
*15X, ' RECEIVER ANTENNA GAIN -----
69 CONTINUE

```

```

CC          START PROGRAM AGAIN
          9999 GO TO 19
          CONTINUE
          STOP
          END
CC          SUBROUTINE CIFF
CC          SUBROUTINE TO COMPUTE DIFFRACTION ATTENUATION
          IMPLICIT REAL*8(A-H,O-Z)
          COMMON /NR/ SW3,SW4,SA3,SA4,SAFO,JZ
          COMMON /MH/ F,D,NS,A,DH,DHS,S,E,POL,KM
          COMMON /MP/ H1E,H2E,H1G,H2G,DL1,DL2,DL,DLS,TE1,TE2,TE,KL
          COMMON /MLDS/ AG,AD,AS,ACR,AED,MD,AH50,AH5,D5,MS,AES,DX,H5
          REAL*8 NS,MC,MDO,MS,MSS,MDS,K1,K2,K3,K4
          X=180.00.*S/F
          RDL=DL
          KK=0
          10 KK=KK+1
          D3=DL+.5*(A*A/F)**.333333333
          IF (D3 .LT. DLS) D3=DLS
          D4=D3+(A*A/F)**.333333333
          T3=TE+D3/A
          T4=TE+D4/A
          CALCULATION OF KNIFE EDGE DIFFRACTION
          V13=1.2915*I3*DSORT(F*DL1*(D3-DL)/(D3-DL2))
          V23=1.2915*I3*DSORT(F*DL2*(D3-DL)/(D3-DL1))
          V14=1.2915*I4*DSORT(F*DL1*(D4-DL)/(D4-DL2))
          V24=1.2915*I4*DSORT(F*DL2*(D4-DL)/(D4-DL1))
          AV13=FNA(V13)
          IF (V13 .GT. 2.4) AV13=FNB(V13)
          AV23=FNA(V23)
          IF (V23 .GT. 2.4) AV23=FNB(V23)
          AV14=FNA(V14)
          IF (V14 .GT. 2.4) AV14=FNB(V14)
          AV24=FNA(V24)
          IF (V24 .GT. 2.4) AV24=FNB(V24)
          AK3=AV13+AV23
          AK4=AV14+AV24

```

CALCULATION OF ROUNDED EARTH DIFFRACTION

```

A1=DL1*DL1/(.002*H1E)
A2=DL2*DL2/(.002*H2E)
A3=(D3-DL1)/T3
A4=(D4-DL1)/T4
K1=FND(A1,F,E,X)
K2=FND(A2,F,E,X)
K3=FND(A3,F,E,X)
K4=FND(A4,F,E,X)
IF (POL(E,X)-1.) GO TO 15
K1=FNE(K1,E,X)
K2=FNE(K2,E,X)
K3=FNE(K3,E,X)
K4=FNE(K4,E,X)
B1=FNC(K1,F)
B2=FNC(K2,F)
B3=FNC(K3,F)
B4=FNC(K4,F)
X1=B1*DL1/A1** .6666666666
X2=B2*DL2/A2** .6666666666
X3=B3*(D3-DL1)/A3** .6666666666+X1+X2
X4=B4*(D4-DL1)/A4** .6666666666+X1+X2
XL1=450./DABS(DLOG10(K1)**3)
XL2=450./DABS(DLOG10(K2)**3)
IF (X1.GT.0..AND.X1.LE.200. .AND.K1.GE.0..AND.K1.LE.0.00001)
  C GO TO 16
16 T=40.*DLOG10(X1)-117.
   T1=-117.
   T2=DMINI((DABS(T)),(DABS(T1)))
   FX1=T
   IF (T2.EQ.DABS(T1)) FX1=T1
17 IF (X2.GT.0..AND.X2.LE.200. .AND.K2.GE.0..AND.K2.LE.0.00001)
  C GO TO 18
18 T=40.*DLOG10(X2)-117.
   T1=-117.
   T2=DMINI((DABS(T)),(DABS(T1)))
   FX2=T
   IF (T2.EQ.DABS(T1)) FX2=T1
19 IF (X1.GT.0..AND.X1.LE.200. .AND.K1.GT.0.00001 .AND.K1.LT.1.
  C) GO TO 21
   GO TO 22
21 FX1=40.*DLOG10(X1)-117.
   XL1=LE.XL1)FX1=20.*DLOG10(K1)+2.5*1. E=5*X1/K1-15.
22 IF (X2.GT.0..AND.X2.LE.200. .AND.K2.GT.0.00001 .AND.K2.LT.1.
  C) GO TO 23

```

```

23 GO TO 24 *DLOG10(X2) -117.
FX2=40. LE(XL2) FX2=20. *DLOG10(K2)+2.5*1. E-5*X2*X2/K2-15.
24 IF(X2) *DEXP(-.005*X1)
W1=.0134*X2 *DEXP(-.005*X2)
IF(X1) *GT.200. AND X1 LE 117. 2000.
IF(X2) *GT.200. *DLOG10(X1) +11. -W1*(.05751*X1-10.*DLOG10(X1))
C IF(X2) *GT.200. *AND. X2 LE. 2000.
IF(X1) *GT.2000. *DLOG10(X2) -117. +11. -W2*(.05751*X2-10.*DLOG10(X2))
IF(X2) *GT.2000. ) FX2=.05751*X1-10.*DLOG10(X1)
IF(X1) *GT.2000. ) FX2=.05751*X2-10.*DLOG10(X2)
GX3=.05751*X3-10.*DLOG10(X3)
GX4=.05751*X4-10.*DLOG10(X4)
AR3=GX3-FX1-FX2-20.
AR4=GX4-FX1-FX2-20.

```

COMBINATION OF ROJNDED EARTH AND KNIFE EDGE DIFFRACTION

```

28 DH03=DH*(1.-.8*DEXP(-.02*D3))
DH04=DH*(1.-.8*DEXP(-.02*D4))
P13=DSQRT((H1E*H2E)/(H1G*H2G))+(A*TE+DL)/D3
P14=DSQRT((H1E*H2E)/(H1G*H2G))+(A*TE+DL)/D4
D0L3=DMINI(1000.0D0.(DH03*F/299.7925))
D0L4=DMINI(1000.0D0.(DH04*F/299.7925))
W3=1./((1.+1*DSQRT(D0L3*P13))
W4=1./((1.+1*DSQRT(D0L4*P14))
A3=(1.-W3)*AK3+W3*AR3
A4=(1.-W4)*AK4+W4*AR4
MD=(A4-A3)/(D4-D3)
AED=A4-MD*D4
DH0LS=DH*(1.-.8*DEXP(-.02*DLS))
SHDLS=.78*DHL$*DEXP(-.5*(DHL$**25))
AF0=DMINI(AFO,15.0D0)
AED=AED+AF0
91 IF (KM .EQ. 2) GO TO 40
IF (KK .EQ. 2) GO TO 20
SAFO=AF0
SW3=W3
SW4=W4
SA3=A3
SA4=A4
AD=AED+MD*D
32 TD=(TE+D/A)*D
SDL1=DL1
SDL2=DL2
STE1=TE1

```

```

CC
STE2=IE2
STE=TE
CALCULATION OF SCATTER ATTENUATION
CALL SCATT
IF (H5 .LE. 10.) AES=AH5 -MS*D5
IF (H5 .LE. 10.) AS=AES+MS*D
IF (H5 .LE. 10.) GO TO 30
MDS=HD
AEDS=AED
DH=0.
GO TO 10
20 ADO=AED
MD=MS
AED=AEDS
DX1=(AHL50-MS*D5-ADO)/(MDO-MS)
DX2=(RD1+.25*(A*A/F))*+.3333333333333333*DLOG10(F)
DXO=DX1*(3.-.2*H5)+DX2*(.2*H5-2.)
AXO=ADO+MDO*DXO
ASX=AXO+(AH5-AH50)
AS=AES+MS*D
30 DX=(AES-AED)/(MD-MS)
DXN=DL+.25*(A*A/F))*+.3333333333333333*DLOG10(F)
IF (DXN .GT. DX) AES=AES+MS*D
IF (DXN .GT. DX) DX=DXN
ACR=AD
IF (D .GT. DX) ACR=AS
DL1=SDL1
DL2=SDL2
DL=SDL
TE1=STE1
TE2=STE2
TE=STE
DH=DHS
41 CONTINUE
40 END
SUBROUTINE SCATT
SUBROUTINE TO COMPUTE SCATTER PARAMETERS
IMPLICIT REAL*8(A-H,O-Z)

```

```

COMMON /MM/ F,D,NS,A,DH,DHS,S,E,POL,KM
COMMON /NP/ H1E,H2E,H1G,H2G,DLS1,DL2,DL1,DL2,DL,DLS,TE1,TE2,TE,KL
COMMON /MAR/ 14/03,04,05
COMMON /MLDS/ AG,AD,AS,ACR,AED,MD,AH50,AH5,D5,MS,AFS,DX,H5
REAL*8 NS,MD,MDO,MS,MSS,MDS,K1,K2,K3,K4
KK=0
10 KK=KK+1
D5=DL+200.
D6=DL+400.
11 T5=TE+D5/A
T6=TE+D6/A
H5=DMINI(((1./H1E+1./H2E)/(T5*F*DABS(.007-.058*T5))),{(15.000)})
H5=H5+10.*DLOG10(F*T5**4)-.1*(NS-301.)*DEXP(-T5*D5/40.)
S6=H6+10.*DLOG10(F*T6**4)-.1*(NS-301.)*DEXP(-T6*D6/40.)
IF (T5*D5 .LT. 10.) AH5=S5+103.4+.332*T5*D5
IF (T6*D6 .LT. 10.) AH6=S6+103.4+.332*T6*D6-10.*DLOG(T6*D6)
IF (T5*D5 .GT. 10.) .AND.T5*D5.LE.70.) AH5=S5+97.1+.212*T5*D5-2.5*
CDLOG10(T5*D5)
IF (T6*D6 .GT. 10.) .AND.T6*D6.LE.70.) AH6=S6+97.1+.212*T6*D6-2.5*
CDLOG10(T6*D6)
IF (T5*D5 .GT. 70.) AH5=S5+86.8+.157*T5*D5+5.*DLOG10(T5*D5)
IF (T6*D6 .GT. 70.) AH6=S6+86.8+.157*T6*D6+5.*DLOG10(T6*D6)
MS=(AH6-AH5)/(D6-D5)
IF (KK .EQ. 2) GO TO 25
IF (H5 .LE. 10.) GO TO 30
IF (KK .EQ. 1) GO TO 20
25 MS=MSS
AH50=AH5
AH5=AH5
D5=D5
GO TO 30
20 DH=0.
DL1=DL*S1*DEXP(-.07*DSQRT(DH/DMAX1(5.000,H1E)))
DL2=DL*S2*DEXP(-.07*DSQRT(DH/DMAX1(5.000,H2E)))
DL=DL1+DL2
TE1=(.00065/DLS1)*{(DLS1/DL1-1)*DH-3.077*H1E}
TE2=(.00065/DLS2)*{(DLS2/DL2-1)*DH-3.077*H2E}
TE=DMA XI((TE1+TE2),(-DL/A))
T=TE+D/A
AH5S=AH5
MSS=MS
D5S=D5
GO TO 10
30 CONTINUE
RETURN
END

```

```

SUBROUTINE LOS
SUBROUTINE TO COMPUTE LINE OF SIGHT ATTENUATION
IMPLICIT REAL*8(A-H,O-Z)
COMMON /MM/F,D,NS,A,DH,DHS,S,E,POL,KM
COMMON /NR/W,SM3,SM4,SA3,SA4,SAFO,JZ
COMMON /MP/H1E,H2E,HIG,H2G,DL1,DL2,DL1,DL2,DL1,DL2,DL1,DL2,TE1,TE2,TE,KL
COMMON /MLD/AG,AD,AS,ACR,AED,MD,AH5,D5,MS,AES,DX,H5
COMMON /ML/DO,D1,DO2,AO,A1,K1,K2,AL,ALS,AUG
REAL*8 NS,MD,MDO,V,S,MSS,MDS,K1,K2,K3,K4,M
KM=2
CALL DIFF
KM=0

```

CALCULATION OF TWO RAY THEORY

```

D01=.0004*H1E*H2E*F
D02=DMINI((-AED/MD),(DL-2.))
IF (AED .GE. 0.) D0=DMINI(D01,(.5*DL))
IF (AED .LT. 0.) D0=.5*DL
IF (AED .LT. 0.) .AND. D02 .GE. D0) D0=D02
D1=D0+.25*(DL-D0)
IF (D1 .LE. D0) D1=D0+.25*(DL-D0)
D5=0
IF (J .EQ. 0) D=D0
PSI=DATA TAN((H1E+H2E)/(1000.*D))
DHD=DH*(1.-.8*DEXP(-.02*D))
SH=.78*DHD*DEXP(-.5*DHD*.25)
SP=DSIN(PSI)
X=18000.*S/F
P2=(DSQRT((E-DCOS(PSI))*2.+X*X)+E-DCOS(PSI))*DCOS(PSI)/
C2.
P=DSQRT(P2)
Q=X/(2.*P)
IF (POL .EQ. 1.) B=(E*X*X)/(P2+Q*Q)
IF (POL .EQ. -1.) B=1./(P2+Q*Q)
IF (POL .EQ. 1.) M=2.*(P*E+Q*X)/(P2+Q*Q)
IF (POL .EQ. -1.) M=2.*P/(P2+Q*Q)
R2=(1.+B*SP*SP-M*SP)/(1.+B*SP*SP+M*SP)
RS=DSQRT(SP)
SQEXF=DSQRT(R2)*DEXP(-.0209584473*F*SH*SP)*DIV

```

22
2

000 000

0000

```

IF (SQEXF .GT. .5 .AND. SQEXF .GT. RE) RE=SQEXF
C=DATAN(Q/(P+SP))-DATAN(Q/(P-SP))
IF (POL .EQ. -1) GO TO 40
Y1=(X*SP+Q)/(E*SP+P)
IF (E*SP .GE. P) C=DATAN(Y1)-DATAN(Y2)+3.141592654
IF (E*SP .LT. P .AND. P*SP .GT. .5) C=DATAN(Y1)+DATAN(Y2)
IF (E*SP .LT. P .AND. P*SP .LE. .5) C=DATAN(Y1)-DATAN(Y2)
40 IF (I .EQ. 0)
CAO=-1.0*DLG10(1.+RE*RE-2.*RE*DCOS(.000041917*F*H1E*H2E/D0-C))
IF (J .EQ. 1) GO TO 3
D=D1
J=1 TO 22
GO TO 22
CONTINUE
D=DS
IF (J .EQ. 1)
CAL=-1.0*DLG10(1.+RE*RE-2.*RE*DCOS(.000041917*F*H1E*H2E/D1-C))
COMBINATION OF TWO RAY THEORY AND DIFFRACTION
ALS=AED+MD*DLS
AL=AED+MD*DL
DEDO=AED+MD*DO
DEDI=AED+MD*DI
SAO=AO
SAL=A1
W=1./((1.+F*DH*.0001)
A0=DMINI((W*A1+(1.-W)*DEDO),DEDO)
A1=DMINI((W*A1+(1.-W)*DEDI),DEDI)
K2=((ALS-A0)*(D1-D0)-(A1-A0)*(DLS-D0))/((D1-D0)*DLG10(DLS/D0)-
C(DLS-D0)*DLG10(D1/D0))
K2=DMAX(K2,0,0D0)
K1=((ALS-A0)-K2*DLG10(DLS/D0))/(DLS-D0)
IF (K1 .GT. 0.) GO TO 50
K1=0.
K2=(ALS-A0)/(DLG10(DLS/D0))
50 AG=AO+K1*(D-D0)+K2*DLG10(D/D0)
IF (AG .LT. 0.) AG=0.
51 AOG=AO
53 ACR=AG
RETURN
END
SUBROUTINE UTIPLT (X ,Y ,NDATA,XMAX,XMIN,YMAX,YMIN,KKZ,MODCUR)
DIMENSION GRID(61,81),XSCALE(5),YSCALE(7)
DIMENSION X (1),Y (1)

```



```

INTEGERS 2 GRID, BLANK, DOT, XCHAR(4)/1H., 1H., 1H., 1H., 1H., 1H./
DATA DOT, BLANK/248 40, 240 40/
KDATA=NDATA*KKZ
IF(MOOCUR.GT.1) GO TO 444

```

```

C C C
C C C
C C C

```

```

GRID IS THE MATRIX USED TO PLOT THE POINTS

```

```

IERR=0

```

```

CHECKING X AND Y POINTS AND PLOTTING THOSE OUT OF RANGE
AT THE MARGIN

```

```

DO 30 I=1, KDATA, KKZ
IF(X(I).GT.XMAX.OR.X(I).LT.XMIN.OR.Y(I).GT.YMAX.OR.Y(I).LT.YMIN)
1 IF(IERR)=IERR+1
IF(X(I).LE.XMAX) GO TO 205
X(I)=XMAX
GO TO 210
IF(X(I).GE.XMIN) GO TO 210
X(I)=XMIN
205 IF(Y(I).LE.YMAX) GO TO 215
Y(I)=YMAX
210 IF(Y(I).GE.YMIN) GO TO 30
Y(I)=YMIN

```

```

C 30 CONTINUE
C C C
PLOTTING X AND Y AXIS, IF NECESSARY

```

```

JERR=0
XRANGE=XMAX-XMIN
YRANGE=YMAX-YMIN
IF(YRANGE.NE.0.) GO TO 298
IF(XRANGE.NE.0.) GO TO 889
YMIN=0
YRANGE=YMAX
GO TO 299
IF(XRANGE.NE.0.) GO TO 299
XMIN=0
XRANGE=XMAX

```

```

C C C
BLANKING OUT MATRIX-(GRID)

```

```

299 DO 300 I=1, 61
DO 301 JJ=1, 81
301 GRID(I, JJ)=BLANK

```

```

300 CONTINUE
   IF (XMAX#XMIN.GE.0.) GO TO 222
   IYAXIS=80.#(-XMIN)/XRANGE+1.5
   DO 40 I=1,61
   GRIDI(I,IYAXIS)=DOT
222 IF (YMAX#YMIN.GE.0.) GO TO 333
   IXAXIS=60.#YMAX/YRANGE+1.5
   DO 60 I=1,81
   GRID(I,IXAXIS,II)=DOT
CC
CC
   COMPUTE PROPER SCALE NUMBERS
333 XINCR=XRANGE/4.
   YINCR=YRANGE/6.
   XSCALE(1)=XMAX
   XSCALE(5)=XMIN
   DO 80 I=2,4
   XSCALE(I)=XSCALE(I-1)-XINCR
   IF (ABS(XSCALE(I)).LT.1.E-4) XSCALE(I)=0.
80 CONTINUE
   YSCALE(1)=YMAX
   YSCALE(7)=YMIN
   DO 81 I=2,6
   YSCALE(I)=YSCALE(I-1)-YINCR
   IF (ABS(YSCALE(I)).LT.1.E-4) YSCALE(I)=0.
81 CONTINUE
   I=1,2
   JJ=6-11
   XT=XSCALE(JJ)
   XSCALE(YJ)=XSCALE(II)
85 XSCALE(III)=XT
CC
CC
   PLACING POINTS IN THEIR PROPER GRID POSITIONS
444 IF (MODCUR.LT.2) JSET=0
   IF (JERR.GT.0) GO TO 885
   JSET=JSET+1
   IF (JSET.GT.4) JSET=1
   DO I=1,KDA*AKKZ
   IPTX=60.#(YMAX-Y(I))/YRANGE+1.5
   IPTY=80.#(X(I)-XMIN)/XRANGE+1.5
   IF (IPTX.GT.61.OR.IPTY.GT.81) GO TO 70
   IF (IPTX.LE.0.OR.IPTY.LE.0) GO TO 70
   GRIDI(IPTY,IPTX)=XCHAR(JSET)
   GO TO 700
70 IERR=IERR+1
700 CONTINUE
CC
C

```

```

C
OUTPUT SECTION WITH GRAPH
IF (MODCUR.EQ.1,OR.MODCUR.EQ.2) RETURN
AXR=ABS(XRANGE)
IF (AXR.LT.1.E+8.AND.AXR.GE..95) GO TO 400
WRITE(6,17) XSCALE
FORMAT(12X,1PE10.3,4(10X,E10.3),***,8(*****),***)
GO TO 401
400 WRITE(6,17) XSCALE
FORMAT(8X,F11.2,4(9X,F11.2)/15X,***,8(*****),***)
401 DO 101 IK=1,61
IF (MOD(IK-1,10).NE.0) GO TO 92
IF (AYR.LT.1.E+8.AND.AXR.GE..95) GO TO 404
WRITE(6,18) YSCALE((IK,IX),IX=1,81),YSCALE(11)
FORMAT(3X,1PE10.3,2X,1H+,1X,81A1,1X,1H+,2X,E10.3)
18 GO TO 405
404 WRITE(6,118) YSCALE(11),((GRID(IK,IX),IX=1,81),YSCALE(11)
118 FORMAT(2X,F11.2,*,*,81A1,*,*,F11.2)
405 II=II+101
GO TO 101
WRITE(6,19) (GRID(IK,IX),IX=1,81)
19 FORMAT(15X,*,*,81A1,*,*)
101 CONTINUE
IF (AXR.LT.1.E+8.AND.AXR.GE..95) GO TO 402
WRITE(6,22) XSCALE
FORMAT(15X,***,8(*****),***/12X,1PE10.3,4(10X,E10.3),***)
22 GO TO 403
402 WRITE(6,217) XSCALE
217 FORMAT(15X,***,8(*****),***/8X,F11.2,4(9X,F11.2),***)
403 IF (IERR.GT.0) WRITE(6,20) IERR
20 FORMAT(10X,'NUMBER OF POINTS OUT OF RANGE =',I4)
1000 RETURN
C
888 WRITE(6,888)
888 FORMAT(' ALL Y VALUES=0. CANNOT SETUP PLOT GRID. CHECK MAX & MIN Y
1 JERR=10
RETURN
887 WRITE(6,886)
886 FORMAT(' ALL X VALUES=0. CANNOT SETUP PLOT GRID. CHECK MAX & MIN X
1 JERR=10
RETURN
885 WRITE(6,884)
884 FORMAT(' GRID NOT SETUP WHEN MODCUR LAST 0 OR 1. NO PLOT UNTIL GRI
10 PROPERLY SETUP')

```

RETURN
END

C

FUNCTION FNA(C)
IMPLICIT REAL*8(A-H,O-Z)
FNA=6.02+9.11*C-1.27*C*C
RETURN
END

C

FUNCTION FNB(C)
IMPLICIT REAL*8(A-H,O-Z)
FNB=12.953+20.*DLOG10(C)
RETURN
END

C

FUNCTION FNC(C,F)
IMPLICIT REAL*8(A-H,O-Z)
FNC=4.16.4*F**.333333333*(1.607-C)
RETURN
END

C

FUNCTION FNE(C,F,E,X)
IMPLICIT REAL*8(A-H,O-Z)
FND=(.36278/(C*F)**.333333333)*1./((E-1.)**2.+X*X)**.25
RETURN
END

C

FUNCTION FNE(C,E,X)
IMPLICIT REAL*8(A-H,O-Z)
FNE=C*DSQRT(E+E*X)
RETURN
END

--- PROGRAM PARAMETERS ---

POLARIZATION (POL), -----VERTICAL
 FREQUENCY OF SIGNAL (F) -----5025.00 MEG-HERTZ
 SURFACE CONDUCTIVITY (S) -----0.00500 MHO/METER
 SURFACE REFRACTIVITY (NS) -----250.00 N-UNITS
 SUM OF ELEVATION ANGLES (TEI) -----0.1423 RADIANS
 DISTANCE BETWEEN ANTENNAS (DIST) -----300.00 K-METERS
 ATTENUATION BELOW FREE SPACE (AE) -----84.27 DB
 INTERDECILE RANGE OF TERRAIN HEIGHT (DH) -----60.00 METERS
 SUM OF SMOOTH-EARTH HORIZON DISTANCES (DLS) -----115.70 K-METERS
 DIFFRACTION ATTENUATION AT DISTANCE DLS (ALS) -----29.91 DB
 PERMITTIVITY OR RELATIVE DIELECTRIC CONSTANT (E) -----15.00
 ESTIMATED SCATTER ATTENUATION BELOW FREE SPACE (AES) -----30.13 DB
 STRUCTURAL RECEIVER ANTENNA HEIGHT ABOVE GROUND (H2G) -----610.00 METERS
 STRUCTURAL TRANSMITTER ANTENNA HEIGHT ABOVE GROUND (H1G) -----20.00 METERS
 ESTIMATED DIFFRACTION ATTENUATION BELOW FREE SPACE (AED) -----84.24 DB
 COEFFICIENT THAT DEFINES SLOPE OF A SMOOTH CURVE OF ACR (K1) -----0.98624 DB/KM
 COEFFICIENT THAT DEFINES SLOPE OF A SMOOTH CURVE OF ACR (K2) -----0.0 DB/KM
 SLOPE OF THE CURVE OF SCATTER ATTENUATION AS VERSUS DISTANCE (MS) -----0.12136 DB/KM
 DISTANCE WHERE DIFFRACTION AND SCATTER ATTENUATIONS ARE EQUAL (DA) -----132.20 K-METERS
 ATTENUATION WHERE DIFFRACTION AND SCATTER ATTENUATIONS ARE EQUAL (ADX) -----46.18 DB
 SLOPE OF THE CURVE OF DIFFRACTION ATTENUATION AS VERSUS DISTANCE (MD) -----0.98597 DB/KM

--- SIGNAL STRENGTH DATA INPUT ---

TRANSMITTER POWER OUT -----100000.00 WATTS
 TRANSMITTER TRANSMISSION LINE LOSS -----2.00 DB
 TRANSMITTER ANTENNA GAIN -----45.60 DB
 RECEIVER SENSITIVITY -----40.00 DBM
 RECEIVER TRANSMISSION LINE LOSS -----2.00 DB
 RECEIVER ANTENNA GAIN -----10.00 DB

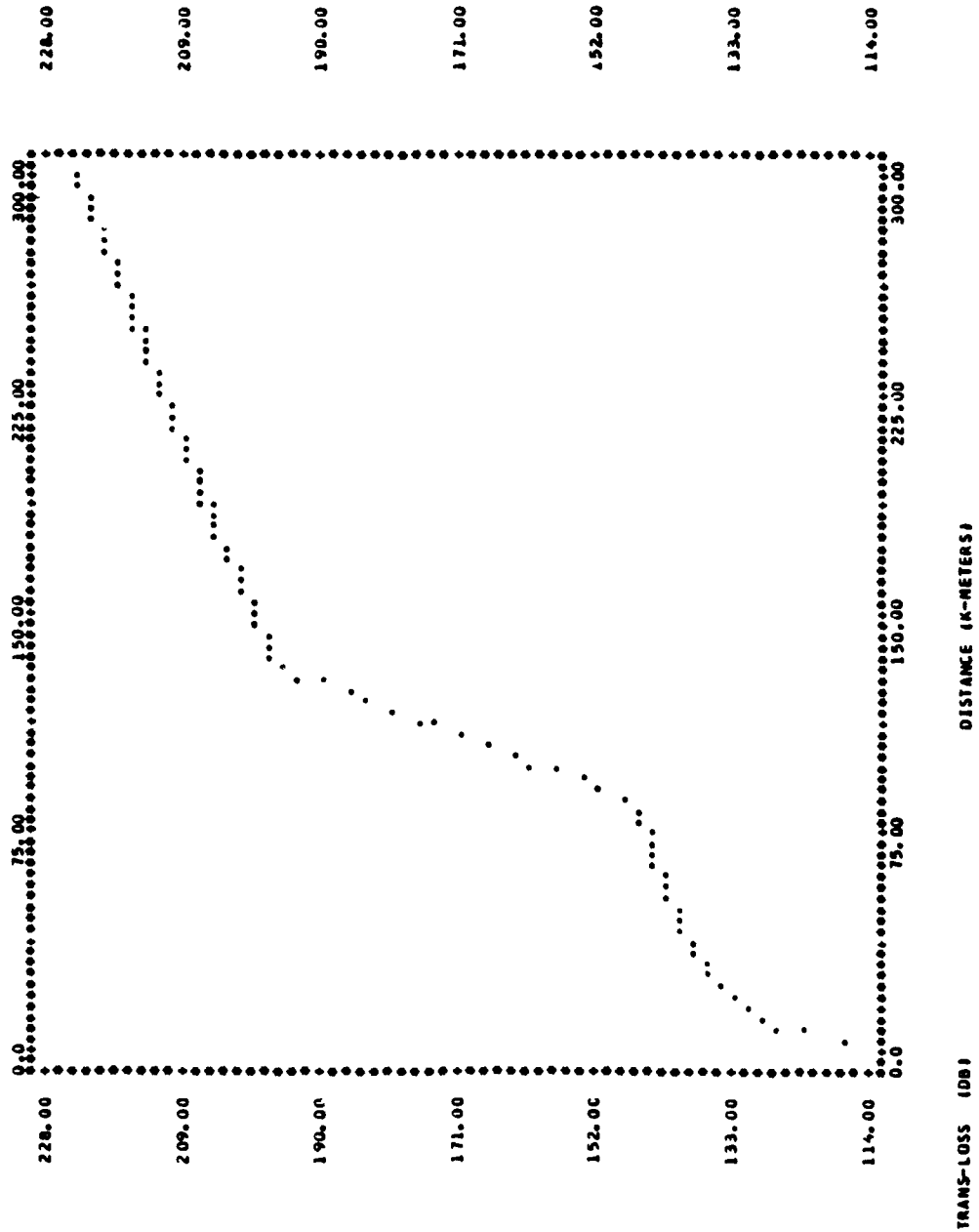
--- USER TERRAIN DATA ---

FREQUENCY OF SIGNAL --F-- (MEG-HERTZ) 5825.00000

DISTANCE TRANS-LOSS (DB)	DISTANCE (KM)	TRANS-LOSS (DB)	DISTANCE TRANS-LOSS (DB)	DISTANCE (KM)	TRANS-LOSS (DB)	DISTANCE TRANS-LOSS (DB)	DISTANCE (KM)	TRANS-LOSS (DB)	
3.0000	117.30	63.0000	143.74	123.0000	184.58	183.0000	205.34	243.0000	215.09
6.0000	123.32	66.0000	144.15	126.0000	189.75	186.0000	205.85	246.0000	215.56
9.0000	126.84	69.0000	144.53	129.0000	192.91	189.0000	206.35	249.0000	216.03
12.0000	129.34	72.0000	144.90	132.0000	196.07	192.0000	206.85	252.0000	216.50
15.0000	131.28	75.0000	145.26	135.0000	196.88	195.0000	207.35	255.0000	216.96
18.0000	132.86	78.0000	145.60	138.0000	197.43	198.0000	207.85	258.0000	217.43
21.0000	134.20	81.0000	145.93	141.0000	197.98	201.0000	208.34	261.0000	217.89
24.0000	135.36	84.0000	146.24	144.0000	198.53	204.0000	208.84	264.0000	218.36
27.0000	136.38	87.0000	146.07	147.0000	199.07	207.0000	209.33	267.0000	218.82
30.0000	137.30	90.0000	151.33	150.0000	199.61	210.0000	209.82	270.0000	219.28
33.0000	138.13	93.0000	154.57	153.0000	200.15	213.0000	210.30	273.0000	219.74
36.0000	138.88	96.0000	157.81	156.0000	200.68	216.0000	210.79	276.0000	220.20
39.0000	139.58	99.0000	161.03	159.0000	201.21	219.0000	211.27	279.0000	220.66
42.0000	140.22	102.0000	164.25	162.0000	201.74	222.0000	211.76	282.0000	221.12
45.0000	140.82	105.0000	167.46	165.0000	202.26	225.0000	212.24	285.0000	221.57
48.0000	141.38	108.0000	170.66	168.0000	202.78	228.0000	212.72	288.0000	222.03
51.0000	141.91	111.0000	173.86	171.0000	203.30	231.0000	213.19	291.0000	222.48
54.0000	142.40	114.0000	177.05	174.0000	203.81	234.0000	213.67	294.0000	222.93
57.0000	142.87	117.0000	180.23	177.0000	204.33	237.0000	214.14	297.0000	223.39
60.0000	143.32	120.0000	183.41	180.0000	204.84	240.0000	214.62	300.0000	223.84

PLOT OF TRANS.-LOSS VERSUS DISTANCE

• NOTE •• TO FIND SIGNAL STRENGTH FROM GRAPH, SUBTRACT TRANS.-LOSS FROM 141.60



--- SIGNAL STRENGTH VERSUS DISTANCE FOR GIVEN SYSTEM PARAMETERS ---

DISTANCE (KM)	SIG-STRENGTH (DBM)	DISTANCE (KM)	SIG-STRENGTH (DBM)	DISTANCE (KM)	SIG-STRENGTH (DBM)	DISTANCE (KM)	SIG-STRENGTH (DBM)	DISTANCE (KM)	SIG-STRENGTH (DBM)	DISTANCE (KM)	SIG-STRENGTH (DBM)
3.0000	24.30	63.0000	-2.14	123.0000	-44.98	183.0000	-63.74	243.0000	-73.49		
6.0000	18.28	66.0000	-2.55	126.0000	-48.15	186.0000	-64.25	246.0000	-73.96		
9.0000	14.76	69.0000	-2.93	129.0000	-51.31	189.0000	-64.75	249.0000	-74.43		
12.0000	12.26	72.0000	-3.30	132.0000	-54.47	192.0000	-65.25	252.0000	-74.90		
15.0000	10.32	75.0000	-3.66	135.0000	-55.28	195.0000	-65.75	255.0000	-75.36		
18.0000	8.74	78.0000	-4.00	138.0000	-55.83	198.0000	-66.25	258.0000	-75.83		
21.0000	7.40	81.0000	-4.33	141.0000	-56.38	201.0000	-66.74	261.0000	-76.29		
24.0000	6.24	84.0000	-4.64	144.0000	-56.93	204.0000	-67.24	264.0000	-76.76		
27.0000	5.22	87.0000	-6.47	147.0000	-57.47	207.0000	-67.73	267.0000	-77.22		
30.0000	4.30	90.0000	-9.73	150.0000	-58.01	210.0000	-68.22	270.0000	-77.68		
33.0000	3.47	93.0000	-12.97	153.0000	-58.55	213.0000	-68.70	273.0000	-78.14		
36.0000	2.72	96.0000	-16.21	156.0000	-59.08	216.0000	-69.19	276.0000	-78.60		
39.0000	2.02	99.0000	-19.43	159.0000	-59.61	219.0000	-69.67	279.0000	-79.06		
42.0000	1.38	102.0000	-22.65	162.0000	-60.14	222.0000	-70.16	282.0000	-79.52		
45.0000	0.78	105.0000	-25.86	165.0000	-60.66	225.0000	-70.64	285.0000	-79.97		
48.0000	0.22	108.0000	-29.06	168.0000	-61.18	228.0000	-71.12	288.0000	-80.43		
51.0000	-0.31	111.0000	-32.26	171.0000	-61.70	231.0000	-71.59	291.0000	-80.88		
54.0000	-0.80	114.0000	-35.45	174.0000	-62.21	234.0000	-72.07	294.0000	-81.33		
57.0000	-1.27	117.0000	-38.63	177.0000	-62.73	237.0000	-72.54	297.0000	-81.79		
60.0000	-1.72	120.0000	-41.81	180.0000	-63.24	240.0000	-73.02	300.0000	-82.24		

**** FOR A RECEIVER INPUT LEVEL OF -40.00 DBM, DISTANCE BETWEEN ANTENNAS CAN BE AT LEAST 117.00 KM ****

--- PROGRAM PARAMETERS ---

POLARIZATION (POL1) -----VERTICAL
 FREQUENCY OF SIGNAL (F) -----5025.00 MEG-HERTZ
 SURFACE CONDUCTIVITY (S) -----0.00500 MHO/METER
 SURFACE REFRACTIVITY (NS) -----200.00 N-UNITS
 SUM OF ELEVATION ANGLES (TE) -----0.1392 RADIAN
 DISTANCE BETWEEN ANTENNAS (DIST) -----300.00 K-METERS
 ATTENUATION BELOW FREE SPACE (AE) -----03.49 DB
 INTERDECILE RANGE OF TERRAIN HEIGHT (DH) -----60.00 METERS
 SUM OF SMOOTH-EARTH HORIZON DISTANCES (DLS) -----116.30 K-METERS
 DIFFRACTION ATTENUATION AT DISTANCE DLS (ALS) -----29.82 DB
 PERMITTIVITY OR RELATIVE DIELECTRIC CONSTANT (E) -----15.00
 ESTIMATED SCATTER ATTENUATION BELOW FREE SPACE (AES) -----29.37 DB
 STRUCTURAL RECEIVER ANTENNA HEIGHT ABOVE GROUND (H2G) -----610.00 METERS
 STRUCTURAL TRANSMITTER ANTENNA HEIGHT ABOVE GROUND (H1G) -----20.00 METERS
 ESTIMATED DIFFRACTION ATTENUATION BELOW FREE SPACE (AED) -----03.43 DB
 COEFFICIENT THAT DEFINES SLOPE OF A SMOOTH CURVE OF ACR (K1) -----0.95788 DB/KM
 COEFFICIENT THAT DEFINES SLOPE OF A SMOOTH CURVE OF ACR (K2) -----0.0 DB/KM
 SLOPE OF THE CURVE OF SCATTER ATTENUATION AS VERSUS DISTANCE (NS) -----0.12378 DB/KM
 DISTANCE WHERE DIFFRACTION AND SCATTER ATTENUATIONS ARE EQUAL (DX) -----135.32 K-METERS
 ATTENUATION WHERE DIFFRACTION AND SCATTER ATTENUATION ARE EQUAL (ADX) -----46.12 DB
 SLOPE OF THE CURVE OF DIFFRACTION ATTENUATION AS VERSUS DISTANCE (MO) -----0.95732 DB/KM

--- SIGNAL STRENGTH DATA INPUT ---

TRANSMITTER POWER OUT -----1000000.00 WATTS
 TRANSMITTER TRANSMISSION LINE LOSS -----2.00 DB
 TRANSMITTER ANTENNA GAIN -----65.60 DB
 RECEIVER SENSITIVITY -----40.00 DBM
 RECEIVER TRANSMISSION LINE LOSS -----2.00 DB
 RECEIVER ANTENNA GAIN -----10.00 DB

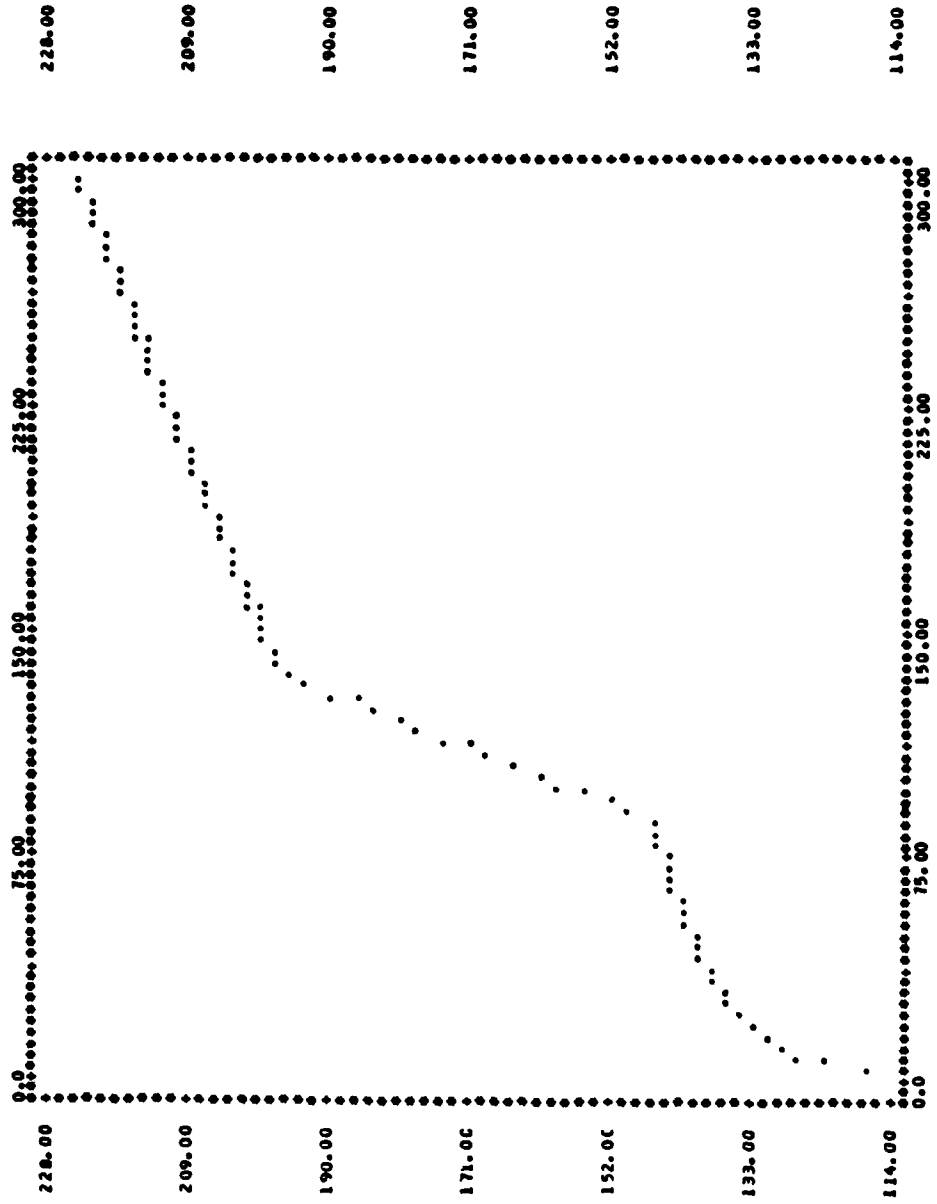
--- USER TERRAIN DATA ---

FREQUENCY OF SIGNAL -F- (MEG-HERTZ) 5825.00000

DISTANCE (KM)	TRANS-LOSS (DB)	DISTANCE (KM)	TRANS-LOSS (DB)	DISTANCE (KM)	TRANS-LOSS (DB)	DISTANCE (KM)	TRANS-LOSS (DB)	DISTANCE (KM)	TRANS-LOSS (DB)
3.0000	117.30	63.0000	143.74	123.0000	183.88	183.0000	205.02	243.0000	214.91
6.0000	123.32	66.0000	144.15	126.0000	186.96	186.0000	205.54	246.0000	215.39
9.0000	126.84	69.0000	144.53	129.0000	190.04	189.0000	206.05	249.0000	215.87
12.0000	129.34	72.0000	144.90	132.0000	193.11	192.0000	206.55	252.0000	216.34
15.0000	131.28	75.0000	145.26	135.0000	196.17	195.0000	207.06	255.0000	216.82
18.0000	132.86	78.0000	145.60	138.0000	197.00	198.0000	207.56	258.0000	217.29
21.0000	134.20	81.0000	145.93	141.0000	197.56	201.0000	208.07	261.0000	217.76
24.0000	135.36	84.0000	146.24	144.0000	198.11	204.0000	208.57	264.0000	218.23
27.0000	136.38	87.0000	146.55	147.0000	198.67	207.0000	209.06	267.0000	218.70
30.0000	137.30	90.0000	146.86	150.0000	199.21	210.0000	209.56	270.0000	219.17
33.0000	138.13	93.0000	147.17	153.0000	199.76	213.0000	210.06	273.0000	219.64
36.0000	138.88	96.0000	147.47	156.0000	200.30	216.0000	210.55	276.0000	220.10
39.0000	139.58	99.0000	147.76	159.0000	200.83	219.0000	211.04	279.0000	220.57
42.0000	140.22	102.0000	148.04	162.0000	201.37	222.0000	211.53	282.0000	221.03
45.0000	140.82	105.0000	148.32	165.0000	201.90	225.0000	212.02	285.0000	221.50
48.0000	141.38	108.0000	148.59	168.0000	202.42	228.0000	212.50	288.0000	221.96
51.0000	141.91	111.0000	148.86	171.0000	202.95	231.0000	212.99	291.0000	222.42
54.0000	142.40	114.0000	149.12	174.0000	203.47	234.0000	213.47	294.0000	222.88
57.0000	142.87	117.0000	149.37	177.0000	203.99	237.0000	213.95	297.0000	223.34
60.0000	143.32	120.0000	149.62	180.0000	204.51	240.0000	214.43	300.0000	223.80

PLOT OF TRANS.-LOSS VERSUS DISTANCE

• NOTE •• TO FIND SIGNAL STRENGTH FROM GRAPH, SUBTRACT TRANS.-LOSS FROM 141.60



--- SIGNAL STRENGTH VERSUS DISTANCE FOR GIVEN SYSTEM PARAMETERS ---

DISTANCE (KM)	SIG-STRENGTH (DBM)	DISTANCE (KM)	SIG-STRENGTH (DBM)	DISTANCE (KM)	SIG-STRENGTH (DBM)	DISTANCE (KM)	SIG-STRENGTH (DBM)	DISTANCE (KM)	SIG-STRENGTH (DBM)
3.0000	26.30	63.0000	-2.14	123.0000	-42.28	183.0000	-63.62	243.0000	-73.31
6.0000	18.28	66.0000	-2.55	126.0000	-45.36	186.0000	-63.94	246.0000	-73.79
9.0000	14.76	69.0000	-2.93	129.0000	-48.44	189.0000	-64.45	249.0000	-74.27
12.0000	12.26	72.0000	-3.30	132.0000	-51.51	192.0000	-64.95	252.0000	-74.74
15.0000	10.32	75.0000	-3.66	135.0000	-54.57	195.0000	-65.46	255.0000	-75.22
18.0000	8.74	78.0000	-4.00	138.0000	-55.40	198.0000	-65.96	258.0000	-75.69
21.0000	7.60	81.0000	-4.33	141.0000	-55.96	201.0000	-66.47	261.0000	-76.16
24.0000	6.24	84.0000	-4.64	144.0000	-56.51	204.0000	-66.97	264.0000	-76.63
27.0000	5.22	87.0000	-4.95	147.0000	-57.07	207.0000	-67.46	267.0000	-77.10
30.0000	4.30	90.0000	-7.94	150.0000	-57.61	210.0000	-67.96	270.0000	-77.57
33.0000	3.47	93.0000	-11.12	153.0000	-58.16	213.0000	-68.46	273.0000	-78.04
36.0000	2.72	96.0000	-14.27	156.0000	-58.70	216.0000	-68.95	276.0000	-78.50
39.0000	2.02	99.0000	-17.41	159.0000	-59.23	219.0000	-69.44	279.0000	-78.97
42.0000	1.38	102.0000	-20.54	162.0000	-59.77	222.0000	-69.93	282.0000	-79.43
45.0000	0.78	105.0000	-23.66	165.0000	-60.30	225.0000	-70.42	285.0000	-79.90
48.0000	0.22	108.0000	-26.78	168.0000	-60.82	228.0000	-70.90	288.0000	-80.36
51.0000	-0.31	111.0000	-29.89	171.0000	-61.35	231.0000	-71.39	291.0000	-80.82
54.0000	-0.80	114.0000	-33.00	174.0000	-61.87	234.0000	-71.87	294.0000	-81.28
57.0000	-1.27	117.0000	-36.10	177.0000	-62.39	237.0000	-72.35	297.0000	-81.74
60.0000	-1.72	120.0000	-39.19	180.0000	-62.91	240.0000	-72.83	300.0000	-82.20

***** FOR A RECEIVER INPUT LEVEL OF -40.00 DBM, DISTANCE BETWEEN ANTENNAS CAN BE AT LEAST 120.00 KM *****

---- PROGRAM PARAMETERS ----

POLARIZATION (POL) ----- VERTICAL
 FREQUENCY OF SIGNAL (F) ----- 5825.00 MCG-HERTZ
 SURFACE CONDUCTIVITY (S) ----- 0.00500 MO/METER
 SURFACE REFRACTIVITY (NS) ----- 310.00 M-UNITS
 SUM OF ELEVATION ANGLES (TE) ----- 0.01356 RADIANMS
 DISTANCE BETWEEN ANTENNAS (DIST) ----- 300.00 K-METERS
 ATTENUATION BELOW FREE SPACE (AE) ----- 82.49 DB
 INTERDECILE RANGE OF TERRAIN HEIGHT (DM) ----- 60.00 METERS
 SUM OF SMOOTH-EARTH HORIZON DISTANCES (DLS) ----- 121.50 K-METERS
 DIFFRACTION ATTENUATION AT DISTANCE DLS (ALS) ----- 29.72 DB
 PERMITTIVITY OR RELATIVE DIELECTRIC CONSTANT (E) ----- 15.00
 ESTIMATED SCATTER ATTENUATION BELOW FREE SPACE (AES) ----- 28.57 DB
 STRUCTURAL RECEIVER ANTENNA HEIGHT ABOVE GROUND (H2G) ----- 610.00 METERS
 STRUCTURAL TRANSMITTER ANTENNA HEIGHT ABOVE GROUND (H1G) ----- 20.00 METERS
 ESTIMATED DIFFRACTION ATTENUATION BELOW FREE SPACE (AED) ----- 82.42 DB
 COEFFICIENT THAT DEFINES SLOPE OF A SMOOTH CURVE OF ACR (K1) ----- 0.92350 DB/KM
 COEFFICIENT THAT DEFINES SLOPE OF A SMOOTH CURVE OF ACR (K2) ----- 0.0 DB/KM
 SLOPE OF THE CURVE OF SCATTER ATTENUATION AS VERSUS DISTANCE (MS) ----- 0.12549 DB/KM
 DISTANCE WHERE DIFFRACTION AND SCATTER ATTENUATIONS ARE EQUAL (DX) ----- 139.18 K-METERS
 ATTENUATION WHERE DIFFRACTION AND SCATTER ATTENUATION ARE EQUAL (ADAX) ----- 46.03 DB
 SLOPE OF THE CURVE OF DIFFRACTION ATTENUATION AS VERSUS DISTANCE (MD) ----- 0.92293 DB/KM

---- SIGNAL STRENGTH DATA INPUT ----

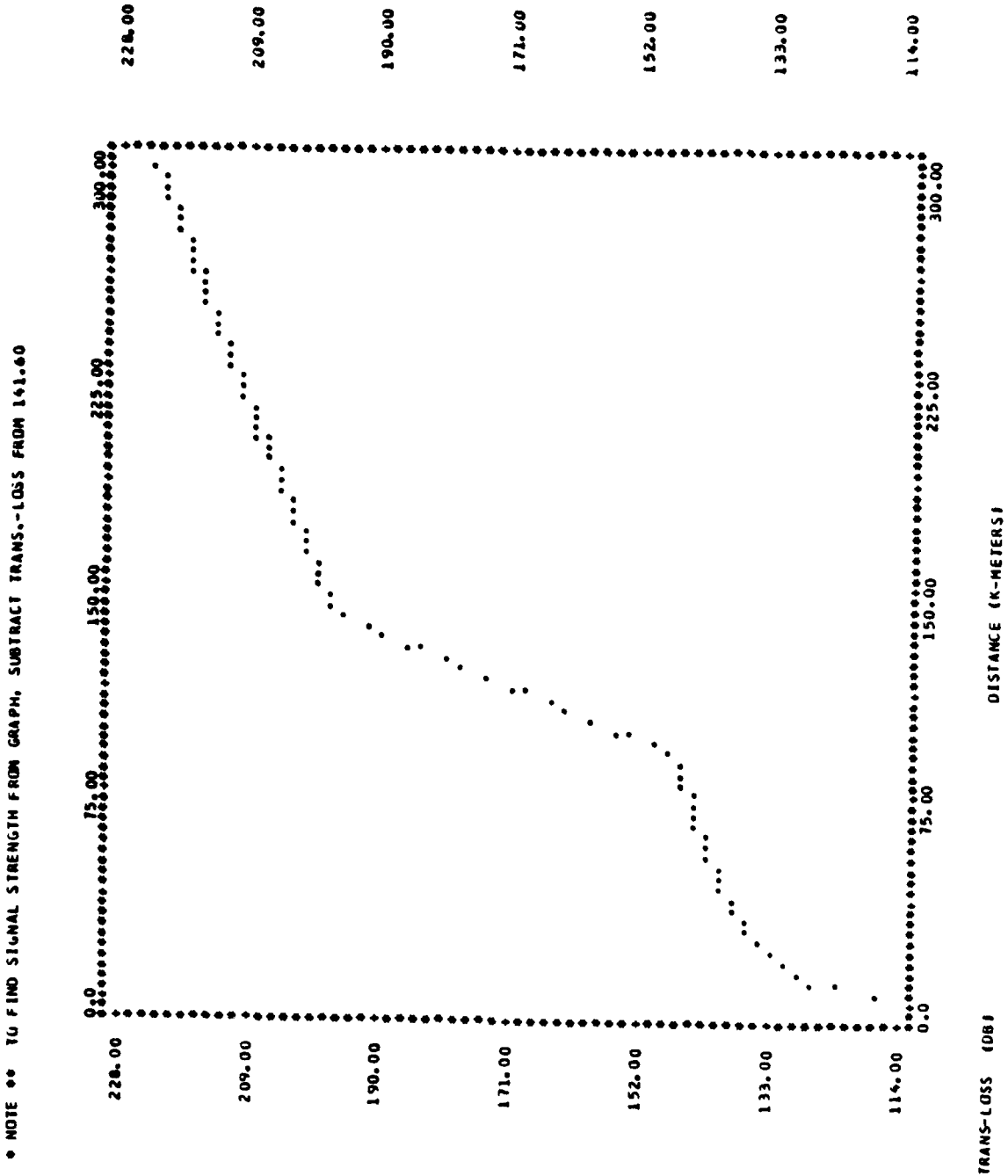
TRANSMITTER POWER OUT ----- 1000000.00 WATTS
 TRANSMITTER TRANSMISSION LINE LOSS ----- 2.00 DB
 TRANSMITTER ANTENNA GAIN ----- 45.60 DB
 RECEIVER SENSITIVITY ----- 40.00 DBM
 RECEIVER TRANSMISSION LINE LOSS ----- 2.00 DB
 RECEIVER ANTENNA GAIN ----- 10.00 DB

--- USER TERRAIN DATA ---

FREQUENCY OF SIGNAL -F- (MEG-HERTZ) 5825.00000

DISTANCE (KM)	TRANS-LOSS (DB)	DISTANCE (KM)	TRANS-LOSS (DB)	DISTANCE (KM)	TRANS-LOSS (DB)	DISTANCE (KM)	TRANS-LOSS (DB)
3.0000	117.30	63.0000	143.74	123.0000	180.65	183.0000	204.54
6.0000	123.32	66.0000	144.15	126.0000	183.63	186.0000	205.06
9.0000	126.84	69.0000	144.53	129.0000	186.61	189.0000	205.57
12.0000	129.34	72.0000	144.90	132.0000	189.57	192.0000	206.08
15.0000	131.28	75.0000	145.26	135.0000	192.54	195.0000	206.59
18.0000	132.86	78.0000	145.60	138.0000	195.50	198.0000	207.10
21.0000	134.20	81.0000	145.93	141.0000	197.00	201.0000	207.61
24.0000	135.36	84.0000	146.24	144.0000	197.56	204.0000	208.12
27.0000	136.38	87.0000	146.55	147.0000	198.12	207.0000	208.62
30.0000	137.30	90.0000	147.47	150.0000	198.67	210.0000	209.12
33.0000	138.13	93.0000	150.52	153.0000	199.22	213.0000	209.62
36.0000	138.88	96.0000	153.57	156.0000	199.76	216.0000	210.12
39.0000	139.58	99.0000	156.61	159.0000	200.30	219.0000	210.61
42.0000	140.22	102.0000	159.64	162.0000	200.84	222.0000	211.11
45.0000	140.82	105.0000	162.66	165.0000	201.38	225.0000	211.60
48.0000	141.38	108.0000	165.67	168.0000	201.91	228.0000	212.09
51.0000	141.91	111.0000	168.68	171.0000	202.44	231.0000	212.58
54.0000	142.40	114.0000	171.68	174.0000	202.97	234.0000	213.07
57.0000	142.87	117.0000	174.68	177.0000	203.50	237.0000	213.56
60.0000	143.32	120.0000	177.67	180.0000	204.02	240.0000	214.05

● NOTE ●● TO FIND SIGNAL STRENGTH FROM GRAPH, SUBTRACT TRANS.-LOSS FROM 141.60



--- SIGNAL STRENGTH VERSUS DISTANCE FOR GIVEN SYSTEM PARAMETERS ---

DISTANCE (KM)	SIG-STRENGTH (DBM)	DISTANCE (KM)	SIG-STRENGTH (DBM)	DISTANCE (KM)	SIG-STRENGTH (DBM)	DISTANCE (KM)	SIG-STRENGTH (DBM)	DISTANCE (KM)	SIG-STRENGTH (DBM)
3.0000	24.30	63.0000	-2.14	123.0000	-39.05	183.0000	-62.94	243.0000	-72.93
6.0000	18.28	66.8000	-2.55	126.0000	-42.03	186.0000	-63.46	246.0000	-73.41
9.0000	14.76	69.0000	-2.93	129.0000	-45.01	189.0000	-63.97	249.0000	-73.89
12.0000	12.26	72.0000	-3.30	132.0000	-47.97	192.0000	-64.48	252.0000	-74.37
15.0000	10.32	75.0000	-3.66	135.0000	-50.94	195.0000	-64.99	255.0000	-74.85
18.0000	8.74	78.0000	-4.00	138.0000	-53.90	198.0000	-65.50	258.0000	-75.33
21.0000	7.40	81.0000	-4.33	141.0000	-55.40	201.0000	-66.01	261.0000	-75.81
24.0000	6.24	84.0000	-4.64	144.0000	-55.96	204.0000	-66.52	264.0000	-76.28
27.0000	5.22	87.0000	-4.95	147.0000	-56.52	207.0000	-67.02	267.0000	-76.76
30.0000	4.30	90.0000	-5.27	150.0000	-57.07	210.0000	-67.52	270.0000	-77.23
33.0000	3.47	93.0000	-5.52	153.0000	-57.62	213.0000	-68.02	273.0000	-77.71
36.0000	2.72	96.0000	-5.77	156.0000	-58.16	216.0000	-68.52	276.0000	-78.18
39.0000	2.02	99.0000	-6.01	159.0000	-58.70	219.0000	-69.01	279.0000	-78.65
42.0000	1.38	102.0000	-6.24	162.0000	-59.24	222.0000	-69.51	282.0000	-79.12
45.0000	0.78	105.0000	-6.46	165.0000	-59.78	225.0000	-70.00	285.0000	-79.58
48.0000	0.22	108.0000	-6.67	168.0000	-60.31	228.0000	-70.49	288.0000	-80.05
51.0000	-0.31	111.0000	-6.88	171.0000	-60.84	231.0000	-70.98	291.0000	-80.52
54.0000	-0.80	114.0000	-7.08	174.0000	-61.37	234.0000	-71.47	294.0000	-80.98
57.0000	-1.27	117.0000	-7.27	177.0000	-61.90	237.0000	-71.96	297.0000	-81.45
60.0000	-1.72	120.0000	-7.47	180.0000	-62.42	240.0000	-72.45	300.0000	-81.91

***** FOR A RECEIVER INPUT LEVEL OF -40.00 DBM, DISTANCE BETWEEN ANTENNAS CAN BE AT LEAST 123.00 KM *****

--- PROGRAM PARAMETERS ---

POLARIZATION (POL): -----VERTICAL
 FREQUENCY OF SIGNAL (F) -----5825.00 MEG-HERTZ
 SURFACE CONDUCTIVITY (S) -----0.00500 MIU/METER
 SURFACE REFRACTIVITY (NS) -----340.00 N-UNITS
 SUM OF ELEVATION ANGLES (TE) -----0.1311 RADIANS
 DISTANCE BETWEEN ANTENNAS (DIST) -----300.00 K-METERS
 ATTENUATION BELOW FREE SPACE (AE) -----81.19 DB
 INTERDECILE RANGE OF TERRAIN HEIGHT (DM) -----60.00 METERS
 SUM OF SMOOTH-EARTH HORIZON DISTANCES (DLS) -----125.65 K-METERS
 DIFFRACTION ATTENUATION AT DISTANCE DLS (ALS) -----29.59 DB
 PERMITTIVITY OR RELATIVE DIELECTRIC CONSTANT (E) -----15.00
 ESTIMATED SCATTER ATTENUATION BELOW FREE SPACE (AES) -----27.72 DB
 STRUCTURAL RECEIVER ANTENNA HEIGHT ABOVE GROUND (H2R) -----610.00 METERS
 STRUCTURAL TRANSMITTER ANTENNA HEIGHT ABOVE GROUND (H1G) -----20.00 METERS
 ESTIMATED DIFFRACTION ATTENUATION BELOW FREE SPACE (AEO) -----81.17 DB
 COEFFICIENT THAT DEFINES SLOPE OF A SMOOTH CURVE OF ACR (K1) -----0.88162 DB/KM
 COEFFICIENT THAT DEFINES SLOPE OF A SMOOTH CURVE OF ACR (K2) -----0.0 DB/KM
 SLOPE OF THE CURVE OF SCATTER ATTENUATION AS VERSUS DISTANCE (NS) -----0.12627 DB/KM
 DISTANCE WHERE DIFFRACTION AND SCATTER ATTENUATIONS ARE EQUAL (DX) -----144.19 K-METERS
 ATTENUATION WHERE DIFFRACTION AND SCATTER ATTENUATION ARE EQUAL (ADX) -----45.93 DB
 SLOPE OF THE CURVE OF DIFFRACTION ATTENUATION AS VERSUS DISTANCE (MD) -----0.88149 DB/KM

--- SIGNAL STRENGTH DATA INPUT ---

TRANSMITTER POWER OUT -----1000000.00 WATTS
 TRANSMITTER TRANSMISSION LINE LOSS -----2.00 DB
 TRANSMITTER ANTENNA GAIN -----45.60 DB
 RECEIVER SENSITIVITY -----40.00 UWM
 RECEIVER TRANSMISSION LINE LOSS -----2.00 DB
 RECEIVER ANTENNA GAIN -----10.00 DB

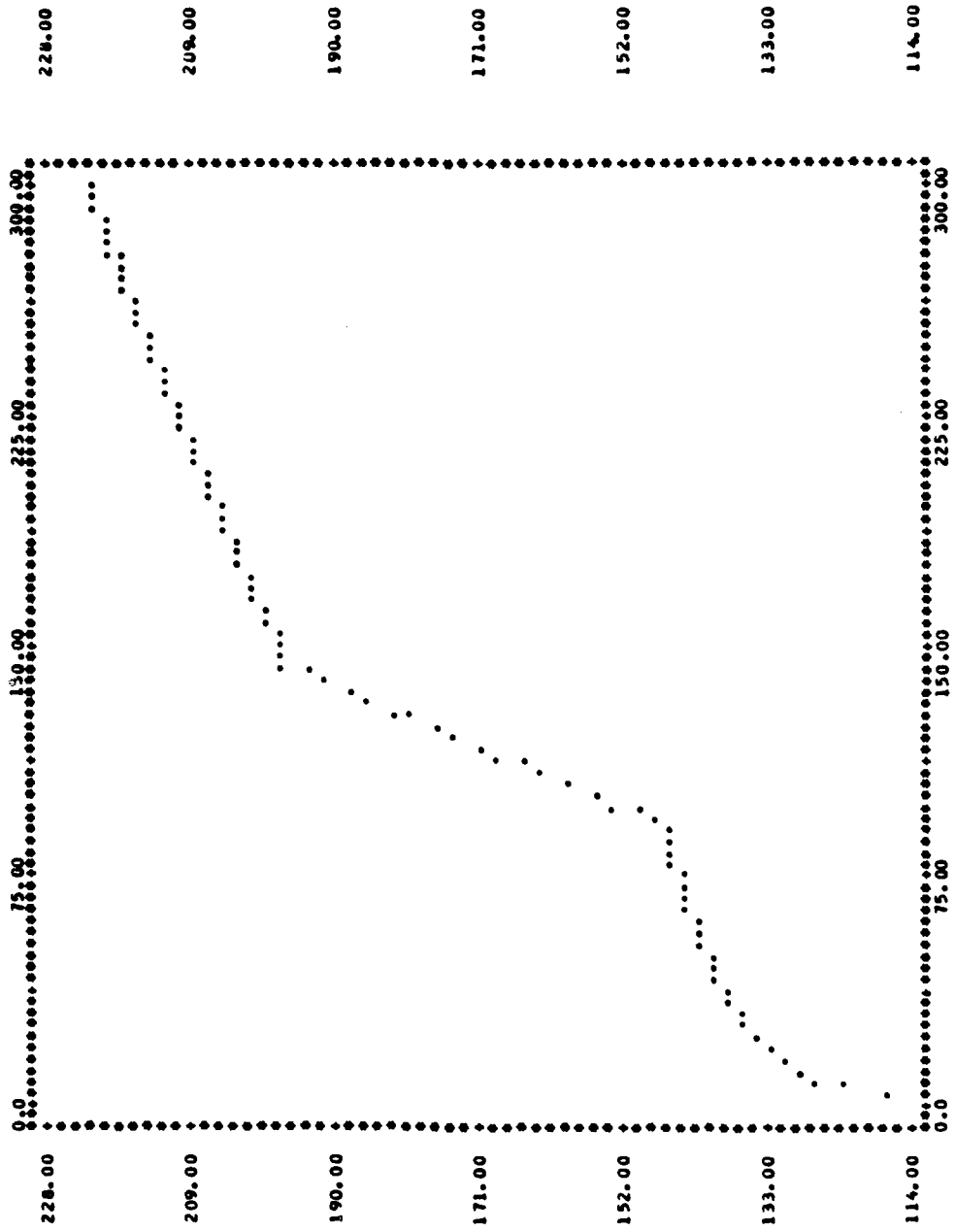
--- USER TERRAIN DATA ---

FREQUENCY OF SIGNAL -F- (MEG-HERTZ) 5825.00000

DISTANCE TRANS-LOSS (DB)	DISTANCE (KM)	TRANS-LOSS (DB)	DISTANCE TRANS-LOSS (DB)	DISTANCE (KM)	TRANS-LOSS (DB)	DISTANCE TRANS-LOSS (DB)	DISTANCE (KM)	TRANS-LOSS (DB)	DISTANCE TRANS-LOSS (DB)
117.30	3.0000	143.74	123.0000	176.81	183.0000	203.84	243.0000	213.88	
123.32	6.0000	144.15	126.0000	179.66	186.0000	204.36	246.0000	214.36	
126.84	9.0000	144.53	129.0000	182.51	189.0000	204.87	249.0000	214.84	
129.34	12.0000	144.90	132.0000	185.35	192.0000	205.39	252.0000	215.33	
131.28	15.0000	145.26	135.0000	188.19	195.0000	205.90	255.0000	215.81	
132.86	18.0000	145.60	138.0000	191.03	198.0000	206.41	258.0000	216.29	
134.20	21.0000	145.93	141.0000	193.86	201.0000	206.92	261.0000	216.77	
135.36	24.0000	146.24	144.0000	196.69	204.0000	207.43	264.0000	217.25	
136.38	27.0000	146.55	147.0000	197.39	207.0000	207.94	267.0000	217.72	
137.30	30.0000	146.84	150.0000	197.94	210.0000	208.44	270.0000	218.20	
138.13	33.0000	147.93	153.0000	198.49	213.0000	208.94	273.0000	218.67	
138.88	36.0000	150.85	156.0000	199.04	216.0000	209.44	276.0000	219.15	
139.58	39.0000	153.76	159.0000	199.58	219.0000	209.94	279.0000	219.62	
140.22	42.0000	156.67	162.0000	200.13	222.0000	210.44	282.0000	220.09	
140.82	45.0000	159.56	165.0000	200.66	225.0000	210.93	285.0000	220.56	
141.38	48.0000	162.45	168.0000	201.20	228.0000	211.43	288.0000	221.03	
141.91	51.0000	165.33	171.0000	201.73	231.0000	211.92	291.0000	221.50	
142.40	54.0000	168.21	174.0000	202.26	234.0000	212.41	294.0000	221.97	
142.87	57.0000	171.08	177.0000	202.79	237.0000	212.90	297.0000	222.44	
143.32	60.0000	173.95	180.0000	203.31	240.0000	213.39	300.0000	222.90	

PLOT OF TRANS.-LOSS VERSUS DISTANCE

• NOTE •• TO FIND SIGNAL STRENGTH FROM GRAPH, SUBTRACT TRANS.-LOSS FROM 141.60



DISTANCE (K-METERS)

TRANS-LOSS (DB)

--- SIGNAL STRENGTH VERSUS DISTANCE FOR GIVEN SYSTEM PARAMETERS ---

DISTANCE (KM)	SIG-STRENGTH (DBM)	DISTANCE (KM)	SIG-STRENGTH (DBM)	DISTANCE (KM)	SIG-STRENGTH (DBM)	DISTANCE (KM)	SIG-STRENGTH (DBM)
3.0000	24.30	63.0000	-2.14	123.0000	-35.21	183.0000	-64.24
6.0000	18.28	66.0000	-2.55	126.0000	-38.06	186.0000	-62.76
9.0000	14.76	69.0000	-2.93	129.0000	-40.91	189.0000	-63.27
12.0000	12.26	72.0000	-3.30	132.0000	-43.75	192.0000	-63.79
15.0000	10.32	75.0000	-3.66	135.0000	-46.59	195.0000	-64.30
18.0000	8.74	78.0000	-4.00	138.0000	-49.43	198.0000	-64.81
21.0000	7.40	81.0000	-4.33	141.0000	-52.26	201.0000	-65.32
24.0000	6.24	84.0000	-4.64	144.0000	-55.09	204.0000	-65.83
27.0000	5.22	87.0000	-4.95	147.0000	-55.79	207.0000	-66.34
30.0000	4.30	90.0000	-5.24	150.0000	-56.34	210.0000	-66.84
33.0000	3.47	93.0000	-5.53	153.0000	-56.89	213.0000	-67.34
36.0000	2.72	96.0000	-5.79	156.0000	-57.44	216.0000	-67.84
39.0000	2.02	99.0000	-6.02	159.0000	-57.98	219.0000	-68.34
42.0000	1.38	102.0000	-6.22	162.0000	-58.53	222.0000	-68.84
45.0000	0.78	105.0000	-6.40	165.0000	-59.06	225.0000	-69.33
48.0000	0.22	108.0000	-6.55	168.0000	-59.60	228.0000	-69.83
51.0000	-0.31	111.0000	-6.68	171.0000	-60.13	231.0000	-70.32
54.0000	-0.80	114.0000	-6.79	174.0000	-60.66	234.0000	-70.81
57.0000	-1.27	117.0000	-6.88	177.0000	-61.19	237.0000	-71.30
60.0000	-1.72	120.0000	-6.95	180.0000	-61.71	240.0000	-71.79
63.0000	-2.14	123.0000	-7.00	183.0000	-62.21	243.0000	-72.28
66.0000	-2.55	126.0000	-7.04	186.0000	-62.71	246.0000	-72.76
69.0000	-2.93	129.0000	-7.07	189.0000	-63.21	249.0000	-73.24
72.0000	-3.30	132.0000	-7.10	192.0000	-63.71	252.0000	-73.73
75.0000	-3.66	135.0000	-7.12	195.0000	-64.21	255.0000	-74.21
78.0000	-4.00	138.0000	-7.14	198.0000	-64.71	258.0000	-74.69
81.0000	-4.33	141.0000	-7.15	201.0000	-65.21	261.0000	-75.17
84.0000	-4.64	144.0000	-7.16	204.0000	-65.71	264.0000	-75.65
87.0000	-4.95	147.0000	-7.17	207.0000	-66.21	267.0000	-76.12
90.0000	-5.24	150.0000	-7.18	210.0000	-66.71	270.0000	-76.60
93.0000	-5.53	153.0000	-7.18	213.0000	-67.21	273.0000	-77.07
96.0000	-5.79	156.0000	-7.18	216.0000	-67.71	276.0000	-77.55
99.0000	-6.02	159.0000	-7.17	219.0000	-68.21	279.0000	-78.02
102.0000	-6.22	162.0000	-7.16	222.0000	-68.71	282.0000	-78.49
105.0000	-6.40	165.0000	-7.15	225.0000	-69.21	285.0000	-78.96
108.0000	-6.55	168.0000	-7.14	228.0000	-69.71	288.0000	-79.43
111.0000	-6.68	171.0000	-7.13	231.0000	-70.21	291.0000	-79.90
114.0000	-6.79	174.0000	-7.12	234.0000	-70.71	294.0000	-80.37
117.0000	-6.88	177.0000	-7.11	237.0000	-71.21	297.0000	-80.84
120.0000	-6.95	180.0000	-7.10	240.0000	-71.71	300.0000	-81.30

***** FOR A RECEIVER INPUT LEVEL OF -40.00 DBM, DISTANCE BETWEEN ANTENNAS CAN BE AT LEAST 126.00 KM *****

--- PROGRAM PARAMETERS ---

POLARIZATION (POL), -----VERTICAL
 FREQUENCY OF SIGNAL (F) -----5825.00 MEG-HERTZ
 SURFACE CONDUCTIVITY (S) -----0.00500 MHO/METER
 SURFACE REFRACTIVITY (NS) -----370.00 N-UNITS
 SUM OF ELEVATION ANGLES (TE) -----0.1256 RADIAN
 DISTANCE BETWEEN ANTENNAS (DIST) -----300.00 K-METERS
 ATTENUATION BELOW FREE SPACE (AE) -----79.60 DB
 INTEROCCULE RANGE OF TERRAIN HEIGHT (DH) -----60.00 METERS
 SUM OF SMOOTH-EARTH HORIZON DISTANCES (DLS) -----131.15 K-METERS
 DIFFRACTION ATTENUATION AT DISTANCE DLS (ALS) -----29.43 DB
 PERMITTIVITY OR RELATIVE DIELECTRIC CONSTANT (E) -----15.00
 ESTIMATED SCATTER ATTENUATION BELOW FREE SPACE (AES) -----26.82 DB
 STRUCTURAL RECEIVER ANTENNA HEIGHT ABOVE GROUND (HZG) -----610.00 METERS
 STRUCTURAL TRANSMITTER ANTENNA HEIGHT ABOVE GROUND (HIG) -----20.00 METERS
 ESTIMATED DIFFRACTION ATTENUATION BELOW FREE SPACE (AED) -----79.60 DB
 COEFFICIENT THAT DEFINES SLOPE OF A SMOOTH CURVE OF ACR (K1) -----0.83130 DB/KM
 COEFFICIENT THAT DEFINES SLOPE OF A SMOOTH CURVE OF ACR (K2) -----0.0 DB/KM
 SLOPE OF THE CURVE OF SCATTER ATTENUATION AS VERSUS DISTANCE (NS) -----0.12583 DB/KM
 DISTANCE WHERE DIFFRACTION AND SCATTER ATTENUATIONS ARE EQUAL (DX) -----150.84 K-METERS
 ATTENUATION WHERE DIFFRACTION AND SCATTER ATTENUATION ARE EQUAL (ADX) -----45.80 DB
 SLOPE OF THE CURVE OF DIFFRACTION ATTENUATION AS VERSUS DISTANCE (MD) -----0.83130 DB/KM

--- SIGNAL STRENGTH DATA INPUT ---

TRANSMITTER POWER OUT -----1000000.00 WATTS
 TRANSMITTER TRANSMISSION LINE LOSS -----2.00 DB
 TRANSMITTER ANTENNA GAIN -----45.60 DB
 RECEIVER SENSITIVITY -----40.00 DBM
 RECEIVER TRANSMISSION LINE LOSS -----2.00 DB
 RECEIVER ANTENNA GAIN -----10.00 DB

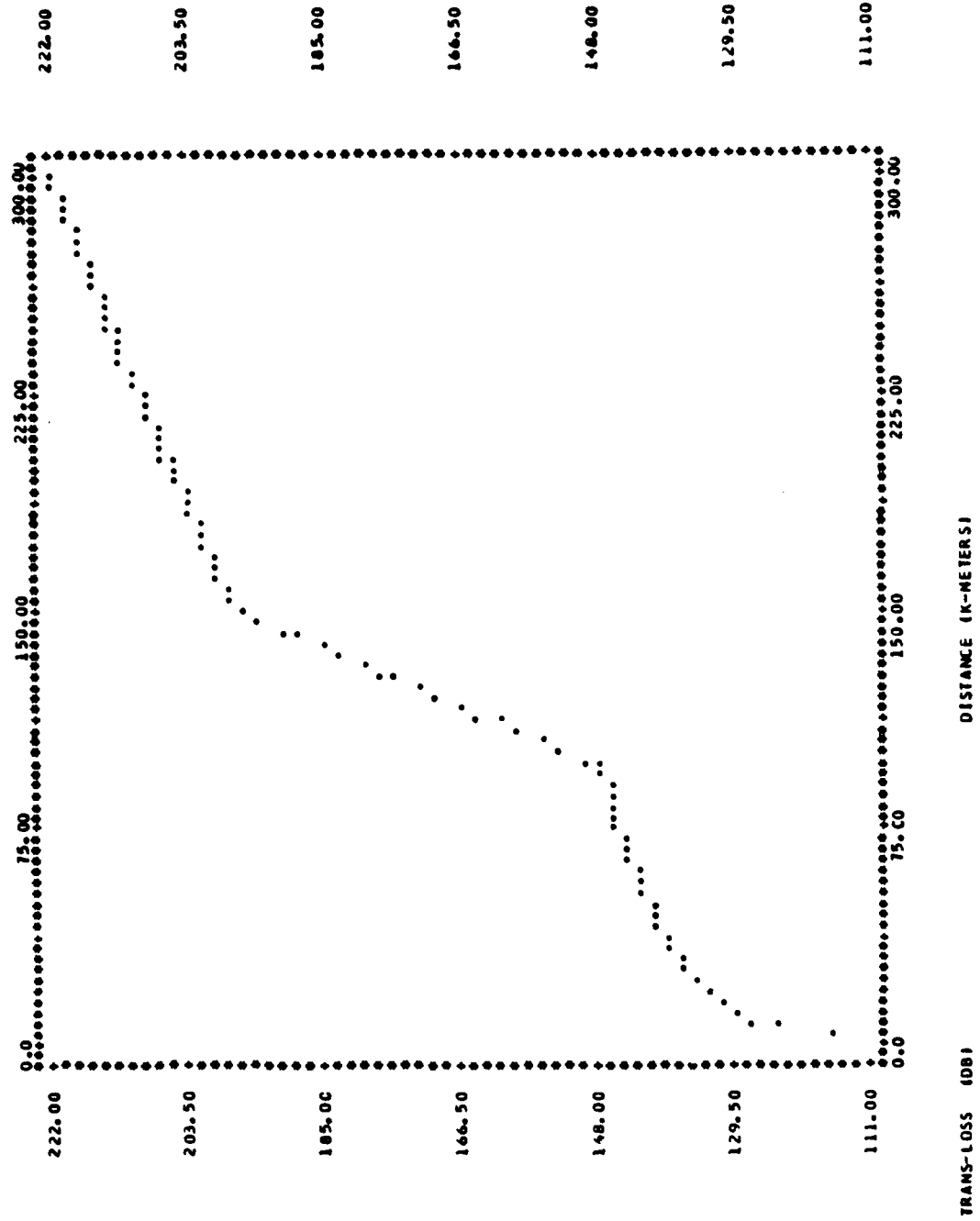
--- USER TERRAIN DATA ---

FREQUENCY OF SIGNAL -F- (MEG-HERTZ) 5825.00000

DISTANCE (KM)	TRANS-LOSS (DB)	DISTANCE (KM)	TRANS-LOSS (DB)	DISTANCE (KM)	TRANS-LOSS (DB)	DISTANCE (KM)	TRANS-LOSS (DB)	DISTANCE (KM)	TRANS-LOSS (DB)
3.0000	117.30	63.0000	143.74	123.0000	172.21	183.0000	202.85	243.0000	212.86
6.0000	123.32	66.0000	144.15	126.0000	174.91	186.0000	203.37	246.0000	213.35
9.0000	126.84	69.0000	144.53	129.0000	177.61	189.0000	203.89	249.0000	213.83
12.0000	129.34	72.0000	144.90	132.0000	180.30	192.0000	204.40	252.0000	214.31
15.0000	131.28	75.0000	145.26	135.0000	182.99	195.0000	204.91	255.0000	214.79
18.0000	132.86	78.0000	145.60	138.0000	185.67	198.0000	205.42	258.0000	215.27
21.0000	134.20	81.0000	145.93	141.0000	188.36	201.0000	205.93	261.0000	215.75
24.0000	135.36	84.0000	146.24	144.0000	191.03	204.0000	206.44	264.0000	216.23
27.0000	136.38	87.0000	146.55	147.0000	193.71	207.0000	206.94	267.0000	216.70
30.0000	137.30	90.0000	146.84	150.0000	196.37	210.0000	207.44	270.0000	217.18
33.0000	138.13	93.0000	147.13	153.0000	197.52	213.0000	207.94	273.0000	217.65
36.0000	138.88	96.0000	147.61	156.0000	198.07	216.0000	208.44	276.0000	218.12
39.0000	139.58	99.0000	150.37	159.0000	198.61	219.0000	208.94	279.0000	218.59
42.0000	140.22	102.0000	153.12	162.0000	199.15	222.0000	209.44	282.0000	219.06
45.0000	140.82	105.0000	155.87	165.0000	199.69	225.0000	209.93	285.0000	219.53
48.0000	141.38	108.0000	158.61	168.0000	200.22	228.0000	210.42	288.0000	220.00
51.0000	141.91	111.0000	161.34	171.0000	200.75	231.0000	210.91	291.0000	220.47
54.0000	142.40	114.0000	164.06	174.0000	201.28	234.0000	211.40	294.0000	220.93
57.0000	142.87	117.0000	166.78	177.0000	201.81	237.0000	211.89	297.0000	221.40
60.0000	143.32	120.0000	169.50	180.0000	202.33	240.0000	212.38	300.0000	221.87

PLOT OF TRANS.-LOSS VERSUS DISTANCE

* NOTE ** TO FIND SIGNAL STRENGTH FROM GRAPH, SUBTRACT TRANS.-LOSS FROM 141.60



--- SIGNAL STRENGTH VERSUS DISTANCE FOR GIVEN SYSTEM PARAMETERS ---

DISTANCE (KM)	SIG-STRENGTH (DBM)	DISTANCE (KM)	SIG-STRENGTH (DBM)	DISTANCE (KM)	SIG-STRENGTH (DBM)	DISTANCE (KM)	SIG-STRENGTH (DBM)	DISTANCE (KM)	SIG-STRENGTH (DBM)
3.0000	24.30	63.0000	-2.14	123.0000	-30.61	183.0000	-61.25	243.0000	-71.26
6.0000	18.28	66.0000	-2.55	126.0000	-33.31	186.0000	-61.77	246.0000	-71.75
9.0000	14.76	69.0000	-2.93	129.0000	-36.01	189.0000	-62.29	249.0000	-72.23
12.0000	12.26	72.0000	-3.30	132.0000	-38.70	192.0000	-62.80	252.0000	-72.71
15.0000	10.32	75.0000	-3.66	135.0000	-41.39	195.0000	-63.31	255.0000	-73.19
18.0000	8.74	78.0000	-4.00	138.0000	-44.07	198.0000	-63.82	258.0000	-73.67
21.0000	7.40	81.0000	-4.33	141.0000	-46.76	201.0000	-64.33	261.0000	-74.15
24.0000	6.24	84.0000	-4.64	144.0000	-49.43	204.0000	-64.84	264.0000	-74.63
27.0000	5.22	87.0000	-4.95	147.0000	-52.11	207.0000	-65.34	267.0000	-75.10
30.0000	4.30	90.0000	-5.24	150.0000	-54.77	210.0000	-65.84	270.0000	-75.58
33.0000	3.47	93.0000	-5.53	153.0000	-57.92	213.0000	-66.34	273.0000	-76.05
36.0000	2.72	96.0000	-6.01	156.0000	-56.47	216.0000	-66.84	276.0000	-76.52
39.0000	2.02	99.0000	-6.77	159.0000	-57.01	219.0000	-67.34	279.0000	-76.99
42.0000	1.38	102.0000	-11.52	162.0000	-57.55	222.0000	-67.84	282.0000	-77.46
45.0000	0.78	105.0000	-14.27	165.0000	-58.09	225.0000	-68.33	285.0000	-77.93
48.0000	0.22	108.0000	-17.01	168.0000	-58.62	228.0000	-68.82	288.0000	-78.40
51.0000	-0.31	111.0000	-19.74	171.0000	-59.15	231.0000	-69.31	291.0000	-78.87
54.0000	-0.80	114.0000	-22.46	174.0000	-59.68	234.0000	-69.80	294.0000	-79.33
57.0000	-1.27	117.0000	-25.18	177.0000	-60.21	237.0000	-70.29	297.0000	-79.80
60.0000	-1.72	120.0000	-27.90	180.0000	-60.73	240.0000	-70.78	300.0000	-80.27

***** FOR A RECEIVER INPUT LEVEL OF -40.00 DBM, DISTANCE BETWEEN ANTENNAS CAN BE AT LEAST 132.00 KM *****

--- PROGRAM PARAMETERS ---

POLARIZATION (POL), -----VERTICAL
 FREQUENCY OF SIGNAL (F) -----5825.00 MEG-HERTZ
 SURFACE CONDUCTIVITY (S) -----0.00500 MHO/METER
 SURFACE REFRACTIVITY (NS) -----400.00 N-UNITS
 SUM OF ELEVATION ANGLES (TE) -----0.1100 RADIANS
 DISTANCE BETWEEN ANTENNAS (DIST) -----300.00 K-METERS
 ATTENUATION BELOW FREE SPACE (AE) -----77.58 DB
 INTERDECILE RANGE OF TERRAIN HEIGHT (DM) -----60.00 METERS
 SUM OF SMOOTH-EARTH HORIZON DISTANCES (DLS) -----138.69 K-METERS
 DIFFRACTION ATTENUATION AT DISTANCE DLS (ALS) -----29.22 DB
 PERMITTIVITY OR RELATIVE DIELECTRIC CONSTANT (E) -----15.00
 ESTIMATED SCATTER ATTENUATION BELOW FREE SPACE (AES) -----25.84 DB
 STRUCTURAL RECEIVER ANTENNA HEIGHT ABOVE GROUND (H2G) -----610.00 METERS
 STRUCTURAL TRANSMITTER ANTENNA HEIGHT ABOVE GROUND (H1G) -----20.00 METERS
 ESTIMATED DIFFRACTION ATTENUATION BELOW FREE SPACE (AED) -----77.58 DB
 COEFFICIENT THAT DEFINES SLOPE OF A SMOOTH CURVE OF ACR (K1) -----0.77009 DB/KM
 COEFFICIENT THAT DEFINES SLOPE OF A SMOOTH CURVE OF ACR (K2) -----0.0 DB/KM
 SLOPE OF THE CURVE OF SCATTER ATTENUATION AS VERSUS DISTANCE (NS) -----0.12369 DB/KM
 DISTANCE WHERE DIFFRACTION AND SCATTER ATTENUATIONS ARE EQUAL (UX) -----160.00 K-METERS
 ATTENUATION WHERE DIFFRACTION AND SCATTER ATTENUATION ARE EQUAL (ADX) -----45.63 DB
 SLOPE OF THE CURVE OF DIFFRACTION ATTENUATION AS VERSUS DISTANCE (ND) -----0.77009 DB/KM

--- SIGNAL STRENGTH DATA INPUT ---

TRANSMITTER POWER OUT -----1000000.00 WATTS
 TRANSMITTER TRANSMISSION LINE LOSS -----2.00 DB
 TRANSMITTER ANTENNA GAIN -----45.60 DB
 RECEIVER SENSITIVITY -----40.00 DBM
 RECEIVER TRANSMISSION LINE LOSS -----2.00 DB
 RECEIVER ANTENNA GAIN -----10.00 DB

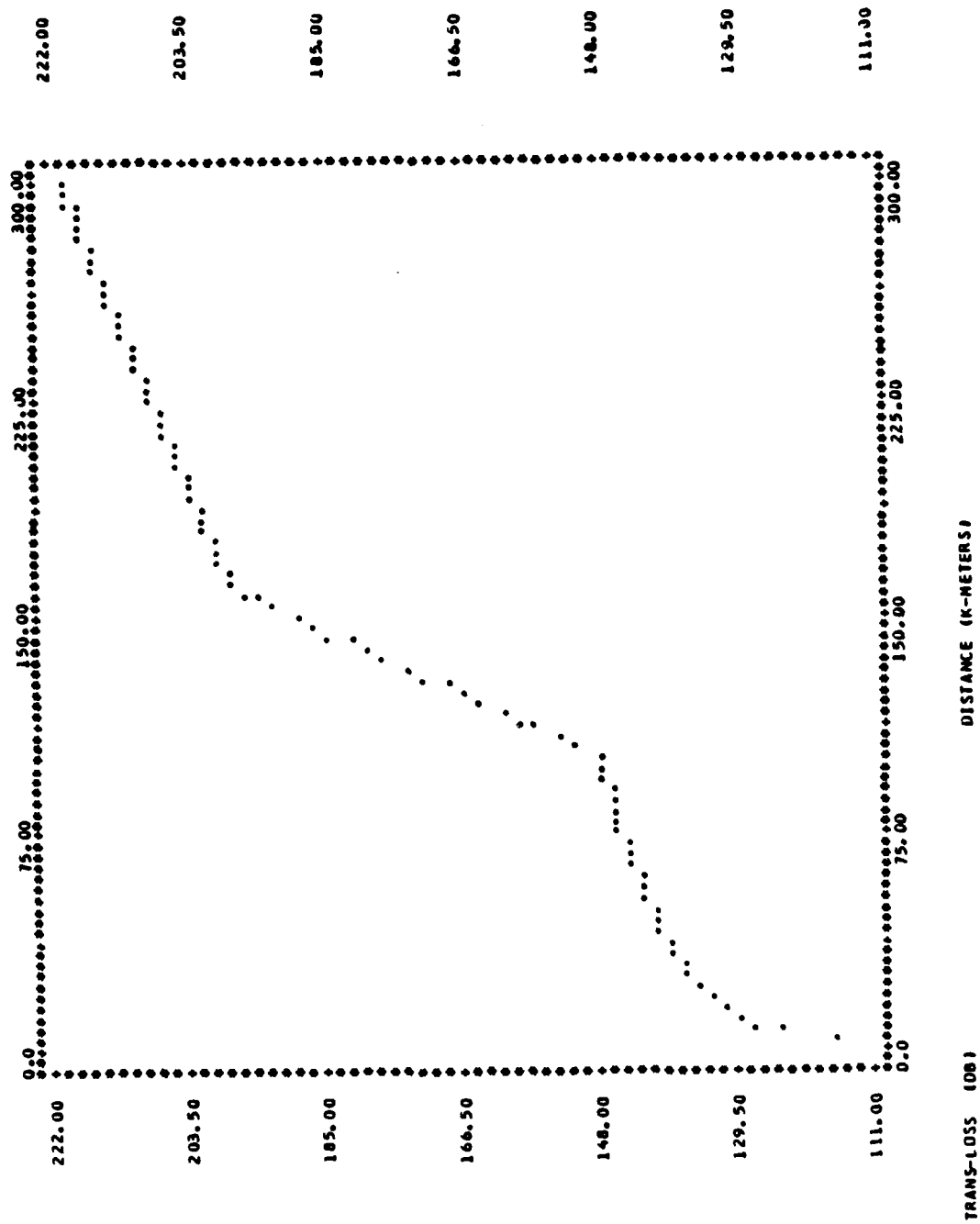
--- USER TERRAIN DATA ---

FREQUENCY OF SIGNAL -F- (MEG-HERTZ) 5825.00000

DISTANCE (KM)	TRANS-LOSS (DB)	DISTANCE (KM)	TRANS-LOSS (DB)	DISTANCE (KM)	TRANS-LOSS (DB)	DISTANCE (KM)	TRANS-LOSS (DB)	DISTANCE (KM)	TRANS-LOSS (DB)
3.0000	117.30	63.0000	143.74	123.0000	166.69	183.0000	201.48	243.0000	211.36
6.0000	123.32	66.0000	144.15	126.0000	169.21	186.0000	201.99	246.0000	211.84
9.0000	126.84	69.0000	144.53	129.0000	171.73	189.0000	202.50	249.0000	212.32
12.0000	129.34	72.0000	144.90	132.0000	174.24	192.0000	203.01	252.0000	212.79
15.0000	131.28	75.0000	145.26	135.0000	176.74	195.0000	203.52	255.0000	213.27
18.0000	132.86	78.0000	145.60	138.0000	179.24	198.0000	204.02	258.0000	213.74
21.0000	134.20	81.0000	145.93	141.0000	181.74	201.0000	204.52	261.0000	214.21
24.0000	135.36	84.0000	146.24	144.0000	184.23	204.0000	205.02	264.0000	214.68
27.0000	136.38	87.0000	146.55	147.0000	186.72	207.0000	205.52	267.0000	215.15
30.0000	137.30	90.0000	146.84	150.0000	189.21	210.0000	206.02	270.0000	215.62
33.0000	138.13	93.0000	147.13	153.0000	191.69	213.0000	206.51	273.0000	216.09
36.0000	138.88	96.0000	147.40	156.0000	194.17	216.0000	207.00	276.0000	216.55
39.0000	139.58	99.0000	147.67	159.0000	196.65	219.0000	207.49	279.0000	217.02
42.0000	140.22	102.0000	148.90	162.0000	197.82	222.0000	207.98	282.0000	217.48
45.0000	140.82	105.0000	151.46	165.0000	198.35	225.0000	208.47	285.0000	217.94
48.0000	141.38	108.0000	154.01	168.0000	198.88	228.0000	208.96	288.0000	218.41
51.0000	141.91	111.0000	156.56	171.0000	199.41	231.0000	209.44	291.0000	218.87
54.0000	142.40	114.0000	159.10	174.0000	199.93	234.0000	209.92	294.0000	219.33
57.0000	142.87	117.0000	161.64	177.0000	200.45	237.0000	210.41	297.0000	219.79
60.0000	143.32	120.0000	164.17	180.0000	200.97	240.0000	210.89	300.0000	220.25

PLOT OF TRANS-LOSS VERSUS DISTANCE

• NOTE •• TO FIND SIGNAL STRENGTH FROM GRAPH, SUBTRACT TRANS-LOSS FROM 141.60



--- SIGNAL STRENGTH VERSUS DISTANCE FOR GIVEN SYSTEM PARAMETERS ---

DISTANCE (KM)	SIG-STRENGTH (DBM)	DISTANCE (KM)	SIG-STRENGTH (DBM)	DISTANCE (KM)	SIG-STRENGTH (DBM)	DISTANCE (KM)	SIG-STRENGTH (DBM)	DISTANCE (KM)	SIG-STRENGTH (DBM)
3.0000	24.30	63.0030	-2.14	123.0000	-25.09	183.0000	-59.88	243.0000	-69.76
6.0000	18.28	66.0030	-2.55	126.0000	-27.61	186.0000	-60.39	246.0000	-70.24
9.0000	14.76	69.0030	-2.93	129.0000	-30.13	189.0000	-60.90	249.0000	-70.72
12.0000	12.26	72.0030	-3.30	132.0000	-32.64	192.0000	-61.41	252.0000	-71.19
15.0000	10.32	75.0030	-3.66	135.0000	-35.14	195.0000	-61.92	255.0000	-71.67
18.0000	8.74	78.0000	-4.00	138.0000	-37.64	198.0000	-62.42	258.0000	-72.14
21.0000	7.60	81.0000	-4.33	141.0000	-40.14	201.0000	-62.92	261.0000	-72.61
24.0000	6.24	84.0000	-4.64	144.0000	-42.63	204.0000	-63.42	264.0000	-73.08
27.0000	5.22	87.0000	-4.95	147.0000	-45.12	207.0000	-63.92	267.0000	-73.55
30.0000	4.30	90.0000	-5.24	150.0000	-47.61	210.0000	-64.42	270.0000	-74.02
33.0000	3.67	93.0030	-5.53	153.0000	-50.09	213.0000	-64.91	273.0000	-74.49
36.0000	2.72	96.0030	-5.80	156.0000	-52.57	216.0000	-65.40	276.0000	-74.95
39.0000	2.32	99.0000	-6.07	159.0000	-55.05	219.0000	-65.89	279.0000	-75.42
42.0000	1.38	102.0030	-7.30	162.0000	-56.22	222.0000	-66.38	282.0000	-75.88
45.0000	0.78	105.0000	-9.86	165.0000	-56.75	225.0000	-66.87	285.0000	-76.34
48.0000	0.22	108.0000	-12.41	168.0000	-57.28	228.0000	-67.36	288.0000	-76.81
51.0000	-0.31	111.0000	-14.96	171.0000	-57.81	231.0000	-67.84	291.0000	-77.27
54.0000	-0.80	114.0030	-17.50	174.0000	-58.33	234.0000	-68.32	294.0000	-77.73
57.0000	-1.27	117.0000	-20.04	177.0000	-58.85	237.0000	-68.81	297.0000	-78.19
60.0000	-1.72	120.0000	-22.57	180.0000	-59.37	240.0000	-69.29	300.0000	-78.65

***** FOR A RECEIVER INPUT LEVEL OF -40.00 DBM, DISTANCE BETWEEN ANTENNAS CAN BE AT LEAST 138.00 KM *****

--- PROGRAM PARAMETERS ---

POLARIZATION (POL) -----VERTICAL
 FREQUENCY OF SIGNAL (F) ----- 40.00 MEG-HERTZ
 SURFACE CONDUCTIVITY (S) ----- 0.00500 MHO/METER
 SURFACE REFRACTIVITY (NS) ----- 250.00 N-UNITS
 SUM OF ELEVATION ANGLES (TE) ----- .00300 RADIAN
 DISTANCE BETWEEN ANTENNAS (DIST) ----- 30.00 K-METERS
 ATTENUATION BELOW FREE SPACE (AE) ----- 13.79 DB
 INTERDECILE RANGE OF TERRAIN HEIGHT (DH) ----- 10.00 METERS
 SUM OF SMOOTH-EARTH HORIZON DISTANCES (DLS) ----- 25.22 K-METERS
 DIFFRACTION ATTENUATION AT DISTANCE DLS (ALS) ----- 50.27 DB
 PERMITTIVITY OR RELATIVE DIELECTRIC CONSTANT (E) ----- 15.00
 ESTIMATED SCATTER ATTENUATION BELOW FREE SPACE (AES) ----- 59.91 DB
 STRUCTURAL RECEIVER ANTENNA HEIGHT ABOVE GROUND (H2G) ----- 10.00 METERS
 STRUCTURAL TRANSMITTER ANTENNA HEIGHT ABOVE GROUND (H1G) ----- 10.00 METERS
 ESTIMATED DIFFRACTION ATTENUATION BELOW FREE SPACE (AED) ----- 43.51 DB
 COEFFICIENT THAT DEFINES SLOPE OF A SMOOTH CURVE OF ACR (K1) ----- 0.67760 DB/KM
 COEFFICIENT THAT DEFINES SLOPE OF A SMOOTH CURVE OF ACR (K2) ----- 13.035637 DB/KM
 SLOPE OF THE CURVE OF SCATTER ATTENUATION AS VERSUS DISTANCE (MS) ----- 0.10521 DB/KM
 DISTANCE WHERE DIFFRACTION AND SCATTER ATTENUATIONS ARE EQUAL (DX) ----- 100.65 K-METERS
 ATTENUATION WHERE DIFFRACTION AND SCATTER ATTENUATION ARE EQUAL (ADX) ----- 70.50 DB
 SLOPE OF THE CURVE OF DIFFRACTION ATTENUATION AS VERSUS DISTANCE (MD) ----- 0.26020 DB/KM

--- SIGNAL STRENGTH DATA INPUT ---

TRANSMITTER POWER OUT ----- 35.00 WATTS
 TRANSMITTER TRANSMISSION LINE LOSS ----- 2.00 DB
 TRANSMITTER ANTENNA GAIN ----- 10.00 DB
 RECEIVER SENSITIVITY ----- -80.00 DBM
 RECEIVER TRANSMISSION LINE LOSS ----- 2.00 DB
 RECEIVER ANTENNA GAIN ----- 10.00 DB

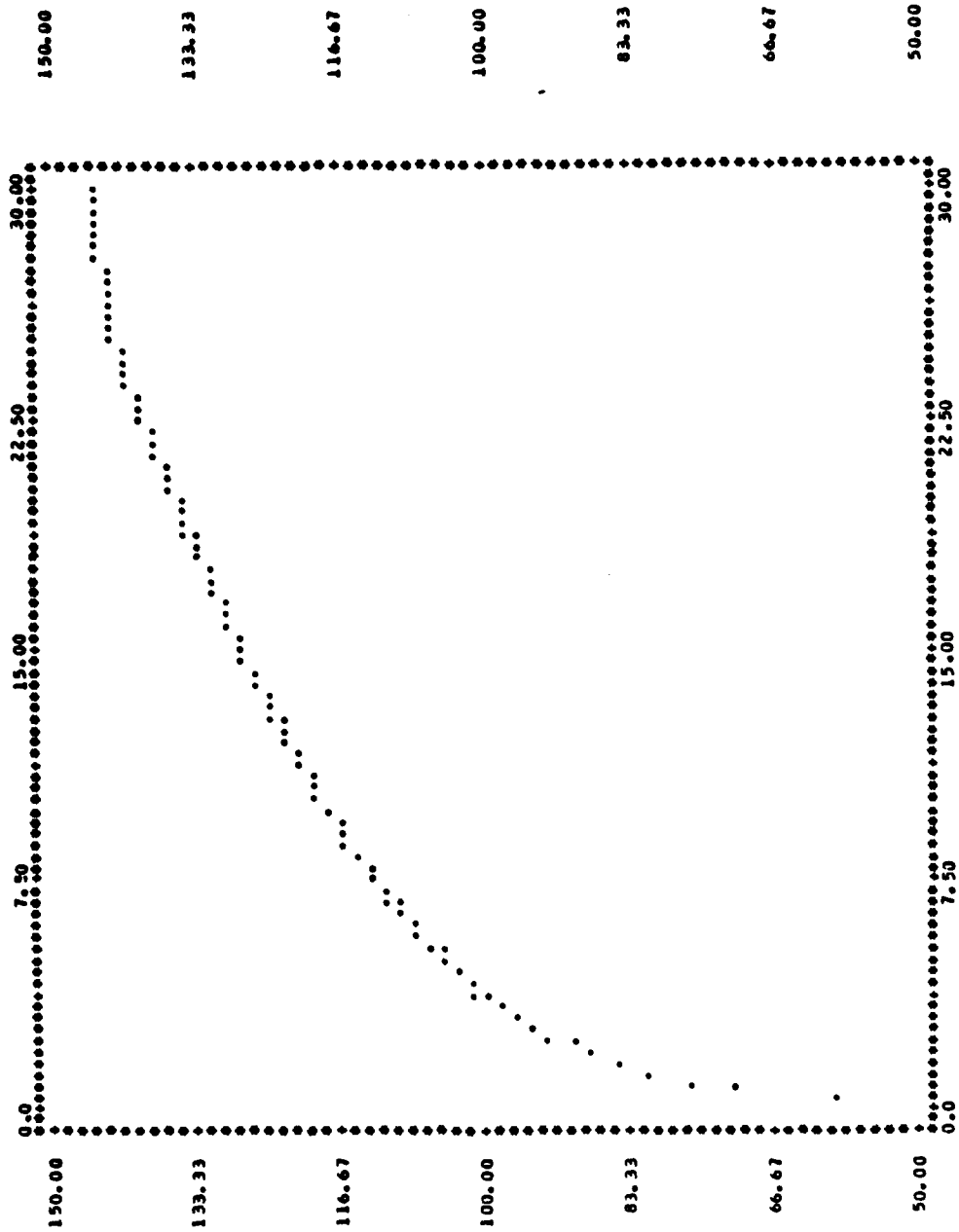
--- USER TERRAIN DATA ---

FREQUENCY OF SIGNAL -F- (MEG-HERTZ) 40.00000

DISTANCE TRANS-LOSS (DB)	DISTANCE (KM)	DISTANCE TRANS-LOSS (DB)	DISTANCE (KM)	DISTANCE TRANS-LOSS (DB)	DISTANCE (KM)	DISTANCE TRANS-LOSS (DB)	DISTANCE (KM)
60.79	6.3000	109.59	12.3000	123.49	18.3000	133.39	24.3000
71.18	6.6000	110.48	12.6000	124.05	18.6000	133.83	24.6000
77.34	6.9000	111.34	12.9000	124.60	18.9000	134.27	24.9000
81.77	7.2000	112.16	13.2000	125.14	19.2000	134.71	25.2000
85.25	7.5000	112.97	13.5000	125.67	19.5000	135.14	25.5000
88.13	7.8000	113.75	13.8000	126.20	19.8000	135.57	25.8000
90.60	8.1000	114.50	14.1000	126.72	20.1000	135.99	26.1000
92.77	8.4000	115.24	14.4000	127.23	20.4000	136.41	26.4000
94.70	8.7000	115.96	14.7000	127.73	20.7000	136.83	26.7000
96.45	9.0000	116.66	15.0000	128.23	21.0000	137.24	27.0000
98.06	9.3000	117.35	15.3000	128.73	21.3000	137.66	27.3000
99.54	9.6000	118.02	15.6000	129.22	21.6000	138.06	27.6000
100.92	9.9000	118.67	15.9000	129.70	21.9000	138.47	27.9000
102.21	10.2000	119.31	16.2000	130.18	22.2000	138.87	28.2000
103.43	10.5000	119.94	16.5000	130.65	22.5000	139.27	28.5000
104.58	10.8000	120.56	16.8000	131.12	22.8000	139.67	28.8000
105.67	11.1000	121.17	17.1000	131.58	23.1000	140.07	29.1000
106.72	11.4000	121.76	17.4000	132.04	23.4000	140.46	29.4000
107.71	11.7000	122.35	17.7000	132.50	23.7000	140.85	29.7000
108.67	12.0000	122.92	18.0000	132.95	24.0000	141.24	30.0000

PLOT OF TRANS.-LOSS VERSUS DISTANCE

• NOTE •• TO FIND SIGNAL STRENGTH FROM GRAPH, SUBTRACT TRANS.-LOSS FROM 61.66



TRANS-LOSS (DB) DISTANCE (K-METERS)

--- SIGNAL STRENGTH VERSUS DISTANCE FOR GIVEN SYSTEM PARAMETERS ---

DISTANCE (KM)	SIG-STRENGTH (DBM)	DISTANCE (KM)	SIG-STRENGTH (DBM)	DISTANCE (KM)	SIG-STRENGTH (DBM)	DISTANCE (KM)	SIG-STRENGTH (DBM)	DISTANCE (KM)	SIG-STRENGTH (DBM)
0.3000	0.65	6.3000	-68.15	12.3000	-62.05	18.3000	-71.95	24.3000	-80.18
0.6000	-9.74	6.6000	-69.04	12.6000	-62.61	18.6000	-72.39	24.6000	-80.57
0.9000	-15.90	6.9000	-69.89	12.9000	-63.15	18.9000	-72.83	24.9000	-80.95
1.2000	-20.33	7.2000	-70.72	13.2000	-63.70	19.2000	-73.27	25.2000	-81.33
1.5000	-23.81	7.5000	-71.53	13.5000	-64.23	19.5000	-73.70	25.5000	-81.53
1.8000	-26.69	7.8000	-72.31	13.8000	-64.76	19.8000	-74.13	25.8000	-81.71
2.1000	-29.16	8.1000	-73.06	14.1000	-65.27	20.1000	-74.55	26.1000	-81.89
2.4000	-31.33	8.4000	-73.80	14.4000	-65.79	20.4000	-74.97	26.4000	-82.07
2.7000	-33.26	8.7000	-74.52	14.7000	-66.29	20.7000	-75.39	26.7000	-82.25
3.0000	-35.01	9.0000	-75.22	15.0000	-66.79	21.0000	-75.80	27.0000	-82.43
3.3000	-36.62	9.3000	-75.91	15.3000	-67.29	21.3000	-76.22	27.3000	-82.60
3.6000	-38.10	9.6000	-76.58	15.6000	-67.78	21.6000	-76.62	27.6000	-82.78
3.9000	-39.48	9.9000	-77.23	15.9000	-68.26	21.9000	-77.03	27.9000	-82.95
4.2000	-40.77	10.2000	-77.87	16.2000	-68.74	22.2000	-77.43	28.2000	-83.12
4.5000	-41.99	10.5000	-78.50	16.5000	-69.21	22.5000	-77.83	28.5000	-83.30
4.8000	-43.14	10.8000	-79.12	16.8000	-69.68	22.8000	-78.23	28.8000	-83.47
5.1000	-44.23	11.1000	-79.73	17.1000	-70.14	23.1000	-78.63	29.1000	-83.64
5.4000	-45.28	11.4000	-80.32	17.4000	-70.60	23.4000	-79.02	29.4000	-83.81
5.7000	-46.27	11.7000	-80.91	17.7000	-71.06	23.7000	-79.41	29.7000	-83.98
6.0000	-47.23	12.0000	-81.48	18.0000	-71.51	24.0000	-79.80	30.0000	-84.14

***** FOR A RECEIVER INPUT LEVEL OF -80.00 DBM, DISTANCE BETWEEN ANTENNAS CAN BE AT LEAST 24.00 KM *****

--- PROGRAM PARAMETERS ---

POLARIZATION (POL), -----VERTICAL
 FREQUENCY OF SIGNAL (F) ----- 40.00 MEG-HERTZ
 SURFACE CONDUCTIVITY (S) -----0.00500 MO/METER
 SURFACE REFRACTIVITY (NS) ----- 300.00 N-UNITS
 SUM OF ELEVATION ANGLES (TE) -----0.0200 RADIAN
 DISTANCE BETWEEN ANTENNAS (DIST) ----- 30.00 K-METERS
 ATTENUATION BELOW FREE SPACE (AE) ----- 13.86 DB
 INTERDECIBLE RANGE OF TERRAIN HEIGHT (DH) ----- 10.00 METERS
 SUM OF SMOOTH-EARTH HORIZON DISTANCES (DLS) ----- 26.22 K-METERS
 DIFFRACTION ATTENUATION AT DISTANCE DLS (ALS) ----- 50.55 DB
 PERMITTIVITY OR RELATIVE DIELECTRIC CONSTANT (E) ----- 15.00
 ESTIMATED SCATTER ATTENUATION BELOW FREE SPACE (AES) ----- 59.71 DB
 STRUCTURAL RECEIVER ANTENNA HEIGHT ABOVE GROUND (HZG) ----- 10.00 METERS
 STRUCTURAL TRANSMITTER ANTENNA HEIGHT ABOVE GROUND (HIG) ----- 10.00 METERS
 ESTIMATED DIFFRACTION ATTENUATION BELOW FREE SPACE (AED) ----- 43.86 DB
 COEFFICIENT THAT DEFINES SLOPE OF A SMOOTH CURVE OF ACR (K1) -----0.64713 DB/KM
 COEFFICIENT THAT DEFINES SLOPE OF A SMOOTH CURVE OF ACR (K2) -----13.903013 DB/KM
 SLOPE OF THE CURVE OF SCATTER ATTENUATION AS VERSUS DISTANCE (MS) -----0.10000 DB/KM
 DISTANCE WHERE DIFFRACTION AND SCATTER ATTENUATIONS ARE EQUAL (DX) ----- 107.97 K-METERS
 ATTENUATION WHERE DIFFRACTION AND SCATTER ATTENUATIONS ARE EQUAL (ADX) ----- 71.38 DB
 SLOPE OF THE CURVE OF DIFFRACTION ATTENUATION AS VERSUS DISTANCE (MD) -----0.25487 DB/KM

--- SIGNAL STRENGTH DATA INPUT ---

TRANSMITTER POWER OUT ----- 35.00 WATTS
 TRANSMITTER TRANSMISSION LINE LOSS ----- 2.00 DB
 TRANSMITTER ANTENNA GAIN ----- 10.00 DB
 RECEIVER SENSITIVITY ----- -80.00 DBM
 RECEIVER TRANSMISSION LINE LOSS ----- 2.00 DB
 RECEIVER ANTENNA GAIN ----- 10.00 DB

9

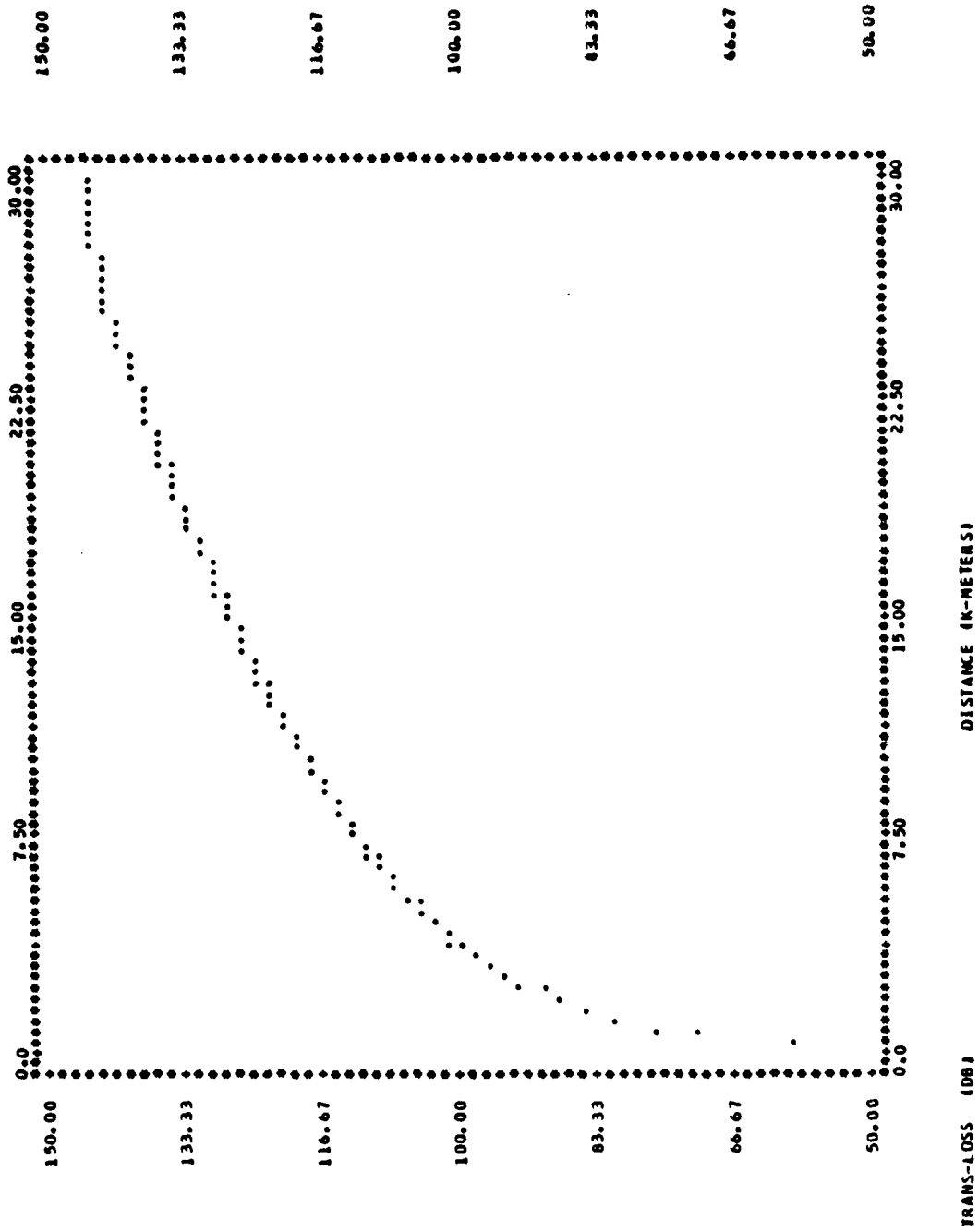
--- USER TERRAIN DATA ---

FREQUENCY OF SIGNAL - F- (MEG-HERTZ) 40.00000

DISTANCE (KM)	TRANS-LOSS (DB)	DISTANCE (KM)	TRANS-LOSS (DB)	DISTANCE (KM)	TRANS-LOSS (DB)	DISTANCE (KM)	TRANS-LOSS (DB)		
0.3000	60.82	6.3000	-109.53	12.3000	-123.26	18.3000	-132.99	24.3000	-141.05
0.6000	71.22	6.6000	-110.40	12.6000	-123.81	18.6000	-133.43	24.6000	-141.42
0.9000	77.38	6.9000	-111.25	12.9000	-124.35	18.9000	-133.85	24.9000	-141.80
1.2000	81.81	7.2000	-112.07	13.2000	-124.88	19.2000	-134.28	25.2000	-142.17
1.5000	85.29	7.5000	-112.87	13.5000	-125.41	19.5000	-134.70	25.5000	-142.54
1.8000	88.17	7.8000	-113.64	13.8000	-125.92	19.8000	-135.12	25.8000	-142.90
2.1000	90.63	8.1000	-114.39	14.1000	-126.43	20.1000	-135.54	26.1000	-143.27
2.4000	92.79	8.4000	-115.12	14.4000	-126.94	20.4000	-135.95	26.4000	-143.52
2.7000	94.72	8.7000	-115.83	14.7000	-127.44	20.7000	-136.36	26.7000	-143.69
3.0000	96.67	9.0000	-116.52	15.0000	-127.93	21.0000	-136.77	27.0000	-143.86
3.3000	98.06	9.3000	-117.20	15.3000	-128.41	21.3000	-137.17	27.3000	-144.04
3.6000	99.54	9.6000	-117.86	15.6000	-128.89	21.6000	-137.57	27.6000	-144.21
3.9000	100.91	9.9000	-118.51	15.9000	-129.37	21.9000	-137.97	27.9000	-144.38
4.2000	102.20	10.2000	-119.14	16.2000	-129.84	22.2000	-138.36	28.2000	-144.55
4.5000	103.41	10.5000	-119.76	16.5000	-130.30	22.5000	-138.75	28.5000	-144.72
4.8000	104.55	10.8000	-120.37	16.8000	-130.76	22.8000	-139.14	28.8000	-144.88
5.1000	105.64	11.1000	-120.97	17.1000	-131.22	23.1000	-139.53	29.1000	-145.05
5.4000	106.67	11.4000	-121.56	17.4000	-131.67	23.4000	-139.91	29.4000	-145.22
5.7000	107.66	11.7000	-122.13	17.7000	-132.11	23.7000	-140.29	29.7000	-145.38
6.0000	108.61	12.0000	-122.70	18.0000	-132.55	24.0000	-140.67	30.0000	-145.54

PLOT OF TRANS.-LOSS VERSUS DISTANCE

• NOTE •• TO FIND SIGNAL STRENGTH FROM GRAPH, SUBTRACT TRANS.-LOSS FROM 61.44



--- SIGNAL STRENGTH VERSUS DISTANCE FOR GIVEN SYSTEM PARAMETERS ---

DISTANCE (KM)	SIG-STRENGTH (DBM)	DISTANCE (KM)	SIG-STRENGTH (DBM)	DISTANCE (KM)	SIG-STRENGTH (DBM)	DISTANCE (KM)	SIG-STRENGTH (DBM)	DISTANCE (KM)	SIG-STRENGTH (DBM)
0.3000---	0.63	6.3000---	-48.08	12.3000---	-61.82	18.3000---	-71.55	24.3000---	-79.61
0.6000---	-9.77	6.6000---	-48.96	12.6000---	-62.37	18.6000---	-71.98	24.6000---	-79.98
0.9000---	-15.94	6.9000---	-49.81	12.9000---	-62.91	18.9000---	-72.41	24.9000---	-80.36
1.2000---	-20.37	7.2000---	-50.63	13.2000---	-63.44	19.2000---	-72.84	25.2000---	-80.73
1.5000---	-23.85	7.5000---	-51.43	13.5000---	-63.97	19.5000---	-73.26	25.5000---	-81.10
1.8000---	-26.73	7.8000---	-52.20	13.8000---	-64.48	19.8000---	-73.68	25.8000---	-81.46
2.1000---	-29.19	8.1000---	-52.95	14.1000---	-64.99	20.1000---	-74.10	26.1000---	-81.83
2.4000---	-31.35	8.4000---	-53.68	14.4000---	-65.50	20.4000---	-74.51	26.4000---	-82.08
2.7000---	-33.28	8.7000---	-54.39	14.7000---	-66.00	20.7000---	-74.92	26.7000---	-82.25
3.0000---	-35.02	9.0000---	-55.08	15.0000---	-66.49	21.0000---	-75.32	27.0000---	-82.42
3.3000---	-36.62	9.3000---	-55.76	15.3000---	-66.97	21.3000---	-75.73	27.3000---	-82.60
3.6000---	-38.10	9.6000---	-56.42	15.6000---	-67.45	21.6000---	-76.13	27.6000---	-82.77
3.9000---	-39.47	9.9000---	-57.07	15.9000---	-67.93	21.9000---	-76.52	27.9000---	-82.94
4.2000---	-40.76	10.2000---	-57.70	16.2000---	-68.40	22.2000---	-76.92	28.2000---	-83.11
4.5000---	-41.97	10.5000---	-58.32	16.5000---	-68.86	22.5000---	-77.31	28.5000---	-83.28
4.8000---	-43.11	10.8000---	-58.93	16.8000---	-69.32	22.8000---	-77.70	28.8000---	-83.44
5.1000---	-44.20	11.1000---	-59.53	17.1000---	-69.78	23.1000---	-78.09	29.1000---	-83.61
5.4000---	-45.23	11.4000---	-60.12	17.4000---	-70.23	23.4000---	-78.47	29.4000---	-83.77
5.7000---	-46.22	11.7000---	-60.69	17.7000---	-70.67	23.7000---	-78.85	29.7000---	-83.94
6.0000---	-47.17	12.0000---	-61.26	18.0000---	-71.11	24.0000---	-79.23	30.0000---	-84.10

***** FOR A RECEIVER INPUT LEVEL OF -80.00 DBM, DISTANCE BETWEEN ANTENNAS CAN BE AT LEAST 24.60 KM *****

--- PROGRAM PARAMETERS ---

POLARIZATION (POL) -----VERTICAL
 FREQUENCY OF SIGNAL (F) ----- 60.00 MEG-HERTZ
 SURFACE CONDUCTIVITY (S) -----0.00500 MHO/METER
 SURFACE REFRACTIVITY (NS) ----- 350.00 N-UNITS
 SUM OF ELEVATION ANGLES (TE) -----0.0273 RADIAN
 DISTANCE BETWEEN ANTENNAS (DIST) ----- 40.00 K-METERS
 ATTENUATION BELOW FREE SPACE (AE) ----- 13.96 DB
 INTERDECILE RANGE OF TERRAIN HEIGHT (DH) ----- 10.00 METERS
 SUM OF SMOOTH-EARTH HORIZON DISTANCES (DLS) ----- 27.73 K-METERS
 DIFFRACTION ATTENUATION AT DISTANCE DLS (ALS) ----- 50.95 DB
 PERMITTIVITY OR RELATIVE DIELECTRIC CONSTANT (E) ----- 15.00
 ESTIMATED SCATTER ATTENUATION BELOW FREE SPACE (AES) ----- 59.67 DB
 STRUCTURAL RECEIVER ANTENNA HEIGHT ABOVE GROUND (HZG) ----- 10.00 METERS
 STRUCTURAL TRANSMITTER ANTENNA HEIGHT ABOVE GROUND (HIG) ----- 10.00 METERS
 ESTIMATED DIFFRACTION ATTENUATION BELOW FREE SPACE (AED) ----- 64.39 DB
 COEFFICIENT THAT DEFINES SLOPE OF A SMOOTH CURVE OF ACR (K1) -----0.60348 DB/KM
 COEFFICIENT THAT DEFINES SLOPE OF A SMOOTH CURVE OF ACR (K2) -----13.997371 DB/KM
 SLOPE OF THE CURVE OF SCATTER ATTENUATION AS VERSUS DISTANCE (MS) -----0.10830 DB/KM
 DISTANCE WHERE DIFFRACTION AND SCATTER ATTENUATIONS ARE EQUAL (DX) ----- 119.05 K-METERS
 ATTENUATION WHERE DIFFRACTION AND SCATTER ATTENUATION ARE EQUAL (ADX) ----- 72.56 DB
 SLOPE OF THE CURVE OF DIFFRACTION ATTENUATION AS VERSUS DISTANCE (MD) -----0.23668 DB/KM

--- SIGNAL STRENGTH DATA INPUT ---

TRANSMITTER POWER OUT ----- 35.00 WATTS
 TRANSMITTER TRANSMISSION LINE LOSS ----- 2.00 DB
 TRANSMITTER ANTENNA GAIN ----- 10.00 DB
 RECEIVER SENSITIVITY ----- -80.00 DBM
 RECEIVER TRANSMISSION LINE LOSS ----- 2.00 DB
 RECEIVER ANTENNA GAIN ----- 10.00 DB

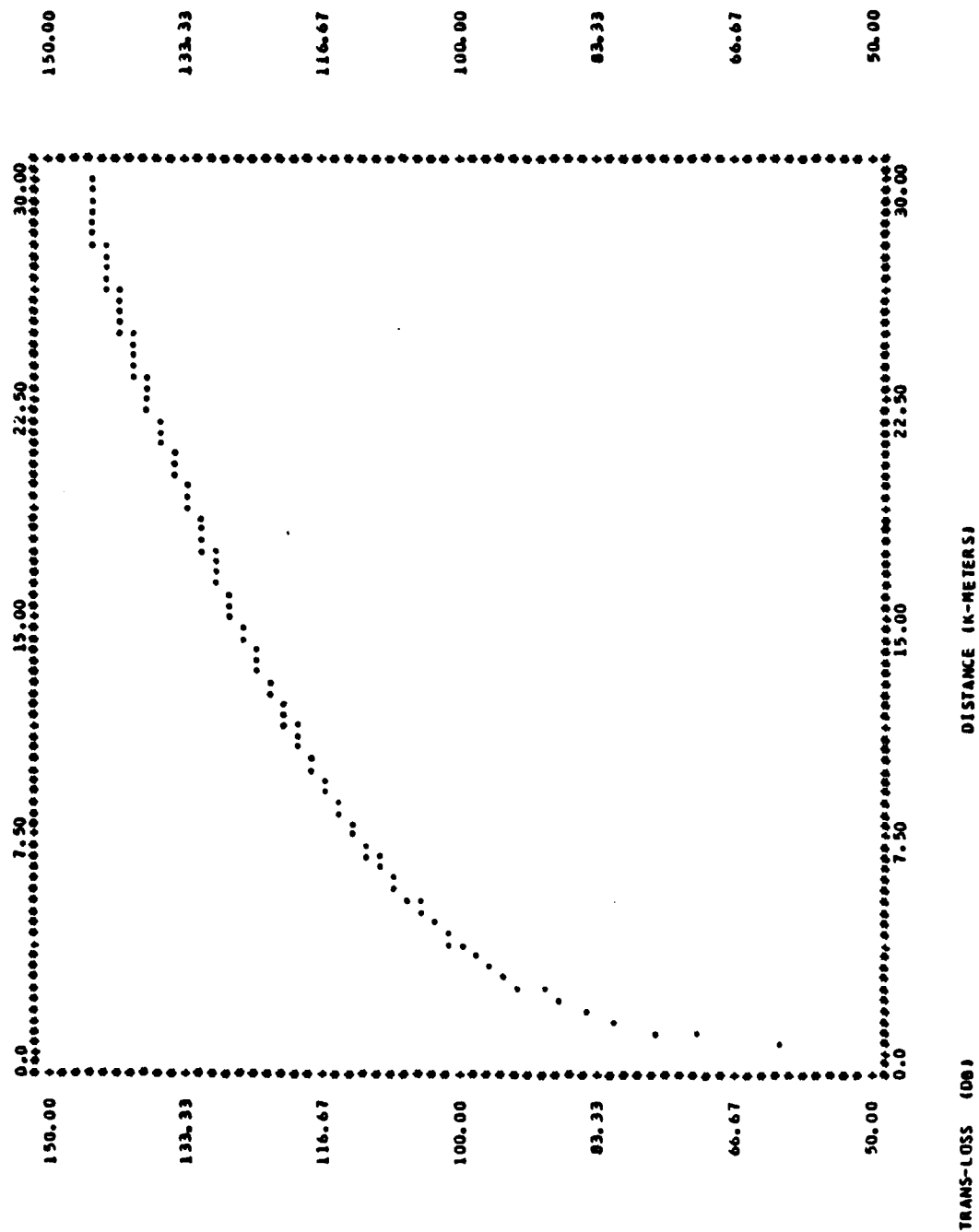
--- USER TERRAIN DATA ---

FREQUENCY OF SIGNAL -F- (MEG-HERTZ) 40.00000

DISTANCE (KM)	TRANS-LOSS (DB)	DISTANCE (KM)	TRANS-LOSS (DB)	DISTANCE (KM)	TRANS-LOSS (DB)	DISTANCE (KM)	TRANS-LOSS (DB)
0.3000	60.85	6.3000	109.44	12.3000	122.95	18.3000	132.45
0.6000	71.27	6.6000	110.31	12.6000	123.49	18.6000	132.87
0.9000	77.44	6.9000	111.15	12.9000	124.02	18.9000	133.29
1.2000	81.87	7.2000	111.96	13.2000	124.54	19.2000	133.70
1.5000	85.34	7.5000	112.74	13.5000	125.05	19.5000	134.11
1.8000	88.22	7.8000	113.50	13.8000	125.56	19.8000	134.52
2.1000	90.68	8.1000	114.24	14.1000	126.06	20.1000	134.92
2.4000	92.83	8.4000	114.96	14.4000	126.55	20.4000	135.33
2.7000	94.75	8.7000	115.66	14.7000	127.04	20.7000	135.72
3.0000	96.49	9.0000	116.34	15.0000	127.52	21.0000	136.12
3.3000	98.08	9.3000	117.01	15.3000	127.99	21.3000	136.51
3.6000	99.54	9.6000	117.66	15.6000	128.46	21.6000	136.90
3.9000	100.91	9.9000	118.29	15.9000	128.92	21.9000	137.28
4.2000	102.18	10.2000	118.92	16.2000	129.38	22.2000	137.66
4.5000	103.38	10.5000	119.52	16.5000	129.83	22.5000	138.04
4.8000	104.52	10.8000	120.12	16.8000	130.28	22.8000	138.42
5.1000	105.59	11.1000	120.71	17.1000	130.72	23.1000	138.80
5.4000	106.62	11.4000	121.28	17.4000	131.16	23.4000	139.17
5.7000	107.60	11.7000	121.85	17.7000	131.59	23.7000	139.54
6.0000	108.54	12.0000	122.40	18.0000	132.02	24.0000	139.90
6.3000	109.27	12.3000	122.95	18.3000	132.45	24.3000	140.27
6.6000	110.31	12.6000	123.49	18.6000	132.87	24.6000	140.63
6.9000	111.15	12.9000	124.02	18.9000	133.29	24.9000	140.99
7.2000	111.96	13.2000	124.54	19.2000	133.70	25.2000	141.35
7.5000	112.74	13.5000	125.05	19.5000	134.11	25.5000	141.71
7.8000	113.50	13.8000	125.56	19.8000	134.52	25.8000	142.06
8.1000	114.24	14.1000	126.06	20.1000	134.92	26.1000	142.41
8.4000	114.96	14.4000	126.55	20.4000	135.33	26.4000	142.77
8.7000	115.66	14.7000	127.04	20.7000	135.72	26.7000	143.11
9.0000	116.34	15.0000	127.52	21.0000	136.12	27.0000	143.46
9.3000	117.01	15.3000	127.99	21.3000	136.51	27.3000	143.80
9.6000	117.66	15.6000	128.46	21.6000	136.90	27.6000	144.15
9.9000	118.29	15.9000	128.92	21.9000	137.28	27.9000	144.39
10.2000	118.92	16.2000	129.38	22.2000	137.66	28.2000	144.56
10.5000	119.52	16.5000	129.83	22.5000	138.04	28.5000	144.72
10.8000	120.12	16.8000	130.28	22.8000	138.42	28.8000	144.88
11.1000	120.71	17.1000	130.72	23.1000	138.80	29.1000	145.04
11.4000	121.28	17.4000	131.16	23.4000	139.17	29.4000	145.20
11.7000	121.85	17.7000	131.59	23.7000	139.54	29.7000	145.36
12.0000	122.40	18.0000	132.02	24.0000	139.90	30.0000	145.52

PLOT OF TRANS.-LOSS VERSUS DISTANCE

• NOTE •• TO FIND SIGNAL STRENGTH FROM GRAPH, SUBTRACT TRANS.-LOSS FROM 61.44



--- SIGNAL STRENGTH VERSUS DISTANCE FOR GIVEN SYSTEM PARAMETERS ---

DISTANCE (KM)	SIG-STRENGTH (DBM)	DISTANCE (KM)	SIG-STRENGTH (DBM)	DISTANCE (KM)	SIG-STRENGTH (DBM)	DISTANCE (KM)	SIG-STRENGTH (DBM)	DISTANCE (KM)	SIG-STRENGTH (DBM)
0.3000	0.59	6.3000	-48.00	12.3000	-61.51	18.3000	-71.01	24.3000	-78.83
0.6000	-9.83	6.6000	-48.87	12.6000	-62.05	18.6000	-71.53	24.6000	-79.19
0.9000	-16.00	6.9000	-49.71	12.9000	-62.58	18.9000	-71.85	24.9000	-79.55
1.2000	-20.43	7.2000	-50.52	13.2000	-63.10	19.2000	-72.26	25.2000	-79.91
1.5000	-23.90	7.5000	-51.30	13.5000	-63.61	19.5000	-72.67	25.5000	-80.27
1.8000	-26.78	7.8000	-52.06	13.8000	-64.12	19.8000	-73.08	25.8000	-80.62
2.1000	-29.23	8.1000	-52.80	14.1000	-64.62	20.1000	-73.48	26.1000	-80.97
2.4000	-31.39	8.4000	-53.52	14.4000	-65.11	20.4000	-73.88	26.4000	-81.32
2.7000	-33.31	8.7000	-54.22	14.7000	-65.60	20.7000	-74.28	26.7000	-81.67
3.0000	-35.05	9.0000	-54.90	15.0000	-66.08	21.0000	-74.68	27.0000	-82.02
3.3000	-36.63	9.3000	-55.57	15.3000	-66.55	21.3000	-75.07	27.3000	-82.36
3.6000	-38.10	9.6000	-56.22	15.6000	-67.02	21.6000	-75.46	27.6000	-82.71
3.9000	-39.46	9.9000	-56.85	15.9000	-67.48	21.9000	-75.84	27.9000	-82.95
4.2000	-40.74	10.2000	-57.47	16.2000	-67.94	22.2000	-76.22	28.2000	-83.12
4.5000	-41.94	10.5000	-58.08	16.5000	-68.39	22.5000	-76.60	28.5000	-83.28
4.8000	-43.08	10.8000	-58.68	16.8000	-68.84	22.8000	-76.98	28.8000	-83.44
5.1000	-44.15	11.1000	-59.27	17.1000	-69.28	23.1000	-77.35	29.1000	-83.60
5.4000	-45.18	11.4000	-59.84	17.4000	-69.72	23.4000	-77.73	29.4000	-83.76
5.7000	-46.16	11.7000	-60.41	17.7000	-70.15	23.7000	-78.10	29.7000	-83.92
6.0000	-47.10	12.0000	-60.96	18.0000	-70.58	24.0000	-78.46	30.0000	-84.08

***** FOR A RECEIVER INPUT LEVEL OF -80.00 DBM, DISTANCE BETWEEN ANTENNAS CAN BE AT LEAST 25.20 KM *****

--- PROGRAM PARAMETERS ---

POLARIZATION (POL) -----VERTICAL
 FREQUENCY OF SIGNAL (F) ----- 60.00 MEG-HERTZ
 SURFACE CONDUCTIVITY (S) -----0.00500 MMHO/METER
 SURFACE REFRACTIVITY (NS) ----- 400.00 N-UNITS
 SUM OF ELEVATION ANGLES (YE) -----.00250 RADIANMS
 DISTANCE BETWEEN ANTENNAS (DIST) ----- 30.00 K-METERS
 ATTENUATION BELOW FREE SPACE (AE) ----- 0.0 DB
 INTERDECILE RANGE OF TERRAIN HEIGHT (DM) ----- 10.00 METERS
 SUM OF SMOOTH-EARTH HORIZON DISTANCES (DLS) ----- 30.21 K-METERS
 DIFFRACTION ATTENUATION AT DISTANCE DLS (ALS) ----- 51.97 DB
 PERMITTIVITY OR RELATIVE DIELECTRIC CONSTANT (E) ----- 15.00
 ESTIMATED SCATTER ATTENUATION BELOW FREE SPACE (AES) ----- 0.0 DB
 STRUCTURAL RECEIVER ANTENNA HEIGHT ABOVE GROUND (H2A) ----- 10.00 METERS
 STRUCTURAL TRANSMITTER ANTENNA HEIGHT ABOVE GROUND (H1G) ----- 10.00 METERS
 ESTIMATED DIFFRACTION ATTENUATION BELOW FREE SPACE (AEO) ----- 45.18 DB
 COEFFICIENT THAT DEFINES SLOPE OF A SMOOTH CURVE OF ACR (K1) -----0.54765 DB/KM
 COEFFICIENT THAT DEFINES SLOPE OF A SMOOTH CURVE OF ACR (K2) -----16.134013 DB/KM
 SLOPE OF THE CURVE OF SCATTER ATTENUATION AS VERSUS DISTANCE (MS) -----0.0 DB/KM
 DISTANCE WHERE DIFFRACTION AND SCATTER ATTENUATIONS ARE EQUAL (DX) ----- 0.0 K-METERS
 ATTENUATION WHERE DIFFRACTION AND SCATTER ATTENUATION ARE EQUAL (ADX) ----- 0.0 DB
 SLOPE OF THE CURVE OF DIFFRACTION ATTENUATION AS VERSUS DISTANCE (MD) -----0.21145 DB/KM

--- SIGNAL STRENGTH DATA INPUT ---

TRANSMITTER POWER OUT ----- 35.00 WATTS
 TRANSMITTER TRANSMISSION LINE LOSS ----- 2.00 DB
 TRANSMITTER ANTENNA GAIN ----- 10.00 DB
 RECEIVER SENSITIVITY ----- -80.00 DBM
 RECEIVER TRANSMISSION LINE LOSS ----- 2.00 DB
 RECEIVER ANTENNA GAIN ----- 10.00 DB

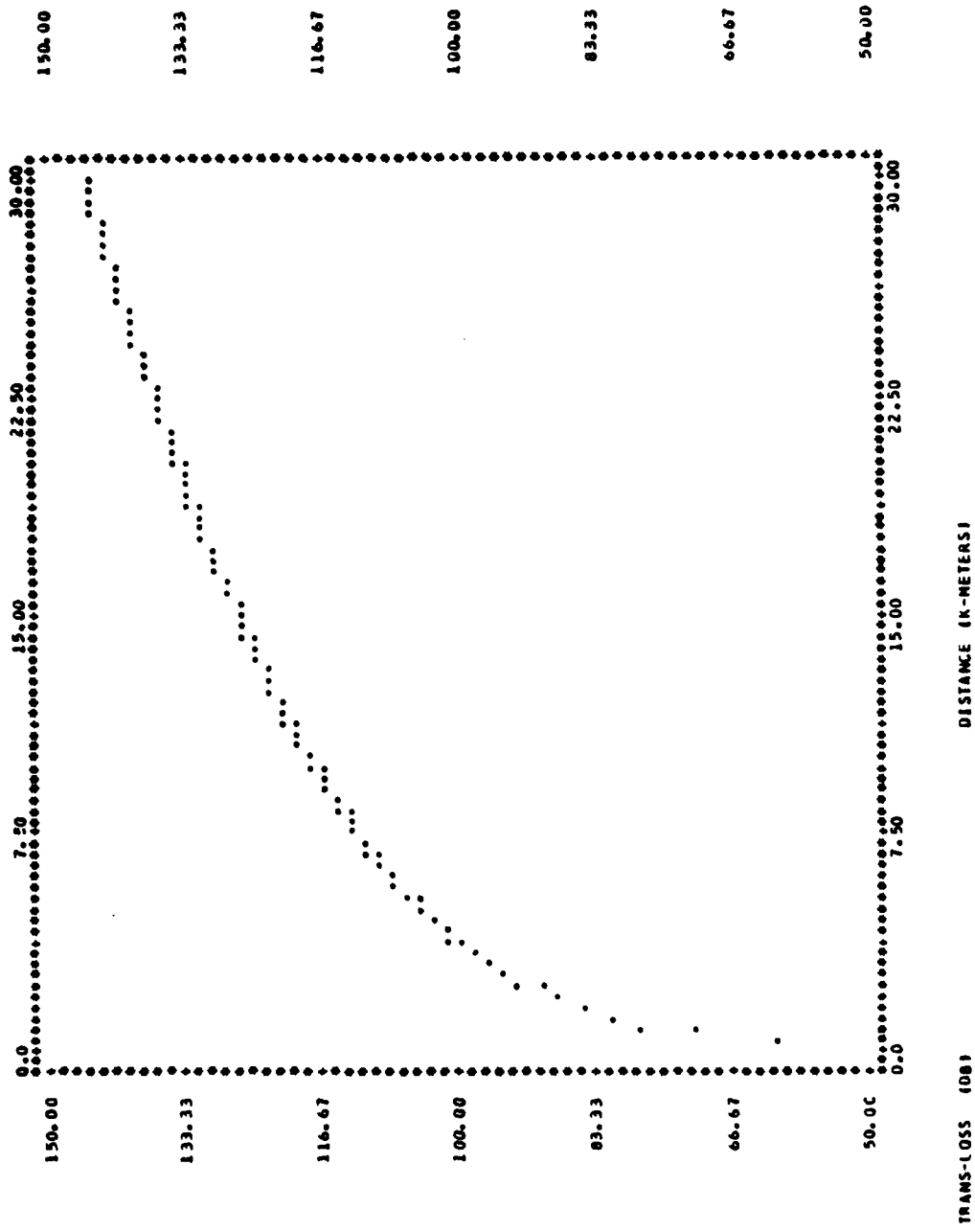
--- USER TERRAIN DATA ---

FREQUENCY OF SIGNAL -F- (MEG-HERTZ) 40.00000

DISTANCE TRANS-LOSS (KM)	DISTANCE TRANS-LOSS (DB)	DISTANCE TRANS-LOSS (KM)	DISTANCE TRANS-LOSS (DB)	DISTANCE TRANS-LOSS (KM)	DISTANCE TRANS-LOSS (DB)	DISTANCE TRANS-LOSS (KM)	DISTANCE TRANS-LOSS (DB)
0.3000	60.91	6.3000	129.33	12.3000	122.54	18.3000	131.71
0.6000	71.35	6.6000	110.19	12.6000	123.06	18.6000	132.12
0.9000	77.53	6.9000	111.01	12.9000	123.57	18.9000	132.52
1.2000	81.96	7.2000	111.80	13.2000	124.07	19.2000	132.92
1.5000	85.63	7.5000	112.57	13.5000	124.57	19.5000	133.31
1.8000	88.30	7.8000	113.32	13.8000	125.06	19.8000	133.70
2.1000	90.74	8.1000	114.04	14.1000	125.55	20.1000	134.09
2.4000	92.89	8.4000	114.75	14.4000	126.02	20.4000	134.47
2.7000	94.80	8.7000	115.43	14.7000	126.49	20.7000	134.85
3.0000	96.53	9.0000	116.10	15.0000	126.96	21.0000	135.23
3.3000	98.10	9.3000	116.75	15.3000	127.41	21.3000	135.60
3.6000	99.56	9.6000	117.38	15.6000	127.87	21.6000	135.98
3.9000	100.91	9.9000	118.00	15.9000	128.31	21.9000	136.34
4.2000	102.17	10.2000	118.61	16.2000	128.75	22.2000	136.71
4.5000	103.36	10.5000	119.20	16.5000	129.19	22.5000	137.07
4.8000	104.48	10.8000	119.79	16.8000	129.62	22.8000	137.43
5.1000	105.54	11.1000	120.36	17.1000	130.05	23.1000	137.79
5.4000	106.55	11.4000	120.92	17.4000	130.47	23.4000	138.15
5.7000	107.52	11.7000	121.47	17.7000	130.89	23.7000	138.50
6.0000	108.44	12.0000	122.00	18.0000	131.30	24.0000	138.85
6.3000	109.20					24.3000	139.20
6.6000	109.85					24.6000	139.55
6.9000	110.49					24.9000	139.89
7.2000	111.01					25.2000	140.23
7.5000	111.57					25.5000	140.57
7.8000	112.13					25.8000	140.91
8.1000	112.64					26.1000	141.25
8.4000	113.12					26.4000	141.58
8.7000	113.57					26.7000	141.91
9.0000	114.00					27.0000	142.24
9.3000	114.40					27.3000	142.57
9.6000	114.78					27.6000	142.90
9.9000	115.14					27.9000	143.22
10.2000	115.48					28.2000	143.54
10.5000	115.80					28.5000	143.86
10.8000	116.10					28.8000	144.18
11.1000	116.38					29.1000	144.50
11.4000	116.64					29.4000	144.82
11.7000	116.88					29.7000	145.13
12.0000	117.10					30.0000	145.45

PLOT OF TRANS.-LOSS VERSUS DISTANCE

• NOTE •• TO FIND SIGNAL STRENGTH FROM GRAPH, SUBTRACT TRANS.-LOSS FROM 63.44



--- SIGNAL STRENGTH VERSUS DISTANCE FOR GIVEN SYSTEM PARAMETERS ---

DISTANCE (KM)	SIG-STRENGTH (DBM)	DISTANCE (KM)	SIG-STRENGTH (DBM)	DISTANCE (KM)	SIG-STRENGTH (DBM)	DISTANCE (KM)	SIG-STRENGTH (DBM)	DISTANCE (KM)	SIG-STRENGTH (DBM)
0.3000	0.53	6.3000	-47.89	12.3000	-61.09	18.3000	-70.27	24.3000	-77.76
0.6000	-9.91	6.6000	-48.74	12.6000	-61.62	18.6000	-70.68	24.6000	-78.11
0.9000	-16.09	6.9000	-49.57	12.9000	-62.13	18.9000	-71.08	24.9000	-78.45
1.2000	-23.52	7.2000	-50.36	13.2000	-62.63	19.2000	-71.47	25.2000	-78.79
1.5000	-23.99	7.5000	-51.13	13.5000	-63.13	19.5000	-71.87	25.5000	-79.13
1.8000	-26.85	7.8000	-51.88	13.8000	-63.62	19.8000	-72.26	25.8000	-79.47
2.1000	-29.30	8.1000	-52.60	14.1000	-64.10	20.1000	-72.65	26.1000	-79.80
2.4000	-31.45	8.4000	-53.31	14.4000	-64.58	20.4000	-73.03	26.4000	-80.14
2.7000	-33.36	8.7000	-53.99	14.7000	-65.05	20.7000	-73.41	26.7000	-80.47
3.0000	-35.08	9.0000	-54.66	15.0000	-65.52	21.0000	-73.79	27.0000	-80.80
3.3000	-36.66	9.3000	-55.31	15.3000	-65.97	21.3000	-74.16	27.3000	-81.13
3.6000	-38.12	9.6000	-55.94	15.6000	-66.43	21.6000	-74.54	27.6000	-81.45
3.9000	-39.47	9.9000	-56.56	15.9000	-66.87	21.9000	-74.90	27.9000	-81.78
4.2000	-40.73	10.2000	-57.17	16.2000	-67.31	22.2000	-75.27	28.2000	-82.10
4.5000	-41.92	10.5000	-57.76	16.5000	-67.75	22.5000	-75.63	28.5000	-82.42
4.8000	-43.04	10.8000	-58.35	16.8000	-68.18	22.8000	-75.99	28.8000	-82.74
5.1000	-44.10	11.1000	-58.92	17.1000	-68.61	23.1000	-76.35	29.1000	-83.06
5.4000	-45.11	11.4000	-59.48	17.4000	-69.03	23.4000	-76.71	29.4000	-83.38
5.7000	-46.08	11.7000	-60.02	17.7000	-69.45	23.7000	-77.06	29.7000	-83.69
6.0000	-47.00	12.0000	-60.56	18.0000	-69.86	24.0000	-77.41	30.0000	-84.01

***** FOR A RECEIVER INPUT LEVEL OF -80.00 DBM, DISTANCE BETWEEN ANTENNAS CAN BE AT LEAST 26.10 KM *****

APPENDIX C

COMPUTER SIMULATION 2 LISTING AND OUTPUT

This Appendix contains the program and output for Simulation 2. The output consists of Tables which are referenced by number in the main text of the thesis. At the top of each data Table, is an explanation of the parameters used in the run. Each Table represents one run of the program.

THIS PROGRAM WAS WRITTEN BY TOM HOUSER AND TED MOURAS AT THE
 NAVAL POSTGRADUATE SCHOOL IN MAY 1983. ITS PURPOSE IS TO
 SIMULATE AN AIRBORNE SEARCH IN FINDING SYSTEM IN ORDER TO
 EVALUATE SOURCES OF FIX ERROR. THE PROGRAM INTRODUCES
 ERRORS IN LCB ACCURACY RESULTING FROM REFRACTIVE AND
 INHERENT SYSTEM INACCURACIES OR ERRORS RESULTING FROM ERRONEOUS
 PLAYFORM LOCATION REPORTING. IT USES A TWO BEARING CROSS GEO-
 METRY TO PRODUCE FIXES. AN AIRCRAFT IS FLOWN ON A 200 KILOMETER
 BASELINE SIMULATING A CORPS FRONT.

NOTE: SOME OF THE EXECUTABLE STATEMENTS IN THE PROGRAM
 WHICH DEAL WITH GRAPHICAL OUTPUT OR STATISTICAL OUTPUT
 HAVE "COMMENT" SYMBOLS IN FRONT OF THEM TO REDUCE THE
 AMOUNT OF OUTPUT DURING VARIOUS DATA RUNS. THESE CAN BE
 REMOVED TO FIT THE NEEDS OF THE INDIVIDUAL USER.

DOUBLE PRECISION DSEED1 XC, XD, ACTX, REPX, RAND1, RAND2
 REAL*8 YA, YB, YC, YD, XA, XB, XE, XG, XH, XI, XJ, XK, XL, XM, XN, XO, XP, XQ, XR, XS, XT, XU, XV, XW, XZ, YL, YM, YN, YO, YP, YQ, YR, YS, YT, YU, YV, YW, YZ, ZL, ZM, ZN, ZO, ZP, ZQ, ZR, ZS, ZT, ZU, ZV, ZW, ZY, ZZ, A, B, C, D, DD, COUNTA, COUNTB, COUNTC, COUNTD
 REAL*8 DRIFT, ERR, MAXERR, SELECT, ANGA, XA1, XB1, XC1, XD1
 REAL*8 ANGB, ANGC, ANG, LOBA1(40,3), LOBA2(40,3), LOBB1(40,3)
 REAL*8 LUBB2(40,3), LOBC1(40,3), LOBC2(40,3), LOBD1(40,3), LOBD2(40,3)
 REAL*8 TEMP1, TEMP2, HUM1, HUM2, PRESS1, PRESS2, DNDZ, GRAD
 REAL*8 ANGLE1, RANG, SIDE1, SIDE2, SIDE3, SIDE4, SIDE5, SIDE7
 REAL*8 SFLAG1, SFLAG2, SFLAG3, SFLAG4, SFLAG5, SFLAG6, SFLAG7, MSKEEP
 INTEGER A, AA, B, BB, B8B, C, CC, D, DD, COUNTA, COUNTB, COUNTC, COUNTD

EXPLANATION OF FLAGS:
 FLAG1 - FILE LOB'S ARE PLACED INTO FOR LATER
 CORRELATION. DOES NOT HAVE TO BE SET (AUTOMATIC).
 FLAG2 - CONTROLS WHETHER ERROR IS INTRODUCED IN THE LOB OR NOT.
 MUST BE SET. ONE IS "ON".
 FLAG3 - CONTROLS WHETHER RANDOM NAV ERROR IS INTRODUCED. MUST
 BE SET. ONE IS "ON".
 FLAG4 - CONTROLS WHETHER DRIFT NAV ERROR IS INTRODUCED. MUST BE
 SET. ONE IS "ON".
 FLAG5 - CONTROLS TURNING THE AIRCRAFT (REVERSE TRACK). AUTOMATIC.
 FLAG6 - CONTROLS WHETHER DRIFT ERROR IS ADDED OR SUBTRACTED FROM
 TRUE POSITION. ONE IS ADD. ZERO IS SUBTRACT.
 FLAG7 - ALL CWS FOR NAVIGATION UPDATE AT END OF TRACK. MUST BE
 SET. ONE IS "ON".
 NOTE: FLAGS THREE AND FOUR CANNOT BE SET TO "ON" SIMULTANEOUSLY
 OR WARNING WILL APPEAR.

DATA FLAG2/1/, FLAG3/0/, FLAG4/0/, FLAG6/0/, FLAG7/0/

CCCCCCCCCCCCCCCC

CCCCCCCCCCCCCCCC C

C
C
MAXERR=2.0
DRIFTX=.005

SWEEP=0
COUNTA=0
COUNTB=0
COUNTC=0
COUNTD=0
A=0
AA=0
BB=0
BBB=0
C=0
CC=0
D=0
DD=0

C
DSEED1=12315.7

C
C
C
C
FOUR EMITTERS ARE USED: A, B, C, D WITH THE FOLLOWING VARIABLES
REPRESENTING THE X AND Y COORDINATES OF THESE EMITTERS.

YA=100.00
YB=70.0
YC=250.0
YD=100.0

C
XA=80.0
XB=120.0
XC=150.0
XD=80.0

C
C
C
C
THE TOTAL OF THE FOLLOWING THREE VARIABLES MUST EQUAL THE Y
DISTANCE TO THE EMITTER.

GRAD=30.0
SIDE7=45.0

C
C
C
MET DATA FOLLOWS. SEE TEXT FOR EXPLANATION.

TEMP1=90.0
TEMP2=70.0
HUM1=.80
HUM2=.20
PRESS1=1013
PRESS2=1013

```

C      CALL METRO(TEMP1,TEMP2,HUM1,HUM2,PRESS1,PRESS2,DNDZ,G3AD)
C      WRITE(6,550) DNDZ
550    FORMAT(I1,////,9X,DNDX=-,F7.3,///)
C      THE FOLLOWING VARIES THE PLACE ON THE BASELINE WHERE THE FIRST
C      LOB IS TAKEN.
C      ACTX=(GGUBFS(DSEED1)*3.0)
C      REPX=ACTX
C      THE FOLLOWING LOOP CONTROLS THE NUMBER OF TIMES THE AIRCRAFT
C      MAKES A ROUND TRIP OF THE CORPS FRONT.
C      DO 5 M=1,2
C        FLAG5=0
C      THE FLAG CONTROLS THE FILE THAT THE LOB'S ARE PLACED INTO
C      FOR LATER CORRELATION (SEE EXPLANATORY TEXT).
C      CONTINUE
C      THE VARIABLE ACTX IS THE AIRCRAFT POSITION ON THE BASELINE. THE
C      CHANGE OF 1.5433333 REPRESENTS AN AIRCRAFT SPEED OF 200 KTS.
C      ACTX=ACTX+1.5433333
C      THE FOLLOWING STEP CHECKS TO SEE IF THE FLIGHT ACROSS THE
C      CORPS FRONT IS COMPLETE.
C      IF (ACTX.LT.200.0) GO TO 30
C      CALL CORL8(LOB1,LOB2,LOB3,LOB4,LOB5,LOB6,LOB7,LOB8,LOB9,LOB10,LOB11,LOB12,
C      A,AA,BB,BB8,C,CC,D,DD,COUNTA,COUNTB,COUNTC,COUNTD,YA,XA,YB,
C      XB,YC,XC,YD,XD,MAXERR,SWEEP)
C      FLAG5=1
C      GO TO 56
C      FOLLOWING INSURES THAT BOTH TYPES OF NAV ERROR CANNOT BE
C      INADVERTENTLY INTRODUCED AT THE SAME TIME.
C      CONTINUE
C      IF (FLAG3.EQ.1.AND.FLAG4.EQ.1) WRITE(6,100)
C      THE FOLLOWING STEP, IF THE FLAG IS SET, INTRODUCES RANDOM
C      ERROR IN THE POSITION REPORTED BY THE NAVIGATION SYSTEM.
C      IF (FLAG3.EQ.0) GO TO 91
C      RAND1=GGUBFS(DSEED1)

```



```

RAND2=GGUBFS(DSEED1)
IF (RAND1.GT.0.5) GO TO 90
  REPX=ACTX+RAND2
  GO TO 66
CONTINUE
REPX=ACTX-RAND2
GO TO 66
CONTINUE

```

90
91

C
C
C

THE FOLLOWING STEP IF THE FLAG IS SET, INTRODUCES A DRIFT
ERROR IN THE POSITION REPORTED BY THE NAVIGATION SYSTEM.

```

IF (FLAG4.EQ.0) GO TO 93
IF (FLAG6.EQ.0) GO TO 92
  REPX=REPX+1.5433333+DRIFTX
  GO TO 66
CONTINUE

```

92
93
66

C
C
C
C
C

```

CONTINUE
REPX=REPX+1.5433333-DRIFTX
GO TO 66
CONTINUE
REPX=ACTX
CONTINUE

```

FLAG1=0

FOLLOWING FLAG CONTROLS WHETHER ERROR IN THE LOB IS INTRODUCED
OR NOT. THE "IF" STATEMENT CONTROLS WHETHER THE ERROR IS ADDED
OR SUBTRACTED FROM THE LOB. IT USES A UNIFORM DISTRIBUTION.

```

ERROR=0.0
IF (FLAG2.EQ.0) GO TO 11
  ERROR=(GGUBFS(DSEED1))
  IF (ERROR.GT.0.5) GO TO 12
  IF (ERROR=MAXERR)
    GO TO 11
CONTINUE
ERROR=MAXERR*(-1.0)
CONTINUE

```

12
11

C
C
C
C
C

THE FOLLOWING "IF" STATEMENTS SELECT THE EMITTER THAT THE LOB
WILL BE TAKEN ON. IT USES A UNIFORM DISTRIBUTION AND ASSUMES
THAT ALL EMITTERS CAN BE RECEIVED FOR OF PURPOSES. THE OTHER IF
STATEMENT IS PERTINENT TO THE GEOMETRY (SEE TEXT).

```

SELECT=(GGUBFS(DSEED1))*10.0)
IF (SELECT.GT.2.5) GO TO 13
  SIDE5=YA-(SIDE7+GRAD)
  IF (ACTX.GT.XA) GO TO 14

```

```

A=A+1
XA1=XA-ACIX
ANGA=(DATAN(YA/XA1))

CALCULATION OF THE RADIUS OF CURVATURE
RADIUS=(1/(DNDZ*(DCOS(ANGA))))*1000000.0

ANG1=(3.14159265/2.0)-ANGA
SIDE1=RADIUS*DSIN(ANG1)
SIDE2=DSQRT((RADIUS**2)-(SIDE1**2))
SIDE3=DABS(SIDE1-GRAD)
SIDE4=DSQRT((RADIUS**2)-(SIDE3**2))
SIDE5=SIDE2-SIDE4
SIDE6=XA-((SIDE5*DSIN(ANG1))/DSIN(ANGA))
ANGA=DARCOS(SIDE4/RADIUS)
SIDE8=SIDE7*DTAN(ANGA)
GO TO 990
IF (SIDE1.LE.GRAD) GO TO 990
SIDE6=SIDE6-SIDE8
ANG=(3.14159265/2.0)-ANGA
ANG=(180.0*ANG)/3.14159265
CALL STORA(ANG,SIDE6,LOBAL,LOB2,FLAG1,A,AA)
GO TO 56
CONTINUE
SIDE6=SIDE6+SIDE8
ANG=(3.14159265/2.0)-ANGA
ANG=(180.0*ANG)/3.14159265
FLAG1=1
CALL STORA(ANG,SIDE6,LOBAL,LOB2,FLAG1,A,AA)
GO TO 56
CONTINUE
AA=AA+1
XA1=ACIX-XA
ANGA=(DATAN(YA/XA1))

```

CC C

990

14

CC C

```

SIDE8=SIDE7*DTAN(ANGA)
IF (SIDE1.LE.GRAD) GO TO 991
SIDE6=SIDE6+SIDE8
ANG=(13.14159265/2.0)-ANGA
FLAG1=(180.0*ANG)/3.14159265
CALL STORA(ANG,SIDE6,LOBA1,LOBA2,FLAG1,A,AA)
GO TO 56
991 CONTINUE
SIDE6=SIDE6-SIDE8
ANG=(13.14159265/2.0)-ANGA
ANG=(180.0*ANG)/3.14159265
CALL STORA(ANG,SIDE6,LOBA1,LOBA2,FLAG1,A,AA)
GO TO 56
C 13 CONTINUE
IF (SELECT.GT.5.0) GO TO 16
SIDE5=YB-(SIDE7+GRAD)
IF (ACTX.GT.XB) GO TO 17
BB=BB+1
XB1=XB-AC TX
ANGB=(DATAN(YB/XB1))
C 13 CONTINUE
CALCULATION OF THE RADIUS OF CURVATURE
RADIUS=(1/(DNDZ*(DCOS(ANGB))))*1000000.0
C
ANG1=(3.14159265/2.0)-ANGB
SIDE1=RADIUS*DSIN(ANG1)
SIDE2=DSQRT((RADIUS**2)-(SIDE1**2))
SIDE3=DSQRT((RADIUS**2)-(SIDE3**2))
SIDE4=DSQRT((RADIUS**2)-(SIDE3**2))
SIDE5=XB-(SIDE4
SIDE6=SIDE6+DIFF
ANGB=DARCO5(SIDE4/RADIUS)
SIDE8=SIDE7*DTAN(ANGB)
IF (SIDE1.LE.GRAD) GO TO 890
SIDE6=SIDE6-SIDE8
ANG=(13.14159265/2.0)-ANGB
ANG=(180.0*ANG)/3.14159265
CALL STORB(ANG,SIDE6,LOBB1,LOBB2,FLAG1,BB,888)
GO TO 56
C 890 CONTINUE
SIDE6=SIDE6+SIDE8
ANG=(13.14159265/2.0)-ANGB
ANG=(180.0*ANG)/3.14159265
FLAG1=1

```

```

17      CALL STOR B(ANG,SIDE6,LOBB1,LOBB2,FLAG1,BB,BBB)
        GO TO 56
        CONTINUE
        BBF=BBB+1
        XBI=ACTX-XB
        ANGB=(DATAN(YB/XB1))

        CALCULATION OF THE RADIUS OF CURVATURE
        RADIUS=(1/(DNDZ*(DCOS(ANGB))))*1000000.0
        ANGL=(3.14159265/2.0)-ANGB
        SIDE1=RADIUS*DSIN(ANG1)
        SIDE2=DSQRT((RADIUS**2)-(SIDE1**2))
        SIDE3=DA8S(SIDE1-GRAD)
        SIDE4=DSQRT((RADIUS**2)-(SIDE3**2))
        DIFF=SIDE4-SIDE2
        SIDE6=XB+((SIDE5*DSIN(ANG1))/DSIN(ANGB))
        SIDE6=SIDE6+DIFF
        ANGB=DARCOS(SIDE4/RADIUS)
        SIDE8=SIDE7*DTAN(ANGB)
        IF (SIDE6=LE.GRAD) GO TO 891
        SIDE6=SIDE6+SIDE8
        ANGL=(3.14159265/2.0)-ANGB
        ANGB=(180.0*ANG)/3.14159265
        FLAG1=1
        CALL STOR B(ANG,SIDE6,LOBB1,LOBB2,FLAG1,BB,BBB)
        GO TO 56
        CONTINUE

891     CONTINUE
        SIDE6=SIDE6-SIDE8
        ANGL=(3.14159265/2.0)-ANGB
        ANGB=(180.0*ANG)/3.14159265
        CALL STOR B(ANG,SIDE6,LOBB1,LOBB2,FLAG1,BB,BBB)
        GO TO 56

16     CONTINUE
        IF (SELECT.GT.7.5) GO TO 19
        SIDE5=YC-(SIDE7+GRAD)
        IF (ACTX.GT.XC) GO TO 20
        C=C+1
        XCI=XC-ACTX
        ANGC=(DATAN(YC/XCI))

        CALCULATION OF THE RADIUS OF CURVATURE
        RADIUS=(1/(DNDZ*(DCOS(ANGC))))*1000000.0
        ANGL=(3.14159265/2.0)-ANGC
        SIDE1=RADIUS*DSIN(ANG1)

```

C
C
C

891

C
16

C
C
C
C

```

SIDE2=DSQRT((RADIUS**2)-(SIDE1**2))
SIDE3=DABS(SIDE1-GRAD)
SIDE4=DSQRT((RADIUS**2)-(SIDE3**2))
DIFF=SIDE2-SIDE4
SIDE6=XC-((SIDE5*DSIN(ANG1))/DSIN(ANGC))
ANGC=DARCOS(SIDE4/RADIUS)
SIDE8=SIDE7*DTAN(ANGC)
IF(SIDE1.LE.GRAD)GO TO 790
SIDE6=SIDE6-SIDE8
ANG=(3.14159265/2.0)-ANGC
ANG=(180.0*ANG)/3.14159265
CALL STORC(ANG,SIDE6,LOBCL,LOBC2,FLAG1,C,CC)
GO TO 56

```

790

```

CONTINUE
SIDE6=SIDE6+SIDE8
ANG=(3.14159265/2.0)-ANGC
ANG=(180.0*ANG)/3.14159265
FLAG1=1
CALL STORC(ANG,SIDE6,LOBCL,LOBC2,FLAG1,C,CC)
GO TO 56

```

20

```

CONTINUE
CC=CC+1
XC1=ACTX-XC
ANGC=(DATAN(YC/XC1))

```

279

CCC

CALCULATION OF THE RADIUS OF CURVATURE

```

RADIUS=(1/(DNDZ*(DCOS(ANGC))))*1000000.0
ANG1=(3.14159265/2.0)-ANGC
SIDE1=RADIUS*DSIN(ANG1)
SIDE2=DSQRT((RADIUS**2)-(SIDE1**2))
SIDE3=DABS(SIDE1-GRAD)
SIDE4=DSQRT((RADIUS**2)-(SIDE3**2))
DIFF=SIDE2-SIDE4
SIDE6=XC+((SIDE5*DSIN(ANG1))/DSIN(ANGC))
SIDE8=SIDE6+DIFF
SIDE6=DARCOS(SIDE4/RADIUS)
ANGC=SIDE7*DTAN(ANGC)
IF(SIDE1.LE.GRAD)GO TO 791
SIDE6=SIDE6-SIDE8
ANG=(3.14159265/2.0)-ANGC
ANG=(180.0*ANG)/3.14159265
FLAG1=1
CALL STORC(ANG,SIDE6,LOBCL,LOBC2,FLAG1,C,CC)
GO TO 56

```

791

```

CONTINUE
SIDE6=SIDE6+SIDE8

```

```

ANG=(3.14159265/2.0)-ANGC
ANG=(180.0*ANG)/3.14159265
CALL STORC(ANG,SIDE6,LOBC1,LOB2,FLAG1,C,CC)
GO TO 56
19 CONTINUE
C IF(ACTX,GT.XD) GO TO 22
D=C+1
XD1=XD-ACIX
ANGD=(DATAN(YD/XD1))
ANGD=(180.0/3.14159265)*ANGD)+ERROR
CALL STORD(ANGD,REPX,ACTX,LOBD1,LOBD2,FLAG1,D,DD)
GO TO 56
22 CONTINUE
DD=DD+1
XD1=ACTX-XD
ANGD=(DATAN(YD/XD1))
ANGD=(180.0/3.14159265)*ANGD)+ERROR
FLAG1=1
CALL STORD(ANGD,REPX,ACTX,LOBD1,LOBD2,FLAG1,D,DD)
C THE FOLLOWING STEP CONTINUES THE FLIGHT.
C
C 56 CONTINUE
IF(FLAG5.EQ.0) GO TO 55
C IF THE SWEEP IS COMPLETE, THE AIRCRAFT WILL RETURN THE OTHER
C DIRECTION.
C ACTX=ACTX-1.5433333
C NEXT STEP ALLOWS THE NAVIGATION SYSTEM TO RECEIVE AN
C UPDATE OF POSITION SUCH AS FROM ORTHOGONAL TACS.
C
C IF(.NOT.(FLAG7.EQ.1.AND.ACTX.GE.120.0)) GO TO 60
C REPX=ACTX
C CONTINUE
C THE FOLLOWING STEP, IF THE FLAG IS SET, INTRODUCES RANDOM
C ERROR IN THE POSITION REPORTED BY THE NAVIGATION SYSTEM.
C
C IF(FLAG3.EQ.0) GO TO 41
C RAND1=GGUBFS(DSEED1)
C RAND2=GGUBFS(DSEED1)
C IF(RAND1.GT.0.5) GO TO 40
C REPX=REPX-1.5433333+RAND2
C GO TO 67
C CONTINUE
C REPX=REPX-1.5433333-RAND2
C GO TO 67
C CONTINUE
40
41 CONTINUE

```

```

C
C
C
    THE FOLLOWING STEP IF THE FLAG IS SET, INTRODUCES A DRIFT
    ERROR IN THE POSITION REPORTED BY THE NAVIGATION SYSTEM.
    IF (FLAG4.EQ.0) GO TO 53
    IF (FLAG6.EQ.0) GO TO 52
    REPX=REPX-1.5433333+DRIFTX
    GO TO 67
52  CONTINUE=REPX-1.5433333-DRIFTX
    GO TO 67
53  CONTINUE
    REPX=ACTX
    CONTINUE
67  C
    IF (ACTX.GT.0.0) GO TO 66
    CALL CORL8 ( LOB1,LOB2,LOB1,LOB2,LOB1,LOB2,LOB1,LOB2,
    *      A,AA,EB,BB,C,CC,DD,COUNTA,COUNTB,COUNTC,COUNTD,
    *      YA,XA,YB,
    *      XB,YC,YD,XD,MAXERR,SWEEP)
    CONTINUE
5  C
C
C
    100 FORMAT('1, //, 5X, * WARNING-CHECK FLAGS, TWO TYPES OF ERROR SPECIFIC
    *D, //')
C
    CALL DONEPL
    STOP
    END
C
C
    FOLLOWING SUBROUTINE CALCULATES THE DNDZ VALUE USED IN THE
    CURVATURE EQUATIONS IN THE MAIN PROGRAM.
C
    SUBROUTINE METRO(TEMP1,TEMP2,HUM1,HUM2,PRESS1,PRESS2,DNDZ,GRAD)
C
    REAL*8 TEMP1,TEMP2,HUM1,HUM2,PRESS1,PRESS2,DNDZ,GRAD,CHANGE
    REAL*8 MR1,MR2,N1,N2
C
    CONVERT TEMPERATURES TO KELVIN
    TEMP1=(TEMP1+59.67)/1.8
    TEMP2=(TEMP2+59.67)/1.8
C
    CALCULATE THE MIXING RATIOS
    MR1=23.84-(2948.0/TEMP1)-(5.05*(DLOG10(TEMP1)))
    MR2=23.84-(2948.0/TEMP2)-(5.05*(DLOG10(TEMP2)))

```

```

C C C
MR1=.625*(1C.0**MR1)
MR2=.625*(1C.0**MR2)
CONVERT THE MIXING RATIOS TO VAPOR PRESSURE IN MILLIBARS
MR1=(PRESS1*(MR1/1000.0))/(.622+(MR1/1000.0))
MR2=(PRESS2*(MR2/1000.0))/(.622+(MR2/1000.0))
ALLCW FOR RELATIVE HUMIDITY
MR1=MR1*HUM1
MR2=MR2*HUM2
CALCULATE THE N VALUES
N1=((PRESS1/TEMP1)*77.6)+{(373000.0*(MR1/(TEMP1**2)))}
N2=((PRESS2/TEMP2)*77.6)+{(373000.0*(MR2/(TEMP2**2)))}
CALCULATE THE DNDZ VALUE
CHANGE=N1-N2
DNDZ=CHANGE/GRAD
DNDZ=100.0
RETURN
END
C C C C C C C C C C C
FOLLOWING SUBROUTINE STORES ALL LOBS AND RELATED AIRCRAFT
POSITIONS ON EMITTER A.
SUBROUTINE STORA(ANG,SIDE6,LOBA1,LOBA2,FLAG1,A,AA)
REAL*8 LOBA1(40,2),LOBA2(40,2),ANG,SIDE6
INTEGER A,AA,FLAG1
IF (FLAG1.EQ.1) GO TO 50
LOBA1(A,1)=ANG
LOBA1(A,2)=SIDE6
WRITE(6,104) ANG,SIDE6
MR1TE(1,2X,'A1',2X,'ANG=',F6.3,2X,'SIDE6=',F9.3)
C 104 FORMAT(1,2X,'A1',2X,'ANG=',F6.3,2X,'SIDE6=',F9.3)
GO TO 51
50 CONTINUE
LOBA2(AA,1)=ANG
LOBA2(AA,2)=SIDE6

```



```

C 105 WRITE(6,105) ANG,SIDE6
51 FORMAT(/,2X,A2,2X,A2,2X,ANG=,F6.3,2X,SIDE6=,F9.3)
RETURN
END

SUBROUTINE TO STORE LOBS AND POSITIONS FOR EMITTER B.
SUBROUTINE STORB (ANG,SIDE6,LOBB1,LOBB2,FLAG1,BB,BB)
REAL*8 LOBB1(40,2),LOBB2(40,2),ANG,SIDE6
INTEGER BB,BB,FLAG1

        IF (FLAG1.EQ.1) GO TO 60
        LOBB1(BB,1)=ANG
        LOBB1(BB,2)=SIDE6
        GO TO 61
CONTINUE
LOBB2(BBB,1)=ANG
LOBB2(BBB,2)=SIDE6
CONTINUE
RETURN
END

SUBROUTINE TO STORE LOBS AND POSITIONS FOR EMITTER C.
SUBROUTINE STORC (ANG,SIDE6,LOBC1,LOBC2,FLAG1,C,CC)
REAL*8 LOBC1(40,2),LOBC2(40,2),ANG,SIDE6
INTEGER C,CC,FLAG1

        IF (FLAG1.EQ.1) GO TO 70
        LOBC1(C,1)=ANG
        LOBC1(C,2)=SIDE6
        GO TO 71
CONTINUE
LOBC2(CC,1)=ANG
LOBC2(CC,2)=SIDE6
CONTINUE
RETURN

```

```

C C C C C
C
C C C
80
81
C C C C C C
C
C

END
SUBROUTINE TO STORE LOBS AND POSITIONS FOR EMITTER D.
SUBROUTINE STORD (ANGD,REPX,ACTX,LOBD1,LOBD2,FLAG1,D,DU)
REAL*8 LOBD1(40,3),LOBD2(40,3),ANGD,REPX,ACTX
INTEGER D,DC,FLAG1

IF (FLAG1.EQ.1) GO TO 80
LOBD1(D,1)=ANGD
LOBD1(D,2)=REPX
LOBD1(D,3)=ACTX
GO TO 81
CONTINUE
LOBD2(DC,1)=ANGD
LOBD2(DC,2)=REPX
LOBD2(DC,3)=ACTX
CONTINUE
RETURN
END

C C C C C C
C
C

FOLLOWING SUBROUTINE CORRELATES THE LOBS AT THE END OF EACH PASS
OF THE CORPS AREA AND REPORTS EMITTER FIXES.

SUBROUTINE CORL8 (LOB1,LOB2,LOB3,LOB4,LOB5,LOB6,LOB7,LOB8,LOB9,LOB10,LOB11,LOB12,
*AZ,AA,BB,BBB,CCCC,DDDD,COUNTA,COUNTB,COUNTC,COUNTD,YA,XA,YB,XB,YC,
*XC,YD,XO,MAXERR,SWEEP)
REAL*8 SUMA,SUMB,SUMC,SUMD,APEXA,APEXB,APEXC,APEXD
REAL*8 LOBA1(40,3),LOB2(40,3),LOB3(40,3),LOB4(40,3),LOB5(40,3),LOB6(40,3),LOB7(40,3),LOB8(40,3)
REAL*8 ALINEB,ALINEC,BLINEC,CLINEC,CLINEB,LINEB,LINEC,LINEB
REAL*8 FIXAX,AX,FIXAXY,TFIXAX,TFIXAY,AVGY,AVGX,AVGERR,FIXBX,FBX
REAL*8 FIXBY,TFIXBY,TFIXBYX,TFIXBYX,TFIXBYX,TFIXBYX,TFIXBYX,TFIXBYX
REAL*8 FIXDX,DX,TFIXDX,TFIXDX,TFIXDX,TFIXDX,TFIXDX,TFIXDX,TFIXDX
REAL*8 YD,XC,MAXERR,YRAYB(800),YRAYC(800),YRAYA(800)
REAL*8 XRAYB(800),YRAYD(800),XRAYA(800),YRAYA(800)
REAL*8 A,B,C,D,AA,BB,BBB,CCCC,DD,COUNTA,COUNTB,COUNTC,COUNTD,I,K
INTEGER J,N,T,U,V,W,SWEEP,L,LA

SWEEP = SWEEP + 1

```

```

TFIXAY=0
TFIXAX=0
TFIXBY=0
TFIXBX=0
TFIXCY=0
TFIXCX=0
TFIXDY=0
TFIXDX=0
XRAYA(1)=XA
XRAYA(2)=YA
XRAYB(1)=XB
XRAYB(2)=YB
XRAYC(1)=XC
XRAYC(2)=YC
XRAYD(1)=XD
XRAYD(2)=YD
L=0
LA=0

```

C

```

DO 55 T=1,A
56 U=1,BA1(T,1)+LOB2(U,1)
SUMA=LOBA1(T,1)+LOB2(U,1)+LOB2(U,1)
IF(SUMA.GT.95.0.OR.SUMA.LT.85.0) GO TO 70
APEXA=180.0-SUMA
ALINEC=(3.14159265/180.0)*APEXA
LOB2=(3.14159265/180.0)*LOB2(U,1)
LOB1=(3.14159265/180.0)*LOB2(U,1)
ALINEB=(ALINEC+DSIN(LOB2))/DSIN(APEXA)
FIXAY=(ALINEB*(DCOS(LOB1)))
AX=ALINEB*(DCOS(LOB1))
FIXAX=LOB2(U,1)+AX
COUNTA=COUNTA+1
XRAYA(COUNTA+1)=FIXAX
XRAYA(COUNTA+1)=FIXAY
WRITE(6,106) FIXAX,FIXAY
C 106 FORMAT(/,2X,FIXAX=,F8.3,/,

```

C

```

CONTINUE
CONTINUE
CONTINUE
IF(.NOT.(COUNTA.EQ.0)) GO TO 93
WRITE(6,200)
GO TO 89
CONTINUE
IF(.NOT.(SWEEP.EQ.2)) GO TO 88

```

C

```

C 88 IF (.NOT. (COUNTA.GE.1)) GO TO 88
      CALL PICHA(XRAYA,YRAYA,COUNTA,MAXERR)
      CONTINUE
      XAY/COUNTA
      AVGX=FIXAX/COUNTA
      AVGERR=DSQRT(((AVGY-YA)**2)+((AVGX-XA)**2))
      PDSRAY(1)=YA
      AVGRAY(1)=AVGERR
      WRITE(6,101) AVGY,AVGX,AVGERR
      COUNTA=2
      XRAYA(2)=AVGX
      YRAYA(2)=AVGY
      IF (.NOT. (SWEEP.EQ.2)) GO TO 89
      CALL PICHA (XRAYA,YRAYA,COUNTA,MAXERR)
      CONTINUE
C 89
C
C
      DO 65 V=1,88
      DO 66 W=1,888
      SUMB=LOBB1(V,1)+LOBB2(W,1)
      IF (SUMB.GT.95.0.OR.SUMB.LT.85.0) GO TO 80
      APEXB=(3.14159265/180.0)*APEXB
      BLINEC=LOBB2(W,2)-LOBB1(V,2)
      LOBE2=(3.14159265/180.0)*LOBB2(W,1)
      LOB1=(3.14159265/180.0)*LOBB1(V,1)
      BLINEB=(BLINEC+DSIN(LOB2))/DSIN(APEXB)
      FIXBY=(BLINEB*(DCOS(LOB1))
      FIXBX=LOBB1(V,2)+BX
      COUNTB=COUNTB+1
      XRAYB(COUNTB+1)=FIXBX
      YRAYB(COUNTB+1)=FIXBY
      WRITE(6,206) FIXBX,FIXBY
      WRITC(6,206) FIXBX,FIXBY
      IF (FIXBX=,F8.3,2X, FIXBY=,F8.3,/)
      CONTINUE
      CONTINUE
C 206 FORMAT(,2X, FIXBX=FIXBX+TFIXBX
      CONTINUE
      CONTINUE
      CONTINUE
      IF (.NOT. (COUNTB.EQ.0)) GO TO 78
      WRITE(6,201)
      GO TO 79
      CONTINUE
      GO TO 79
C 78
C
C
      IF (.NOT. (SWEEP.EQ.2)) GO TO 33
      IF (.NOT. (COUNTB.GE.1)) GO TO 33
      CALL PICFB(XRAYB,YRAYB,COUNTB,MAXERR)

```

```

33 CONTINUE
   AVGY=FIXBY/COUNTB
   AVGX=FIXBX/COUNTB
   AVGERR=DSORT((AVGY-YB)**2)+((AVGX-XB)**2)
   POSGRAY(2)=AVGERR
   WRITE(6,111) AVGY,AVGX,AVGERR
   COUNTB=2
   XRAYB(2)=AVGX
   YRAYB(2)=AVGY
   IF(.NOT.(SWEET.EQ.2)) GO TO 79
   CALL PICHB (XRAYB,YRAYB,COUNTB,MAXERR)
   CONTINUE

C 79 CONTINUE
C
C
C
DO 75 K=1,C
  DO 76 I=1,C
    SUMC=LOBC1(K,1)+LOBC2(I,1)
    IF(SUMC.GT.100.0.OR.SUMC.LT.80.0) GO TO 90
    APEXC=180.0-SUMC
    APNEC={3.14159265/180.0}*APEXC
    LOB2={3.14159265/180.0}*LOBC2(I,1)
    LOB1={3.14159265/180.0}*LOBC1(K,1)
    CLINEB=(CLINEC*DSIN(LOB2))/DSIN(APEXC)
    FIXCY=(CLINEB*(DCOS(LOB1)))
    CX=CLINEB*(DCOS(LOB1))
    FIXCX=LOBC1(K,2)+CX
    COUNTC=COUNTC+1
    XRAYC(COUNTC+1)=FIXCX
    YRAYC(COUNTC+1)=FIXCY
    WRITE(6,207) FIXCX,FIXCY
    FORMAT(1,2X,FIXCY=,F8.3,/)
    CONTINUE
  CONTINUE
  CONTINUE
  IF(.NOT.(COUNTC.EQ.0)) GO TO 68
  WRITE(6,202)
  GO TO 69
68 CONTINUE
  IF(SWEET.GE.1) GO TO 32
  IF(.NOT.(CALL PICHC(XRAYC,YRAYC,COUNTC,MAXERR)
  CONTINUE
  AVGY=FIXCY/COUNTC

```

```

AVGX=FIXCX/COUNTC
AVGERR=DSQRT((AVGY-YC)**2)+((AVGX-XC)**2)
POSRAY(3)=YC
AVGRAY(3)=AVGERR
WRITE(6,121)AVGY,AVGX,AVGERR
COUNTC=2
XRAYC(2)=AVGX
YRAYC(2)=AVGY
IF(SWEEP.GT.1)GO TO 69
CALL PICHC (XRAYC,YRAYC,COUNTC,MAXERR)
CONTINUE

```

C 69
C
C

```

DO 25 J=1,D
26 N=1,DD
SUMD=LOBD1(J,1)+LOBD2(N,1)
IF(SUMD.GT.100.0)SUMD=LT.80.0)GO TO 30
APEXD=180.0-SUMD
APEXD=(3.14159265/180.0)*APEXD
LINEC=LOBD2(N,2)-LOBD1(J,2)
LOB2=(3.14159265/180.0)*LOBD1(J,1)
LOB1=(3.14159265/180.0)*LOBD1(J,1)
LINEB=(LINEC*DSIN(LOB2))/DSIN(APEXD)
YERROR=(LOBD1(J,2)-LOBD1(J,3))
FIXDY=(LINEB*(DSIN(LOB1)))+YERROR
DX=LINEB*(COS(LOB1))
FIXDX=LOBD1(J,2)+DX
COUNTD=COUNTD+1
XRAYD(COUNTD+1)=FIXDX
YRAYD(COUNTD+1)=FIXDY
WRITE(6,208)FIXDX,FIXDY
FORMAT(/,2X,FIXDY=FIXDY,2X,FIXDX=FIXDX,/)

```

C 208

```

30 CONTINUE
25 CONTINUE (COUNTD.EQ.0)GO TO 58
IF(.NOT.WRITE(6,203)
GO TO 55
CONTINUE
IF(.NOT.(SWEEP.EQ.2))GO TO 34
IF(.NOT.(COUNTD.GE.1))GO TO 34
IF(.CALL PICHD(XRAYD,YRAYD,COUNTD,MAXERR)
CONTINUE
AVGY=FIXDY/COUNTD
AVGX=FIXDX/COUNTD

```

C 34
C
C

AD-A134 827

EFFECTS OF ATMOSPHERIC REFRACTION ON US GROUND WARFARE
(U) NAVAL POSTGRADUATE SCHOOL MONTEREY CA
T P MOURAS ET AL. SEP 83

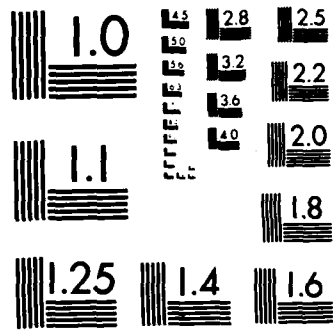
4/4

UNCLASSIFIED

F/G 28/14

NL





MICROCOPY RESOLUTION TEST CHART
NATIONAL BUREAU OF STANDARDS-1963-A


```

C 300  AVGERR=DSQR(((AVGY-YD)**2)+((AVGX-XD)**2))
C      POSRAY(4)=YI
C      AVGRAY(4)=AVGERR
C      WRITE(6,300) POSRAY(1),AVGRAY(1),AVGRAY(2),AVGRAY(3),AVG
C      *RAY(3),POSRAY(4),AVGRAY(4)
C      FORMAT(1,2X,F6.2,1X,F6.4,1X,F6.2,1X,F6.4,1X,F6.2,1X,F6.4,1X,F6.2
C      *1X,F6.4)
C      CALL GRAFIT (POSRAY,AVGERR)
C      WRITE(6,131) AVGY,AVGX,AVGERR
C      COUNTD=2
C      XRAYD(2)=AVGX
C      YRAYD(2)=AVGY
C      IF(.NOT.(SWEEEP.EQ.2)) GO TO 59
C      CALL PICHD (XRAYD,YRAYD,COUNTD,MAXERR)
C      CONTINUE
C 59    IF(.NOT.(SWEEEP.EQ.2.OR.SWEEEP.EQ.4.OR.SWEEEP.EQ.6.OR.SWEEEP.EQ.8)) GO
C      * TO 459
C      WRITE(6,141)
C 459  CONTINUE

```

```

C
A=0
AA=0
BB=0
BBB=0
C=0
CC=0
DD=0
T=0
U=0
V=0
W=0
TT=0
UU=0
VV=0
WW=0
COUNTA=0
COUNTB=0
COUNTC=0
COUNTD=0

```

```

C 101  FORMAT(/,9X,'EMITTER A AVERAGE ERROR',/9X,'AVERAGE Y=',F10.6,2X,
C      *,'AVERAGE X=',F10.6,2X,/9X,'AVERAGE MISSED DISTANCE=',F10.6,7//)
C 111  FORMAT(/,9X,'EMITTER B AVERAGE ERROR',/9X,'AVERAGE Y=',F10.6,2X,
C      *,'AVERAGE X=',F10.6,2X,/9X,'AVERAGE MISSED DISTANCE=',F10.6,7//)
C 121  FORMAT(/,9X,'EMITTER C AVERAGE ERROR',/9X,'AVERAGE Y=',F10.6,2X,

```



```

CALL MARKER (3)
CALL CURVE (XRAYA, YRAYA, COUNTA, -1)
CALL ENDPL (-1)
RETURN
END
FOLLOWING SUBROUTINE IS USED TO PLOT THE FIXES FOR EMITTER B.
SUBROUTINE PICH8 (XRAYB, YRAYB, COUNTB, MAXERR)
REAL*8 XRAYB(225), YRAYB(225), MAXERR
INTEGER COUNTB
CALL COMPRS
CALL NCBRDR
CALL PAGE (11, 8.5)

CALL AREA2D (6.5, 6.5)
CALL SWISSM

CALL XNAME ('X COORDINATE (KILOMETERS) $', 100)
CALL YNAME ('Y COORDINATE (KILOMETERS) $', 100)
CALL HEADIN ('COMPUTED FIXES FOR EMITTER B $', 100, 2, 1)

CALL INTAXS
CALL YAXANG (0)
CALL YTICKS (5)
CALL XTICKS (5)

CALL GRAF (60, 1, 80, 190, 1, 210)
CALL DOT
CALL GRID (1)
CALL RESET ('DOT')

CALL MESSAG ('DEGREES $', 100, 'ABUT', 'ABUT')
CALL MARKER (3)

CALL CURVE (XRAYB, YRAYB, COUNTB, -1)
CALL ENDPL (-2)

```

CC


```

FOLLOWING SUBROUTINE IS USED TO PLOT THE FIXES FOR EMITTER D.
SUBROUTINE FICHD (XRAYD,YRAYD,COUNTD,MAXERR)
REAL*8 XRAYC(800),YRAYD(800),MAXERR
INTEGER COUNTD
CALL TEK618
CALL NOBRDR
CALL PAGE(11.,8.5)

CALL AREA2D(6.5,6.5)
CALL SWISSM

CALL XNAME('X COORDINATE (KILOMETERS)',100)
CALL YNAME('Y COORDINATE (KILOMETERS)',100)
CALL HEADIN('COMPUTED FIXES FOR EMITTER D$',100,2.,1)

CALL INTAXS
CALL YAXANG(0)
CALL YTICKS(5)
CALL XTICKS(5)

CALL GRAF(78.,1.,82.,98.,1.,102.)
CALL DOT
CALL GRID(1,1)
CALL RESET('DOT')

CALL MESSAGE('MAX LOB ERROR EQUAL TO 2.0 DEGREE$',100,0.5,0.5)
CALL MESSAGE('LOB ERROR EQUAL TO 1.0 DEGREE$',100,0.5,0.3)
CALL MARKER(3)

CALL CURVE(XRAYD,YRAYD,COUNTD,-1)
CALL ENOPL(-4)

RETURN
END

SUBROUTINE GRAFIT(POSRAY,AVGRAY)
REAL*8 POSRAY(4),AVGRAY(4)

```

CC

TABLE C-1

Simulation 2, Run 1. Simulation to check program.
Gradient area equal to 15 Km. All values are in
kilometers. Emitter D has system error of 2.0
degrees.

DNDX= - 1.000

EMITTER A AVERAGE ERROR
AVERAGE Y=100.001012 AVERAGE X= 80.000079
AVERAGE MISSED DISTANCE= 0.001015

EMITTER B AVERAGE ERROR
AVERAGE Y= 70.000441 AVERAGE X=119.999938
AVERAGE MISSED DISTANCE= 0.000445

EMITTER C AVERAGE ERROR
AVERAGE Y=250.002003 AVERAGE X=149.999896
AVERAGE MISSED DISTANCE= 0.002006

EMITTER D AVERAGE ERROR
AVERAGE Y= 99.999820 AVERAGE X= 79.999996
AVERAGE MISSED DISTANCE= 0.000180

EMITTER A AVERAGE ERROR
AVERAGE Y=100.000853 AVERAGE X= 80.000006
AVERAGE MISSED DISTANCE= 0.000853

EMITTER B AVERAGE ERROR
AVERAGE Y= 70.000413 AVERAGE X=119.999964
AVERAGE MISSED DISTANCE= 0.000415

EMITTER C AVERAGE ERROR
AVERAGE Y=250.002263 AVERAGE X=149.999909
AVERAGE MISSED DISTANCE= 0.002264

EMITTER D AVERAGE ERROR
AVERAGE Y= 99.999889 AVERAGE X= 79.999996
AVERAGE MISSED DISTANCE= 0.000111

TABLE C-1

Simulation 2, Run 1 (continued).

EMITTER A AVERAGE ERROR
AVERAGE Y=100.000803 AVERAGE X= 80.000032
AVERAGE MISSED DISTANCE= 0.000804

EMITTER B AVERAGE ERROR
AVERAGE Y= 70.000464 AVERAGE X=119.999922
AVERAGE MISSED DISTANCE= 0.000471

EMITTER C AVERAGE ERROR
AVERAGE Y=250.002500 AVERAGE X=149.999883
AVERAGE MISSED DISTANCE= 0.002503

EMITTER D AVERAGE ERROR
AVERAGE Y= 99.999870 AVERAGE X= 79.999997
AVERAGE MISSED DISTANCE= 0.000130

EMITTER A AVERAGE ERROR
AVERAGE Y=100.000808 AVERAGE X= 80.000025
AVERAGE MISSED DISTANCE= 0.000809

EMITTER B AVERAGE ERROR
AVERAGE Y= 70.000431 AVERAGE X=119.999934
AVERAGE MISSED DISTANCE= 0.000436

EMITTER C AVERAGE ERROR
AVERAGE Y=250.002532 AVERAGE X=149.999904
AVERAGE MISSED DISTANCE= 0.002533

EMITTER D AVERAGE ERROR
AVERAGE Y= 99.999909 AVERAGE X= 79.999997
AVERAGE MISSED DISTANCE= 0.000091

TABLE C-2

Simulation 2, Run 2. Gradient area equal to 15 Km.
All values are in kilometers. Emitter D has system
error of 2.0 degrees.

DNDX= - 40.000

EMITTER A AVERAGE ERROR
AVERAGE Y=100.043380 AVERAGE X= 80.002240
AVERAGE MISSED DISTANCE= 0.043438

EMITTER B AVERAGE ERROR
AVERAGE Y= 70.019390 AVERAGE X=119.998662
AVERAGE MISSED DISTANCE= 0.019436

EMITTER C AVERAGE ERROR
AVERAGE Y=250.127474 AVERAGE X=149.999134
AVERAGE MISSED DISTANCE= 0.127477

EMITTER D AVERAGE ERROR
AVERAGE Y=102.759927 AVERAGE X= 81.703879
AVERAGE MISSED DISTANCE= 3.243517

EMITTER A AVERAGE ERROR
AVERAGE Y=100.040231 AVERAGE X= 80.001522
AVERAGE MISSED DISTANCE= 0.040260

EMITTER B AVERAGE ERROR
AVERAGE Y= 70.020793 AVERAGE X=119.997969
AVERAGE MISSED DISTANCE= 0.020892

EMITTER C AVERAGE ERROR
AVERAGE Y=250.126468 AVERAGE X=149.999207
AVERAGE MISSED DISTANCE= 0.126471

EMITTER D AVERAGE ERROR
AVERAGE Y= 98.649566 AVERAGE X= 79.368710
AVERAGE MISSED DISTANCE= 1.490704

TABLE C-2

Simulation 2, Run 2 (continued).

EMITTER A AVERAGE ERROR
 AVERAGE Y=100.042220 AVERAGE X= 80.002135
 AVERAGE MISSED DISTANCE= 0.042274

EMITTER B AVERAGE ERROR
 AVERAGE Y= 70.020391 AVERAGE X=119.997753
 AVERAGE MISSED DISTANCE= 0.020514

EMITTER C AVERAGE ERROR
 AVERAGE Y=250.130829 AVERAGE X=149.998735
 AVERAGE MISSED DISTANCE= 0.130835

EMITTER D AVERAGE ERROR
 AVERAGE Y=102.725045 AVERAGE X= 80.692302
 AVERAGE MISSED DISTANCE= 2.811610

EMITTER A AVERAGE ERROR
 AVERAGE Y=100.042224 AVERAGE X= 80.002115
 AVERAGE MISSED DISTANCE= 0.042277

EMITTER B AVERAGE ERROR
 AVERAGE Y= 70.019693 AVERAGE X=119.998251
 AVERAGE MISSED DISTANCE= 0.019770

EMITTER C AVERAGE ERROR
 AVERAGE Y=250.127309 AVERAGE X=149.999286
 AVERAGE MISSED DISTANCE= 0.127311

EMITTER D AVERAGE ERROR
 AVERAGE Y=102.410316 AVERAGE X= 79.863946
 AVERAGE MISSED DISTANCE= 2.414153

TABLE C-3

Simulation 2, Run 3. Gradient area equal to 15 Km.
 All values are in kilometers. Emitter D has system
 error of 2.0 degrees.

DNDX= - 80.000

EMITTER A AVERAGE ERROR
 AVERAGE Y=100.086917 AVERAGE X= 80.004486
 AVERAGE MISSED DISTANCE= 0.087032

EMITTER B AVERAGE ERROR
 AVERAGE Y= 70.038854 AVERAGE X=119.997338
 AVERAGE MISSED DISTANCE= 0.038945

EMITTER C AVERAGE ERROR
 AVERAGE Y=250.256023 AVERAGE X=149.998342
 AVERAGE MISSED DISTANCE= 0.256029

EMITTER D AVERAGE ERROR
 AVERAGE Y=102.759927 AVERAGE X= 81.703879
 AVERAGE MISSED DISTANCE= 3.243517

EMITTER A AVERAGE ERROR
 AVERAGE Y=100.080602 AVERAGE X= 80.003047
 AVERAGE MISSED DISTANCE= 0.080659

EMITTER B AVERAGE ERROR
 AVERAGE Y= 70.041659 AVERAGE X=119.995953
 AVERAGE MISSED DISTANCE= 0.041855

EMITTER C AVERAGE ERROR
 AVERAGE Y=250.253971 AVERAGE X=149.998479
 AVERAGE MISSED DISTANCE= 0.253975

EMITTER D AVERAGE ERROR
 AVERAGE Y= 98.649566 AVERAGE X= 79.368710
 AVERAGE MISSED DISTANCE= 1.490704

TABLE C-3

Simulation 2, Run 3 (continued).

EMITTER A AVERAGE ERROR
AVERAGE Y=100.084615 AVERAGE X= 80.004267
AVERAGE MISSED DISTANCE= 0.084722

EMITTER B AVERAGE ERROR
AVERAGE Y= 70.040865 AVERAGE X=119.995525
AVERAGE MISSED DISTANCE= 0.041109

EMITTER C AVERAGE ERROR
AVERAGE Y=250.262486 AVERAGE X=149.997556
AVERAGE MISSED DISTANCE= 0.262498

EMITTER D AVERAGE ERROR
AVERAGE Y=102.725045 AVERAGE X= 80.692302
AVERAGE MISSED DISTANCE= 2.811610

EMITTER A AVERAGE ERROR
AVERAGE Y=100.084590 AVERAGE X= 80.004232
AVERAGE MISSED DISTANCE= 0.084696

EMITTER B AVERAGE ERROR
AVERAGE Y= 70.039468 AVERAGE X=119.996522
AVERAGE MISSED DISTANCE= 0.039621

EMITTER C AVERAGE ERROR
AVERAGE Y=250.255841 AVERAGE X=149.998652
AVERAGE MISSED DISTANCE= 0.255845

EMITTER D AVERAGE ERROR
AVERAGE Y=102.410316 AVERAGE X= 79.863946
AVERAGE MISSED DISTANCE= 2.414153

TABLE C-4

Simulation 2, Run 4. Gradient area equal to 15 Km.
 All values are in kilometers. Emitter D has system
 error of 2.0 degrees.

DNDX= -120.000

EMITTER A AVERAGE ERROR
 AVERAGE Y=100.130485 AVERAGE X= 80.006726
 AVERAGE MISSED DISTANCE= 0.130658

EMITTER B AVERAGE ERROR
 AVERAGE Y= 70.058320 AVERAGE X=119.996020
 AVERAGE MISSED DISTANCE= 0.058456

EMITTER C AVERAGE ERROR
 AVERAGE Y=250.384719 AVERAGE X=149.997550
 AVERAGE MISSED DISTANCE= 0.384727

EMITTER D AVERAGE ERROR
 AVERAGE Y=102.759927 AVERAGE X= 81.703879
 AVERAGE MISSED DISTANCE= 3.243517

EMITTER A AVERAGE ERROR
 AVERAGE Y=100.121006 AVERAGE X= 80.004569
 AVERAGE MISSED DISTANCE= 0.121092

EMITTER B AVERAGE ERROR
 AVERAGE Y= 70.062523 AVERAGE X=119.993945
 AVERAGE MISSED DISTANCE= 0.062815

EMITTER C AVERAGE ERROR
 AVERAGE Y=250.381620 AVERAGE X=149.997752
 AVERAGE MISSED DISTANCE= 0.381627

EMITTER D AVERAGE ERROR
 AVERAGE Y= 98.649566 AVERAGE X= 79.368710
 AVERAGE MISSED DISTANCE= 1.490704

TABLE C-4

Simulation 2, Run 4 (continued).

EMITTER A AVERAGE ERROR
AVERAGE Y=100.127041 AVERAGE X= 80.006394
AVERAGE MISSED DISTANCE= 0.127202

EMITTER B AVERAGE ERROR
AVERAGE Y= 70.061337 AVERAGE X=119.993306
AVERAGE MISSED DISTANCE= 0.061702

EMITTER C AVERAGE ERROR
AVERAGE Y=250.394293 AVERAGE X=149.996377
AVERAGE MISSED DISTANCE= 0.394310

EMITTER D AVERAGE ERROR
AVERAGE Y=132.725045 AVERAGE X= 80.692302
AVERAGE MISSED DISTANCE= 2.811610

EMITTER A AVERAGE ERROR
AVERAGE Y=100.126989 AVERAGE X= 80.006345
AVERAGE MISSED DISTANCE= 0.127147

EMITTER B AVERAGE ERROR
AVERAGE Y= 70.059245 AVERAGE X=119.994801
AVERAGE MISSED DISTANCE= 0.059473

EMITTER C AVERAGE ERROR
AVERAGE Y=250.384520 AVERAGE X=149.998019
AVERAGE MISSED DISTANCE= 0.384525

EMITTER D AVERAGE ERROR
AVERAGE Y=132.410316 AVERAGE X= 79.863946
AVERAGE MISSED DISTANCE= 2.414153

TABLE C-5

Simulation 2, Run 5. Gradient area equal to 15 Km.
All values are in kilometers. Emitter D has system
error of 2.0 degrees.

DNDX= -150.000

EMITTER A AVERAGE ERROR
AVERAGE Y=100.163182 AVERAGE X= 80.008403
AVERAGE MISSED DISTANCE= 0.163398

EMITTER B AVERAGE ERROR
AVERAGE Y= 70.072923 AVERAGE X=119.995035
AVERAGE MISSED DISTANCE= 0.073092

EMITTER C AVERAGE ERROR
AVERAGE Y=250.481339 AVERAGE X=149.996957
AVERAGE MISSED DISTANCE= 0.481348

EMITTER D AVERAGE ERROR
AVERAGE Y=102.759927 AVERAGE X= 81.703879
AVERAGE MISSED DISTANCE= 3.243517

EMITTER A AVERAGE ERROR
AVERAGE Y=100.151332 AVERAGE X= 80.005709
AVERAGE MISSED DISTANCE= 0.151440

EMITTER B AVERAGE ERROR
AVERAGE Y= 70.078171 AVERAGE X=119.992447
AVERAGE MISSED DISTANCE= 0.078535

EMITTER C AVERAGE ERROR
AVERAGE Y=250.477453 AVERAGE X=149.997206
AVERAGE MISSED DISTANCE= 0.477462

EMITTER D AVERAGE ERROR
AVERAGE Y= 98.649566 AVERAGE X= 79.368710
AVERAGE MISSED DISTANCE= 1.490704

TABLE C-5

Simulation 2, Run 5 (continued).

EMITTER A AVERAGE ERROR
 AVERAGE Y=100.158883 AVERAGE X= 80.007987
 AVERAGE MISSED DISTANCE= 0.159084

EMITTER B AVERAGE ERROR
 AVERAGE Y= 70.076691 AVERAGE X=119.991647
 AVERAGE MISSED DISTANCE= 0.077144

EMITTER C AVERAGE ERROR
 AVERAGE Y=250.493245 AVERAGE X=149.995494
 AVERAGE MISSED DISTANCE= 0.493266

EMITTER D AVERAGE ERROR
 AVERAGE Y=102.725045 AVERAGE X= 80.692302
 AVERAGE MISSED DISTANCE= 2.811610

EMITTER A AVERAGE ERROR
 AVERAGE Y=100.158809 AVERAGE X= 80.007927
 AVERAGE MISSED DISTANCE= 0.159007

EMITTER B AVERAGE ERROR
 AVERAGE Y= 70.074079 AVERAGE X=119.993514
 AVERAGE MISSED DISTANCE= 0.074363

EMITTER C AVERAGE ERROR
 AVERAGE Y=250.481126 AVERAGE X=149.997545
 AVERAGE MISSED DISTANCE= 0.481133

EMITTER D AVERAGE ERROR
 AVERAGE Y=102.410316 AVERAGE X= 79.863946
 AVERAGE MISSED DISTANCE= 2.414153

TABLE C-6

Simulation 2, Run 6. Gradient area equal to 30 Km.
All values are in kilometers. Emitter D has system
error of 2.0 degrees.

DNDX= - 80.000

EMITTER A AVERAGE ERROR
AVERAGE Y=100.146546 AVERAGE X= 80.007539
AVERAGE MISSED DISTANCE= 0.146740

EMITTER B AVERAGE ERROR
AVERAGE Y= 70.044350 AVERAGE X=119.996988
AVERAGE MISSED DISTANCE= 0.044452

EMITTER C AVERAGE ERROR
AVERAGE Y=250.494021 AVERAGE X=149.996880
AVERAGE MISSED DISTANCE= 0.494030

EMITTER D AVERAGE ERROR
AVERAGE Y=102.759927 AVERAGE X= 81.703879
AVERAGE MISSED DISTANCE= 3.243517

EMITTER A AVERAGE ERROR
AVERAGE Y=100.135913 AVERAGE X= 80.005123
AVERAGE MISSED DISTANCE= 0.136009

EMITTER B AVERAGE ERROR
AVERAGE Y= 70.047533 AVERAGE X=119.995420
AVERAGE MISSED DISTANCE= 0.047753

EMITTER C AVERAGE ERROR
AVERAGE Y=250.490033 AVERAGE X=149.997136
AVERAGE MISSED DISTANCE= 0.490042

EMITTER D AVERAGE ERROR
AVERAGE Y= 98.649566 AVERAGE X= 79.368710
AVERAGE MISSED DISTANCE= 1.490704

TABLE C-6

Simulation 2, Run 6 (continued).

EMITTER A AVERAGE ERROR
AVERAGE Y=100.142684 AVERAGE X= 80.007169
AVERAGE MISSED DISTANCE= 0.142864

EMITTER B AVERAGE ERROR
AVERAGE Y= 70.046624 AVERAGE X=119.994932
AVERAGE MISSED DISTANCE= 0.046898

EMITTER C AVERAGE ERROR
AVERAGE Y=250.506230 AVERAGE X=149.995379
AVERAGE MISSED DISTANCE= 0.506251

EMITTER D AVERAGE ERROR
AVERAGE Y=102.725045 AVERAGE X= 80.692302
AVERAGE MISSED DISTANCE= 2.811610

EMITTER A AVERAGE ERROR
AVERAGE Y=100.142623 AVERAGE X= 80.007113
AVERAGE MISSED DISTANCE= 0.142801

EMITTER B AVERAGE ERROR
AVERAGE Y= 70.045045 AVERAGE X=119.996062
AVERAGE MISSED DISTANCE= 0.045217

EMITTER C AVERAGE ERROR
AVERAGE Y=250.493808 AVERAGE X=149.997484
AVERAGE MISSED DISTANCE= 0.493814

EMITTER D AVERAGE ERROR
AVERAGE Y=102.410316 AVERAGE X= 79.863946
AVERAGE MISSED DISTANCE= 2.414153

TABLE C-7

Simulation 2, Run 7. Gradient area equal to 30 Km.
All values are in kilometers. Emitter D has system
error of 2.0 degrees.

DNDX= -120.000

EMITTER A AVERAGE ERROR
AVERAGE Y=100.220026 AVERAGE X= 80.011285
AVERAGE MISSED DISTANCE= 0.220315

EMITTER B AVERAGE ERROR
AVERAGE Y= 70.066528 AVERAGE X=119.995517
AVERAGE MISSED DISTANCE= 0.066679

EMITTER C AVERAGE ERROR
AVERAGE Y=250.742346 AVERAGE X=149.995360
AVERAGE MISSED DISTANCE= 0.742361

EMITTER D AVERAGE ERROR
AVERAGE Y=102.759927 AVERAGE X= 81.703879
AVERAGE MISSED DISTANCE= 3.243517

EMITTER A AVERAGE ERROR
AVERAGE Y=100.204084 AVERAGE X= 80.007670
AVERAGE MISSED DISTANCE= 0.204228

EMITTER B AVERAGE ERROR
AVERAGE Y= 70.071281 AVERAGE X=119.993181
AVERAGE MISSED DISTANCE= 0.071606

EMITTER C AVERAGE ERROR
AVERAGE Y=250.736341 AVERAGE X=149.995739
AVERAGE MISSED DISTANCE= 0.736353

EMITTER D AVERAGE ERROR
AVERAGE Y= 98.649566 AVERAGE X= 79.368710
AVERAGE MISSED DISTANCE= 1.490704

TABLE C-7

Simulation 2, Run 7 (continued).

EMITTER A AVERAGE ERROR
AVERAGE Y=100.214249 AVERAGE X= 80.010728
AVERAGE MISSED DISTANCE= 0.214518

EMITTER B AVERAGE ERROR
AVERAGE Y= 70.069917 AVERAGE X=119.992449
AVERAGE MISSED DISTANCE= 0.070324

EMITTER C AVERAGE ERROR
AVERAGE Y=250.760544 AVERAGE X=149.993117
AVERAGE MISSED DISTANCE= 0.760575

EMITTER D AVERAGE ERROR
AVERAGE Y=102.725045 AVERAGE X= 80.692302
AVERAGE MISSED DISTANCE= 2.811610

EMITTER A AVERAGE ERROR
AVERAGE Y=100.214143 AVERAGE X= 80.010646
AVERAGE MISSED DISTANCE= 0.214408

EMITTER B AVERAGE ERROR
AVERAGE Y= 70.067568 AVERAGE X=119.994138
AVERAGE MISSED DISTANCE= 0.067822

EMITTER C AVERAGE ERROR
AVERAGE Y=250.742099 AVERAGE X=149.996269
AVERAGE MISSED DISTANCE= 0.742109

EMITTER D AVERAGE ERROR
AVERAGE Y=102.410316 AVERAGE X= 79.863946
AVERAGE MISSED DISTANCE= 2.414153

TABLE C-8

Simulation 2, Run 8. Gradient area of 30 Km. System induced error of 1.5 degrees for all LOB's. Emitters A, B and C have refracted LOB's correlated with straight LOB's. All values are in kilometers.

DNDX= -100.000

EMITTER A AVERAGE ERROR
AVERAGE Y= 96.136822 AVERAGE X= 80.311562
AVERAGE MISSED DISTANCE= 3.875721

EMITTER B AVERAGE ERROR
AVERAGE Y= 70.055440 AVERAGE X= 119.996250
AVERAGE MISSED DISTANCE= 0.055567

EMITTER C AVERAGE ERROR
AVERAGE Y= 250.618112 AVERAGE X= 149.996120
AVERAGE MISSED DISTANCE= 0.618124

EMITTER D AVERAGE ERROR
AVERAGE Y= 101.991913 AVERAGE X= 81.272969
AVERAGE MISSED DISTANCE= 2.363930

EMITTER A AVERAGE ERROR
AVERAGE Y= 101.483913 AVERAGE X= 80.127291
AVERAGE MISSED DISTANCE= 1.489362

EMITTER B AVERAGE ERROR
AVERAGE Y= 70.059409 AVERAGE X= 119.994296
AVERAGE MISSED DISTANCE= 0.059683

EMITTER C AVERAGE ERROR
AVERAGE Y= 250.613116 AVERAGE X= 149.996437
AVERAGE MISSED DISTANCE= 0.613126

EMITTER D AVERAGE ERROR
AVERAGE Y= 100.731179 AVERAGE X= 79.514574
AVERAGE MISSED DISTANCE= 0.877645

TABLE C-8

Simulation 2, Run 8 (continued).

EMITTER A AVERAGE ERROR
 AVERAGE Y= 98.926232 AVERAGE X= 80.760458
 AVERAGE MISSED DISTANCE= 1.315779

EMITTER B AVERAGE ERROR
 AVERAGE Y= 70.058276 AVERAGE X=119.993687
 AVERAGE MISSED DISTANCE= 0.058617

EMITTER C AVERAGE ERROR
 AVERAGE Y=250.633317 AVERAGE X=149.994248
 AVERAGE MISSED DISTANCE= 0.633343

EMITTER D AVERAGE ERROR
 AVERAGE Y=101.946699 AVERAGE X= 80.515853
 AVERAGE MISSED DISTANCE= 2.013887

EMITTER A AVERAGE ERROR
 AVERAGE Y=101.203482 AVERAGE X= 79.673178
 AVERAGE MISSED DISTANCE= 1.247070

EMITTER B AVERAGE ERROR
 AVERAGE Y= 70.056309 AVERAGE X=119.995098
 AVERAGE MISSED DISTANCE= 0.056522

EMITTER C AVERAGE ERROR
 AVERAGE Y=250.617883 AVERAGE X=149.996876
 AVERAGE MISSED DISTANCE= 0.617891

EMITTER D AVERAGE ERROR
 AVERAGE Y=101.649868 AVERAGE X= 79.896641
 AVERAGE MISSED DISTANCE= 1.653102

LIST OF REFERENCES

1. National Oceanic and Atmospheric Administration Document NOAA-S/T 76-1562, U.S. Standard Atmosphere, 1976, p. 20, October 1976.
2. Lake, J. S., "Atmospheric Refraction: A Neglected Fundamental Comes of Age", Defense Electronics, v. 14 no. 10, pp. 22-28, October 1982.
3. Beach, J. B., "Part II, Atmospheric Effects on Radio Wave Propagation", Defense Electronics, v. 12 no. 10, pp. 75-83, October 1980.
4. Naval Research Laboratory Report 7725, Geophysical Aspects of Atmospheric Refraction, by C. G. Purves, p. 14, 7 June 1974.
5. Davidson, K. L., Atmospheric Factors in Electromagnetics/Electro-Optics, material for classroom presentation, Naval Postgraduate School, Monterey, California, pp. 3-1 - 7-31, 1982.
6. Meeks, M. L., Radar Propagation at Low Altitudes, pp. 9-26, Artech House, Inc., 1982.
7. Skolnik, M. I., Introduction to Radar Systems, pp. 448-454, McGraw-Hill, Inc., 1980.
8. Transportation Systems Center - National Aeronautics and Space Administration Report 71-6, Atmospheric Transmission Handbook, by W. I. Thompson III, p. 3, February 1971.
9. Office of Telecommunications Report 76-105, Refractivity and Rainfall Data for Radio Systems Engineering, by C. A. Samson, pp. 6-9, September 1976.
10. Harrington, J. B. and Callaghan, T. G., "UHF/VHF Direction Finding", Watkins - Johnson Company Technotes, v. 8 no. 1, pp. 1-7, February 1981.
11. McCartney, E. J., Optics of the Atmosphere, pp. 100-112, Wiley & Sons, Inc., 1976.
12. Patton, T. N., Petrovic, J. J., and Teti, J., "Propagation Effects of Millimeter Wave Fire Control Systems", S. J. Johnston, editor, Millimeter Wave Radar, p. 170, 1980.

13. Kaelin, C. M., EA-6B Mission Planning: Tactical Considerations for ESM/ECM Employment Under Non-standard Refractive Conditions, Masters Thesis, Naval Postgraduate School, Monterey, California, p. 124, 1980.
14. Naval Ocean Systems Center Technical Note 810, PROCAL-PREOS: A Fast-Running Airborne FLIR System Performance Model, by F. P. Snyder, p. 1, February 1980.
15. Fraser, A. B. and Mach, W. H., "Mirage", Scientific American, pp. 32-36, 1980.
16. Zuev, V. E., Propagation of Visible and Infrared Radiation in the Atmosphere, pp. 348-349, Wiley & Sons, Inc., 1974.
17. Defense Advanced Research Projects Agency Report 1171, Degradation of Laser Systems by Atmospheric Turbulence, By R. F. Lutomirski, R. E. Huschke, W. C. Meecham, and H. T. Yura, pp. 1-230, June 1973.
18. Cooper, A. W., Electro-Optic Principles and Devices, material for classroom presentation, Naval Postgraduate School, Monterey, California, p. A-40, 1982.
19. Hall, F. F., "Index of Refraction Structure Parameter in the Real Atmosphere - an Overview", Technical Digest, Optical Propagation through Turbulence, Rain, and Fog, p. TuCl-1, August 1977.
20. Naval Postgraduate School Report 61-78-003, Optical Resolution in the Turbulent Atmosphere of the Marine Boundary Layer, by E. C. Crittenden, A. W. Cooper, E. A. Milne, G. W. Rodeback, R. L. Armstead, S. H. Kalmbach, D. Land, and B. Katz, pp. 2-16, February 1978.
21. Crittenden, E. C., Cooper, A. W., Milne, E. A., Rodeback, G. W., and Kalmbach, S. H., "Multiwavelength Extinction and Index Fluctuation Measurements", Advisory Group for Aerospace Research and Development Conference Proceedings - 300, Special Topics in Optical Propagation, pp. 13-1 - 13-2, July 1981.
22. McMillan, R. W. and Bohlander, R. A., "Millimeter Wave Atmospheric Turbulence Measurements: Preliminary Results and Instrumentation for Future Measurements", Optical Engineering, v. 22 no. 1, pp. 33-36, January/February 1983.

23. USA Ballistic Research Laboratories Memorandum Report No. 2243, Diurnal Cycles of Refractive Index Structure Function Coefficient, by M. L. Wesely and E.C. Alcaraz, p. 9, November 1972.
24. U.S. Army Field Manual FM 17-12, Tank Gunnery, pp. 4-9 - 4-10, 21 March 1977.
25. Environmental Science Services Administration (ESSA) Research Laboratories Technical Report 79-ITS 67, Prediction of Tropospheric Radio Transmission Loss over Irregular Terrain - A Computer Method-1968, by A. G. Longley, and P. D. Rice, p. 1, July 1968.
26. Callaghan, J. M., Tropoplot: An Improved Fortran Computer Program for Prediction of Long-Term Median Tropospheric Radio Transmission Loss Over Irregular Terrain, Masters Thesis, Naval Postgraduate School, Monterey, California, pp. 10-42, 1973.
27. U.S. Department of Commerce - National Bureau of Standards Monograph 92, Radio Meteorology, by B.R. Bean and E.J. Dutton, p. 63, March 1966.
28. U.S. Army Field Manual FM 24-24, Radio & Radar Reference Data, pp. 1-12, May 1977.
29. U.S. Army Field Manual FM 24-25, Wire and Multichannel Reference Data, pp. 2-16, June 1977.
30. Naval Ocean Systems Center Technical Document 481, IREPS Revision 2.0 User's Manual, by H. V. Hitney, R. A. Paulus, C. P. Hattan, K. D. Anderson, and G. E. Lindem, p. 30, September 1981.

BIBLIOGRAPHY

GTE Sylvania Contract: MDA-904-78-C-0511, Radiosonde Data Analysis III: World Contour Maps, G. K. Miller, W. B. Moreland, and L. N. Ortenburger, December 1979.

GTE Sylvania Contract: MDA-904-87-C-0511, Radiosonde Data Analysis III: Summary Maps of Observed Data, L. N. Ortenburger, S. B. Lawson, and G. K. Miller, December 1978.

National Bureau of Standards Monograph 22, Climatic Charts and Data of the Radio Refractive Index for the United States and the World, by B. R. Bean, J. D. Horn, and A. M. Ozanich Jr., November 1960.

Van Brunt, L. B., Applied ECM, EW Engineering, Inc., 1978.

U.S. Army Atmospheric Sciences Laboratory, Effects of Atmospheric Turbulence on FLIR Performance, by H. A. Quevado and D. E. Snider, January 1983.

B. Khular, K. Thyagaragjan, and A. K. Ghatak, "A note on Mirage Formation", American Journal of Physics, v. 45 no. 1, January 1977.

U.S. Army Field Manual FM 100-5, Operations, 1 July 1976.

U.S. Army Field Manual FM 34-10, Military Intelligence Battalion (Combat Electronic Warfare Intelligence)(Division), 3 July 1981.

Environmental Science Services Administration (ESSA) Research Laboratory Technical Report 65-ITS 58-2, Tabulations of Propagation Data over Irregular Terrain in the 230-to-9200 MHz Frequency Range - Part II Fritz Peak Receiver Site, by P. L. McQuate, J. M. Harman, M. E. Johnson, and A. P. Batsis, December 1968.

Environmental Science Services Administration (ESSA) Research Laboratory Technical Report 65-ITS 58-3, Tabulations of Propagation Data over Irregular Terrain in the 230-to-9200 MHz Frequency Range - Part III North Table Mountain - Golden, by P. L. McQuate, J. M. Harman, M. E. McClanahan, A. P. Batsis, July 1970.

Richter, J. H., Hughes, H. G., and Rose, R. B., "Electromagnetic Propagation Assessment", Electromagnetic Propagation Division, Naval Ocean Systems Center Technical Document 260, Proceedings of Conference on Atmospheric Refractive Effects Assessment, June 1979.

INITIAL DISTRIBUTION LIST

	No. Copies
1. Defense Technical Information Center Cameron Station Alexandria, Virginia 22314	2
2. Deputy Under Secretary of Army of Operations Research Room 2E261, Pentagon Washington, D.C. 20310	1
3. Library, Code 0142 Naval Postgraduate School Monterey, California 93943	2
4. Chairman, Electronic Warfare Academic Group, Code 73 Naval Postgraduate School Monterey, California 93943	1
5. Professor Gordon E. Schacher, Code 61Sq Department of Physics and Chemistry Naval Postgraduate School Monterey, California 93943	1
6. Professor Kenneth L. Davidson, Code 63Ds Department of Meteorology Naval Postgraduate School Monterey, California 93943	1
7. Commander/Director U.S. Army Atmospheric Sciences Laboratory Attn: DEDAS-AE-E (Dr. Don Snider) White Sands Missile Range, New Mexico 88002	3
8. Commander U.S. Army Electronic Proving Grounds Attn: STEEP-MT-T Ft. Huachuca, Arizona 85613	2
9. Lieutenant Colonel Thomas Houser, USA Dep. C-of-S for Ops & Plan(DCSOPS-FDI) Washington, D.C. 20310	1
10. Captain Theodore Mouras, USA Post Office Box 320 Ft. Huachuca, Arizona 85613	1

END

FILMED

12-83

DATIC